Biochemical characterization of the self-splicing GIN1 protein in arbuscular mycorrhizal fungi

Dissertation

der Fakultät für Biologie
der Eberhard Karls Universität Tübingen

zur Erlangung des Grades eines Doktors
der Naturwissenschaften

vorgelegt von
Esther Serrano Padial
aus Elda, Spanien
2005

Tag der mündlichen Prüfung	24.06.2005
Dekan	Prof. Dr. Friedrich Schöffl
1. Berichterstatter	PD Dr. Natalia Requena
2. Berichterstatter	Prof. Dr. Rüdiger Hampp

To my family

Acknowledgments

My special acknowledgement to PD. Dr. Natalia Requena, for giving me the chance to work in this interesting subject, her constant patience and supervision of my work.

I would like to thank the group of Prof. Dr. R. Hampp for nice working atmosphere and the good friends I left there: Alonso, Mónica, Anita, Martin, Silvia, Marion and in special M. Ecke, for being able to solve any problem.

My special regards to Dr. Christian Ottmann and Prof. Dr. C. Oecking and her group. It was really nice to work with you, thanks for being always willing to help and solving so many proteomics and other problems.

My special acknowledgement to Thomas Härtner and Prof. Dr. Wohlleben. Without your advice, patience and good humor I could have not make it with the lipid extraction and characterization. Danke viel mals! Es war wirklich schön mit dir zusammen zum arbeiten.

Specially thanks to G. Mander and Prof. Dr. Reinhardt Fischer and his group, for scientific discussion and that hard week of work.

Thanks to Prof. Dr. R. Süssmuth and his group, Kathrin, Falco, Diane, Timo and Simone, and in special Dr. M. Bertazzo, the chemistry connection, for solving analytical problems and HPLC-MS analyses.

Although we never met, my special regards to Prof. Dr. Sonia Paris. Thanks for your fast email advice. Your protocols, experience and professional discussion brought light to my GTP binding experiments.

Thanks to Dr. T. Haug and all the people in the Isotopenlabour, for being always so nice to me and helping in the set up of the experiments related to radioactivity.

My acknowledgement to Prof. Dr. M. Bölker for providing the Umcdc42 and Umcdc42(Q-L) constructs and P. A. Beachy for the DmHh-C construct and advice.

I would like to thank many groups and people in the Botanical Institute for their contribution to this work in many aspects: Anne, Luz Irina, F. de Courcy, Dr. M. de

Simone, Dr. K. Schumacher, Dr. M. Tarkka, PD. Dr. U. Nehls, Dr. Swechheimer, PD. Dr. D. Begeroff, Prof. Dr. Zeits, Prof. Dr. Kottke, Prof. Dr. Nürnberger, Prof. Dr. Harter.

To Dr. Nina Grunze, for personal and professional advice and critical correction of the thesis. For being a great person, friend and researcher.

To Dr. Mark Trautwein, for hearing and solving my “never ending little lab problems”, thanks for sharing your “common sense”, reviewing my work and unconditional help and friendship.

To Dr. Claudia Lemmel, for supporting me being a great friend and researcher, opening your house and your heart to me. I am sure we will be for long good friends.

Gracias al Prof. Dr. Juan Niclós y Prof. Dr. Pepa González, por introducirme en el campo de la investigación y apoyarme en mi decisión de venir a Alemania.

A mi gran amigo Alonso Leyva por todas las risas, lágrimas y sudores que compartimos estos años.

A Patricia, por las miles de horas y risas al teléfono; a André, por tu guitarra y Ney; a Carla, Cleo, Cintia y Guillerme, por los buenos churrascos; a Malú, por tu gran amistad; a Claudinha, por tu gran corazón; a Dino, Elisette, Renata, Alexandre, Simone y Reiane, por su alegría.

A Daniela, Xavi, Mario, Andrea, Alejandro y Justine, por los buenos momentos.

A mi madre y hermano, a pesar de no comprender mis inquietudes, siempre he contado con vuestro apoyo.

A mi padre, por las cientos de llamadas telefónicas y cartas mandadas todos estos años. No sabes lo que me han ayudado.

Mi agradecimiento especial a Marcelo Bertazzo, por tu incondicional amor y apoyo, tu generosidad, valía profesional y humana. No cambies jamás.

Index

Abbreviations

Aa	Amino acids
AMF	Arbuscular mycorrhizal fungi
Amp	Ampicillin
An	*Aspergillus nidulans*
APS	Ammonium peroxydisulfate
At	*Arabidopsis thaliana*
ATP	Adenosin-triphosphate
Bp	Base pairs
C. albicans	*Candida albicans*
cDNA	Complementary DNA
C. elegans	*Caenorhabditis elegans*
DAG	Diacylglycerol
DIG	Digoxigenin
Disp	Dispatched
Dm	*Drosophila melanogaster*
DNA	Desoxyribonucleic acid
DNase	Desoxyribonuclease
dNTP	Desoxynucleotid-triphosphate
DTT	Dithiotreitol
ESI	Electro spray ionization
GC-MS	Gas chromatography-Mass spectrometry
GiGIN1	*Glomus intraradices* GTPase Intein 1
GIMAP	GTPases from the immune associated protein family
GmGIN1	*Glomus mosseae* GTPase Intein 1
Grd	Groundhog
Gz	*Gibberella zeae*
HC	Hydrocarbons
Hh	Hedgehog
Hint	Hedgehog intein domain
HPLC	High pressure liquid chromatography
IAN	Immune-associated nucleotide

IPTG	Isopropyl β-D-thiogalactopyranoside
Kb	Kilobase
kDa	KiloDalton
LB	Luria Broth
MAG	Monoacylglycerol
Mg	*Magnaporthe grisea*
MeOH	Methanol
mRNA	Messenger RNA
MS	Mass spectrometry
NaCl	Sodium chloride
NBS-LRR	Nucleotide binding site-leucine reach repeat
Nc	*Neurospora crassa*
Nt	*Nicotiana tabacum*
NTA	Nitrilotriaceticacid
PMSF	Phenylmethanesulfonylfluoride
Ptc	Patched
OD	Optical density
Os	*Oriza sativa*
ORF	Open reading frame
P	Pellet
PCR	Polymerase chain reaction
RNA	Ribonucleic acid
RNase	Ribonuclease
Rf	Relative to front
S. cerevisiae	*Saccharomyces cerevisiae*
SDS	Sodiumdodecylsulphate
SE	Sterol esters
Shh	Sonic Hedgehog
Smo	Smoothened
SN	Supernatant
S. pombe	*Schizosaccharomyces pombe*
T	Time
TAE	Tris-acetat-EDTA buffer

Taq-Polymerase	*Thermus aquaticus* DNA polymerase
TAG	Triacylglycerol
TB	Terrific Broth
TBS	Tris buffer saline
TCEP	Tris(carboxyethyl)phosphine
Tet	Tetracycline
TLC	Thin layer chromatography
Tris	Tris (hydroxymethyl) aminoethan
Um	*Ustilago maydis*
UV	Ultraviolet
Wrt	Warthog
X-Gal	5-bromo-4-chloro-3-indolyl-β-D-galactosid

1 Summary

Arbuscular mycorrhizal fungi are obligate symbionts, which means they can not complete their life cycle without establishing symbiosis with a host plant. Nevertheless, mycorrhizal spores are able to germinate and develop a limited hyphal growth in search for a compatible host. In the absence of a host root signal, the fungus stops and arrests growth. When the fungus meets a compatible host root, the fungus forms appressoria on the root rhizodermis and constitutes a functional symbiosis. Because of its beneficial plant effects, it is of outstanding interest to investigate the mechanism of recognition and establishment of the symbiosis between the two partners. Fungal genes that are exclusively expressed during the pre-symbiotic or early developmental stages of the AM symbiosis have been described for the AM fungus *Glomus mosseae* (Requena et al., 2002). A novel gene called *GmGIN1*, coding for GTPase Intein, was identified. *GmGIN1* encodes for a two-domain structure protein, with a putative self-splicing site in the junction of the two domains.

GmGIN1 carboxy terminus shares similarity with the carboxy terminus of Hedgehog (Hh) selfs-plicing proteins. This domain is responsible for self-splicing of the protein precursor into two different peptides. In Hh proteins, the first nucleophilic attack is produced by an internal conserved cysteine, which is situated in GmGIN1 at the 237 amino acid position. The second nucleophilic attack is triggered by a cholesterol molecule, which is covalently attached to the processed N-terminus and determines its localization at raft domains in the cell membrane. In order to investigate an analogous processing mechanism of GmGIN1, the C-terminus was heterologously expressed in *E. coli*. Purified protein was shown to undergo selfsplicing in the same conditions as the carboxy terminus of Hh proteins. Nevertheless, yields of purified protein were not sufficient to appreciate the splicing induction by addition of cholesterol. Lipid extracts from mycorrhizal samples of the closely related fungus *G. intraradices* were performed in order to investigate which molecule could be responsible for the second nucleophilic attack *in vivo*. Mycorrhizal root sterol extracts were able to induce selfsplicing of the carboxy terminus of *D. melanogaster* Hh, expressed and purified under the same conditions as GmGIN1-C. Lipid analysis confirmed the presence of cholesterol derivatives, and traces of cholesterol itself, in the

extracts. Expression of the full length GmGIN1 protein was achieved, but the amount of active purified protein was not enough to observe the self-splicing activity.

The amino terminal domain of GmGIN1 shares homology to a new family of GTPases, the AIG/GIMAP family, conserved among plants, fungi and animals. GmGIN1-N contains three of the five conserved cassettes implicated in GTP binding and hydrolysis. Two of these motifs are also involved in binding to other nucleotide derivatives, such as ATP. In order to investigate the nucleotide binding and possible hydrolysis activity of GmGIN1-N, this domain was heterologously expressed in *E. coli*. No selective binding to α-^{32}P-GTP was observed in overlay assays, neither for GmGIN1-N nor for the positive controls Umcdc42 wild type and Umcdc42(Q-L) mutant. Optimal binding was observed for the positive controls purified under native conditions after incubation with ^{35}S-γ-GTP in solution. GmGIN1-N was shown also to bind to ^{35}S-γ-GTP, but to a lower extent. Competition analysis by ^{35}S-γ-GTP dissociation assays demonstrated that GmGIN1-N has a higher affinity for ATP compared to GTP. This was confirmed by the nucleotide hydrolysis assays, in which GmGIN1-N was shown to actively hydrolyze ATP, but not GTP. This protein could be involved either in recognition events and establishment of the symbiosis upon meeting a host plant, or in growth arrest and programmed cell death in the absence of a compatible partner.

2 Introduction

2.1 Mycorrhiza

2.1.1 Definition and importance

Mycorrhiza is the most widespread root symbiosis. It was estimated that around 90% of land plants are colonized with soil fungi belonging to 3 different phyla: Basidiomycetes, Ascomycetes and Zygomycetes (Smith and Read, 1997). The most common type is the Arbuscular Mycorrhiza (AM), occurring in over 80% of plant species. Based on molecular, morphological, and ecological characteristics AM fungi have been excluded from the Zygomycetes phylum and classified in the new Glomeromycota phylum, in the single class of Glomeromycetes (Schüssler et al. 2001). The occurrence of AM fungi has been dated back to at least 460 million years (Redecker et al. 2000). Fossil records (Remy et al. 1994; Taylor et al. 1995) and molecular data (Simon et al. 1993) have suggested that these fungi evolved together with plants, helping them in the colonization of solid land (Pirozynski and Malloch, 1975). The plant partner of the symbiosis comprises organisms with and without real roots, such as angiosperms, gymnosperms as well as pteridophytes and gametophytes of some mosses, lycopods, and Psilotales (Smith and Read, 1997). Only a few plant families (e.g. Brassicaceae, Cruciferae, Chenopodiaceae, and Proteaceae) as well as some genera (e.g. *Lupinus*) have been described as non-mycorrhizal (Requena and Breuninger, 2004). AM fungi are obligate symbionts, which means they can not complete their life cycle without establishing symbiosis with a host plant. The AM symbiosis confers a direct benefit to the growth and development of the host plants mainly through the acquisition of phosphate as well as other mineral nutrients from the soil by the fungal mycelium (George et al., 1995). In turns, the plant provides the fungus with carbohydrates from the photosynthesis (up to 20% according to Bago et al., 2000; Douds et al., 2000). Mycorrhiza formation has been shown also to enhance plant resistance to biotic and abiotic stresses (Requena et al., 1996; 1998). This can explain some phyto-protection effects observed in AM colonized versus non-colonized plants (Garcia-Garrido and Ocampo 2002). In addition, the fungal mycelium behaves as an extension of the root, and helps maintain the soil structure through the formation of soil aggregates (Bethlenfalvay et al. 1998). Soil structure recovery through mycorrhizal hyphae has also been shown to improve plant growth in degraded soils by restoring the microbial

equilibrium in the rhizosphere (Requena et al. 1997). All these impacts on the balance of the soil-plant ecosystem explain why mycorrhizal diversity determines plant biodiversity, ecosystem variability, and productivity (van der Heijden et al. 1998). Therefore, the mycorrhizal symbiosis can be considered an alternative tool for agriculture and ecosystem conservation (Barea and Jeffries 1995), as well as for the regeneration of degraded areas (Requena et al. 1996, 2001).

2.1.2 Establishment of the symbiosis

Arbuscular mycorrhizal fungi are obligate biotrophs. They are unable to complete their life cycle in asymbiosis (Bonfante and Bianciotto, 1995). The mycelium growing out of mycorrhizal roots produces new spores, which are able to germinate and establish a new mycorrhizal symbiosis. The spore is the only plant-independent phase, and is able to germinate and arrest growth several times without the involvement of plant-derived signals (Mosse 1959; Koske 1981). Independent hyphal growth extends for 2-3 weeks. In the absence of a compatible host root, the fungus stops and arrests growth, before the spore reserves are depleted (Mosse 1988). Although the ability of these spores to establish a symbiosis remains after several growth-arrest cycles (Tommerup 1984), the infectivity decreases with time (Logi et al. 1998).

Upon meeting a compatible host root, the fungus forms appressoria, which are swollen multinucleate structures forming a papilla on the rhizodermis (Bonfante et al., 2000; Giovanetti et al., 1995; Requena and Breuninger 2004). AM fungi, in contrast to other plant-colonizing fungi, do not use a great increase in turgor pressure to penetrate the cell wall, but a combination of mechanical pressure and cell-wall degrading enzymes to penetrate between two epidermal cells (Bonfante and Perotto 1995). The fungus remains in the cortical parenchyma and never crosses the endodermis (Genre and Bonfante 1997). AM fungi produce localized cortical cell wall perforations, but never penetrate the plasma membrane of the host cell. An interface compartment between the plant and fungal cell surfaces is formed at the contact area. This space is composed of the membranes of both organisms, separated by an apoplastic region creating a new compartment in which the bidirectional exchange of nutrients takes place (Bonfante and Scannerini, 1992; Smith and Smith 1990; Smith et al. 1996).

Once the fungus has overcome the epidermis, it grows into the cortex in two different modes (the Arum and Paris types), depending on the plant and fungal species (Smith and Smith 1997). In the Arum type, the fungus spreads with an intercellular growth between the cells of the root cortex. Once in the inner cortex it develops terminal arbuscules on intracellular hyphal branches. In these specialized structures nutrient exchange between the two partners is supposed to occur. The Paris type is defined by the absence of the intercellular phase and the presence of extensive intracellular hyphal coils. Arbuscules, if present, are intercalary structures on the coils, which are rare, small, or absolutely absent (Smith and Smith 1997). This fact opens the possibility that arbuscules may not be the only interface for nutrient exchange (Smith and Smith 1990). The differentiation of the arbuscule is accompanied by a parallel development of the plasma membrane, which invaginates surrounding the fungal surface and gives rise to the peri-arbuscular membrane, increasing the surface contact between the two symbionts (Alexander et al. 1989). This membrane has several characteristics indicating a new role in the symbiosis: a higher ATPase activity (Gianinazzi-Pearson et al. 1991, 2000; Murphy et al. 1997) and the induction of a fungal H^+-ATPase isoenzyme during the *in planta* phase (Requena et al. 2003), both of which might be very important in terms of nutrient transport (Bonfante and Perotto 1995).

The symbiosis is completed with the development of an extraradical mycelium which extends in the soil searching for mineral nutrients to translocate towards the plant. This mycelium is also able to colonize new roots as well as to form a new generation of spores which are the resting propagule of the fungus (Requena and Breuninger 2004). An important role in soil aggregation and erosion control has also been attributed to the extraradical mycelium (Bethlenfalvay et al. 1998).

2.2 Signaling events in the symbiosis

The importance of environmental factors controlling mycorrhizal formation, such as mineral nutrition, which can either depress or stimulate the infection, has long been acknowledged (Harley and Smith, 1983). In contrast, the genetic factors controlling the complex events of recognition, compatibility, and/or resistance have only been studied more recently. Once the spores have germinated the first mycelium extends in search for a compatible host root. No directional growth has been observed towards the root, but several experiments have shown that exudates from host roots

stimulate growth in contrast to non-host exudates (Bécard and Piché, 1989a,b; Gianinazzi-Pearson et al., 1989; Giovannetti et al., 1993a-b, 1996; Nair et al. 1991). This stimulus is hypothesized to start the fungal program necessary for a successful colonization of the root. It has been shown that *Gigaspora gigantea* changes its hyphal branching pattern from dense to scattered in response to a soluble factor derived from host roots (Nagahashi and Douds 2000). This effect was shown to be concentration-dependent and temporal. Formation of appressoria is one of the first morphological changes that point to the recognition between plant and fungus. Giovannetti et al. (1993a,b) have demonstrated that the formation of appressoria is induced by root exudates derived from compatible host plants, while root exudates from non-mycorrhizal plants, such as lupin, stimulated hyphal elongation but not the formation of true appressoria. In contrast to other plant-interacting fungi, appressoria formation is not triggered by root-like surfaces, such as nylon, polyamide, silk, cellulose, or glass threads, even when additionally stimulated with host root exudates (Giovannetti et al. 1993a,b). It has been shown that appressoria formation does not require a signal secreted from the host root or the intact host cell cytoplasm, as isolated cell walls from carrot roots were sufficient to induce appressoria differentiation (Nagahashi and Douds 1997). Nevertheless, further fungal penetration was not observed.

The range of active compounds present in root exudates is still unknown. However, a lipophilic fraction only present in host exudates has been partially purified, which is able to promote growth and branching of the asymbiotic mycelium in *Gigaspora margarita* (Buee et al. 2000). In *Gigaspora rosea* induction of several genes related to mitochondrial activity in response to this root factor was observed (Tamasloukht et al., 2003). One of these genes encodes a putative pyruvate carboxylase, which uses CO_2 as substrate. This could explain the synergistic effect of CO_2 and root exudates in promoting AM fungal growth (Bècard and Piché 1989). An increase in respiration would lead to an increase of the pool of ATP, which could explain the increased plasmalema H^+-ATPase expression and activity, responsible for the alkalinization of the cytoplasm (Requena et al., 2003). This alkalinization is important for controlling many intracellular events, as cellular differentiation, metabolism and cell cycle (Bécard et al., 2004). Germination of AM fungal spores and initial growth of hyphal germ tubes can also be stimulated by volatiles (Koske 1982). CO_2 is able to stimulate extensive hyphal growth of some AM fungi *in vitro*, and high CO_2 concentrations

increase the response to plant exudates (Bècard and Piché 1989a,b). It has been suggested that CO_2 is an essential carbon source for hyphal growth and may be involved in the catabolism of lipids in growing hypha. Supporting this hypothesis it has been shown that carbon from ^{14}C-labeled CO_2 is fixed by *Gigaspora rosea in vitro*, suggesting that an anaplerotic pathway in the fungus uses this carbon source (Bècard and Piché 1989). According to this evidence, CO_2 could be acting as both a trigger for germination and a carbon source. Inducing soluble factors are produced by all mycotrophic plants, but are absent in non-mycorrizal plants, like *Brassica* spp. Preliminary evidence suggests that the molecule that elicits branching of *Glomus mosseae* is a compound smaller than 500 Da in size (Giovannetti et al. 1996). Other possible compounds include flavonoids and phenolic compounds that stimulate the growth of some AM fungi while inhibiting others (Bècard at al. 1992; Douds at al.1996; Poulin et al. 1993; Siqueira et al. 1991; Tsai and Phillips 1991). Flavonoids may act as signaling molecules since they are active at very low concentrations, to stimulate or inhibit growth. Plant flavonoids/isoflavonoids bind to human estrogen receptors (Miksicek, 1993), and experiments using estrogens and anti-estrogens have provided evidence for the presence of an AM fungal receptor able to bind biochanin A and estrogens. Based on the structure of these compounds, it is suggested that the A and C rings of the isoflavonoid and the hydroxyl group at position A-7 are important features for recognition by the receptor (Poulin et al. 1997). Although flavonoids can influence the initial stages of development of the fungus, experiments with flavonoid-deficient mutants of maize have shown that they are not essential for the development of the symbiosis (Bècard et al. 1995), since these plants formed normal mycorrhizas.

Analogs to oligossaccharins have also been proposed as possible signaling candidates in the establishment of the symbiosis. These compounds act as signal molecules in both plant-pathogen and legume-*Rhizobium* interactions (van Brussel et al., 1992). Mycorrhizal fungi have been demonstrated to have weak cellulose and endopolygalacturonase activities (Garcia-Garrido et al., 1992a, b; 1996; Garcia-Romera et al., 1991), and both enzymes have the ability to release oligosaccharides and oligosaccharins from the plant cell wall (Fry et al., 1992). The latter could trigger the colonization and spreading of the fungus by a cascade of events that are autoregulated and controlled by the host (Salzer and Boller, 2000).

The recognition events in mycorrhizal establishment can be compared with those already studied in the *Rhizobium*-legume symbiosis. Legumes have been the model of choice because several mutants have been isolated with impaired symbiotic capabilities in their interaction with both *Rhizobium* and mycorrhiza. Pea mutants originally isolated as being unable to form root nodules (nod^-) have been shown to be resistant to colonization by mycorrhizal fungi and were therefore named myc^- (Duc et al., 1989, Gianinazzi-Pearson et al., 1991). Only aborted infections were observed in roots of these mutants, as a consequence of the formation of ill-defined appressoria by hyphae contacting the root surface. In the cell wall directly in contact with these appressoria, mutant plants produced an abnormally thick papilla where β-1,3-glucans were deposited (Gollote et al., 1993). These pea mutants have been called early mutants while another group of chemically-induced mutants, showing an impaired symbiotic phenotype at later stages of the interaction, were called late mutants (Gianinazzi-Pearson et al., 1996). Mutants do not form truly differentiated arbuscules, although the root is colonized by fungal hyphae and they appear as poorly branched structures. When inoculated with *Rhizobium*, they form non-fixing nodules (nod^+fix^-) (Gianinazzi-Pearson et al., 1996).

The study of nodulation/mycorrhization mutant plants has exposed many similarities between both symbioses, with the recent discovery of shared genes involved in the formation of both mutualistic associations (Stracke et al., 2002). These authors have demonstrated that a plant receptor-like kinase (*LjSYMRK*) is necessary for the perception of symbiotic fungi and bacteria. The mutant plants for these genes are devoid of the signal cascade leading to intracellular microbial accommodation and symbiosis establishment. These studies have corroborated earlier morphological studies and pointed out the active role of the epidermis as a checkpoint for mycorrhizal colonization (Bonfante et al., 2000; Genre and Bonfante, 2002; Novero et al., 2002; Wegel, 1998). Comparisons between the phenotypes of mutant alleles of the plant locus responsible for the perception of the symbiont signal have shown that plant responses to the fungus are cell layer dependent (Novero et al., 2002). While *LjSym15* mutants do not collaborate in the fungal penetration at the epidermal cells (Demchenko et al, 2004; Schauser et al., 1998), *LjSym4* (not characterized) and *LjSYMRK* mutants are not affected at this first step, but do not exhibit fungal intracellular penetration and accomodation in the epidermis and outer cortex (Bonfante et al., 2000; Endre et al., 2002; Novero et al., 2002; Stracke et al., 2002).

Some other genes involved in both nodulation and mycorrhization have been recently characterized in these mutants, as the *M. truncatula* ion channel *DMI1* and the calcium and calmodulin dependent kinase *DMI3* (Ane et al., 2004; Mitra et al., 2004). This is in accordance with what is already known about sequential nodulin induction by mycorrhizal colonization. In *Pisum sativum* the nodulin *PsENOD12* is transitionally induced during appressoria formation and epidermal penetration. Later *PsENOD15* is accumulated during colonization of the cortex (Albrecht et al., 1998). In contrast to *Mendicago sativa MsENOD2* and *MsENOD40*, which are both cytokinin and mycorrhiza-induced, *PsENOD12* and *PsENOD15* are not induced by cytokinin. None of these nodulins are induced when plants are elicited with fungal pathogens such as *Rhizoctonia solani* or *Fusarium oxysporum* (Scheres et al., 1990; Van Rhijn et al., 1997). This suggests their involvement in a plant cascade response specific for mutualistic interactions. In accordance, different arbuscular mycorrhizal fungi produce a diffusible factor that induces the expression of the Nod factor-inducible gene *MtENOD11*, which is not induced by pathogenic fungi, suggesting that the observed root response is specific to AM fungi and *Rhizobium* (Kosuta et al., 2003). Extensive molecular analysis of these plant mutants has been performed in order to identify down-stream gene markers of the colonization process (Martin Laurent et al., 1997; Lapopin et al., 1999; Franken and Requena 2001a, b; Roussel et al., 2001). For instance, MtENOD11, a repetitive proline-rich protein, has been shown to be transiently induced in epidermal cells in contact with appressoria (Chabaud et al., 2002). This protein could have a role in the modification of cell wall plasticity, which could be necessary for hyphal penetration.

2.2.1 The response of the plant

AM fungal signals are perceived by the plant root even before penetration or appressoria formation. Host plants which were non mycorrhizal because of their high P-status level showed an increase in the levels of the flavonoid formononetin when inoculated with *G. intraradices* (Volpin et al., 1994). Application of spore extracts and hyphal fragments has been used to study the effect of these mycorrhizal factors on the plant. Application of spore extracts of *G. intraradices* in tomato roots lead to the synthesis of new polypeptides (Simoneau et al., 1994), while their application together with hyphal fragments to alfalfa roots resulted in alteration in the accumulation pattern of several flavonoids (Larose et al, 2002; Vierheilig et al., 2004).

A similar pattern is obtained when the tissue is treated with Nod factors, resulting in reduced levels of formononetin and medicarpin and increased levels of daidzein and coumestrol. This evidence reasserts once again the functional similarity between signals from the AM fungi and rhizobial Nod factors. The biological significance of these changes, however, remains unclear.

Once the root is colonized by AM fungi, the plant regulates the extent of penetration and colonization by the fungus. Depending on P availability, the AM fungal status of the host plant can vary. In plants with a high P status root colonization is reduced or absent, whereas low P levels enhance root colonization (Vierheilig et al., 2004). The biological activity of root exudates from high-P and low-P plants also differs, showing the same tendency (Vierheilig et al., 2004 and references therein). Accordingly, the accumulation pattern of flavonoids in plants seems to depend on their P status. Alfalfa high-P plants inoculated with *G. intraradices*, accumulated medicarpin at high levels in the absence of fungal structures within the root. This compound exerts an inhibitory effect on spore germination and hyphal growth (Guenoune et al., 2001) and is present at low levels in roots with a low P status. Akiyama et al. (2002) described that another flavonoid, isovitexin 2”-*O*-β-glucoside, was detected in roots of P-deficient melon plants, but not in melons with a high P status. Application of this flavonoid to melon plants inoculated with AM fungi enhanced root colonization.

In plant-pathogen interactions, plants respond to the fungal attack by several mechanisms, altogether known as the plant defense response. Biochemical and physiological responses of the plant to limit the progress of the fungal invasion include production of antifungal metabolites, deposition of lignin, and the production of low-Mr antimicrobial phytoalexins. Although there are indications for elicitor involvement in the early stages of the establishment of the mycorrhizal symbiosis, the elicited defense response is generally less vigorous than that observed during plant-pathogen interactions (Salzer et al., 2000) and is often completely suppressed (David et al., 1998). Expression of defense genes is often localized to arbuscule-containing parenchyma cells, and the elicitation of the defense reaction in other root cells is not overcome (Gianinazzi-Pearson, 1996). Whether the plant recognizes the mycorrhizal fungus as a mutualistic organism or whether the fungus suppresses plant defense responses remains an open question.

The fungus fails to elicit a strong defense, which is often transient and uncoordinatedly expressed. In non-host plant species fungal attempts to penetrate

the root produce a hypersensitive response (Allen et al., 1989). Acordingly, *myc*-mutants respond to penetration attempts with a stronger defense reaction than wild type plants, which includes callose deposition, accumulation of PR1 protein (pathogenesis related protein 1) and phenolic compounds (Gollote et al., 1993), together with an increase in defense transcripts (Ruiz-Lozano et al., 1999). In roots of the AM non-host family *Brassicaceae* the activities of two hydrolases, β-1,3-glucanase and chitinase, and glucosinolate levels were altered when plants were inoculated with AM fungi (Vierheilig et al., 1994; 2000). Giovanetti and Sbrana (1998) in their review about the behavior of AM fungi when coming across a non-compatible host, present evidence of aberrant fungal structures, in dead cells. Both appressoria and arbuscules were absent, suggesting a lack of any recognition event leading to the establishment of a functional symbiosis, but rather a parasitic type of colonization. These facts together suggest that plants susceptible to form mycorrhiza are able to suppress a full expression of the defense response upon recognition of the AM-fungus.

In the mature AM association, when arbuscules start to collapse, fungal cells wall components are released, which could elicit the plant defense response. Accumulation of phenolic compounds in plant cells in response to microorganism attack induces auto-fluorescence (Jahnen and Hahlbrock 1988). This might explain the autofluorescence observed in cells containing collapsing arbuscules. Evidence of the different perception of viable arbuscules compared with collapsed arbuscules by the plant is supported by several observations: (1) H_2O_2 accumulation in *M. truncatula* root cells containing collapsed arbuscules from *G. intraradices*, but never in cells containing active arbuscules (Salzer et al., 1999); (2) In mycorrhizal soybean the phytoalexin glyceollin was not accumulated during early stages of colonization, but increased in the mature association (Morandi et al., 1984; Wyss et al., 1991); (3) At the late stage of the symbiosis, high levels of flavonoids, such as the phytoalexin, medicarpin, could be detected (Larose et al., 2002); (4) In mycorrhizal plants Jasmonic Acid (JA) levels are increased in the later stages of the interaction, rather than during the recognition and establishment of the symbiosis (Hause et al., 2002). Thus, allene oxide synthase, a gene encoding an enzyme involved in the synthesis of JA, was localized by in situ hybridization in arbuscule-containing cells. JA accumulation coincided with the collapsing of arbuscules. We also have to take into account that the AM symbiosis implies a high energetic cost to the plant. Estimated

costs of the mycobiont in a mycorrhizal plant are 4 to 20% (Bago et al., 2000; Douds et al., 2000). The sink strength increases according to the degree of colonization (Lerat et al., 2003). Several evidences point to an autoregulation of the degree of colonization by the host plant, as was already described for the degree of nodulation by rhizobial bacteria in legumes (Gadkar et al., 2003; Vierheilig, 2004). The regulation of both symbioses seems to be similar, as nodulated roots and roots treated with Nod factors in alfalfa split-root systems also systemically suppress AM colonization and vice-versa (Catford et al., 2003). Hypernodulation mutants of pea and *Lotus japonicus* affected in the orthologs of *Gm*NARK (a leucine-rich repeat receptor-like kinase implicated in long-range shoot-to-root signaling) show also a hypermycorrhization phenotype (Morandi et al., 2000; Solaiman et al., 2000). Accordingly, root exudates from mycorrhizal plants do not stimulate hyphal growth and have an inhibitory effect on root colonization (Pinior et al., 1999). Mycorrhizal root exudates contain a different composition compared to non-mycorrhizal root exudates (Franken and Gnädinger 1994), such as a higher content in phenolics (McArthur and Knowles 1992). These mechanisms of regulation of the extent of mycorrhization resemble plant strategies to control pathogenic invasion.

2.3 The *Glomus mosseae GIN1* gene (*GmGIN1*)

To identify genes that are exclusively expressed during the pre-symbiotic or during early developmental stages of the AM symbiosis, a subtractive cDNA library was constructed using suppressive subtractive hybridization (Requena et al., 2002). The library cDNAs are enriched in *G. mosseae* genes up-regulated during the early development versus genes expressed in the extraradical mycelium. Among these genes a novel gene, *GmGIN1* (coding for GTPase Intein), was identified. The full-length *GmGIN1* cDNA encodes a protein of 428 amino acids with a calculated molecular mass of 48 kDa. The protein has a two-domain structure with a putative self-splicing site in the junction of the two domains. The first 209 amino acids (aa) match to the GTP CDC motif (PF 00735) characteristic for proteins involved in cell division, with an ATP/GTP-binding site motif A (P-loop) (PS00017) found between amino acids 11-18. A Hint module (PF01079) characteristic of hedgehog proteins and inteins (both families of proteins undergo self-splicing as post-translational modification) was located between residues 227 and 426 (Fig. 1).

Using the programme BlastP in the NCBI database the full-length protein was analyzed, revealing that the amino (N-) and carboxy (C-) terminus had two different significant homologies (Fig. 1 and 3). The N-terminal domain of GmGIN1 showed homology (46%) to several GTPase proteins, in particular to a novel family of GTP-binding proteins (the IAN-family, Immune Associated Nucleotide), conserved between the plant and animal kingdoms. The C-terminus of the protein presents high homology (50%) to the C-terminal domain of the Hedgehog family of proteins from vertebrates. This conserved domain, essential for the processing of the Hedgehog protein, is not found outside the metazoa. When this gene was published, no significant homology to any fungal protein could be found when the C-terminal domain of GmGIN1 was blasted against fungal databases. However, very recently several genes with homology to the N-terminus of GmGIN1 have been published in the NCBI database from a number of pathogenic fungi, such as *Magnaporthe grisea, Neurospora crassa, Gibberella zea* and *Aspergillus nidulans.*

The self-splicing reaction of hedgehog proteins begins with a first nucleophilic attack from the free electrons of the sulfur atom of the cysteine from the conserved tripeptide GCF. This reaction produces a thio-ester intermediate, which is resolved by a second nucleophilic attack triggered by a cholesterol molecule (Porter et al., 1996 a, b and Fig. 4). The result is the splitting of the protein into two peptides, releasing the N-terminus of the protein covalently modified by a cholesterol moiety and the carboxy terminus (starting at the cysteine). Several conserved amino acids essential for the autoproteolytic activity of hedgehog proteins were also found in the C-terminal domain of GmGIN1. Thus, the conserved cystein residue (Cys-238) within the conserved tripeptide GlyCysPhe (Fig. 1, in red and squared), is localized in the junction of the N-terminus and C-terminus domains. Similarly, Thr-310 and His-313 are also conserved in GmGIN1, shown to be indispensable for the self-splicing ability of hedgehog proteins. An aspartic residue involved in the binding of cholesterol was also found to be conserved in GmGIN1 (Asp-285).

In the following section I will introduce the protein family with highest homology to the N-terminal domain of the GmGIN1 protein. This is a family of GTPase proteins, which include the *Arabidopsis thaliana* (AIG1) and animal proteins (IAN). Recently, both groups of homologs have been included in a family of proteins called GIMAP, for GTPase of the Immunity Associated Protein Family (Krücken 2004).

Figure 1. GmGIN1 gene and two domain protein. Highlighted in blue is the IAN/GIMAP or GTPase of the Immune Associated Protein Family domain; in red the conserved GTP binding motif. Highlighted in green is the Hint (Hedgehog Intein) domain; in red and squared are the conserved amino acids that take part in the auto-splicing and cholesterol binding (Requena et al. 2002).

2.4 The GmGIN1-N terminus orthologues: GTPase proteins

2.4.1 GTPases: conserved structure for a variety of functions

GTPases are proteins that bind and hydrolyze GTP (Bourne et al., 1990). GTPases act as molecular switches whose “on” and “off” states are regulated by binding and hydrolysis of GTP. Their conserved structure and mechanism in many versions of the switch suggest that all derive from a single primordial protein, repeatedly modified in the course of evolution to perform an amazing variety of functions. These include the direction of ribosomal protein synthesis, the mediation of transmembrane signaling by hormones and light, the translocation of nascent proteins into the endoplasmic

reticulum, the control of differentiation and cell proliferation, and the guidance of vesicular traffic within cells (Bourne et al., 1990).

The GTPase cycle includes three conformational states of the protein. Release of the bound GDP converts the “inactive” state of the protein into a transient “empty” state. Under normal conditions in the cytoplasm, GTP it is more likely than GDP to enter the empty nucleotide binding site and upon binding GTP the protein takes on an “active” conformation, which reverts to the GDP-inactive state when GTP is hydrolyzed. The rate constants of GDP release and GTP hydrolysis are quite low in many (but not all) GTPases. These are increased by two types of regulatory proteins; the guanine nucleotide exchange factors (GEFs), which catalyze the release of GDP, promoting its displacement by GTP, and the GTPase-Activating proteins (GAPs), which activate GTP hydrolysis. It can also be reduced by means of guanine nucleotide dissociation inhibitors (GDIs), which inhibit the release of GDP from certain GTPase proteins.

Heterotrimeric GTPases (Gα, β, γ), usually called G proteins, mediate a vast array of signaling processes in all eukaryotes, including mating response, development and pathogenicity in fungi, vision in mammals and metazoans, and neurotransmitter and hormone action in mammals (Bölker, 1998; Borkovich, 1996; Neer, 1995). These regulatory complexes serve as a bridge between transmembrane receptors and intracellular effectors, including adenylate cyclase, phospholipases or protein kinases (Bölker, 1998; Lorenz and Heitman, 1997). Other Gα subunits have been shown to be involved in the regulation of potassium channels and cyclic GMP phosphodiesterase. These proteins consist of three different subunits α, β and γ, with Gα being the nucleotide binding component. Binding of the specific ligand to the receptor induces a structural change that is transduced to the heterotrimeric G protein, which contacts the receptor at the inner membrane. This leads to a decreased affinity of the Gα subunit for GDP, which is then replaced by GTP. The conformation of this subunit changes promoting the dissociation of the $\beta\gamma$ heterodimer. In this activated state the Gα subunit is diffusible in the cytoplasm and can interact with intracellular effectors. Owing to its intrinsic GTPase activity, the activated state persists only for a limited period of time, which prevents from continuous signaling. In different systems, it is either the Gα subunit or the G$\beta\gamma$ heterodimer that transmits the signal (Hamm and Gilchrist, 1996). The Gα subunit in *S. cerevisiae*, Gpa1, regulates mating response by binding to pheromone receptors, being the free $\beta\gamma$ subunit the signal transmitter, while in *S. pombe* the active role is

played by the Gα subunit (Obara et al., 1991). Gpa2 responds to nitrogen starvation in both organisms (Isshiki et al., 1992; Lorenz and Heitman, 1997). Four G proteins have been isolated from the pathogenic fungus *Ustilago maydis*, from which Gpa3 was shown to be indispensable for the pheromone stimulation of mating and pathogenic development (Regenfelder et al., 1997). Several other pathogenic fungi have G proteins implicated in their virulence mechanisms. Thus, disruption of *Magnaporte grisea* magB, a $G\alpha_i$ subunit, affects vegetative growth, conidiation and appressorium formation (Fang and Dean, 2000; Liu and Dean, 1997).

The small GTP-binding proteins of the Ras superfamily have been subdivided in several protein families: Ras, Rho, Arf/Sar, Rab and Ran (Takai et al., 2001). Ras proteins are monomeric, membrane localized and function as molecular switches linking receptor and non-receptor tyrosine kinase activation to downstream cytoplasmic or nuclear events controlling differentiation or proliferation of cells. Oncogenic mutations in these proteins result in constitutive signaling, stimulation of cell proliferation and inhibition of apoptosis (Adjei, 2001). Ras proteins directly bind to and activate Raf protein kinase, which then induces gene expression through the mitogen-activated protein (MAP) kinase cascade in response to various extracellular signaling molecules (Takai, 2001). Ras proteins are targeted to the plasma membrane by lipidic modifications. H- and K-Ras (Harvey and Kirsten murine sarcoma viruses) are both farnesylated, but H-Ras also contains two palmitoyl groups, whereas K-Ras complete the membrane anchor by means of a polybasic domain of six contiguous lysines. Although these proteins a very similar and interact *in vitro* with the same effectors, they generate distinct signaling events *in vivo* and are associated with specific tumor types (Parton and Hancock, 2004). Several pieces of evidence point to the hypothesis that these proteins could be directed to different plasma membrane microdomains, where they would meet different interaction partners. Thus, H-Ras seems to be directed to raft domains enriched in sphingolipids and cholesterol, while K-Ras is not (Mukherjee and Maxfield, 2004).

Members of the Rho family are involved in regulation of a large variety of cell functions. Thus, they have been involved in cell growth, morphogenesis, cell mobility, cytokinesis, trafficking and organization of cell cytoskeleton, but also in transformation and metastasis in cancer (Jaffe and Hall, 2002). Members of this family include the Rho, Rac and Cdc42 subfamilies. In resting cells Rho proteins exist mostly in GDP-bound state, constituting complexes with GDIs in the cytosol (Hoffman

et al., 2000). The GTP-bound state of the protein is associated with cell membranes. In fungi, this family of proteins plays an essential role in cell polarization and cell separation in budding yeast (Ziman et al., 1991; Cabib et al., 1998; Dohlman and Thorner, 2001) and in the phytopathogenic fungus *Ustilago maydis* (Weinzierl et al., 2002). Cdc42 and Rac small GTPases have been described in the ectomycorrhizal fungus *Suillus bovinus*. SbCdc42 has been related to polarized growth, septal formation and the morphological change in mycorrhizal hyphae (Gorfer et al., 2001). Recently, new members of the Rho family of GTPases have been described which display distinct properties, for instance constitutive membrane association, lack of GTPase activity and /or resistance to the effects of GAPs (Sorokina and Chernoff, 2005). Two novel members (Miro-1 and 2, for Mitochondrial Rho) display a unique domain organization and seem to be important for the integrity of the mitochondrial function (Franson et al., 2003). Members of the Rho family only present in plants, called Rop (for Rho-related proteins from Plants), have been identified (Vernoud et al., 2003). Besides the classical roles mentioned above, in plants they are also involved in signal transduction pathways mediated by plant hormones such as abscisic acid (ABA), brassinolide or auxin.

Another group of small GTPases is the Small ADP Ribosylation Factor (Arf) family of proteins. These GTPases are regulators of vesicle biogenesis in intracellular trafficking. Pasqualato et al. (2002) include in this family the Sar (Secretion-associated and Ras-related) proteins. This family of proteins is characterized by an additional control element for nucleotide exchange, the “interswitch toggle”, which establishes a front-back communication between the nucleotide-binding site and an amphipathic membrane-facing N-terminus (Amor et al., 1994; Antonny et al., 1997; Beraud-Dufour et al., 1999). Upon interaction with membranes, this N-terminal part ceases its negative control, and binding to GTP is possible. Thus, the activation of Arf proteins is coupled to its recruitment to membranes (Antonny et al., 1997; Goldberg et al., 1998). Myristoylation of Arf proteins plays an important role in the control of nucleotide exchange (Franco et al., 1993, 1995, 1996), although not all proteins of this family contain myristoylation sequences. Thus, Sar1 may interact directly with phospholipids through the N-terminal peptide region (Pasqualato et al., 2002).

Rab proteins (Ras-related in Brain) are also regulators in membrane traffic pathways, regulating vesicle formation, budding, actin- and tubulin-dependent motility and fusion (Stenmark and Olkkonen, 2001). These proteins are also targeted to

membranes in a reversible manner by a lipophilic modification, consisting of one or two geranylgeranyl groups (Pereira-Leal et al., 2001).

Ran (Ras-related Nuclear protein) proteins play key roles in controlling nuclear processes throughout the cell mitotic cycle. This family of proteins regulates nucleocytoplasmic transport during the G_1, S and G_2 phases of the cell cycle and microtubule organization during the M phase. These small GTPases are not lipid-modified and do not associate with cellular membranes. In contrast, the protein changes its location between the GDP-bound cytoplasm form and the GTP-bound form localized in the nucleus (Clarke and Zhang, 2001).

The resolution of the crystal structure of several GTPases, such as $p21^{ras}$, represented a landmark in understanding the catalytic mechanism of GTPases (de Vos et al., 1988; Pai et al., 1989, 1990; Milburn et al., 1990; Morikawa et al., 1978; Jurnak et al., 1980, 1985). The five polypeptide loops that form the guanine nucleotide-binding site are the most conserved elements in this domain and define the GTPase protein superfamily (Sprang, 1997). They are designated G1 to G5. The diphosphate-binding loop (P-loop or G1-box) with the consensus sequence GXXXXGK(S/T), contacts the α- and β-phosphates of the guanine nucleotide. The primary structure of the G1 loop places it within a larger family of phosphate-binding sequences found in other nucleotide-binding proteins. For instance, it is found in ATP binding proteins, such as adenylate kinases and ATP synthase ß-subunits and myosin heavy chains, kinases (AMP kinase, actin, RecA), adenyltransferases, and the more devergent in the cassette sequence thymidine kinases and phosphoglycerate kinases (Saraste et al., 1990; Traut, 1994). A DXXG consensus sequence located at the N-terminus of the α2-helix, called G3, links the subunits for binding of Mg^{2+} and the γ-phosphate of the GTP. Mg^{2+} is a key cofactor in the GTP binding and nucleotide exchange (Franco et al., 1993, 1995, 1996). The G1 and G3 sequences correspond, respectively, to the WalkerA and WalkerB boxes found in many nucleotide binding proteins, many of which are not GTPases (Traut, 1994). The guanine ring is recognized, in part, by the conserved NKXD sequence (G4). The connection (G2) between the α1 helix and the β2 strand contains a conserved threonine residue involved in Mg^{2+} coordination. The G5 box, with consensus sequence (T/G)(C/S)A, reinforces the guanine base recognition site. Some other sequences have been described as candidates for a G5-like motif, such as

OOM(A/R/P)(G/T)SAL in *E. coli* EF-Tu (O represents an hydrophobic amino acid), or T(C/Q)A(T/V)DT in the α-chain of G_S (Bourne et al., 1991).

2.4.2 Lipid modification and targeting of proteins, particularly GTPases

Membrane localization and function of many proteins are dependent on their covalent modification by specific lipids. Lipid-modified proteins can be classified according to their lipid moiety (Casey, 1995). For example, palmitoylated proteins contain a 16-carbon saturated fatty acyl group attached by a labile thioesther bond to cysteine residues. The acylation is post-translational and reversible, a unique property of this modification that gives cells the potential to control the modification state of the protein, its localization, and activity (Dunphy and Linder, 1998; Linder and Deschenes, 2004). Enzymes that catalyze both attachment and removal of the palmitate have been identified (Duncan and Gilman, 1998; Fujiyama and Tamanoi, 1986; Lobo et al, 2002). For instance, palmitoylation is involved in directing N-Ras and the G_α subunit and the $G_{\beta\gamma}$ complex of trimeric G proteins to the membrane (Hirschman and Jennes, 1999; Magee et al., 1987; Milligan et al., 1995; Wedegaertner et al., 1995). Palmitate has enough affinity to anchor proteins to membranes (Peitzsch and McLaughlin, 1993). Nevertheless, this association is rapidly reversible and for stable association a second lipid modification or other interactions with the membrane are necessary (Baumann and Menon, 2002; Resh, 1999).

Myristoylated proteins contain a saturated acyl group of 14 carbons added in a process involving co-translational modification of the amino-terminal glycine residue through amide bond formation. The result is a very stable modification, although there is at least one report of lipid removal from the mature protein (Manenti et al., 1994). Trimeric G proteins are associated with the inner face of the plasma membrane. Myristoylation greatly increases the affinity of the α_i family of subunits for $\beta\gamma$ and is required for its inhibition of adenylyl cyclase (Taussig et al., 1993). Myristate provides barely enough affinity energy to anchor proteins to membranes. Other additional factors, such as positive charges and protein-protein interactions are necessary to efficiently anchor myristoylated proteins to the membrane (Antonny et al., 1997; McLaughlin and Aderem, 1995). Accordingly, several α subunits contain both myristate and palmitate (Casey, 1995; Wedegaertner et al., 1995). As already

mentioned, myristoylation regulates Arf small GTPases activity and localization (Franco et al., 1993, 1995, 1996; Kahn et al., 1993).

Prenylated proteins contain one or two isoprenoid lipids, either the 15-carbon farnesyl or the 20-carbon geranylgeranyl. The lipids are attached to cysteine groups at or near their carboxy-terminus through stable thioesther bonds in a post-translational process (Sinensky, 2000; Zhang and Casey, 1996). This reaction is catalyzed by three different enzymes, farnesyltransferase (FT) and geranylgeranyltransferase I and II (GGT1 and GGT2) (Maurer-Stroh et al., 2003). As with myristoylated proteins, this process results in a stably modified protein. Proteins containing a cysteine residue fourth from the carboxy-end (the Cys-A-A-X motif) can be modified by either farnesyl or geranylgeranyl, by FT or GGT1, depending on the identity of the X amino acid. Thus, Ras proteins are typically farnesylated (Sinensky, 2000; Zhang and Casey, 1996). Following prenylation, most Cys-A-A-X-type proteins are directed to the ER-membrane compartment for further processing involving removal of the three carboxy-terminal residues and methylation of the carboxylic group of the prenylcysteine (Baumann and Menon, 2002; Pei and Grishin, 2001; Trueblood et al., 2000). A second mechanism for prenylation exists in small GTPases of the Rab family. These proteins are geranylgeranylated at two cystein residues (CC or CXC motif) at or very near the carboxy terminus by GGT2 (Seabra et al., 1992). Another protein, Rab Escort Protein (REP) is necessary to constitute a complex with Rab. This complex is recognized by GGT2 for Rab prenylation (Alexandrov et al., 1994, 1999; Benito-Moreno et al, 1994).

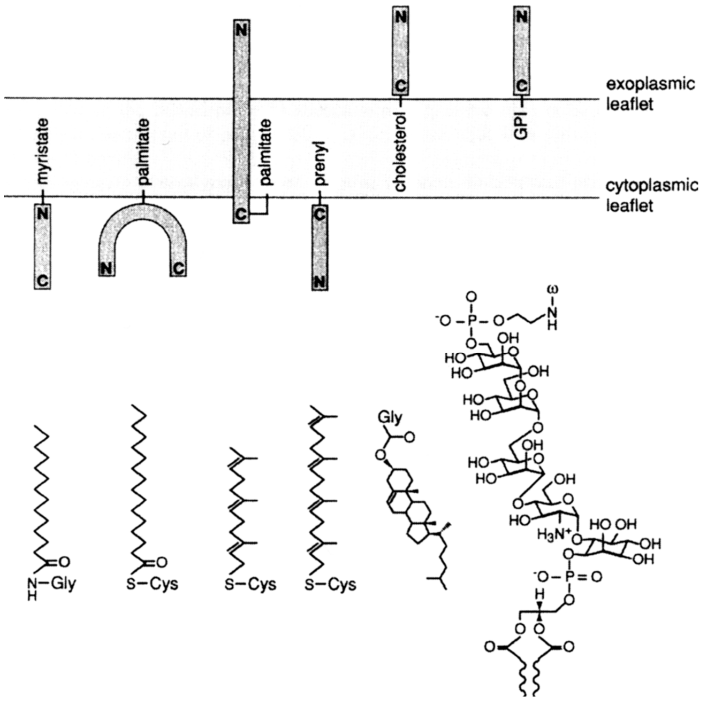

Figure 2. Lipid modifications of proteins: distribution in the cell membrane and lipid structures. From left to right: N-myristoyl glycine, palmitate thioether-linked to cysteine, cholesterol ester-linked to glycine and a GPI anchor linked to the ω amino acid of a GPI-anchored protein (Baumann and Menon, 2002).

Proteins can also contain a complex glycosylphosphatidylinositol (GPI) moiety. The GPI-linked proteins are destined for the cell surface, and function in diverse processes, such as nutrient uptake, cell adhesion, catalysis, and membrane signaling events (Baumann and Menon, 2002; Casey, 1995). GPI-proteins have been localized in membrane domains which are enriched in sphingolipids and cholesterol, and constitute liquid ordered domains called rafts (Brown and Rose, 1992; Jackobson et al., 1995; Friedrichson and Kurzchalia, 1998; Simons and Ikonen, 1997; Varma and Mayor, 1998). In many cells, the detergent-insoluble complex that contains GPI-anchored proteins is also enriched in the protein caveolin (Anderson, 1994; Schroeder et al., 1994). Caveolin is a transmembrane protein which serves as a marker for a type of cell membrane invagination termed caveolae (Rothberg et al., 1992; Sargiacomo et al., 1995; Scherer et al., 1997). A number of signaling molecules, such as trimeric G proteins, G-Protein Coupled Receptors (GPCRs), and small GTPases have been localized in these membrane detergent-insoluble fractions, which could represent specialized signaling compartments at the cell surface (Lisanti, 1994; Mukherjee and Maxfield, 2004; Okamoto et al., 1998; Smart et al., 1999). Accordingly, lipid-depending targeting of trimeric G proteins into rafts has also been demonstrated in the last few years (Moffet et. al., 2000). Both caveolae

and rafts are resistant to Triton X-100 at 4°C, while cell membrane fractions that have a conventional disordered phase are fully solubilized by non-ionic detergents (Rietveld and Simons, 1998). Raft domains are also described in higher plants. Cholesterol derivatives present in plant membranes have been proposed to play the structural role of cholesterol in animal rafts (Peskan et al., 2000; Mongrand et al., 2004). Raft domains have also identified in yeast, in which the Gγ subunit of trimeric G-proteins was localized (Kübler et al., 1996; Moffet et al., 2000). In many fungi, ergosterol is the sterol implicated in raft formation (Bagnat et al., 2000).

2.4.3 GIMAP family of GTP binding proteins

The N-terminus of GmGIN1 shares homology to a family of GTPases called GIMAP (GTPases of the Immunity Associated Protein family), with several members described in higher plants, such as *Arabidopsis thaliana* AIG1. The transcript encoding AtAIG1 protein has been shown to be induced upon *P. syringae* attack of *Arabidopsis* plants (Reuber and Ausubel, 1996). Plants can identify and respond to pathogen attack with a specific reaction, lead by a gene-for-gene recognition event (Flor 1971). In case of interaction between a pathogen that carries an avirulance gene (*avr*) for which the plant carries the corresponding resistance gene, the plant activates a number of inducible responses. Thus, it may react by inducing an oxidative burst, reinforcement of the cell wall by lignification, production of antimicrobial compounds, and programmed cell death, known as the hypersensitive response (HR), in the region of the infection (Lehman, 2002; Nimchuk et al., 2003). When the infecting pathogen is devoid of *avr* genes, the host does not produce an HR and induction of other defense responses is much slower. It is known that different *avr* gene-resistance pairs activate similar defense responses. According to this it is assumed that downstream components of the signal transduction pathway are common to different *avr* gene-resistance pairs (Dangl and Jones, 2001). Using *Arabidopsis* mutants that no longer exert an HR in response to several avirulance factors, the corresponding resistance genes have been isolated (Bent et al., 1994; Debener et al., 1991; Grant et al., 1995; Innes et al., 1993; Kunkel et al., 1993; Mindrinos et al., 1994; Yu et al., 1993). *Pseudomonas syringae* carrying *avrRpt2* and *avrRpm1* avirulance factors was used to infect wild-type and mutant plants without the corresponding resistance genes (*rp2* and *rpm1*), in order to isolate defense-

related genes that are specifically induced as a result of the interaction in the plant. In this screening *AIG1* and *AIG2* (for avrRpt2-induced gene) genes were isolated (Reuber and Ausubel, 1996). These genes exhibit *RPS2* and *avrRpt2*-dependent induction early after infection with *Pseudomonas syringae* carrying *avrRpt2*. However, it is unclear which roles *AIG1* and *AIG2* play in plant defense. Recently, two other plant homologs to AIG1 have been described, *Nicotiana tabacum* NTPG4 and *Oriza sativa* NTPG4.

The N-terminus of GmGIN1 also has homology to the animal protein members of the GIMAP family of GTPases. This family was established after comparison of the animal (IAN) proteins with AIG. In 1999, Poirier et al., described the first animal homolog to plant AIG proteins. The novel gene was called *mIAN-1* (murine Immune-associated nucleotide-1). A new family of putative GTP-binding proteins and the first example of a plant pathogen response gene conserved in animals was defined with this gene. During development, thymocytes are subjected to an extensive selection to only produce functional cells able to establish the immune response against pathogens.

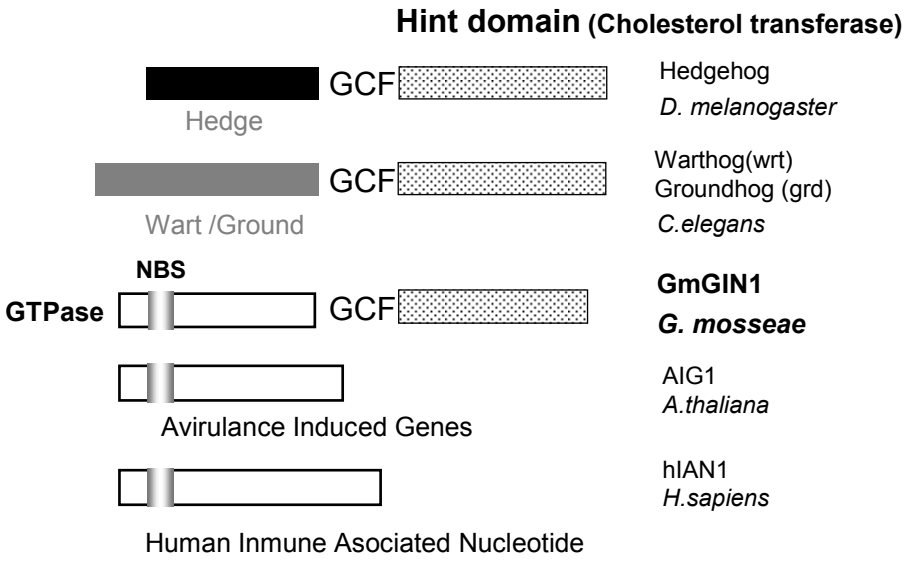

Figure 3. Diagram of the two domain-structure of GmGIN1 and the N- and C-terminus closest homologs. C-terminus homologs containing the Hint module (dotted box), N-terminus homologs in white box, with the Nucleotide Binding Site in grey.

The expression of *mIAN-1* is induced in one of the steps in this process. Moreover, it is predominantly expressed in the lymphoid system, suggesting that it participates in

specific immune responses. As the selection events involve both cell survival and maturation versus induced cell death, the function of mIan-1 is still unclear. mIan4, mIan2 and rat Ian4l1 are also related to processes involving the immune system (Andersen et al., 2004; Krucken et al., 1997, 1999; Hornum et al., 2002; MacMurray et al., 2002). Nevertheless, the function of IAN proteins seems not to be restricted only to the immune system. The high number of genes coding for mammalian IAN proteins, and the expression in organs not associated with the immune system suggest functional diversity (Krücken et al., 2004; MacMurray et al., 2002). This may be reflected by their distinct subcellular localization. mIan4 is mitochondrial (Dáheron et al., 2001; Hornum et al., 2002), and hImap1/hIan2 is associated with the endoplasmic reticulum (ER) (Stamm et al., 2002). In humans, Irod/Ian5 (Inhibitor of Radiation and OA-induced Death) was demonstrated to protect specifically against apoptosis induced by okadaic acid and γ-radiation. Strikingly, this function is not affected by deletion of the GTP-binding domain (Sandal et al., 2003). The widespread expression as its ability to counteract apoptosis in non-immune cells suggests that the function of Irod is not only restricted to the immune system.

Most of the GIMAP proteins contain in their amino acid sequence the five consensus motifs (G1 to G5) that characterize GTPase proteins. These proteins share a high homology at this GTP binding domain, constituting a novel protein family. This amino terminal region constitutes the so-called AIG1 domain (Pfam 04548), while the carboxy-terminal region is more variable (Cambot et al., 2002; Krücken et al., 2004; Poirier et al., 1999; Stamm et al., 2002). Nevertheless, several amino acids in the G3 cassette are changed respecting other GTPases and hImap1 does not contain a clear G5 motif (see discussion) (Cambot et al., 2002). Several members of the family contain putative coiled-coil domains, suggesting the establishment of protein-protein interactions, or transmembrane regions (Cambot et al., 2002; Krücken et al., 2004; McMurray et al., 2002; Poirier et al., 1999; Sandal et al., 2003). Several IAN proteins have been demonstrated to bind selectively to GTP (Cambot et al., 2002; Daheron et al., 2001; Stamm et al., 2002), but only hIAN1 has been demonstrated to exert GTPase activity (Cambot et al., 2002).

2.5 The GmGIN1 C-terminus orthologues: Hedgehog (Hh) proteins

2.5.1 Protein splicing: Inteins and Hedgehog proteins

The C-terminus of GmGIN1 shares similarity with the carboxy terminus of animal Hedgehog (Hh) proteins. Hh proteins are able to undergo auto-splicing mediated by their C-terminus in order to release the active form of the protein, the N-terminus (Lee et al., 1994; Porter et al., 1996a, b). Hh proteins are mechanistically similarly processed as inteins or self-splicing proteins (Paulus, 2000; Pietrovski, 1994, 1998). Protein splicing is a form of posttranslational processing that consists of the excision of an internal polypeptide sequence in the protein, the intein, followed by the concomitant union of the flanking polypeptide sequences, the exteins, by a peptide bond (Fig. 4, Paulus, 2000). The mechanism resembles the intron splicing of the mRNA (Perler et al., 2002). Although intron-splicing is a well known mechanism, little was known about protein splicing until 15 years ago (Hirata et al., 1990; Kane et al., 1990). This post-translational mechanism is shared among the three domains of life, archaea, bacteria, and eukarya, suggesting an ancient evolutionary origin (Pietrovski, 2001). The reaction requires neither cofactors nor auxiliary enzymes and involves four intramolecular reactions (Perler et al., 2002). Some of the reactions characteristic of splicing also occur in other forms of protein autoprocessing, ranging from peptide bond cleavage to attachment of nonprotein moieties, as it is the case of hedgehog proteins. The amino acid residues at the intein-extein borders, the so-called splice junctions, are conserved. The N-terminal splicing junction in inteins has sequence similarity to the splicing junction in hedgehog proteins, constituting the so-called Hint (Hedgehog-Intein) domain (Hall et al., 1997; Pietrovski, 1994, 1998).The C-terminal residue is always an amino acid with a thiol or hydroxyl side chain (cysteine, serine or threonine), suggesting that protein splicing may involve ester intermediates produced by N-S or N-O acyl rearrangements (Wallace, 1993).

Intein splicing proteins have only been found in unicellular organisms, where their distribution has all the hallmarks of parasitic genetic elements (Derbyshire and Belfort, 1998; Pietrovski, 2001). In contrast, the closely related Hedgehog proteins have only been found in animals, where they play a critical regulatory function in early development (Lee et al., 1992; Ingham and McMahon, 2001). Recently, new Hint-like domains have been identified in bacteria, including plant and human pathogenic species (Amitai et al., 2003). An indication of evolutionary relationship

between the splicing mechanisms of the mRNA and proteins is the fact that many introns and inteins represent mobile genetic elements at the DNA level, by means of endonucleases encoded within them (Derbyshire and Belfort, 1998). This allows lateral transfer between genes and even organisms. Nevertheless, this kind of elements is absent in the Hedgehog protein family (Perler, 2002).

Hedgehog proteins (Hh) play key roles during embryonic patterning of multicellular animals, from insects to humans, and the self-splicing of the protein is essential to accomplish this function (Lee et al., 1992, 1994; Echelard et al., 1993; Porter et al., 1995). A well studied example of Hh protein is the *Drosophila melanogaster*. The precursor protein (45 kDa) undergoes self-catalyzed splicing, involving the above mentioned peptide cleavage to yield a 25 kDa C-terminal fragment (Hh-C, the autoprocessing domain) and a 20 kDa protein (Hh-N, the signalling domain) with its carboxy end covalently modified by a cholesterol moiety (Lee et al., 1994; Porter et al., 1996a, b). This lipid modification results in an increased lipophilic character of the Hh-N domain, allowing the protein to interact with specific receptors on the surface of adjacent cells after being secreted (Chen and Struhl, 1996; Burke et al., 1999; Fuse et al., 1999; Marigo et al, 1996; Stone et al, 1996).

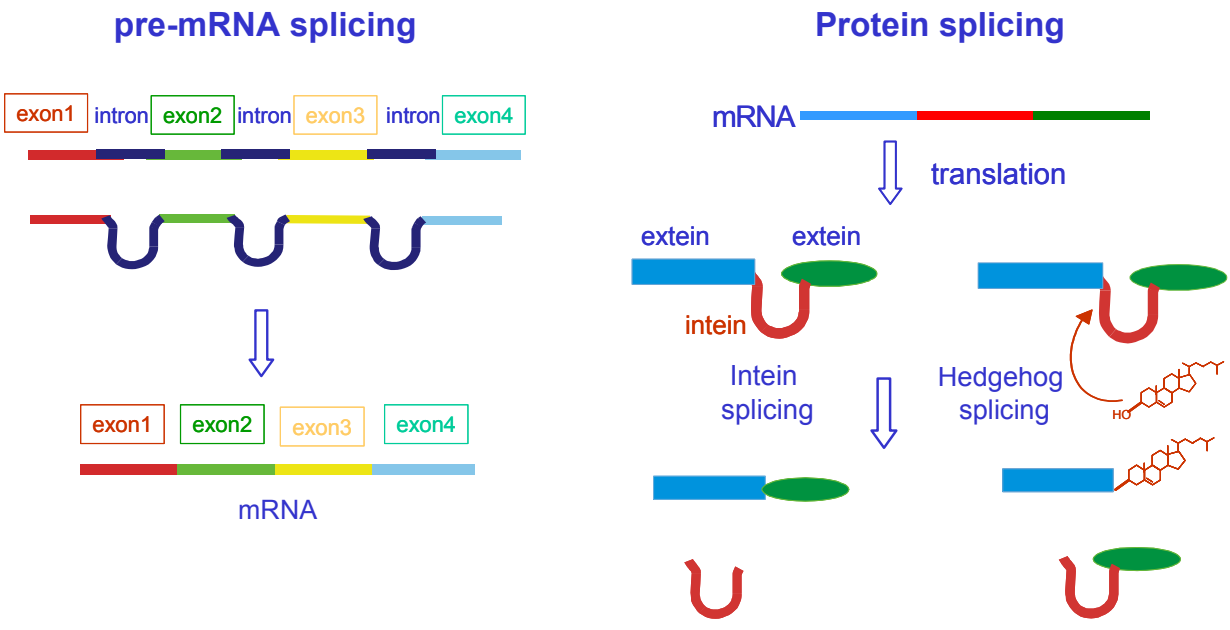

Figure 4. Comparison between intron-RNA splicing and protein splicing. In protein splicing are included intein splicing and Hedgehog proteins splicing.

The autocleavage of hedgehog proteins occurs adjacent to a cysteine residue (Cys-258), within the conserved dipeptide Cys-Phe (Fig. 5). These residues are located in

a highly conserved region that resembles the N-terminal protein splicing motif N1 of inteins, called Hint-domain (Hall et al., 1997; Pietrovski, 1994, 1998). The N-terminal 145-amino-acid segment of the *D. melanogaster* hedgehog autoprocessing domain (Hh-C_{17}), composing the entire region homologous to the protein splicing domain, was crystallized and solved to 1.9-Å resolution (Hall et al., 1997). To assess the autocleavage ability of the *D. melanogaster* Hh a chimeric protein where most of the Hh-N terminus was replaced by a hexahistidine sequence to allow protein purification was constructed (Porter et. al., 1996a). *In vitro* cleavage of the purified chimeric protein (Hh-C) was shown to require a thiol or hydroxylamine molecule and it was blocked when cysteine (Cys-258) at the N-terminus of the Hh-C domain (Fig. 4) was substituted by alanine, and much attenuated by replacement with serine (Porter et. al., 1996a). Several other observations are consistent with the involvement of a thioester intermediate (Fig. 5, A), as it happens in the first step of intein protein splicing. Thus, His-329 in *Drosophila* Hh, which is essential for the autocleavage (Lee et al., 1994), is also found in this conserved region that resembles the intein protein splicing motif implicated in the N-S acyl rearrangement (Perler et al., 2002). In Hh proteins, the thioester intermediary (Fig. 5, B) undergoes a transesterification reaction, triggered by cholesterol (Porter et al, 1996b). Mutation of His-329 to alanine prevented splicing using both thiol reagents and cholesterol (Hall et al., 1997). In the same region, replacement of the highly conserved Thr-326 also results in deficient thiol and cholesterol induced cleavage (Hall et al., 1997). On the other hand, mutation of the conserved Asp-303 to alanine had no effect in splicing induced with thiols, but avoided splicing using cholesterol (Hall et al., 1997). Accordingly, no amino acid analog to Asp-303 is found in intein splicing proteins (Perler et al., 2002). These conserved amino acids are in close proximity in the crystal structure of *Drosophila* Hh-C_{17} (Hall et al., 1997) (Fig. 6). These evidences imply that Asp-303 is important for the cholesterol attachment, while Thr-326 and His-329 are involved in the N-S acyl rearrangement (Perler et al., 2002). Deletion of the last 63 C-terminal residues of the Hh-C domain, which are not required for the N-S acyl rearrangement, prevents esterification with cholesterol (Hall. et al., 1997). Whether this part of the domain functions as a cholesterol binding/sensing site or participates in the catalysis of transesterification is not yet clear.

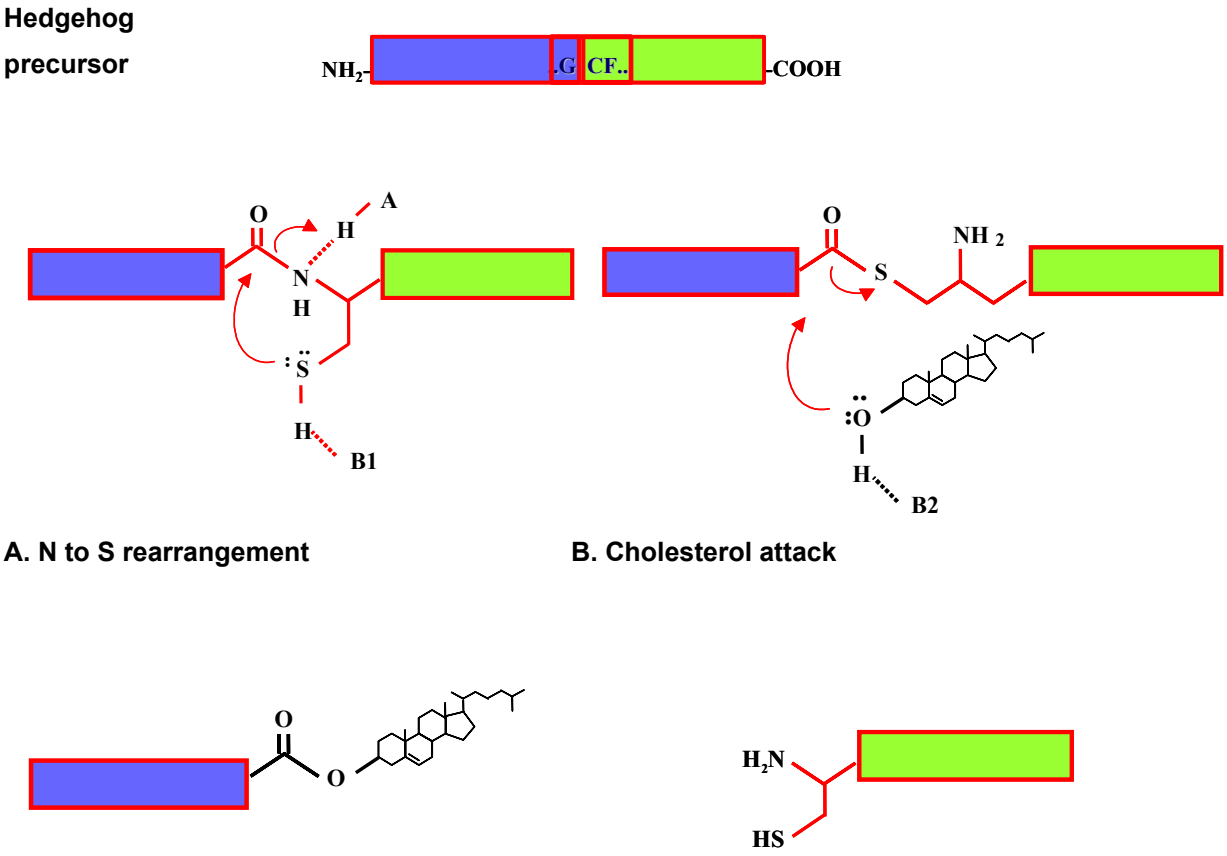

Figure 5. Splicing mechanism in Hedgehog proteins. A- First nucleophilic attack by the conserved cysteine residue. B- Trans-ester intermediary and second nucleophilic attack by a cholesterol molecule. C- Release of the active Hh-N terminus and Hh-C. In the square are the conserved amino acids at the splice junction (Porter et al., 1996a, b).

2.5.2 Lipid modification of Hedgehog proteins and localization to rafts

Depending on the context, Hedgehog (Hh) signals can promote cell proliferation, prevent apoptosis, or induce specific cell fates. Hh are secreted proteins which function as morphogens in neighboring or more distant cells (Ingham and McMahon, 2001). While only one gene is found in *Drosophila*, multiple members of this family of proteins are described in vertebrates. Hh receptor Patched (Ptc) is a negative regulator of the pathway repressing the downstream activator Smoothened (Smo) (Chen and Struhl, 1996; Fuse et al., 1999; Marigo et al, 1996; Stone et al, 1996). Binding of Hh to Ptc prevents this inhibition, leading to cellular responses via specific transcription factors (Alcedo et al., 1996; Hooper et al., 1994; van der Heuvel and Ingham, 1996). Ptc is an integral-membrane protein that posses a Sterol Sensing Domain (SSD). While the N-terminus of Ptc seems to be responsible for

internalization of Hh, the C-terminus takes part in the signaling pathway (Johnson et al., 2000).

Hedgehog proteins are modified *in vivo* by the addition of a cholesterol moiety at the carboxy terminus of the processed N-terminus and by palmitoylation at the N-terminus (Lee et al., 1994; Pepinski et al., 1998; Porter et al., 1996a, b). The processed signaling protein Hh-N^{chol} is released from the producing cells. A protein called Dispatched (Disp), which is a putative 12-pass transmembrane protein with a sterol sensing domain (SSD), seems to be involved in this process (Burke et al., 1999). In *Disp* mutants, Hh-N^{chol} is no longer released and accumulates in the producing cells. Possible roles of this protein include a function in the intracellular trafficking of Hh-N^{chol} in the secretory pathway or displacement of the cholesterol anchor from the membrane once it reaches the cell surface. Disp might be involved in the formation of an aggregate of Hedgehog-N protein that is then capable of diffusing away from Hh-producing cells. Conversely, effective sequestration by Ptc requires the cholesterol moiety (Jeong and McMahon, 2002). Quite striking is the fact that Ptc mutated in its SSD is not affected in the sequestration of Hh-N^{chol}. For this reason, the enhanced sequestration of Hh-N^{chol} by Ptc is most likely due to some other cholesterol-dependent process, such as lipid raft association. GPI protein modification is similar to the cholesterol modification in that both are attached to extracellular proteins and serve as lipid raft targeting signals. Nevertheless, the finding that Hh-N^{GPI} lacks the long-range activity of Hh-N^{chol} shows that GPI cannot replace cholesterol (Burke et. al., 1999). Therefore, a possible function of the cholesterol modification is targeting of the protein to lipid rafts, as demonstrated by the association of Hh-N^{chol} to these areas of the membrane (Rietveld et. al., 1999). Lipid rafts are sphingolipid- and cholesterol-rich microdomains in lipid bilayers, which associate with specific proteins and behave as docking platforms (Simons and Ikonen, 1997). They are thought to be important in some signaling pathways by acting as organizing centers for signaling components, and to be important in protein sorting. Concentration of Hh-N^{chol} in lipid rafts may promote its hexamerization, or the interaction with Ptc, which also accumulates in these microdomains (Chen et al., 2004; Karpen et. al. 2001).

A **B**

Figure 6. A. Crystal structure from Hedgehog-C (Hh-C_{17}) (Hint domain) from Hall et al., 1997. **B.** 3D structure prediction for GmGIN-C (Requena et al. unpublished).

Sonic Hedgehog (Shh) is another member of the Hh protein family. The enhanced activity of Shh-N^{chol} versus Shh-N could be due to an indirect effect of the cholesterol modification, facilitating a second modification such as palmitoylation. Palmitoylation has been shown to enhance its activity (Pepinski, et al., 1998; Taylor et. al., 2001). However, the mechanism of this enhancement is unclear, as it is not accompanied of an increase in binding affinity to Ptc (Pepinski et al, 1998). In *Drosophila*, mutants in a putative membrane acyl transferase required for this palmitoylation produce an inactive Hh signal, regardless of its cholesterol modification (Chamoun et al., 2001; Micchelli et al., 2002). Similarly, a form of Hh that cannot be palmitoylated because of a mutation at its modification site lacks activity (Lee et al., 2001). Palmitoylation seems to collaborate with cholesterol to anchor Hh proteins to the membrane, more tightly than by means of the cholesterol moiety (Pepinski et. al., 1998). Nevertheless, this modification also affects Shh long-range distance signaling (Lewis et al., Chen et al., 2004). Shh protein lacking this modification, but with the cholesterol moiety, are secreted but fail to form a multimeric complex of increased signaling inducing activity (Chen et al., 2004; Zeng et al., 2001). In this multimeric complex lipid modifications would be hidden, resulting in increased solubility and diffusion (Chen et al., 2004; Zeng et al., 2001). Accordingly, secretion does not seem to be affected by this modification (Lee et al., 2001).

Replacement of the N-terminal cysteine residue by a hydrophobic residue is sufficient to increase signaling activity, indicating that it is the hydrophobicity per se rather than

the specific nature of the palmitoyl moiety that promotes the activity (Taylor et al., 2001; Ingham and MacMahon, 2001). Accordingly, rat Shh was modified with a wide variety of lipid modifications (palmitoyl, myristoyl, stearoyl, arachidoyl residues) under the same conditions in which palmitoylation of human Shh was described (Pepinski et al., 1998).

Exposure of mammalian embryos to inhibitors of cholesterol synthesis or steroidal alkaloids such as jervine and cyclopamine causes holoprosencephaly, the same phenotype found in mice and humans with mutations in *Shh*. However, instead of affecting cholesterol modification of Shh, these steroidal alkaloids appear to inhibit the response in signal-receiving cells (Cooper et. al., 1998; Incardona et. al., 1998). Further analysis of the effect of cyclopamine points to a role in directly antagonizing further downstream components, such as Smo activity (Taipale et. al., 2000). Accordingly, several studies point to the possibility that a molecule similar to these compounds is actively transported by Ptc in order to inhibit Smo activity (Chen et al., 2002; Frank-Kamenetsky et al., 2002; Taipale et al., 2002).

2.5.3 The Hog domain is found in other proteins

GmGIN1 is not the only protein which contains the C-terminal domain of Hedgehog proteins attached to an N-terminus different of Hh-N. Searches through the *Caenorhabditis elegans* genome, revealed that despite of the absence of Hedgehog proteins as such, several protein sequences were found to contain similarities to Hedgehog proteins (Bürgling, 1996). The similarity is restricted to the carboxyl-terminus of the Hedgehog proteins. The authors named this conserved carboxy terminus as the “Hog” domain. The autoproteolytic cleavage site in Hedgehog proteins at the Cys-Phe pair is conserved in the *C. elegans* homologs (Bürgling, 1996). The cleavage site was also predicted by computer comparison to be similar to the amino-terminal splice sites of “intein” protein domains. Thus, the N-terminal splice junction motif of intein proteins matches all Hog domains (Koonin, 1995; Pietrokovski, 1994). Accordingly, Wrt1 has been shown to undergo autosplicing heterologously expressed in *Drosophila* cells (Porter et al, 1996a). The similarity extends beyond the Hint domain, and is also observed in a series of hydrophobic residues that occur at conserved intervals (Aspöck et al., 1999). In hedgehog protein this region has been called the Sterol Recognition Region (SRR) (Beachy et al., 1997; Hall et al., 1997; Mann and Beachy, 2000).

Database searches and comparison of the amino-terminal domains of these proteins revealed two new protein domains (Aspöck et al., 1999; Bürgling, 1996). The “Wart” domain is present in ten *C. elegans* proteins (Aspöck et al., 1999). Five of them are associated with the Hog domain. Two common features of the Wart domains are: cysteins seem to play a significant role and they have signal sequences for protein export immediately upstream of the Wart domain (Aspöck et al., 1999; von Heijne, 1986).

The second novel domain, called “Ground”, is found in nine of the *C. elegans* sequences and one from the parasitic nematode *Brugia malayi.* The Ground domain can also occur with or without an associated Hog domain. Like the Wart domain, they are highly divergent, most have clearly identifiable signal sequences at their amino termini, and some of the conserved positions are characterized by cysteins. This is reminiscent of other signaling molecules, thus it is possible that the new Hog family members are novel signaling molecules (Aspöck et al., 1999).

In Aspöck et al. (1999) the authors postulate that Warthog and Hedgehog families could have a common ancestor, the Wedgehog, which could have arisen early in the metazoan evolution from an intein, because this domain is more ancient as it occurs in prokaryotes. Also a new group of genes related to *Ground* (*grd*) genes is described, and named *ground-like* genes (*grl*). They also have signals for protein export, and are in general quite small, but differ from *grd* genes in the patterns of conserved cysteins residues.

The role of *wrt*, *grd* and *grl* genes is still unclear. A known target of Hh is Patched (Ptc) (Fuse et al., 1999), which belongs to a group of integral membrane molecules with a sterol-sensing domain (SSD). Several related genes have been identified in *C. elegans*, such as *ptc-1*, which is involved in nematode development, despite the apparent absence of other components of the Hh/Ptc signaling pathway (Kuwara et al., 2000). In *C. elegans* Ptc-1 is required for germ-line development, affecting cytokinesis, as its absence leads to the formation of multinucleate germ cells and sterility. This could point towards a new or ancestral role of this family of proteins, independent from Hh or the downstream activator Smoothened (Smo) and the role for Ptc in regulating cell proliferation. Another protein related to the Hedgehog pathway, Dispatched, has been found in the *C. elegans* genome (Burke et al., 1999).

Therefore, GmGIN1 could represent the first protein with a Hog domain in lower eukaryotes. By means of the cholesterol moiety it could be targeted to raft domains,

where interaction with proteins, maybe related to patched, could be expected. The expression of GmGIN1 in the presymbiotic stage points towards a role in signaling either towards the establishment of the symbiosis or growth arrest.

2.6 Aim of this work

G. mosseae GmGIN1 is mainly expressed during the pre-symbiotic or early developmental stages of the AM symbiosis (Requena et al., 2002). This means it could be involved in the recognition and signaling events at this developmental stage; either to promote the establishment of the symbiosis with a compatible host plant or growth arrest in its absence. This protein has a two-domain structure with putative self-splicing site in the junction of the two domains. The GmGIN1 carboxy terminus (GmGIN1-C) matched the Hint module, which is characteristic of hedgehog and intein proteins, which undergo self-splicing as post-translational modification. In order to unravel the possible self-splicing activity of GmGIN1-C, the first objective of this work was the heterologous expression and purification of this domain. Purified protein would be tested for the ability to undergo self-splicing in the presence of small nucleophiles and cholesterol, in an analogous manner as Hedgehog C-terminus. Given that cholesterol or sterols could be involved in the splicing reaction *in vivo*, lipid extraction and analysis from the closely related species *G. intraradices* and mycorrhizal carrot roots would be realized and tested for their capacity to induce protein splicing. As cholesterol in hedgehog proteins releases the N-terminus and promotes its activation and localization at the cell membrane, full length protein should be also expressed, purified and tested for its splicing activity.

The GmGIN1 amino terminus (GmGIN1-N) contains a GTP CDC motif, characteristic for proteins involved in cell division, with an ATP/GTP-binding site motif A (P-loop). Moreover, it shares similarity with a novel family of GTPases called GIMAP. This means that the GmGIN1-N could have the ability to bind and hydrolyze either of the two nucleotide derivatives. With this background, a second part of the work was focused on the expression and purification of GmGIN1-N. Purified protein should be tested for nucleotide binding selectivity and hydrolysis.

3 Materials and methods

3.1 Equipment

The equipment employed and the companies to which they belong to, are: BACHOFER GmbH & Co; Thermocycler T personal: BIOMETRA® (Göttingen); Electrophorese cuvette Mupid-21: EUROROGENTEC; Pipettes, Multipette® Plus: EPPENDORF (Hamburg); Centrifuge Mikro 12-24: HETTICH (Germany); Centrifuge Biofuge Fresco: HERAEUS CHRIST GmbH (Osterode); DNA Speed Vac (DNA 110-230): SAVANT Instruments, INC.HOLDBROOK (NY); Vortex-Genie 2: SI (Scientific Industries); Thermoshaker TS-W, SCHUTRON; Spectrophotometer Uvikon: KONTRON INSTRUMENTS; Protein electrophoresis cuvettes and Western transfer module INVITROGEN; GC-9A SHIMADZU; GC-17A SHIMADZU; QS-5000 MS SHIMADZU.

3.2 Standard buffers and solutions

Ampicillin stock solution (1000x)	Ampicillin (Roth) in water filter sterilize	150 mg/ml
Citric buffer	Citric acid Trisodium citrate pH 6.0, autoclave	1.7 mM 8.3 mM
Chloramphenicol stock solution (1000x)	Chlor in ethanol filter sterilize	34 mg/ml
Denaturation solution (for Southern and Northern blot)	NaOH NaCl	0.5 M 1.5 M
Denaturation solution (for colony hybridization)	NaOH NaCl SDS	0.5 M 1.5 M 0.1%
DEPC Water (Diethyl-pyrocarbonate)	DEPC autoclave	0.1%

DIG-buffer 1	Maleic acid	0.1 M
	NaCl	0.15 M
	pH 7.5	
DIG-buffer 2	Buffer 1	
	Blocking reagent	1%
DIG-buffer 3	Tris/HCl, pH 9.5	100 mM
	NaCl	100 mM
	$MgCl_2$	50 mM
DIG-Standard hybridization buffer	SSC	5x
	N-Laurylsarcosine	0.1%
	SDS	0.02%
	Blocking reagent	1%
IPTG (Isopropyl β-D-thiogalactopyranoside)	Stock solution (50 µL/plate)	0.1 M
	For protein induction (stock solution)	1 M
Kanamycin stock solution (1000x)	Kan in water	50 mg/ml
Loading dye DNA (6x)	Glycerol	30 %
	Bromophenol blue	0.25 %
Neutralization solution (for Southern and Northern blot)	Tris-HCl, pH 7.0	0.5 M
	NaCl	1.5 M
Neutralization solution (for colony hybridization)	Tris-HCl, pH 7.5	1.0 M
	NaCl	1.5 M
PMSF (Phenylmethanesulfonylfluoride)	PMSF in isopropanol	200mM
Protein extraction buffer	Maleic acid/KOH pH 6.8	100 mM
	Sucrose	100 mM
	ß-mercaptoethanol	2 % (v/v)
	Ethylenglycol	15 % (v/v)

	PVPP	5 % (w/v)
	PMSF	1.5 mM
	(Added in moment of extraction)	
SSC buffer (20x)	NaCl	3 M
	Trisodium citrate $2H_2O$/NaOH	0.3 M
	pH 7.0	
Plasmid DNA minipreparation		
Solution I	Tris/HCl, pH 7.5	50 mM
	EDTA	10 mM
	Ribonuclease A	100 μg/ml
Solution II	NaOH	0.2 M
	SDS	1%
Solution III	KAc	1.5 M
	pH 4.8	
TE-Buffer	Tris/HCl, pH 8.0	10 mM
	EDTA	1 mM
Tetracycline stock solution (200x)	Tet in water	15 mg/ml
Washing buffer	Buffer 1	
(for DIG-detection)	Tween 20	0.3%
Washing solution	SSC	1x
(for DIG-detection)	SDS	0.1%
Washing solution	SSC	3x
(for colony hybridization)	SDS	0.1%
X-Gal	stock solution in	2%
	NN-Dimethylformamid (50 μl/plate)	

3.3 Culture Media

LB agar	LB broth
	2% agar
LB amp	LB broth

		Ampicilin	150 μg/ml
LB amp/chlor		LB broth	
		Ampicilin	150 μg/ml
		Chloramphenicol	34 μg/ml
LB amp/kan		LB broth	
		Ampicillin	150 μg/ml
		Kanamycin	50 μg/ml
LB amp/tet		LB broth	
		Ampicillin	150 μg/ml
		Tetracycline	15 μg/ml
LB tet		LB broth	
		Tetracycline	15 μg/ml
LB broth		Casein hydrolysate (MERCK)	10 g/L
		NaCl	10 g/L
		Yeast extract (DIFCO)	5 g/L
Terrific Broth	Part 1	Tryptone	12 g
		Yeast extract	24 g
		Glycerol	4 ml
		Deionised water	900 ml
	Part 2	KH_2PO_4	2.31 g
		K_2HPO4	12.54 g
		Deionised water	100 ml
	Prepare and autoclave separately and combine to make 1 L medium for use.		
2xYT		Tryptone	16 g
		Yeast extract	10 g
		NaCl	5 g
		pH 7.0 with NaOH and adjust to 1 L	
M medium	Macroelements	KNO_3	80 mg/L

		$MgSO_4 \cdot 7H_2O$	731 mg/L
		KCl	65 mg/L
	KH_2PO_4		4.8 mg/L
	$Ca(NO_3)_2$		288 mg/L
	Na-FeEDTA		8 mg/L
	Microelements	$MnCl_2 \cdot 4H_2O$	6 mg/L
		H_3BO_3	1.5 mg/L
		$ZnSO_4 \cdot 5H_2O$	2.65 mg/L
	Other microelements	$Na_2MoO_4 \cdot 2H_2O$	2.4 μg/L
		$CuSO_4 \cdot 5H_2O$	0.13 mg/L
	Vitamines	Glycin	3 mg/L
		Myo inositol	50 mg/L
		Nicotinic acid	0.5 mg/L
		Piridoxine-HCl	0.1 mg/L
		Thiamine-HCl	0.1 mg/L
	pH 5.5 with KOH		
	Phytagel (Sigma)		0.3%
M medium	M medium		
+sucrose	Sucrose		1%
M medium-Mes+P	M medium		
	Sucrose		30 g/L
	Mes		1.952 g/L (10 mM)
	KH_2PO_4		5.4 mg/L
M medium liquid	Macroelements	KNO_3	160 mg/L
		$MgSO_4 \cdot 7H_2O$	1462 mg/L
		KCl	130 mg/L
	KH_2PO_4		4,8 mg/L
	$Ca(NO_3)_2$		576 mg/L
	Na-FeEDTA		16 mg/L
	Microelements	$MnCl_2 \cdot 4H_2O$	12 mg/L
		H_3BO_3	3 mg/L
		$ZnSO_4 \cdot 5H_2O$	5.3 mg/L

	Other microelements	$Na_2MoO_4 \cdot 2H_2O$	4.8 μg/L
		$CuSO_4 \cdot 5H_2O$	0.26 mg/L
	Vitamines	Glycin	6 mg/L
		Myo inositol	100 mg/L
		Nicotinic acid	1 mg/L
		Piridoxine HCl	0.2 mg/L
		Thiamine HCl	0.2 mg/L
		pH 5.5 with KOH	
SOB medium		Casein hydrolysed	20 g/L
		Yeast extract	5 g/L
		NaCl	0.58 g/L
		KCl	0.186 g/L
		pH 7.0	
SOC medium		SOB medium	98 ml
		2 M $MgCl_2$	1 ml
		2 M Glucose	1 ml

3.4 Protein SDS-PAGE reagents

Tris-Glycine Gels	APS (ammonium peroxydisulfate)	10% in water
	SDS (sodiumdodecylsulphate)	10% in water
	Stacking buffer	
	Tris/HCl pH 6.8	1 M
	Running gel buffer	
	Tris/HCl pH 8.8	1.5 M
Schägger/Jagov PAGE Gels	Gel Buffer	
	Tris/HCl pH 8.45	3 M
	SDS (sodiumdodecylsulphate)	0.3%
	Glycerol	87 % in water

Protein Tris-Glycine Sample Buffer (4x)	Glycerol	4.00 g
	Tris base	0.682 g
	Tris HCl	0.666 g
	SDS	0.80 g
	EDTA	0.006 g
	Serva Blue G250	0.75 ml of 1% solution
	Phenol Red	0.25 ml of 1% solution
	Deionized water to 10 ml	
	1X buffer pH 8.5	
	Do not use acid or base to adjust pH.	
Protein S-J Sample Buffer	Tris-HCl pH 6.8	50 mM
	SDS	4%
	Glycerol	12%
	ß-mercaptoethanol	2% (v/v)
	Serva BlueG	0.01%
Tris-Glycine Running Buffer (10x)	Tris base	30 g/L
	Glycine	144 g/L
	SDS	1%
	pH 8.3, do not adjust.	
MES SDS Running Buffer (20x)	MES [*2-(N-morpholino) ethane sulfonic acid*]	1.0 M
	Tris Base	1.00 M
	SDS	69.3 mM
	EDTA	20.5 mM
	1X buffer should be pH 7.3	
	Do not use acid or base to adjust pH.	
S-J Running Buffer	Tris	0.1 M
	Tricine	0.1 M
	SDS	0.1%
	pH 8.25, do not adjust.	
Coomassie staining solution	Acetic acid	10%

	Methanol	15%
	Serva Blue R250	1.2 g/L
	Deionized water	
Destaining solution	Acetic acid	10%
	Methanol	15%
	Deionized water	
Tris-Glycine Transfer Buffer (10x)	Tris Base	29.28 g/L
	Glycine	58.14 g/L
	SDS	3.70 g/L
	pH must be 8.3, do not adjust.	
1X Transfer buffer Tris-Glycine	10X Trys-Glycine buffer	100 ml
	Methanol	200 ml
	H_2O	700 ml
	Final volume of 1000 ml	
Nupage novex Bis-Tris 20x Transfer Buffer	Bicine	10.2 g/100 ml
	Bis-Tris	13.1 g/100 ml
	EDTA	0.75 g/100 ml
	pH should be 7.2.	
Nupage novex Bis-Tris 1x Transfer Buffer	20x Transfer B.	50 ml
	Methanol	100 ml
	H_2O	850 ml

When transferring 2 gels at the same time, methanol was increased to 20%.

3.4.1 In gel trypsin digest

Ammonium bicarbonate (BiCa)	100 mM in Milli-Q-water
	Filter through 0.45 μm Nitrocellulose filter
	Aliquot and store at -20°C
Dithiothreitol (DTT) solution	10 mM in 100 mM BiCa
Formic acid solution	5% in Milli-Q-water
Iodacetamid solution	55 mM in 100 mM BiCa

	Prepare just before use and store in the dark
Trypsin solution (Promega)	Dilute one drop (20 μg) in 200 μl of Resuspension buffer, distribute in 10 μl aliquots and store at -80°C until use. For working dilution add to one aliquot 40 μl Milli-Q-water and 50 μl 100 mM BiCa. Prepare just before use

3.5. Western blot detection buffers and solutions.

0.5% Blocking solution (peroxidase-labeled 2ry antibody)	5 ml Blocking reagent of Chemiluminescence Detection Kit BM/Roche Nr 1 500 708 to 95ml TBS.	
1st Blocking Buffer	5% BSA (Merck) or skimmed milk (Difco) in TBST.	
2nd Blocking Buffer	2.5% Skimmed milk in TBST.	
Ponceau S staining	Ponceau S 0.3% in 7% Trichloroacetic acid	
Tris Buffered Saline (TBS)	Tris Base	6.05 g/L (50mM)
	NaCl	8.76 g/L (150mM)
	Adjust pH to 7.5 with HCl	
	H_2O	adjust to 1000 ml
TBS-Tween 20 (TBST)	1 ml Tween 20 (0.1%) in 1L TBS	

3.5.1 Primary Antibodies.

-AntiXpress (Invitrogen, Nr R910-25), dilution 1:5.000 in Blocking B.2
-AntiHis (Novagen, Nr 70796-4), dilution 1:2.000 in Blocking B. 2.
-RGS-AntiHis (Qiagen, Nr 34650), dilution 1:2.000 in Blocking B. 2.
-Rabbit antisera 461 and 476 antiCREN (Seqlab). First bleeding diluted 1:10.000 in Blocking B. 2.
-Rabbit antisera 474 and 475 antiCKQD and CRVT (Seqlab). First bleeding diluted 1:10.000 in Blocking B. 2.

3.5.2 Secondary Antibodies.

-Anti-mouse Ig-POD (Fab fragment) (Sigma), dilution 1:12000 in Blocking B. 2.
-Anti-mouse Ig-Alkaline phosphatase conjugate (Sigma), dilution 1:10.000 in Blocking B. 2.
-Goat Anti-rabbit Ig (H+L)-POD (BioRad), dilution 1:3.000 to 1:10.000 in Blocking B. 2.
-Goat Anti-rabbit Ig (H+L)-Alkaline phosphatase conjugate (BioRad), dilution 1:10.000 in Blocking B. 2.

Detection solution	Chemiluminescence Detection Kit BM/Roche Nr 1 500 708 (peroxidase-labeled 2ry antibody). Mix substrate solution A (bottle 1) and starting solution B (cup 2) in a ratio of 100:1 and equilibrate to 15-25°C, covered with aluminium foil.	
Stripping Buffer	ß-mercaptoethanol	100 mM
	SDS	2%
	in TBS pH 7.5	

3.6 Ni-NTA Purification Buffers

3.6.1 Native Purification Buffers

Lysis Buffer	NaH_2PO_4 H_2O	50 mM
	NaCl	500 mM
	Imidazol	10 mM
	Triton X-100	0.3%
	Glycerol	6%
	PMSF	1 mM
	pH 8.0	
Washing Buffer	NaH_2PO_4 H_2O	50 mM
	NaCl	500 mM
	Imidazol	20 mM to 50 mM
	Triton X-100	0.5%
	Glycerol	6%
	PMSF	1 mM

	pH 7.0			
Elution Buffer	NaH_2PO_4 H_2O		50 mM	
	NaCl		300 to 500 mM	
	Imidazol		500 mM	
	PMSF		1 mM	
	pH 8.0			

3.6.2 Denaturing Buffers

Lysis Buffer	NaH_2PO_4 H_2O		50 mM	
	NaCl		500 mM	
	Imidazol		10 mM	
	Triton X-100		0.3%	
	Glycerol		6%	
	Urea		8 M	
	pH 8.0			
Washing Buffer	NaH_2PO_4 H_2O		50 mM	
	NaCl		500 mM	
	Imidazol		20 mM to 50 mM	
	Triton X-100		0.5%	
	Glycerol		6%	
	Urea		8 M	
	pH 8.0			
Elution Buffer	NaH_2PO_4 H_2O		50 mM	
	NaCl		500 mM	
	Imidazol		500 mM	
	Urea		8 M	
	pH 8.0			
Refolding Buffers	Buffer A	Tris/HCl	20 mM	pH 8.0
		NaCl	500 mM	
		Glycerol	20%	
		Urea	6 M	
	Buffer B	Tris/HCl	20 mM	pH 8.0

		NaCl	500 mM
		Glycerol	20%
DEAE sepharose purification	Buffer A	MOPS	50 mM
			pH 6.5 with KOH
	Buffer B	MOPS	50 mM
			NaCl 2 M
			pH 6.5 with KOH, filter.

3.7 Organisms and culture conditions

3.7.1. *Escherichia coli*

3.7.1.1 Strains

XL1-Blue (Invitrogen)	endA1, gyrA96, hsdR17, lac^-, recA1, relA1,supE44, thi-1, [F' $lacI^qZ$ ΔM15, proAB, Tn 10]
TOP 10 (Invitrogen)	F^- mcrA Δ(mrr-hsdRMS-mcrBC) Φ 80lacZΔM15 ΔlacX74 recA1 deoR araD139 Δ(ara-leu)7697 galU galK rpsL (Str^R) endA1 nupG
M-15 [pREP4] (Qiagen)	NalS StrS RifS Thi- Lac- Ara+ Gal- Mtl- F- RecA+ Uvr+ Lon+
BL21 (Novagen)	F-ompT hsdSB (rB- mB-) gal dcm)
BL21 (DE3) (Novagen)	F-ompT hsdSB (rB- mB-) gal dcm (DE3)
BL21 (DE3) pLys(Novagen)	F-ompT hsdSB (rB- mB-)gal dcm (DE3) pLysS (CmR).

3.7.1.2 Standard culture conditions

E. coli XL1-Blue and TOP 10 strains were cultured in LB-tet or LB-Str, respectively, solid or liquid medium, at 37ºC. For liquid culture, bacteria were incubated by shaking at 160 rpm overnight. In case of M15 [pREP4] strain, kanamycin was used as antibiotic, and chloramphenicol for BL21 (DE3) pLyS.

3.7.1.3 Standard protein induction conditions

Cells from glycerol stocks were streaked out on LB-broth plates supplemented with the appropriate antibiotics and grown overnight. One colony was incubated over night in LB-broth liquid medium supplemented with the corresponding antibiotics according to the *E. coli* strain and 0.5% glucose. Next day fresh medium was inoculated with this pre-inoculum in a ratio 1:500 or to an OD_{600} of 0.1. Cells were grown at 37°C and 200 rpm until an OD_{600} of 0.6-0.9, collected and resuspended in the same volume of medium without glucose and with the corresponding concentration of IPTG (from 0.1 to 1 mM). Induction was performed either at 37°C during 3-5 hours or overnight at 20°C.

3.7.2 Mycorrhizal fungi

3.7.2.1 Strains

Glomus mosseae (BEG12)
Glomus intraradices (line DC-1), Bécard and Fortin, (1988).
Amanita muscaria [L. ex Fr] Hooker, strain CS83

3.7.2.2 Standard culture conditions

Ri T-DNA-transformed carrot (*Daucus carota* L.) roots colonized with *G. intraradices* line DC-1 were grown in bi-compartmental Petri plates as described by St-Arnaud et al. (1996) at 27ºC in the dark. Carrot roots were grown in the proximal compartment of the divided plate containing solid M medium supplemented with 1% of sucrose (Bécard and Fortin, 1988; Figure 7). Only hyphae were allowed to grow in the distal compartment containing solid or liquid M medium without sucrose. Spores from solid medium were recovered by dissolving the medium in 3 volumes of citric buffer/volume of solid medium for 1 h at 30ºC. Spores were recovered in a 40 μm sieve and washed with water to eliminate the remaining medium. Solid medium was removed once the fungus reached the second compartment and re-filled with 8 ml liquid M medium in order to allow hyphal growth in liquid medium. For negative

control cultures without *G. intraradices*, roots were grown in solid M-medium-Mes+P, which contains a higher amount of sucrose and phosphate.

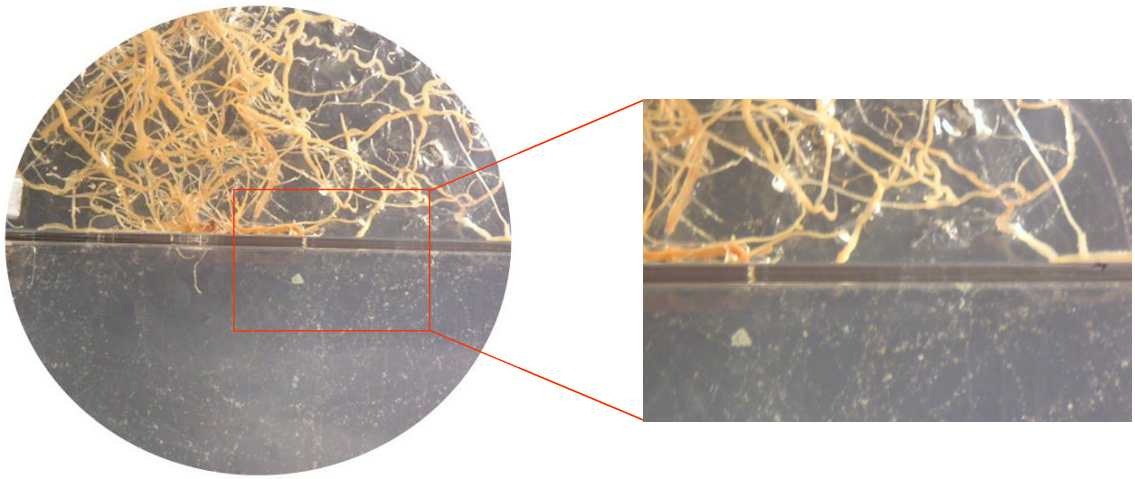

Figure 7. *In vitro* bi-compartmental system. Divided plate with root proximal compartment (carrot roots colonized with *G. intraradices* in solid M medium supplemented with sucrose) and fungal distal compartment (*G. intraradices* extraradical hyphae and spores in M medium without sucrose) (Ocón, 2004).

Amanita muscaria was cultured on Melin-Norkrans medium (MMN 1/2 C medium) agar plates (Guttenberger & Hampp, 1992) for one month at 20 °C. Suspension cultures were prepared from one month old solid cultures by homogenisation of two 1.5 cm diameter fungal colonies, using an Ultra Turrax T25, Janke & Kunkel, Staufen, Germany; tip S25N-18G. The mycelium was then resuspended in 60 ml of MMN 1/2 C medium and shaken at 81 rpm at a constant temperature of 20°C.

3.8 Molecular biological methods

3.8.1 Plasmids

pTrcHis-TOPO — Invitrogen, Karlsruhe, Germany

trc promoter, *lac* operator site, T7 gene 10 translational enhancer, pTrcHis forward priming site, initiation ATG, 6XHis tag, Xpress™ epitope, Xpress™ foward priming site, Enterokinase cleavage site, TOPO® Cloning site, pTrcHis reverse priming site, *bla* promoter, Ampicillin resistance gene (*bla*), pBR322-derived origin, Lac Repressor (*lacI*^{q}).

pRSETb — Invitrogen, Karlsruhe, Germany
T7 promoter, 6XHis tag, Xpress™ epitope, Enterokinase cleavage site, Multiple cloning site, pRSET reverse priming site,T7 transcription terminator, f1 origin, *bla* promoter, Ampicillin (*bla*) resistance gene (ORF), pUC origin.

pCR 2.1-TOPO — Invitrogen, Karlsruhe, Germany
LacZα gene, M13 Reverse priming site, Sp6 promoter, Multiple Cloning Site, T7 promoter, M13 (-20) Forward priming site, M13 (-40) Forward priming site, f1 origin, kanamycin resistance ORF, ampicillin resistance ORF, pUC origin.

pET15b — T7 promoter, T7 transcription start, 6XHis tag, Multiple Cloning Site, T7 terminator, Lac Repressor (*lacI)*, pBR322 origin, Ampicillin (*bla*) resistance gene (ORF).

3.8.2 Oligonucleotides

Name	Sequence 5'-3'
79F1	GAT GTC TCG GAT TCA GCT GC
79R1	TAT GGC GCA CGA CAA TTG GG
79F2	GGA GAC TAC GTA TGT TGT GG
79R2	AAC AAG AGC AGA GAA CCT CG
GmGINExF1	GGA TTC CTT ACT CGT AAA CCT G
GmGINExR1	ATT TAA AGG CAC CCC ATG ATC C
GmGINExF0	CCT TAA GCA GTG GTA ACA ACG C
GmGINExF2	CGG GGG AAG TTG ATA CAA TGT C
GmGINExR2	GCG GCA AAT CAT CCT TCG AAA TC
GmGINExF3	AGA TCT GAT ACA ATG TCA AAT TGC CCA TC
GmGINExF4	AGC GGC CGC CAG TGT GAT G
GmGINExR4	GCG GCA AAA CCT CCT TCG AAA TC
GmGINExR5	AGG CAC CCC ATG ATC CAG CG

3.8.3 Plasmid DNA extraction from *E. coli*

An alkaline lysis method was used to extract the plasmid DNA from transformed cells. The treatment with lysing and precipitant agents resulted in the liberation of plasmid DNA, which was then precipitated with isopropanol. An isolated colony was used to inoculate 3 ml of LB medium containing ampicillin. The over-night culture was pelleted at 13.000 rpm for 3 minutes. After resuspension with 200 μl of Solution I, the cells were lysed using 200 μl of Solution II. Following protein and cell debris precipitation with 200 μl of Solution III, samples were centrifuged at 13.000 rpm for 15 minutes. The supernatant was transferred to a new reaction tube containing 600 μl of isopropanol. Plasmid DNA was then precipitated by 15 minutes centrifugation at 13.000 rpm. The pellet was washed with 500 μl of cold 70% ethanol and centrifuged at 13.000 rpm for 5 minutes. Plasmid DNA was resuspended in 50 μl TE buffer at 68ºC for 2 min.

3.8.4 Restriction enzyme analysis of plasmid DNA preparations

Three microliters of the extracted plasmid DNA were analysed by digestion with 5 U of *Eco*RI or the correspondent enzyme (Fermentas) restriction enzyme in a 10 μL volume. The reaction was incubated at 37ºC for 1 h and analysed by gel electrophoresis.

3.8.5 PCR

The standard PCR reaction components and the concentration in which they were used are listed below:

Components	Volume (μl)	Final concentration
10x PCR buffer	2.5	1x
2.5 mM dNTPs mixture	2	0.2 mM each
50 mM $MgCl_2$	1	2 mM
Forward primer (10 μM)	1	0.4 μM
Reverse primer (10 μM)	1	0.4 μM
Template DNA	1	as required
Taq-Polymerase (5 U/μl)	0.5	2.5 units
DEPC water	up to 25	

3.8.6 Synthesis of DIG-labelled probes by PCR

DIG-labelled probes were synthesized by PCR using the PCR DIG probe synthesis kit (Roche) according to manufacturer's instructions. For the synthesis of probes, 0.5 μL of Expand Polymerase (Roche) enzyme were used in 25 μL reaction volume.

3.8.7 Standard ligation of PCR products

PCR fragments were ligated into the pCR 2.1-TOPO vector from the TOPO-TA cloning kit (Invitrogen). After gel electrophoresis, PCR fragments were excised from the agarose gel, frozen and recovered by the "freeze-squeeze" method. This method consists on eluting directly the DNA contained in the agarose gel. For that, after ethidium bromide staining, the desired band was recognized under UV light and excised using a scalpel from the agarose gel. The band was placed on parafilm at -20ºC until frozen. DNA was then eluted by thawing the fragment within the parafilm with the fingers. Six microliters of the eluted fragment were ligated to 0.5-1 μl of pCR 2.1-TOPO vector according to the supplier's instructions. Ligations were used for transformation of chemically competent *E. coli* or kept at 4ºC until analyzed.

3.8.8 Cloning for protein expression

The C-terminus of the *GmGIN1* gene was amplified by PCR with the Expand High Fidelity system (Roche) using GmGINExF1 and GmGINExR1 as primers and *G. mosseae* cDNA as template. The amplification proceeded with 3 minutes at 94°C, followed by 30 cycles consisting of 30 seconds at 94°C, 30 seconds at 58.4°C and 45 seconds at 68°C, followed by a final elongation of 10 minutes at 68°C. After addition of Taq Polymerase, the reaction was incubated at 72°C for another 10 minutes. The resulting product of the reaction was run in an agarose gel and the corresponding band was excised and DNA was eluted by freeze-squeeze. 5 μl of the eluted band were ligated into the pTrcHis-TOPO® vector (Invitrogen) and the resulting product was transformed into *E. coli* TOP-10. The resulting clones were analyzed by BamHI-EcoRI (Fermentas) digestion

and analytical PCR using the pTrcHis Forward primer and the GmGINExR1 primer to check for the correct orientation of the insert. For subcloning of the insert to the pRSETb® vector (Invitrogen), the previous construct was digested with *BamHI-EcoRI* and the insert was ligated into the *BamHI-EcoRI*-restricted pRSETb vector.

For cloning of the full length *GmGIN1* cDNA, the GmGINExF3 and GMGINExR1 primers were used, following the amplification protocol of 3 minutes at 94°C, followed by 35 cycles consisting of 15 seconds at 94°C, 30 seconds at 58.4°C and 2 minutes at 68°C, followed by a final elongation of 10 minutes at 68°C. For changing the insert to the pRSETb® vector (Invitrogen), the previous construct was digested with *BamHI-HindIII* and ligated into the digested vector. Transformants were analyzed by bacterial colony hybridization.

The N-terminus of *GmGIN1* was PCR amplified using the primers GmGINExF3 and GmGINExR2 according to the protocol: 3 minutes at 94°C, followed by 30 cycles consisting of 15 seconds at 94°C, 30 seconds at 60.6°C and 90 seconds at 68°C, followed by a final elongation of 10 minutes at 68°C.

3.8.9 *E. coli* chemically competent cells

A single colony of the *E. coli* strain was inoculated in 3 ml of LB medium supplemented with the corresponding antibiotic and grown overnight at 37ºC shaking. One ml of the overnight culture was used to inoculate 100 ml of LB medium in a 250-ml Erlenmeyer flask. The culture was shaken at 180 rpm at 37ºC until the OD_{600} reached 0.4-0.6. After 5-10 min on ice, cells were harvested by centrifugation at 5.000 rpm for 10 min. The supernatant was discarded and the cells were carefully resuspended in the same volume of chilled sterile 0.1 M $MgCl_2$. Following centrifugation at 5.000 rpm for 5 min, the supernatant was discarded and cells were resuspended in half of the initial volume of sterile, chilled 0.1 M $CaCl_2$. They were then placed on ice for about 4 h (from 1 h to 24 h) and centrifuged at 5.000 rpm for 5 min. Pellet was air dried and resuspended in 2.5 ml of chilled 0.1 M $CaCl_2$/20% glycerol. Aliquots of 100 µl were placed in 1.5 ml chilled eppendorf cups. Competent cells were stored at -80ºC until use.

3.8.10 *E. coli* electro-competent cells

5 ml of SOB medium without magnesium were inoculated in a 250 ml flask. Cells were grown under vigorous aeration overnight at 37°C. On the next day 500 ml SOB medium without magnesium were inoculated with 0.5 ml of the overnight culture. The cells were grown under vigorous shaking at 37°C until OD_{600} was 0.7 to 0.8. The cells were harvested by centrifugation for 10 minutes at 4000 x g and 4°C. The pellet was resuspended in 500 ml of ice cold bidestillated sterile water. The cell suspension was centrifuged at 4.000 x g and 4°C for 15 minutes. The supernatant was carefully discarded and the same step repeated twice. The pellet was resuspended in 25 ml of ice cold 10% glycerol. The cell suspension was centrifuged and the supernatant discarded. The pellet was resuspended in 1 to 2 ml of ice cold 10% glycerol and cells were frozen in 200 µl aliquots in liquid nitrogen. Frozen cells were stored at -80°C

3.8.11 *E. coli* transformation

Chemically competent *E. coli* cells were transformed with 3.5-5 µl of vector-DNA insert ligation by heat shock at 42ºC for 1 min. After addition of 500 µl of SOC medium, the cells were incubated at 37ºC for 1 h shaking at 180 rpm. Transformed bacteria were plated in LB plates supplemented with the corresponding antibiotic and containing 50 µl of X-gal and 50 µl of IPTG stock solutions and incubated over night at 37ºC. Selection of positive clones was performed by blue-white screening.

Electro-competent cells were thawed on ice and an 80 µl aliquot was mixed with 8 µl of vector-DNA insert ligation. After one minute on ice the mixture was transferred to the cell for electroshock and 800 µl of SOC were added immediately. Cells were grown for 1 hour at 37°C and plated in the same manner.

3.8.12 Northern and Southern Blot

DNA or RNA was transferred from agarose (DNA) or formaldehyde-agarose (RNA) gel to nitrocellulose membrane (Hybond N^+, Amersham). For DNA

transfers (Southern blot; Southern, 1979), DNA was denatured after electrophoresis in agarose gel for 30 min with denaturation solution, and then neutralized in neutralization solution for 30-45 min. After incubation for 5 min in 2x SSC buffer, gels were blotted according to Sambrook et al. (1989). For RNA (Northern blot), formaldehyde-agarose gels were washed for 15 min with 20x SSC buffer, followed by 5 min in 2x SSC buffer. After overnight transfer, DNA or RNA were crosslinked to the membranes by UV radiation (1 min at 254 nm each membrane side). Membranes were pre-hybridised with DIG-Standard hybridation buffer at 65-68ºC for 1 h and then hybridized overnight at the same temperature with a DIG-labelled probe. Washing of the membranes was carried out by standard techniques. Membranes were washed twice with 2x washing solution for 5 min at RT. Then, they were washed twice with 0.5x washing solution for 15 min at the hybridization temperature. After this time, membranes were placed in a tray containing washing buffer and shaken at 50 rpm for 5 min. Membranes were blocked with buffer 2 (1% blocking reagent) for 30 min. Then, alkaline phosphatase-conjugated antibody specific for digoxigenin (Roche) was added. After washing 2 times with washing buffer for 15 min and 5 min in buffer 3, signal detection was performed by addition of the chemiluminiscent substrate, according to the manufacter's recommendations.

3.8.13 Bacterial colony hybridization

Colony hybridization on a nylon membrane was used for large-scale analysis of clones from an *E. coli* transformation. Three different LB amp plates were used for that purpose. The first plate contained bacterial clones obtained after the transformation. The surface the second plate was covered with a nylon membrane previously washed in distilled water and then imbibed in 2x SSC buffer. The third plate was used as a replica stock of the different clones. Single colonies were picked from the first plate using a sterile tooth-pick and transferred to the nylon membrane on the second plate and third plate. The second and third plates were incubated at 37ºC overnight to allow for bacterial growth. On the next day, the nylon membrane was removed from the LB amp plate and the third plate was stored as a stock at 4ºC. Plasmid DNA was cross linked to the membrane by UV radiation. The membrane was first incubated for

15 min on a filter paper imbibed on denaturation solution. Then, the membrane was moved to a filter paper imbibed on neutralization solution where it was kept for 5 min. After washing for 15 min with 2x SSC buffer, the DNA was cross-linked into the membrane by UV radiation (5 min at 254 nm). The membrane was washed in distilled water and allowed to dry. In order to reduce background and eliminate cell debris, the membrane was washed from 1 to 3 h with 3x SSC at 68ºC before hybridization. After that, the membrane was pre-hybridized and hybridized as described for Northern or Southern blot.

3.9 Biochemical methods

3.9.1 Protein purification

3.9.1.1 Native purification of His-tagged proteins from *E. coli*

One hundred ml *E. coli* cells were harvested and resuspended in a minimum volume of ice cold native lysis buffer (1 ml). One mg/ml of lysozyme was added and incubated for 1 hour in ice. 0.1 mM PMSF was added to the suspension every 30 minutes in order to prevent protein degradation. The suspension was treated with 5 μg/ml DNAse and 10 μg/ml RNase for 20 minutes and sonified in 3-4 cycles for 2 to 4 minutes on ice. In case the suspension was very viscous, freeze-thawing cycles were employed in between. The lysate was centrifuged for 20 minutes at 10.000 rpm at 4°C. When the supernatant was very viscous, a second centrifugation at 35.000 rpm for 45 minutes at 4°C was performed. The supernatant was incubated for one hour in pre-equilibrated Ni-NTA agarose resin (Qiagen) at 4°C (0.4 ml resin). The resin was spun down and the supernatant was discarded. Then the resin was washed thoroughly with large volumes of native washing buffer containing 20 mM Imidazol (10 times with 2 ml buffer), and the last washing step was performed with a small volume of native washing buffer containing 50 mM Imidazol (0.5 ml). Samples of all fractions were taken for SDS-PAGE analysis. Elution was performed with small volumes of native elution buffer (0.3 ml). Fractions were collected and stored at -20°C. When protein minipurification was performed, the pellet from 2 mL *E. coli* cell culture was resuspended in 150 µl ice cold native lysis buffer. Incubation with

lysozyme was performed, but DNAse and RNase incubation was not necessary. Sonication was performed in 2-3 cycles for 30 seconds on ice. Subsequent steps were performed as described above. 40µl Ni-NTA agarose resin were used, only 3 washing steps were necessary (1 ml buffer each) and elutions were performed with 25 µl buffer.

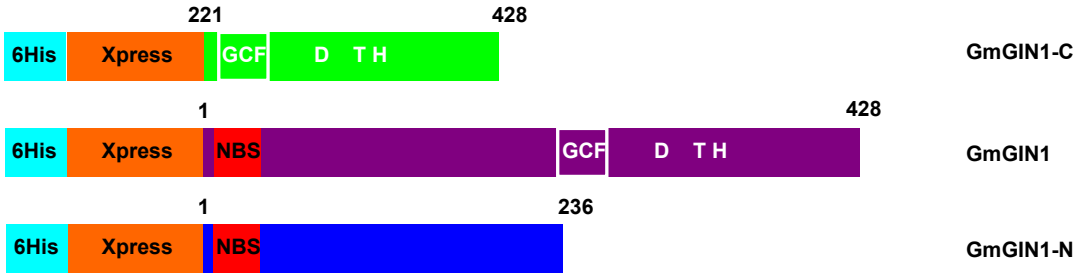

Figure 8. Schematic representation of the different *G. mosseae* GIN1 recombinant proteins expressed in *E. coli*. pTrcHis and pRSETb vectors add an N-terminal 6-Histidine tag for purification and Xpress epitope for immunodetection. GmGIN1-C construct expressed the protein from amino acid 221 until 428. GmGIN1 constituted the full length protein, from amino acid 1 to 428. GmGIN1-N construct expressed from amino acid 1 to 236, just before the splice junction. The splice junction is boxed and conserved amino acids implicated in the splicing are remarked. The N-terminal Nucleotide Binding Site (NBS) is remarked in red.

3.9.1.2 Denaturing purification of His-tagged proteins from *E. coli*

Frozen cell pellets from 100 mL cultures were thawed at room temperature in 1 ml of denaturing lysis buffer and were stirred for 45 minutes at room temperature. The suspension was subjected to four cycles of freezing and thawing and then to a centrifugation at room temperature of 15.000 rpm for 30 minutes. The supernatant was incubated for one hour with pre-equilibrated Ni-NTA agarose resin (Qiagen) at room temperature. Subsequent purification steps were performed in the same way as in 3.6.1.1.

3.9.1.3 Ion exchange purification of GmGIN-C terminus

pRSETbGmGIN-C has a pI of 7.4. DEAE-Sepharose was used as anion exchanger, using Buffer A and B in combination to obtain an increasing gradient of 20% salt every 100 ml. At pH 6.5 pRSETbGmGIN1-C must be positively charged. For this reason it will not be bound to the resin. Fractions were

collected every 8 ml. Eluted fractions were run in SDS-page gels and analyzed by immunoblotting.
A Mono S column was used as cation exchanger to trap the protein from positive fractions eluted from the DEAE column. Positively charged protein will bind to the column. A linear gradient of salt, from 0 to 100 % was used to elute the protein. One milliliter fractions were collected and analyzed as above.

3.9.2 Protein precipitation

Very diluted samples were concentrated by precipitation with four volumes of ice cold acetone. The mixture was kept for 30 minutes at -20°C and centrifuged at 13.000 rpm for 20 minutes at 4°C. Samples were then resuspended in smaller volumes of the appropriate buffer.

3.9.3 Splicing reaction

Protein splicing reactions were performed in the elution buffer with addition of Triton X-100 to 0.5% and the corresponding splicing agent. The concentrations used for reducing agents ranged between 1 mM and 200 mM for DTT, 1 mM and 10 mM for TCEP and 100 mM for ß-mercaptoethanol. In case of reactions containing cholesterol (Sigma), a concentration of 500 mM was used and in the buffer was included 1mM of DTT or TCEP. Cholesterol was diluted in water in the stock solution. This low concentration of reducing agent was also added in reactions containing lipid extracts. Cholesterol and lipid extracts stocks were sonified in a bath sonicator before and after addition to the reaction mixture for 15 minutes. Standard incubation conditions were 27°C for 16 to 24 hours. The reaction was stopped by addition of SDS-sample buffer.

3.9.4 Production of antibodies directed against the N- and C-terminus of GmGIN1

Production of antibodies directed against the GmGIN1 amino and carboxy terminus was performed by Seqlab. For the production of antibodies directed against the GmGIN1 amino terminus, 2 rabbits were immunized with the *CREN*

peptide. The two different antisera obtained were called 461 and 476 *antiCREN*. For the GmGIN-C terminus, two different peptides (*CKQD* and *CRVT*) were designed, which were both injected together in two different rabbits. The corresponding antisera obtained were called 474 and 475 *antiCKQD-CRVT*. We first compared the pre-immune sera for the different rabbits and the first bleeding (already with the corresponding antibodies). Samples from cells expressing the His-tagged GmGIN1-C and GmGIN1-N constructs (3.5 µl from 1 ml total cell extract samples resuspended in 100 µl of 1X loading dye) were separated by 14% Tris-Glycine gels. The gels were blotted on Nitrocellulose membranes (Schleicher & Schuell, in this case of 0.45 µm pore size) during 2 h in the Semidry-system from Biorad (60 mA per gel). After Ponceau S staining and blocking, the membranes in pieces were incubated with the two different antibodies at two different concentrations, 1:5000 and 1:10000. Detection continued as described in 3.9.7. The second antibody Goat Anti-Rabbit IgG (H^+L)-Alkaline Phosphatase conjugate (BioRad 170-6518), in dilution 1:10.000 in 2.5% milk in TBST was used for detection. Membranes were equilibrated for two minutes in alkaline buffer (0.1 M Tris-HCl pH 9.5) to adjust to optimal pH for the Alkaline Phosphatase activity. Detection was performed in phosphoimager using the ECF substrate from Amersham.

3.9.5 SDS-Polyacrylamide Gel Electrophoresis of proteins.

3.9.5.1 Tris-Glycine gels

Reagents	5% Stacking gel	12% Running gels	14% Running gels	15% Running gels	16% Running gels
H_2O	3 ml	4.75 ml	4 ml	3.75 ml	3.5 ml
Acrylamide-BisAcry. 40%	500 µl	3 ml	3.5 ml	3.75 ml	4.0 ml
Buffer 1.5 M TrisHCl pH 8.8		2.5 ml	2.5 ml	2.5 ml	2.5 ml
Buffer 1.0 M TrisHCl pH 6.8	500 µl				
SDS 10%	40 µl	150 µl	150 µl	150 µl	150 µl
APS 10%	40 µl	150 µl	150 µl	150 µl	150 µl
TEMED	3 µl	5 µl	5 µl	5 µl	5 µl
Final volume	4 ml	10 ml	10 ml	10 ml	10 ml

3.9.5.2 Schägger-Jagov gels

Reagents	Stacking gel	Running gel
H_2O	4.032 ml	2.17 ml
Acrylamide/bisacrylamide mix (48%solution/1.5%)	480 µl	3.61 ml
S/J gel buffer	1.488 ml	3.61 ml
Glycerol 87%		1.45 ml
APS 10%	100 µl	145 µl
TEMED	10 µl	14.5 µl

3.9.5.3 Casting and running of gels

The components of the running gel were mixed in the order described in the table above in a small beaker. The mix should be homogeneous and care should be taken to avoid bubbles. Once the TEMED was added, the mixture would start to polymerize, therefore it had to be poured immediately in precast plastic plates sealed with agarose. The mixture was covered with isopropanol, as contact with oxygen during polymerization should be avoided. When polymerization was completed (30 minutes), the isopropanol was removed and the surface was washed with distilled water. The space between plates was dried with filter paper and the stacking gel mixture was poured in. Care should be taken when placing the comb not to introduce bubbles.

Samples were prepared by adding the sample buffer in the corresponding dilution. Samples were boiled during 8 minutes to denature proteins and briefly spun down. Very dense samples were centrifuged for 3 minutes.

After polymerization was completed, the comb was removed and the remaining unpolymerized acrylamide was washed away with 1X Running Buffer. The gel was mounted in the electrophoresis apparatus. Running buffer was added in the inner chamber until the gel was covered. Then samples were loaded and the outer chamber was filled with running buffer. The chamber was closed and connected to the power supply. 50 mA was used as starting current, once the sample front had reached the running gel current was increased up to 100 mA

When running Schägger-Jagov gels, 25 mA were used as starting current and it was increased afterwards to 30 mA. Electrophoresis was stopped once the loading dye has reached the bottom. Gels were either assembled for western blotting or stained. Staining was performed in Coomassie Blue staining solution either for one hour at room temperature or for 2 minutes with heating in the microwave and followed by 10 minutes shaking. Then the staining solution was replaced by destaining solution and was changed as many times as necessary to remove the background staining.

3.9.6 Western-blot transfer

Gloves have to be worn all the time and the membrane should never be touched without them. The membrane and filter paper (2 sheets) were cut

according to the gel size. Nitrocellulose membranes (Schleicher & Schuell, 0.2 µm pore size) were directly equilibrated in transfer buffer. When using PVDF membranes (Schleicher & Schuell, 0.2 µm pore size), membranes were pre-wetted in 100% methanol. After that, deionized water was slowly added while shaking until methanol was diluted to 20%. Then the membrane was equilibrated in transfer buffer.

Blotting pads were soaked in transfer buffer until saturated. Air bubbles were removed by squeezing the pads while submerged in buffer. Watmann 3MM filter papers (two, for each side) were soaked briefly in transfer buffer immediately before use. The gel should be immediately transferred following the run. The remaining SDS of the running buffer in the surface of the gel facilitates the transfer. The cassette was opened and the wells and stacking gel were cut out of the gel. A piece of presoaked watmann paper was laid on top of the gel just above the foot of the gel leaving this uncovered. Filter paper was kept saturated and air bubbles were removed. The sandwich was put facing down in order to remove the gel from the plate. Once the gel was over a flat surface the foot was cut off. The surface of the gel was wetted with transfer buffer and the membrane was placed on top of it. Air bubbles were removed and the other filter paper was placed on top of the membrane. Two presoaked pads were located in the deeper part of the module (cathode) and then the sandwich with the gel closer to the cathode. The other two pads were placed on top and the chamber was closed with the anode chore. The blotting module was assembled inside the transfer chamber and the inner chamber was filled with transfer buffer until the sandwich was covered. The bottom chamber was filled with deionized water. The transfer was run under recommended conditions, either 30 V / 3h (expected current: start 170 mA, end 110 mA) at room temperature or 15-20 V over night at 4°C. After the transfer, the membrane was directly detected or stored at -20°C.

3.9.7 Western blot detection

The membrane was washed with TBS to get rid of the remaining methanol. Transfer efficiency was checked by Ponceau S staining for 15 minutes. Then the membrane was rinsed with water to obtain transient stain. The transferred

gel was also re-stained with Coomassie blue to confirm transfer efficiency. The staining was completely removed from the nitrocellulose membrane by washing in TBS. All steps were performed at room temperature. The membrane was incubated in Blocking Buffer 5% BSA or skimmed milk TBST for 1 h. Then the membrane was transferred into a clean 50 ml reaction tube and incubated with the first antibody solution for another hour. The membrane was then washed four times for 10 minutes with TBST and equilibrated for 20 minutes in the second blocking solution. The membrane was then incubated with the second antibody diluted in blocking buffer 2 for one to two hours. Afterwards the membrane was washed four times for 10 minutes with large volumes of TBST and transferred to a clean tray. Meanwhile the detection substrate was equilibrated in the dark to room temperature. The membrane was dried and placed on a piece of plastic film. Then the substrate solution was added on top of it and left for 60 seconds, after which the excess of reagent was removed and a film is put on top of it. The first film was exposed from 10 to 60 seconds and developed. The luminescence reaction reached its maximum after 1-2 minutes and was relatively constant for 20-30 minutes. If signal intensity was too high, re-exposure was continued after 10 minutes.

3.9.8 Stripping and reprobing

The membrane was incubated in stripping buffer with gentle shaking for 30 minutes at 50°C. After that it was washed twice for 15 minutes with large volumes of TBST at room temperature. Blocking and detection was performed as described above.

3.9.9 In-gel trypsin digest

The protein band was cut out using a clean scalpel and divided into small pieces, which were placed in a 1.5 ml reaction tube. The sample was twice cleaned by shaking for 15 minutes with 2 volumes of Milli-Q-water/ Acetonitril (MQW/ACN 1:1 v/v). The washing solution was discarded and one volume ACN was added, mixed and incubated for 5 minutes at room temperature. The ACN was removed and one volume 100 mM BiCa was added, mixed and 5 minutes incubated at room temperature. Then another volume of ACN was added to

make a BiCa/ACN 1:1 solution, and the mixture was incubated for 15 minutes shaking at room temperature. The solution was discarded and samples were dried in a vacuum centrifuge. For reduction and alkylation of the cystein residues, 2 volumes of DTT solution were added to the samples and they were incubated at 56°C for 45 minutes. Samples were then equilibrated at room temperature for 5 minutes, the solution was discarded and 2 volumes of iodacetamid solution was added and incubated in the dark for 30 minutes. The solution was discarded and one volume of 100 mM BiCa was added and the mixture was incubated with shaking at room temperature for 15 minutes. The same volume of ACN was added and the mixture was incubated for 15 minutes with shaking at room temperature. The solution was removed and the last two steps were repeated as long as the gel exhibited residual Coomassie staining. Samples were dried in a vacuum centrifuge. Trypsin solution was added in 10 µl aliquots and the samples were incubated on ice for 10 minutes. Aliquots of trypsin solution were added until the gel was swollen and saturated with solution. Then the spare trypsin solution was removed and the gel pieces were covered with 25 mM BiCa solution and incubated at 37°C over night. Next day, samples were sonified for 2 minutes and the solution was collected in a clean reaction tube. One volume of 25 mM BiCa was added to the remaining samples and the mixture was incubated with shaking for 15 minutes. After this, one volume of ACN was added to make a BiCa/ACN 1:1 solution and the mixture was incubated for additional 15 minutes. Samples were then sonified for 2 minutes and the solution was removed and combined together with the previous extracts in the clean reaction tube. Then the gel pieces were incubated with shaking in a mixture of 5% (v/v) formic acid/ACN 1:1 for 15 minutes and the solution was collected. The combined extracts were evaporated in a vacuum centrifuge at 60°C to a 10-15 µl volume and stored at -20°C.

3.9.10 Determination of protein concentration by Bradford reagent

Protein concentration was determined with the Bio-Rad Protein Assay (Bio-Rad, Hercules. Calif. USA) in microtiter plates. Fifty microliters of protein extract were analysed using 50 µl of a 1:5 dilution (Bradford reagent:H_2O) in 100 µl extraction buffer. Three repetitions of every sample were carried out. The

absorbance was determined at 620 nm in a plate photometer (340 ATTC, SLT Lab Instruments). A BSA calibration curve with concentrations between 0 and 1 mg/ml was used to calculate protein concentration in the extracts.

3.9.11 Protein extraction of mycorrhizal samples

Samples of *G. intraradices* spores, hyphae or mycorrhizal roots from *D. carota* were homogenized with pistile and mortar after addition of 250 µl ice cold extraction buffer in liquid nitrogen. The mixture was put into a reaction tube and the volume of buffer was adjusted to 500 µl, thawed and centrifuged at 4°C and 10,000 rpm for 20 minutes. The supernatant was collected in a new eppendorf and stored at -20°C.

3.9.12 Lipid extraction

Samples from external mycelium and spores from *Glomus intraradices* and carrot roots mycorrhizal with *Glomus intrarradices* and non-mycorrhizal were taken in order to perform lipid extraction following different extraction methods for neutral lipids. Root samples were extracted by the Folch method and the Nichol method protocols described by Christie (*Lipid Analysis*, 1982, Pergamon). Hyphae and spores were extracted according to Beilby et al. All organic-lipidic fractions were dried in a rotor evaporator and resuspended in chloroform. Fractions used in splicing reactions were resuspended in water or in water added with 0.7% Triton X-100.

3.9.12.1 Folch method (Folch et al., 1957).

One g *G. intrarradices* mycorrhizal roots were homogenized for 1 minute in 10 ml methanol with pestle and mortar. Afterwards 20 ml Chloroform were added and samples were homogenized for 2 additional minutes. The mixture was filtered and the solid residue was resuspended in 30 ml chloroform/methanol (2/1, v/v). It was homogenized for 3 minutes. The sample was filtered again and the solid residue was washed first with 20 ml chloroform and then with 10 ml methanol. The combined filtrates were set in a measuring cylinder and 0.25 volumes of a 0.88% KCl/water solution were added. The mixture was shaken

and allowed to settle down. The upper layer was removed by aspiration. To the lower layer, 1/4 of the volume of a mixture methanol/water (1/1, v/v) was added. The washing step was repeated with KCl solution. The purified lipids were retained in the bottom layer, which was dried on a rotary evaporator and resuspended in a small volume of chloroform (0.3 ml). Samples were stored at –20°C.

3.9.12.2 Lipid extraction according to Beilby et al. (1980).

The material to be extracted (spores and hyphae from *G. intraradices*) were broken in mortar and pestle first with liquid nitrogen and then with a small volume of methanol at 0°C. The volume of methanol was adjusted to 0.5 ml and the tube was shaken. 1ml of chloroform was added and the tube was shaken for 1 hour at 4°C. The extraction process was repeated three times, the last time at room temperature. The extracts were washed with 0.2 volumes of a 0.9% w/v NaCl solution. After phase separation the chloroform phase was removed and the aqueous phase was extracted twice with 40 volumes of a chloroform/methanol/saline (86/14/1, v/v) mixture. All chloroform extracts were combined together for drying in a rotary evaporator. Lipids were resuspended in a small volume of chloroform and stored at –20°C.

3.9.12.3 Lipid extraction according to Nichols et al. (1965).

This method was also applied to *G. intrarradices* mycorrhizal roots. This method includes a preliminary incubation in isopropanol to inactivate plant lipases. 100 ml of isopropanol was added to 1g of roots ground by with a pestle using liquid nitrogen and macerated in a mortar. The mixture was filtered and the filtrate was kept at room temperature. The solid was extracted again with 200 ml of a chloroform/isopropanol (1/1, v/v) mixture. The extract was filtered and the combined filtrates evaporated. The resulting residue was dissolved in a small volume of chloroform/methanol (2/1, v/v) and washed according to the Folch method (with 0.88%KCl solution). The lipids were recovered from the lower phase, dried and resuspended in chloroform.

3.9.12.4 Lipid extraction according to Blight and Dyer (1959)

The material was first ground with mortar and pestle using liquid nitrogen. Samples corresponding to spores (2.4 g), non-mycorrhizal roots, mycorrhizal roots (3 g) and *A. muscaria* mycelium (3 g) as control were extracted with 10 ml of a mixture of methanol/dichloromethane (2/1, v/v) for 2 hours with vigorous shaking. The extracts were then pelleted at 10,000 rpm for 10 minutes and the supernatant was loaded over a separatory funnel and the pellet was once again extracted with methanol/dichloromethane/water (2/1/0.8, v/v/v) for 2 hours. This extract was pelleted again, and the extracts combined and the pellet extracted with the same solvent mixture. To the combined extracts (30 ml) 10 ml of water and 10 ml dichloromethane were added and the mixture was shaken 5 times by hand and the phases were allowed to separate overnight. The lipid extracts (lower phase) were dried in a rotary evaporator and stored at -20°C.

3.9.12.5 Extraction of unsaponified fraction (Entenman, 1957).

This extraction method was performed with spores and external mycelium from *G. intraradices*, non-mycorrhizal roots, and mycorrhizal roots. The material was first ground in liquid nitrogen with a pestle in a mortar. Then it was digested and saponificated with KOH. 2 ml of 30% KOH per gram of tissue were added and the mixture was heated to 80-100°C. Ethanol was added to make a final 50% suspension. Digestion was carried out for 4 hours. After this, ethanol was allowed to evaporate and the material was filtered and washed with a small volume of ethanol. Ethanol was added to the filtrate to make a 50% solution, which was extracted 3 times in a separatory funnel with petroleum ether in a ratio of 5 to 1 volume of ethanol solution. The combined petroleum ether extracts were washed with small portions of 2 N KOH twice and over 5 times, or until the washes were neutral, with distilled water. The petroleum ether extract contained the unsaponificable material, including sterols. The extract was dried in a rotary evaporator and resuspended in water added with 0.7% Triton X-100 by sonication. These fractions were stored at -20°C.

3.9.13 Lipid column chromatography

The silica gel soil (G60 Merck) was packed into a glass column with dichloromethane and allowed to settle to give a bed volume of 4 to 4.5 ml. Lipid extracts were loaded with a Pasteur pipette. The lipids were eluted using 10 volumes of dichloromethane, 40 volumes of acetone and 10 volumes of methanol in subsequent steps. Fractions corresponding to the three elutions were dried in a rotary evaporator and kept at -20°C. For analysis of the fractions, lipids were dissolved in the same solvent used during the elution.

3.9.14 Thin layer chromatography (TLC)

Samples from the silica gel chromatography were loaded in TLC plates dissolved in the same solvent in which they were eluted. Lipid standards and total lipids, as insaponificable lipid extracts were loaded as dichloromethane solutions. For routine analysis of lipid samples, silica gel G plates without fluorescent indicator were used (Merck, Silica gel 60). After a first migration in dichloromethane/methanol (1/1, v/v) in a specialized tank followed by rapid drying, lipids were applied as spots at 1.5 cm from the bottom, and plates were developed in the solvent mixture: hexane/diethyl ether/acetic acid (70/30/1, v/v/v). Using the same type of plates, lipids were also resolved using two runs of dichloromethane in order to distinguish among different types of sterols, according to the degree of methyl group substitution at C-4. For analysis of the unsaponificable fractions, HPTLC- Alufolien plates (Merck, Silica gel 60 F254) were used. Plates were developed in a dichloromethane/methanol/water (85/15/0.5) solvent mixture. Acetylated lipids were resolved in analytical TLC on 10% $AgNO_3$-silica gel plates. In these plates sterols differing by the degree of unsaturation and position of double bonds in either the ring system or the side chain can be separated. Migration was performed for 15 hr with cyclohexane/toluene (7/3, v/v) to separate the 4,4-dimethyl and 4-demethyl steryl acetates and (3/2, v/v) to separate the 4α-methyl steryl acetates. The TLC plates were sprayed with a 0.1% berberin-HCl ethanol solution and revealed in UV-light or using a Molibdatephosphoric acid solution (Merck) followed by heating at 120°C for 10 minutes.

3.9.15 Lipid acetylation

Dry lipid samples were resuspended in 500 μl of dry pyridine and 500 μl of acetic acid anhydride, mixed and left for 16 hours at room temperature.

3.9.16 Sterol content quantification

Sterol-acetylated samples were dried and weighted. 0.2 mg of acetyl-cholesterol, used as standard, were added to each sample and sterols were analysed by Gas Chromatography (GC) in GC-9A (Shimadzu) with the following programme.

Integrator	C-R3A Chromatopac (Shimadzu)
Detector	flame ionization detector
Unpolar soil	capilar soil DB1701 (Phenyl-Cyanopropyl-Methylsilicone phase)
	length 20 m
	internal diameter 0,32 mm
	soil thickness 0,25 μm
Programme temperature	250-320°C with 4°/min
	320°C 10 min isotherm
Injector temperature	330°C
Split	1:10

Areas from peaks corresponding to 0,2 mg of acyl-cholesterol were compared with the areas obtained for the different sterols, obtaining the subsequent mass values. These values were relative ro the total dry weight of the samples before addition of the standard, and were standardized for 10 mg of total lipid weight for comparison.

3.9.17 Gas liquid chromatography- mass spectrometry (GC-MS)

GC-17A (Shimadzu), coupled to QS-5000 MS (Shimadzu).

Programme		
Oven temperature	250°C	
Injector temperature	320°C	
Interface temperature	300°C	
Unpolar soil	capilar soil DB5 (Methylsilicone phase)	
	length	15 m
	internal diameter	0,25 mm
	soil thickness	0,25 µm
Column pressure	4,3 (KPa)	
Column flow	0,4 ml/min	
Linear velocity	36,0	
Split ratio	15	
Total flow	6,5 (ml/min)	
Initial	250-320°C with 4°/min	
	320°C 10 min isotherm	
Detector	2,00 (KV)	
Mass range	start 50,00	end 700,00
	scan modus	

3.9.18 GTP-binding and hydrolysis activity

3.9.18.1 GTP overlay assays

Ni-NTA agarose purified proteins (GmGIN1-N, Umcdc42 wild type and Umcdc42(Q-L) mutant) and total lysates of *E. coli* expressing these proteins were tested for their ability to specifically bind GTP. Samples were run in Tris-Glycine SDS-PAGE gels and transferred to nitrocellulose membranes (Schleicher and Shuell). After transfer the membranes were rinsed in Binding Buffer and blocked for 30 minutes at room temperature. After this the membrane was incubated in Binding Buffer containing 2 µCi/mmol of α-^{32}P-GTP for 2 hours at room temperature. Then the membrane was washed several times with Binding Buffer for 30 minutes to one hour. Membranes were air dried and exposed to an X-ray film from 24 to 120 hours at -80°C. Two different binding buffers were tested in this assay: GTP-Binding buffer1 [Tris/HCl pH 7.5

(20 mM); Tween 20 (0.1%), milk powder (1%), $MgCl_2$ (5 mM)] and GTP-Binding buffer2 [Tris/HCl pH 7.5 (50 mM), Tween 20 (0.1%), BSA (5%), $MgCl_2$ (5 mM), EGTA, (5 mM)].

3.9.18.2 GTP binding filtration assays

His-tagged proteins (GmGIN1-N, Umcdc42 wild type and Umcdc42(Q-L) mutant) purified under native conditions were assayed for their capacity to bind GTP in solution under native conditions. The elution buffer for purification of these proteins contained a lower amount of NaCl (300 mM) and Imidazol (300 mM) not to interfere with the activity of the proteins in the final reaction. The stock solution of ^{35}S-γ-GTP (Amersham), a non-hydrolyzable analogue of GTP, consisted of a mixture of radioactive and cold S-γ-GTP (Roche), resulting in a concentration of 200 µM nucleotide and 2000 cpm/pmol radioactive labelling. This solution results from mixing 90 µCi ^{35}S-γ-GTP and 50 µl cold S-γ-GTP (2 mM), and completing to 0.5 µl with water. The reaction mixture contained 10 µM ^{35}S-γ-GTP, in a final volume of 50 µL reaction. After incubation of the proteins in GTP binding activity buffer [Hepes/NaOH pH 7.5, (50 mM), Dithiothreitol (DTT) (1 mM), EDTA (2 mM), $MgCl_2$ (1 mM)] at 37°C, 50 µl of the reaction mixture were diluted in 2 ml washing buffer [Hepes/NaOH pH 7.5 (20 mM), NaCl (100 mM), $MgCl_2$ (10 mM)] in order to stop the binding reaction. These aliquots were filtered through nitrocellulose filters (0.45 µm pore size, Sartorius) using a vacuum filtration manifold unit. Filters were washed twice with washing buffer, dried and counted.

3.9.18.3 Dissociation assay using competing nucleotides

Purified GmGIN1-N and Umcdc42 wild type under native conditions were allowed to bind ^{35}S-γ-GTP in the same conditions as described in 3.6.18.3 for 45 minutes. After this, aliquots of 50 µl were collected, filtered and radioactivity was measured as described above. At this initial time point, an excess of competing cold nucleotide (GDP, GTP, ADP or ATP) was added to a

concentration of 1 mM. Aliquots were collected at different time points to asses the decrease in bound ^{35}S-γ-GTP.

3.9.18.4 Enzymatic activity of GmGIN1-N

Native purified GmGIN1-N was incubated with 1 µl radiolabelled α^{32}P-ATP or α^{32}P-GTP (10 mCi/ml) (Amersham) in 10 µl hydrolysis buffer [Tris-HCl pH 7.5, (50 mM), NaCl (50 mM), DTT (1.5 mM), EDTA (0.1 mM), $MgCl_2$ (10 mM)] at 30°C. Two µL aliquots from the reaction mixture were removed at different time points and frozen to stop the hydrolysis reaction. The same reaction mixture but lacking the protein was used as negative control. Aliquots were spotted onto silica gel G60 thin layer chromatography (TLC) plates (Merck) and resolved for 12 h with a mixture of isobutyl alcohol:isoamyl alcohol:2-ethoxyethanol:ammonia:water (9:6:18:9:15). Plates were dried and exposed to an X-ray film for 10 h. Nucleotide non-radioactive standards were resolved in an analogous manner in silica gel 60 F254 TLC plates (Merck) in order to compare the running distances of the spots. Non-radioactive standards were visualized with UV light.

4 Results

4.1 Recombinant expression in *E. coli* of GmGIN-1 C terminus

4.1.1 Expression using the pTrcHis-TOPO vector

The C-terminus from GmGIN1 protein shares similarity with the auto-splicing domain of Hedgehog proteins (Requena et al., 2002; Figure 9). Accordingly, it contains the conserved amino acids that have been demonstrated to be indispensable to perform self-splicing of Hedgehog proteins (Figure 9). In order to demonstrate that GmGIN1 can also be processed in an analogue manner, its C-terminus (GmGIN1-C), which should be sufficient to induce self-splicing, was expressed recombinantly in *E. coli*. For this purpose the GmGIN-C terminus was cloned into the expression vector pTrcHisTOPO from Invitrogen. This vector allows recombinant production of proteins with a tight control of expression. The pTrcHis vector incorporates a hexahistidine tag (His-tag) in the N-terminus of the protein to allow its purification by metal affinity chromatography with Ni-NTA agarose. This tag was chosen because of its small size, which was shown not to interfere with the protein self-splicing function in Hedgehog proteins (Porter et al., 1996a). The vector also incorporates the HisG epitope and the Xpress epitope, which enable the recognition of the protein by immunodetection after Western blot (Table 1). The vector also incorporates an enterokinase cleavage site for removal of the His-tag.

Peptide	Size	AntiXpress recognition
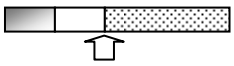	28 kDa	+
	7 kDa	+
	21 kDa	-

Table 1. His-tag construct of GmGIN1-C. Scheme showing position of the His-tag (in grey), Splicing junction in GmGIN1-C (arrow) and peptides resulting from the self-splicing: His-tag plus N-terminal fragment (white square) and C-terminal fragment (black dots). The molecular weight of the peptides is indicated, and their recognition or not by immunodetection with AntiXpress antibody.

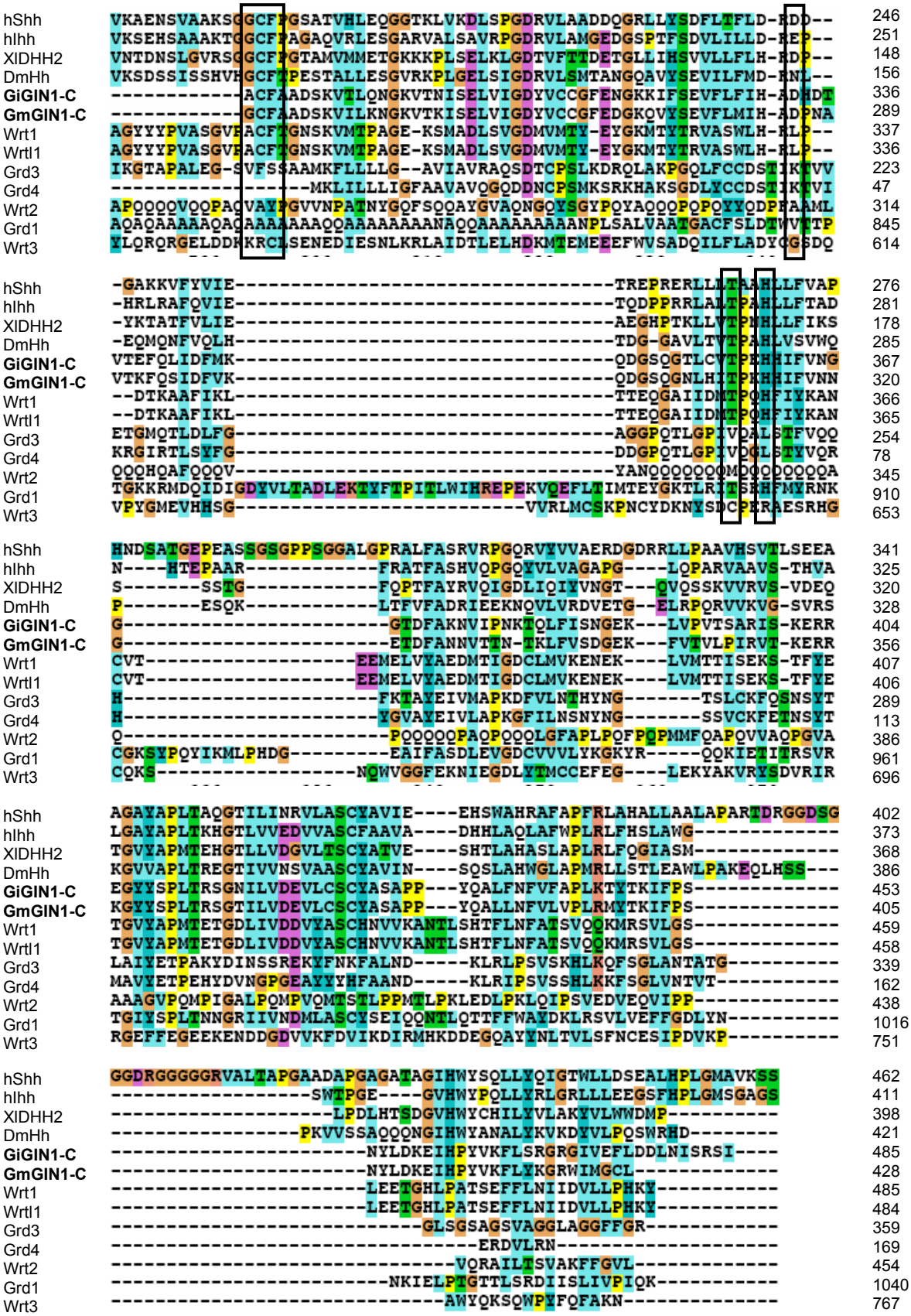

Figure 9 . Multiple alignment GmGIN1-C and GiGIN1-C with the C-terminus of several Hedgehog (Hh) proteins: hShh, human Sonic Hh (NP000184); hIhh, Indian Hh (NP002172); XlDHH2, *X. laevis* Dessert Hh (Q91611); *C. elegans* Warthog (Wrt) proteins: Wrt1 (NP495579); Wrt2 (NP508529); Wrt3 (NP501673); Wart-like protein Wrtl1 (AAB93321); and Ground (Grd) proteins: Grd1 (NP741901); Grd3 (NP500346); Grd4 (NP509442). Amino acids involved in splicing are boxed.

Cloning of GmGIN1-C terminus was achieved by PCR amplification with the primers GmGINExF1 and GmGINExR1 as described in material and methods. The corresponding fragment of 626 bp (Fig. 10, A) was ligated into pTrcHisTOPO and transformed into chemically competent XL1-Blue and TOP-10 *E. coli* cells. Recombinant clones were analyzed by plasmid DNA extraction and restriction analysis. Positive clones were verified to contain the insert in the forward orientation by PCR using the pTrcHis Forward and GinExR1 primers. The sequence of the insert was checked not to contain any error by sequencing.

First protein expression studies were preformed with TOP-10 *E. coli* cells, using empty cells as negative control and the lacZ reporter gene also expressed in pTrcHis as positive control. Cells expressing the lacZ produced a protein of 40 KDa in comparison to empty cells, while cells containing the pTrcHisGmGIN1-C produced a protein of 28 KDa (Fig 10, B).

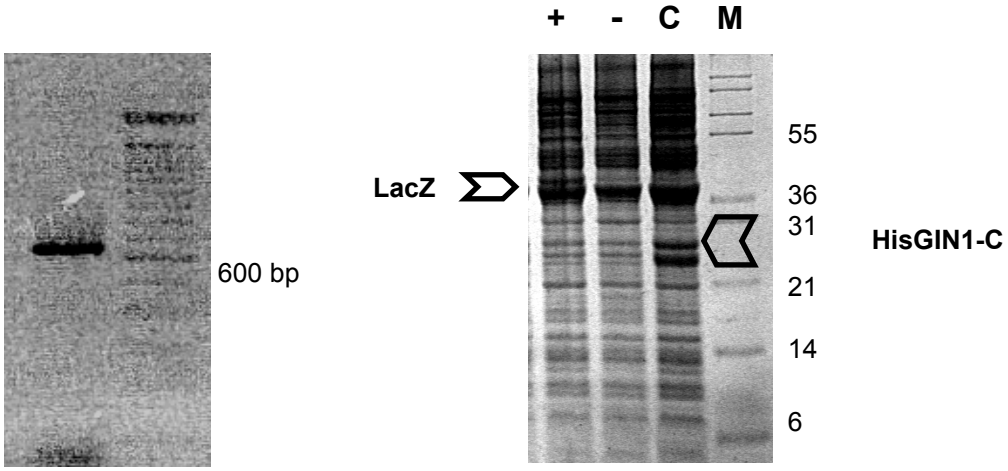

Figure 10. A. PCR product GinExF1/R1. B. Expression pTrcHisGmGIN1-C in TOP10 cells. Comparison between TOP10 expressing the positive control lacZ protein (+),negative control empty TOP10 cells (-) and TOP10 expressing the pTrcHisGmGIN1-C construct (C).

A time course of protein production was performed in order to know which time point after induction provided the optimal yield. It could be shown that levels of protein expression reached a maximum after 4 hours of induction (Fig. 11).

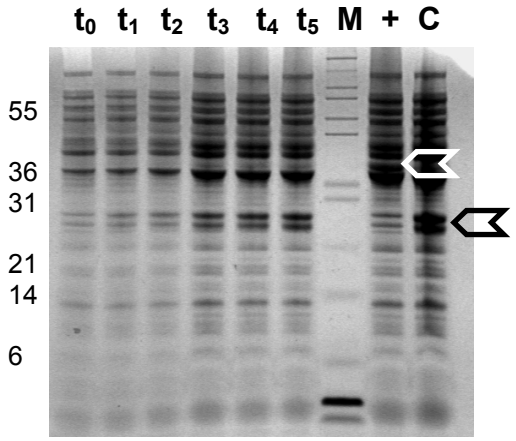

Figure 11. Time course of expression of pTrcHisGmGIN1-C in TOP10 cells. t_0 before addition of inducer, t_1 to t_5 - samples collected each hour after induction with IPTG, TOP10 expressing the positive control lacZ protein (+), TOP10 expressing the pTrcHisGmGIN1-C construct (C). Arrows indicate the protein band positions.

The protein of 28 kDa was confirmed to correspond to the C-terminus of the GmGIN1 protein by immunodetection and mass spectrometry (Fig. 12 and Table 2). This construct was also cloned into other *E. coli* cells such as XL1-Blue, M-15[pREP4] and BL21. M-15[pREP4] produced the highest yield of protein (Fig. 12).

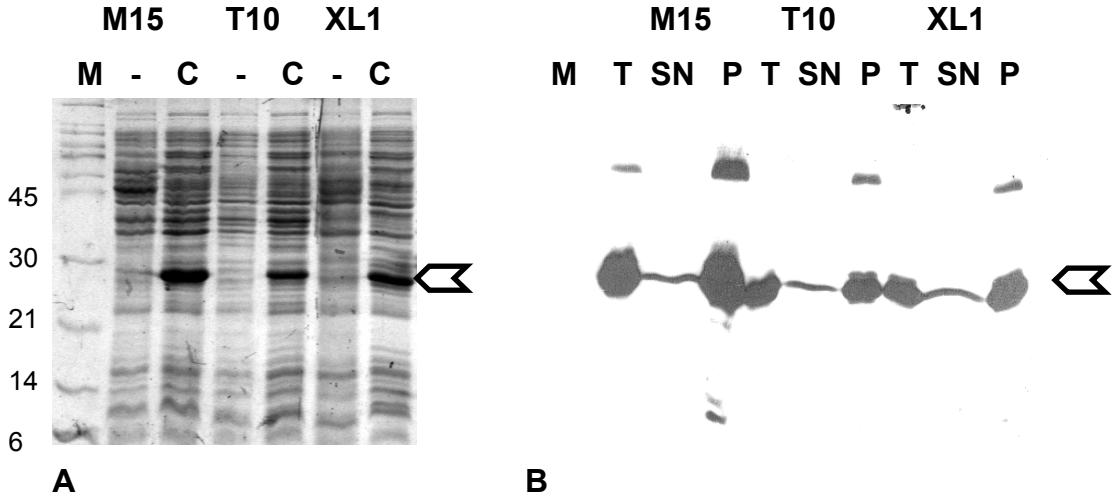

Figure 12. GmGIN1-C expressed in pTrcHis vector in M15, T10 and XL1-Blue *E. coli* cells. A-Coomassie stained gel comparing empty cells (-) with cells expressing GmGIN1-C (C). **B.** Immunodetection with AntiHis antibody (Novagen) comparing the yield of soluble GmGIN1-C produced in the different *E.coli* strains. Total lysate (T), supernatant after native lysis (SN) and pellet (P). Molecular weight marker (M). Arrows indicate the protein band position.

cleavage site	Resulting peptide sequence	Peptide length [aa]	Theoretical mass: Peptide mass [Da]	Theoretical mass: $[M+H]^+$	Theoretical mass: $[M+2H]^{2+}$	Experimentally detected mass
23	MGGSHHHHHHGMASMTGGQQMGR	23	2467	2467,7	1234,4	n. d.
40	DLYDDDDKDPTLGFLTR	17	1999	2000,1	1000,6	√
58	KPVELINDFEGCFAADSK	18	1983	1984,2	992,6	√
62	VILK	4	472	472,6	236,8	√
65	NGK	3	317	318,3	159,7	n. d.
68	VTK	3	346	347,4	174,2	√
86	ISELVIGDYVCCGFEDGK	18	1947	1948,2	974,6	√
105	QVYSEVFLMIHADPNAVTK	19	2162	2163,5	1082,2	√
113	FQSIDFVK	8	983	984,1	492,6	√
126	QDGSQGNLHITPK	13	1395	1395,5	698,3	√
147	HHIFVNNGETDFANNVTTNTK	21	2374	2374,5	1187,8	√
155	LFVSDGGK	8	822	822,9	412	√
163	FVTVLPTR	8	932	933,1	467,1	√
166	VTK	3	346	347,4	174,2	√
168	ER	2	303	304,3	152,7	n. d.
169	R	1	174	175,2	88,1	n. d.
170	K	1	146	147,2	74,1	n. d.
178	GYYSPLTR	8	956	957,1	479	√
210	SGTILVDEVLCSCYASAPPYQALLNFVLVPLR	32	3453	3454,1	1727,5	n. d.
214	MYTK	4	542	542,7	271,8	√
223	IFPSNYLDK	9	1096	1097,2	549,1	√
230	EIHPYVK	7	885	886	443,5	√
234	FLYK	4	570	570,7	285,9	√
236	GR	2	231	232,3	116,6	n. d.
242	WIMGCL	6	722	722,9	362	√

Table 2. Peptide fragments detected experimentally by mass spectrometry (HPLC-ESI-MS). Detected (√) and non detected (n. d.) peptides from all theoretical peptide fragments obtained after trypsin digestion of pTrcHisGmGIN1-C.

4.1.2 Purification of GmGIN1-C expressed in pTrcHis

GmGIN1-C was first purified by Ni-affinity chromatography under denaturing conditions (Fig. 13-A). TOP-10 cells expressing pTrcHisGmGIN1-C were grown at 37°C to an OD_{600} of 0.6-0.7, after which production of the protein was induced with 1 mM IPTG. Denaturing purification was performed from 1 mL of culture in a small scale approach. A single band of 28 kDa corresponding to GmGIN-C was observed (Fig. 13-A). In contrast, purification under native conditions from 100 mL culture resulted in much lower yield of protein. This was the same even when using two different types of resins appropriate for His-tagged protein purification, such as Ni-IDA (Probond system, Invitrogen) and Ni-

NTA (Novagen). When protein solubility was analyzed, we could observe that most of the protein was located in the insoluble fraction after cell lysis, possibly in inclusion bodies (Fig. 13-B). Therefore, only after denaturing purification the protein could be clearly observed in the SDS gels.

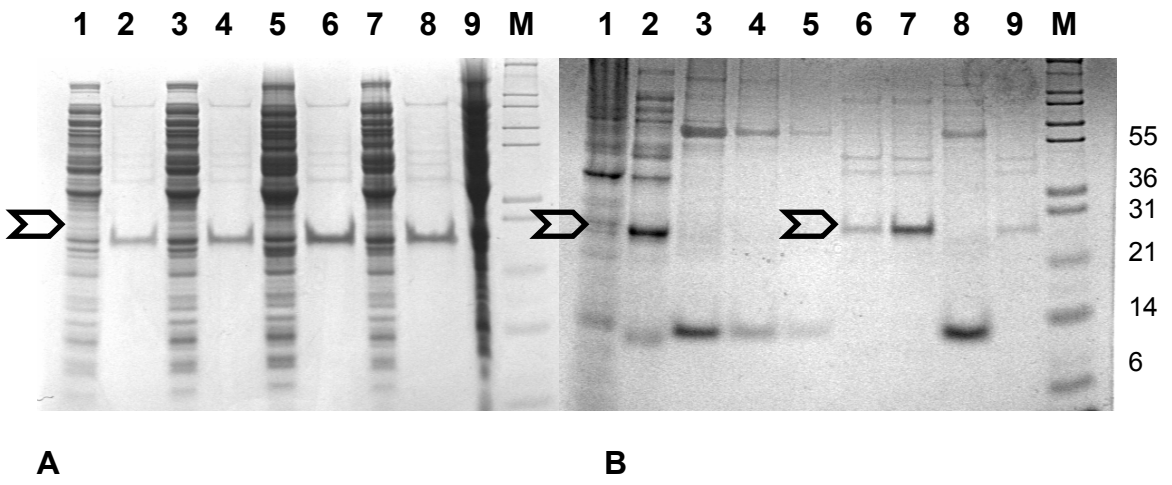

Figure 13. A. total lysates of TOP10 cells expressing pTrcHisGmGIN1-C (1, 2 and 3) compared to purified protein under denaturing conditions (2, 4, 6 and 8). 1- (t_0) before addition of inducer, 2 and 3- 1 h after induction (t_1), 4 and 5- 2 h after induction (t_2), 6 and 7- 3 h after induction (t_3), 8 and 9- 6 h after induction (t_6), M- molecular weight marker. **B. Analysis of pTrcHisGmGIN-C solubility.** 1- Soluble fraction after native lysis 50 mL cell culture; 2- Pellet after native lysis 50 mL cell culture; purifications from 1 mL culture: 3 to 5- elutions of the protein after native purification (6 h induction); 6 and 7- elutions after denaturing purification (6 h induction); 8- elutions after native purification (5 h induction); 9- elutions after denaturing purification (5 h induction).

Several changes in growth conditions (temperature, time of induction, OD before induction) and in induction (time of induction, concentration of IPTG) were tested in order to improve the yield and solubility of the protein. Temperatures of 18° (performing overnight induction), 26° and 37°C were tested. Concentrations of inducer (IPTG) ranged between 0.1 and 1 mM, added once the cell culture had reached an OD_{600} of 0.600, 1.200 or 3.00. Longer times of induction (4 to 6 h) were preferred when induction was performed with cultures induced at OD_{600} of 0.600, while shorter times of induction (3 to 4 h) were chosen for later induction. The best conditions for native GmGIN1-C purification were an induction at OD_{600}= 0.600 using 0.35 mM of IPTG, while keeping the original growth temperature at 37ºC (Fig 14-A). Different strains of *E. coli* were tested as BL21 (protease deficient), XL-1 Blue and M-15[pREP4]. The most efficient strain was M-15[pREP4].

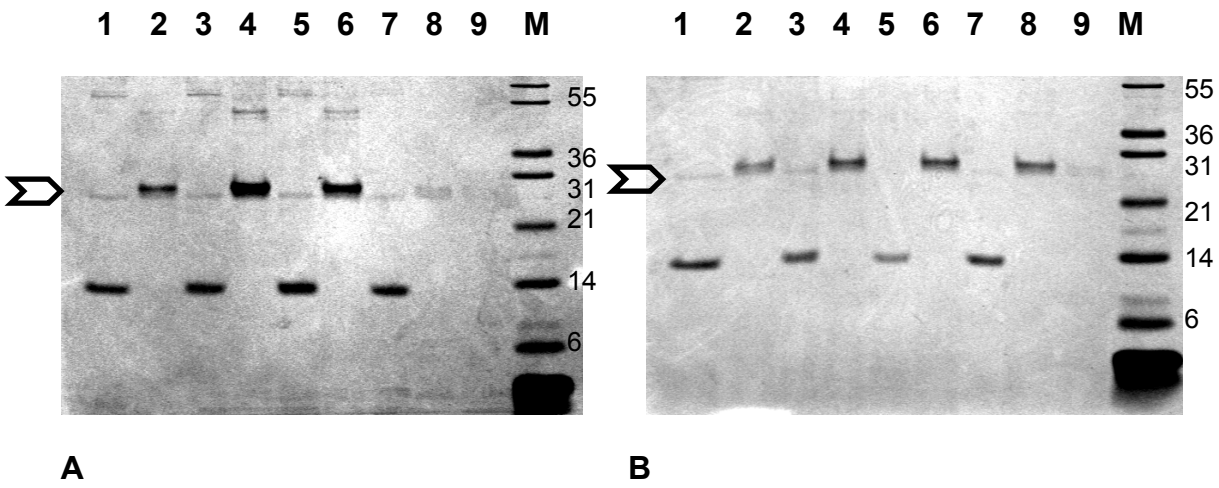

Figure 14. Test for incresing solubility of pTrcHisGmGIN1-C. Induction was performed at an OD_{600} of 0.6 **(A)** or 1.2 **(B)** at 37°C changing the amount of inducer.1,2- 0.1 mM IPTG purification under native (1) and denaturing conditions (2); 3, 4- 0.25 mM IPTG purification under native (3) and denaturing conditions (4); 5, 6- 0.35 mM IPTG purification under native (5) and denaturing conditions (6) ; 7, 8, 9- 1 mM IPTG purification under native (7) and elution 1 (8) and 2 (9) after purification under denaturing conditions

4.1.3 Cloning and expression in pRSETb vector

GmGIN1-C was also cloned in the pRSETb vector from Invitrogen. This vector was previously used by P. A. Beachy group to express the C-terminus of *D. melanogaster* Hedgehog protein of (DmHh-C) (Lee et al. 1994; Porter et al., 1996a). DmHh-C comprises amino acids 83 to 471 with a deletion from 89 to 254, which deletes most of the N-terminus from Hh mature protein (Lee et al, 1992). This construct contains the amino acids sufficient to provoke the self-splicing processing of the protein *in vitro*. We used DmHh-C protein as a control of expression and purification with the Ni-NTA resin and as a positive control for the splicing reaction. The pRSETb vector also incorporates a hexahistidine tag at the N-terminus of the protein. The vector also incorporates the RGSHis and the Xpress epitopes at the N-terminus of the protein to enable recognition of the protein by immunodetection. It also contains the enterokinase cleavage site. In order to express both proteins, GmGIN1-C and DmHh-C, in the same vector and with the same cellular background we transferred *GmGIN1-C* from pTrcHis vector into pRSETb.

For that pTrcHisGmGIN1-C was excised from pTrcHis vector using EcoRI and BamHI, and subsequently ligated in pRSETb vector linearized with the same enzymes (Fig. 15-A). Positive clones were obtained by bacterial colony

hybridization, and confirmed by enzyme restriction and PCR analysis using GinExF1 and GinExR1 primers (Fig. 15-B).

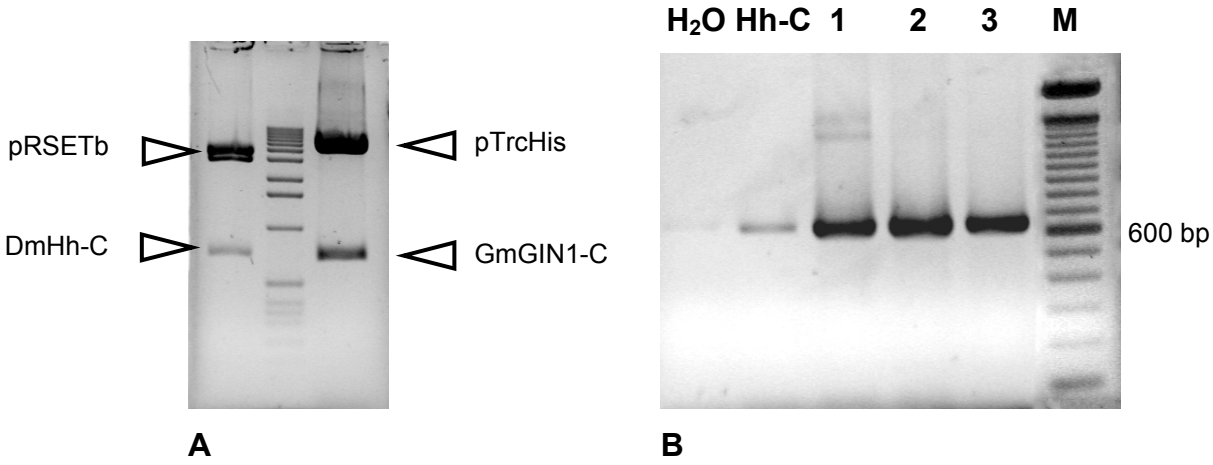

Figure 15. Change of *GmGIN1-C* gene from pTrcHis to pRSETb vector. A. Double digestion with EcoRI and BamHI of pRSETb (2.9 Kb) containing *DmHh-C* insert and pTrcHis (4.39 Kb) containing *GmGIN1-C* gene. **B.** PCR verification with GinExF1/R1 primers. As negative controls water and plasmid containing the *DmHh-C* insert were used. 1 to 3- positive clones after ligation of *GmGIN1-C* in pRSETb vector.

The pRSETb vector allows protein expression under the control of the viral T7 promoter. For this purpose, this vector needs the co-expression of the T7 RNA polymerase. The T7 RNA polymerase gene is present in the *E. coli* genome of BL21(DE3) cells and derivatives. The expression of T7 RNA polymerase is under the control of the lac promoter, and can be induced by addition of IPTG to the cell culture, constituting a double controlled system of expression. For this reason BL21(DE3) *E. coli* cells were used for the expression of the pRSETb constructs. A larger amount of GmGIN1-C protein was obtained when using this expression vector. However, again very little of the protein was located in the soluble fraction after native lysis. Standard expression conditions consisted of an overnight induction with 0.5 mM IPTG at 18°C after the cells had reached an OD_{600} of 0.6. Induction at 37°C for 4 hours rendered similar results (Fig 16-B). Surprisingly, protein expression was not controlled at all, and expression of protein can be detected even without induction with IPTG (Fig. 16 and Fig. 17, t_0). Different media were also tested to see whether the amount of soluble protein could be increased. While LB media render higher yield of GmGIN1-C protein expressed in pTrcHis vector, similar yields could be obtained when the protein was expressed in the pRSETb vector using LB or TB medium (Fig. 16).

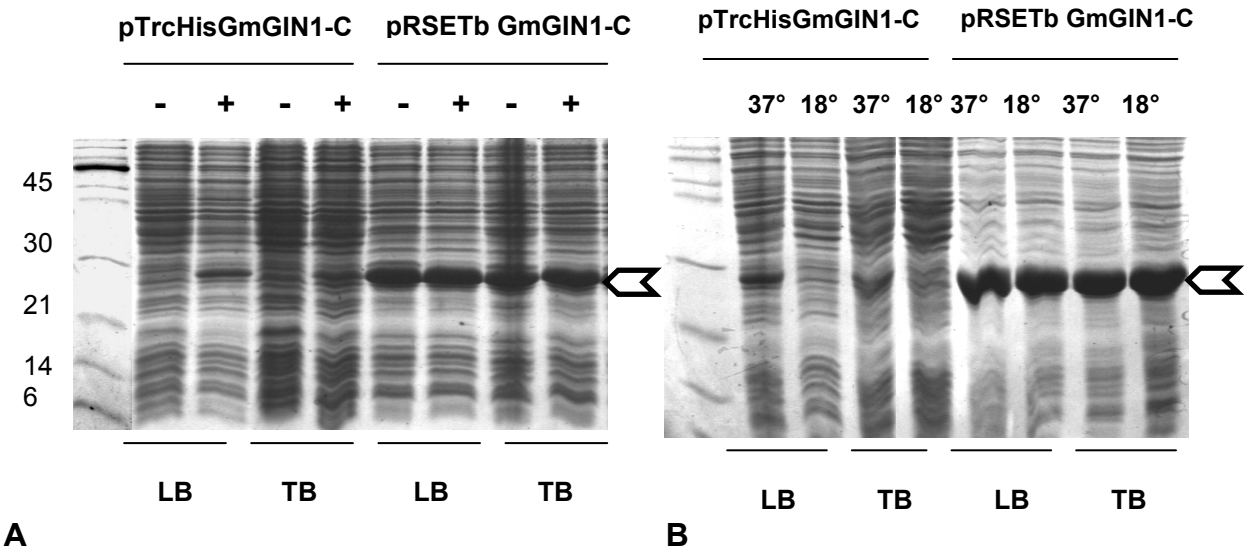

Figure 16. Comparison fo expression of GmGIN1-C in pTrcHis (TOP-10 cells) and pRSETb (BL21(DE3) cells) vectors under different conditions. A. Non-induced (-) and induced (+) cultures with 0.5 mM IPTG after 4 hours of growth were compared. **B.** Induction at 37°C/4 h and at18°C/over night. Two different media, Lb (LB-Broth) and TB (Terrific Broth) were tested. Arrows indicate the GmGIN1-C position.

Expression levels using BL21(DE3)pLyS cells, that theoretically allow a more controlled protein expression, rendered a very low yield of protein (Fig. 17-B). These cells include an extra plasmid (pLyS), which expresses low amounts of lysozyme. This binds and blocks uncontrolled expressed T7 RNA polymerase.

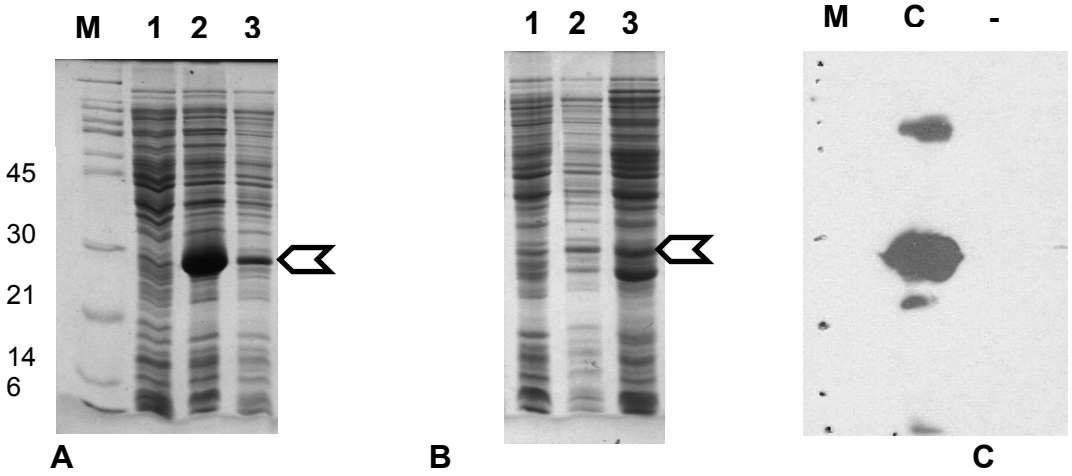

Figure 17. Expression of pRSETbGmGIN1-C in BL21(DE3) cells (A) and BL21(DE3)pLyS cells (B). **A.** 1-Empty BL21(DE3)cells; 2-cells containing pRSETbGmGIN1-C after 6h induction; 3- Cells containing pRSETbGmGIN1-C before induction (t_0). **B.** 1-Empty BL21(DE3)pLys cells; 2- Cells containing pRSETbGmGIN1-C before induction (t_0), BL21(DE3)pLys expressing pRSETbGmGIN1-C after 6h induction. **C.** Immunodetection with AntiHis antibody. Comparison between BL21(DE3) cells expressing GmGIN1-C (C) and empty BL21(DE3) cells (-). Arrows indicate the GmGIN1-C position.

The plasmid expressing GmGIN1-C was often lost in these cells due to competence with the pLyS plasmid, despite selective pressure. In contrast, the *Drosophila* construct in pRSETb yielded high amounts of soluble protein in both types of cells.

4.1.4 Purification of GmGIN1-C expressed in pRSETb vector

4.1.4.1 Purification by Ni-NTA affinity chromatography.

Purification under native conditions was essentially performed as described in materials and methods. Despite of the presence of the His-tag in our protein that should account for the specific binding to the Ni-NTA resin, many contaminant proteins were eluted together with GmGIN1-C due to the low yield of soluble protein. In addition, the use of disulfide-reducing agents, such as β-mercaptoethanol, during purification was reduced or eliminated to avoid splicing of GmGIN1-C during purification. This agent can reduce the unspecific binding of other proteins to the resin and to the target protein. In contrast, the yield of soluble C-terminal DmHh-C protein as well as the amount of purified protein under native conditions was much higher (Fig. 18).

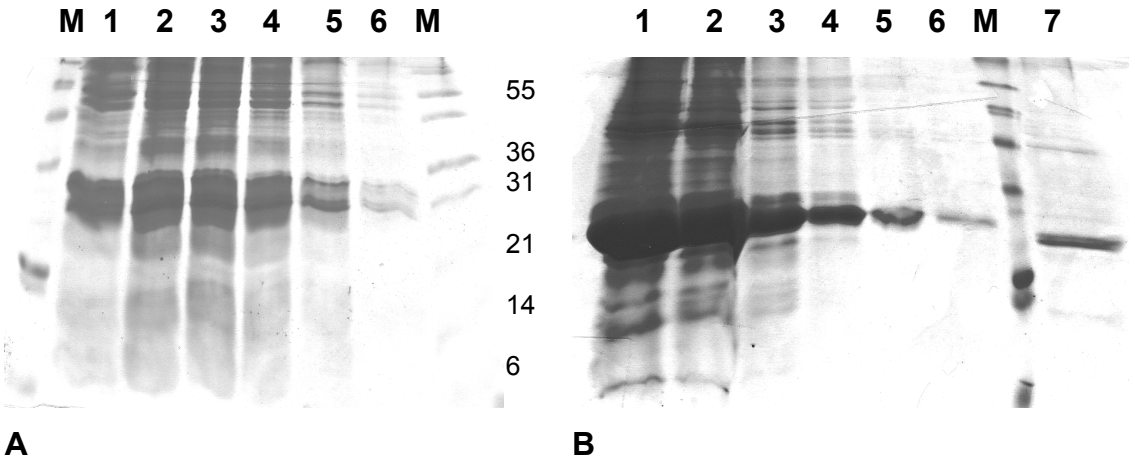

Figure 18. A. Native purification of GmGIN1-C. M-molecular weight markers; 1 to 6-Elutions from Ni-NTA column after purification. **B. Native purification DmHh-C**. M-molecular weight marker; 1 to 6-Elutions from Ni-NTA column after purification; 7- Elution 6 from pRSETbGmGIN1-C.

Several results point to the occurrence of self-splicing of GmGIN1-C during purification. Thus, purification using the Bugbuster® lysis system (Novagen)

showed the presence of a protein band in SDS gels with a lower molecular weight than expected (28 kDa), corresponding to the larger fragment expected after splicing of GmGIN1-C. Accordingly, it could be shown that this band is not detected by western blot using the AntiXpress antibody, which recognizes the Xpress epitope located at the N-terminus of the recombinant GmGIN1-C protein (Fig. 19).

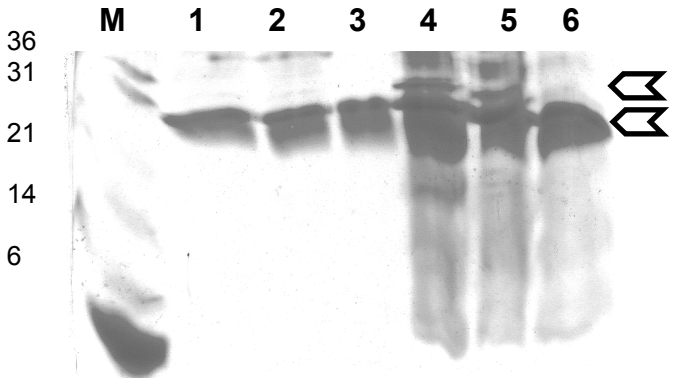

Figure 19. Autosplicing during purification. Comparison between two different native purifications of GmGIN1-C in pRSETb. 1 to 3-Protein purified after lysis with Bugbuster®reagent (Novagen) at room temperature; 4 to 6-Protein purified after lysis with the standard protocol; 1 and 4-Negative control without incubation; 2 and 5-Negative control with incubation; 3 and 6-Splicing reaction with addition 100 mM DTT. Arrows indicate the GmGIN1-C (upper) and spliced large fragment (lower) positions.

Further evidence of the splicing of GmGIN1-C during purification was obtained when several elutions were pooled and upconcentrated six times with a Vivaspin column of 10 kDa MWC. This column allows the small fragment of 7 kDa, resulting from splicing of the full length GmGIN1-C protein, to go through the membrane, and retains only the large fragment (21 kDa) and the entire protein (28 kDa). Nevertheless, a small amount of the N-terminal spliced fragment was also retained and upconcentrated. This enabled its detection by immunodetection with the antiXpress antibody. Like this, both the whole protein and the autospliced fragment could be detected. The small fragment retains also the His-tag. This might explain why it is trapped in the resin during purification. This phenomenon was not so dramatic when the protein was expressed using the pTrcHis construct (Fig. 20).

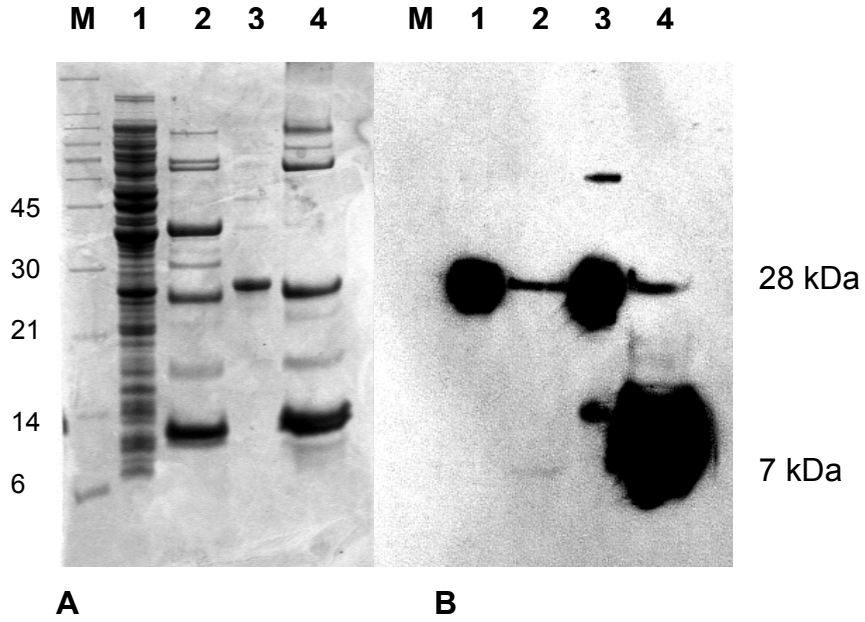

Figure 20. Autosplicing of GmGIN1-C during purification. A. Coomassie stained gel 12% Bis-Tris Nuphage (Invitrogen). **B.** Immunodetection with AntiXpress antibody. 1-Total lysate TOP-10 expressing pTrcHisGmGIN1-C; 2- Elution concentrated after purification; 3- Total lysate BL21(DE3) expressing pRSETbGmGIN1-C 1:10 dilution; 4- Elution concentrated after purification.

In order to obtain a larger amount of native active protein, purification under denaturing conditions and subsequent refolding before elution was carried out. Protein was refolded in the Ni-NTA agarose column using a linear decreasing gradient of urea concentration, from 8 M to cero urea in the refolding buffer (Fig. 21).

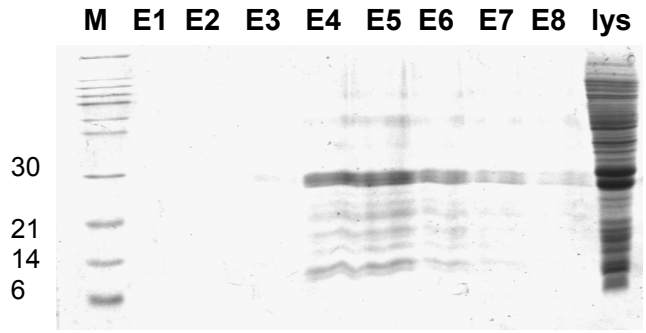

Figure 21. GmGIN1-C purification under denaturing conditions and in column refolding. (E1-E8) Elutions after refolding (one to eight); (lys) Total lysate of BL21(DE3) cells expressing GmGIN1-C in pRSETb.

4.1.4.2 Purification of GmGIN1-C expressed in pRSETb by ion exchange chromatography.

E. coli BL21(DE3) cells expressing pRSETbGmGIN1-C were lysed by 3 passes through French Press after resuspension in native lysis buffer. The lysate was centrifuged twice as described in material and methods. At pH 6.5 pRSETGmGIN1-C is positively charged. As the DEAE matrix is also positively charged, the protein will not bind to the column but. Accordingly, the GmGIN1-C protein appeared in the first fractions of the flow through of the DEAE column before starting the salt gradient, as shown by immunodetection (Fig. 22, fractions 1 to 4). The fraction number 3, containing a higher amount of protein was centrifuged again for 45 minutes at 25000 rpm to remove membrane debris that could interfere in the purification, and the subsequent pellet was analyzed. The remaining supernatant was loaded in a MonoS column, allowing the retention of positively charged proteins, and elutions containing a higher amount of protein were analyzed by immunodetection. However, we could not detect GmGIN1-C using the Anti-Xpress antibody in these fractions. The pellet was resuspended in native Ni-NTA lysis buffer and recombinant protein was purified again by Ni-NTA cromatography (see Fig. 20).

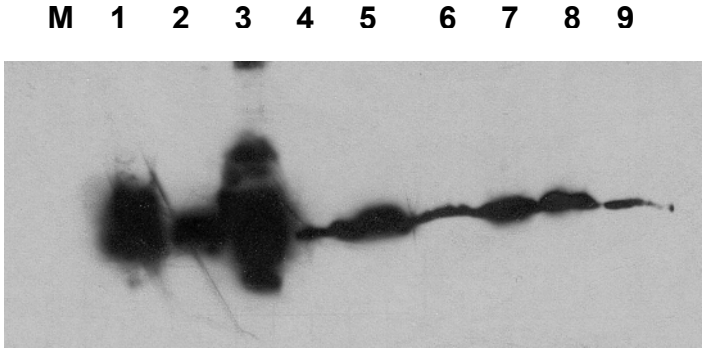

Figure 22. Purification of pRSETbGmGIN1-C by DEAE by ion exchange chromatography. 1-Total lysate BL21(DE3) expressing pRSETbGmGIN1-C; 2-Supernatant 1st centrifugation; 3-Pellet 1st centrifugation; 4-Supernatant 2nd centrifugation; 5-pellet 2nd centrifugation; 6 to 9-DEAE column flow through fractions 1 to 4 respectively.

Although GmGIN1-C could be partially purified by DEAE ion exchange chromatography, the protein needed to be further purified thereafter. Protein could not be recovered after monoS ion exchange chromatography and

fractions after Ni-NTA chromatography were not cleaner as performing directly Ni-NTA purification. The yield of GmGIN1-C protein was also not increased. For these reasons we decided to stick to the less time consuming method of purification.

4.2 Splicing reaction GmGIN1-C

4.2.1 Splicing using small nucleophiles

GmGIN1-C has a molecular weight of 28 kDa. Once the protein suffers self-splicing, two peptides of 21 and 7 kDa molecular weight will result from the auto-processing of the precursor. According to the model of Hedgehog proteins, the first nucleophilic attack leading to the self-splicing is an intramolecular reaction in which the cysteine at the splicing junction is essential. The resulting thioester intermediate is supposed to be resolved *in vivo* by a second nucleophilic attack, presumably performed by a molecule of cholesterol. This second nucleophilic attack can be carried out by small nucleophiles, such as DTT, resulting in the splicing of the protein and attachment of these moieties to the released N-terminal fragment at its carboxy end. DTT has been shown to induce splicing *in vitro* of Hedgehog proteins (Lee et al., 1994; Porter et al., 1996a). The smaller of the two peptides (7 kDa) is the N-terminal fragment, which retains the His-tag and Xpress epitope for detection with specific antibodies. Splicing reactions were performed under standard conditions using as nucleophilic molecules reducing agents such as β-mercaptoethanol, DTT and TCEP (Tris(carboxyethyl)phosphine).

Splicing reactions were performed with the positive control DmHh-C, expressed in the pRSETb vector. This protein has a molecular weight of 29 kDa, producing after cleavage two peptides of 6 and 23 kDa. The N-terminus of the protein corresponds to the lower molecular weight peptide, which retains the His-tag and Xpress epitope. Cleavage could be observed after incubation with TCEP and DTT for 17 h at 27°C in Coomassie stained SDS gels (Fig. 23-A). Appearance of an additional band of 23 KDa could be observed by incubation with both nucleophiles. DTT was more efficient in inducing the splicing reaction.

As a result, appearance of the smaller peptide (6 KDa) could also be observed. This band was detected with the AntiXpress antibody (Fig. 23-B).

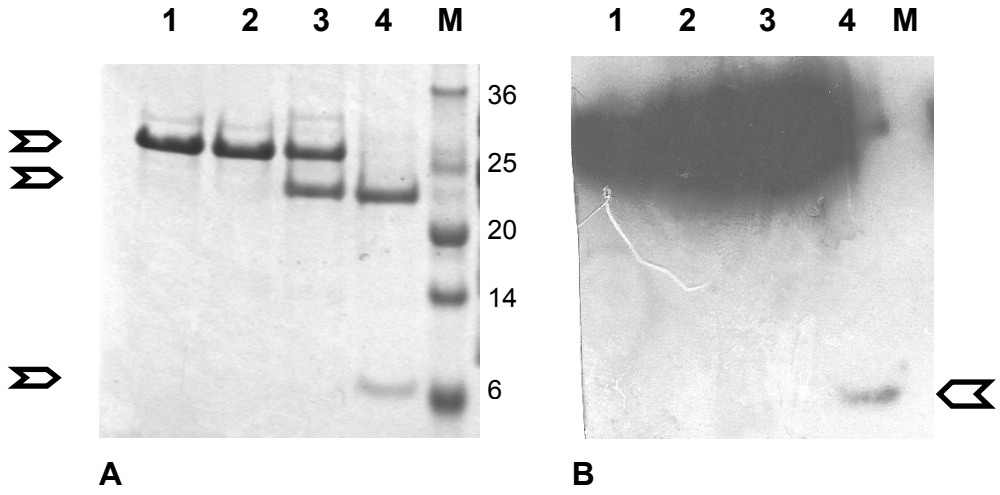

Figure 23. Splicing reaction of DmHh-C expressed in pRSETb. A. SDS-PAGE Coomassie stained 12% bis-tris gel. **B.** immunodetection with AntiXpress antibody. 1-2-Negative controls without incubation (1) and incubated without nucleophile (2); 3-Splicing with 10 mM TCEP; 4-Splicing with 100 mM DTT; M-Molecular weight marker. Arrows indicate Hh-C precursor and the peptides after splicing positions.

First attempts to test GmGIN1-C splicing reaction *in vitro* were performed with protein purified under denaturing conditions. Denatured protein did not retain any splicing activity (data not shown). In contrast, positive results were obtained with GmGIN1-C expressed in pRSETb and purified under native conditions using 100 mM DTT as splicing reagent (Fig. 24). After incubation of GmGIN1-C with this agent at 27°C for 17 hours, disappearance of the band corresponding to the precursor (28 kDa) could be observed in Coomassie stained gels (Fig. 24). As negative controls, protein without incubation and protein incubated under the same conditions but in the absence of nucleophilic agent were used (Fig. 24, lanes 1 and 2). A band of 21 kDa corresponding to the large carboxy terminus after splicing was observed in all lanes. This shows that part of the protein is undergoing self-splicing during purification. In DTT treated samples, the signal corresponding to GmGIN1-C disappeared after western blot and immunodetection with AntiXpress antibody (Fig. 24-B). Although the small fragment of the spliced products was difficult to observe in Coomassie stained gels, it could be detected after immunodetection with the AntiXpress antibody (Fig. 24-B). Splicing performed with TCEP (Fig. 24-A lanes 1 and 2) as nucleophilic agent was not as efficient as in reactions using DTT.

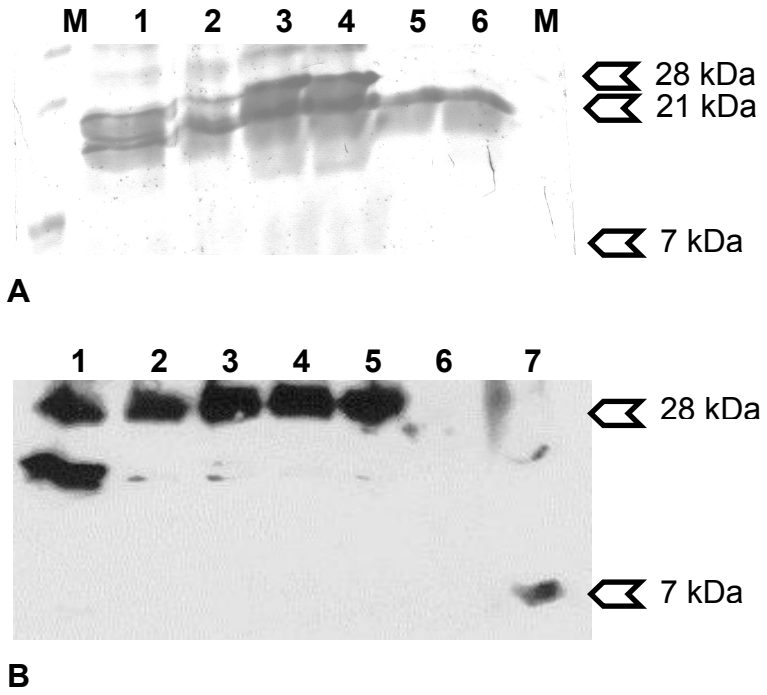

Figure 24. A. Splicing reaction with GmGIN1-C expressed in pRSETb. Coomassie 16% Tris-Glycine gel. 1 and 2-Negative controls, non-incubated (1) and incubated (2) without nucleophile; 3 and 4-Splicing reaction with addition 5 mM TCEP(3) and 10 mM TCEP (4); 5 and 6-Splicing reaction with addition 50 mM DTT(5) and 100 mM DTT (6).
B. Splicing reactions and immunodetection with AntiXpress antibody. 1 and 2-Negative controls, non-incubated (1) and incubated (2) without nucleophile; 3 and 4-Splicing reaction with 500 µM cholesterol with 1mM TCEP (3) and 1mM DTT (4); 5 and 7-Splicing reactions with 1mM (5), 25 mM (6) and 100 mM (7) DTT. Arrows indicate GmGIN1-C precursor and the peptides after splicing positions.

Splicing reaction with GmGIN1-C purified under denaturing conditions and renatured by gradual reduction of urea was also performed. No difference between untreated control samples and samples treated with 100 mM DTT could be observed, neither in Coomassie stained gels nor after western transfer and immunodetection with AntiXpress antibody, showing that most of the protein is probably still under denaturing conditions. However, the amount of native active protein was too low to be clearly differentiated from the denatured protein after the splicing assay (Fig. 25).

Splicing reactions were also performed with pRSETGmGIN1-C protein in fractions obtained from the DEAE column The protein showed to be resistant to self-splicing in this buffer, even after incubation with 100 mM DTT (data not shown). The pellet obtained after centrifugation of the DEAE fraction used for monoS column was resuspended in native purification buffer and subjected to Ni-NTA purification.

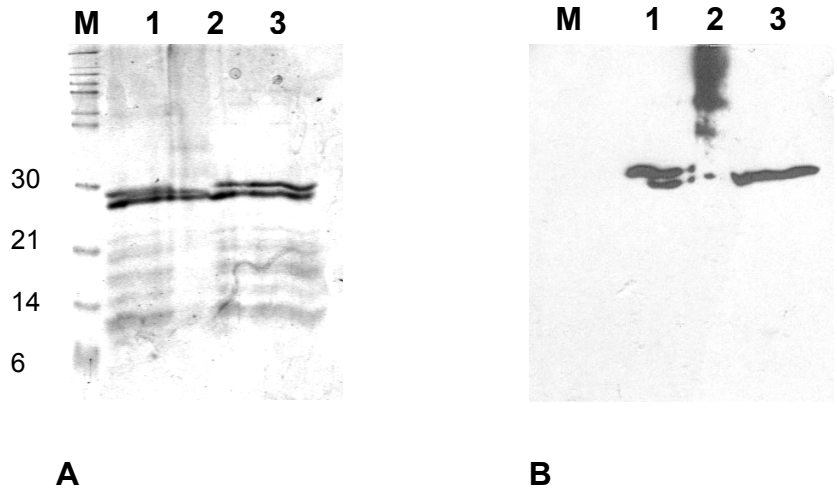

Figure 25. Splicing reaction with GmGIN1-C after denaturing purification and refolding. A. Coomassie stained tris-glycine gel. **B.** Immunodetection with AntiXpress antibody. 1 and 2-GmGIN1-C control without (1) and with incubation during 17h/27°C (2); 3-GmGIN1-C treated with 100 mM DTT.

Elutions were subjected to splicing reaction with 100 mM DTT in a reaction mix containing 80 µL of protein solution, which was precipitated after incubation in order to upconcentrate and load the entire sample in SDS gels. After western transfer, immunodetection with the AntiXpress antibody was performed (Fig. 26). Protein obtained after this purification was able to undergo self-splicing, indicated by the decrease or disappearance of the signal corresponding to GmGIN1-C precursor in three of the elutions after treatment with DTT (Fig. 26-B, lanes 1 to 7). The different splicing efficiency in the DEAE and Ni-NTA elution buffer might reflect a dependence on the pH of the reaction (6.5 and 7.8 respectively) or the influence of the buffer composition itself.

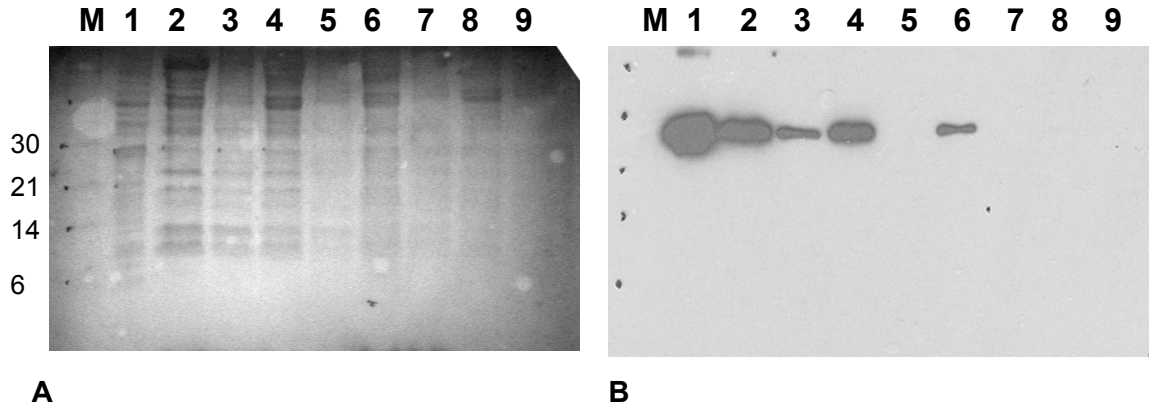

Figure 26. Splicing reactions with GmGIN1-C. A. PonceauS stained membrane after western transfer. **B.** Immunodetection with AntiXpress antibody. 1-Total lysate of BL21(DE3) cells expressing GmGIN1-C; 2 to 9-Different elutions from Ni-NTA resin (E1-E4) incubated without DTT (2,4,6,8) or with 100 mM DTT (3,5,7,9).

4.2.2 Splicing using Cholesterol and lipid extracts

Cholesterol is the molecule known to produce the second nucleophilic attack in hedgehog proteins *in vivo* (Porter et al., 1996a, b). For this reason splicing reactions of GmGIN1-C using cholesterol as nucleophilic agent were performed. Cholesterol is a minor sterol in most fungi, ergosterol being the major sterol (Martin et al., 1990; Sancholle et al., 2001). However, it has been previously shown that arbuscular mycorrhizal fungi contain other sterols rather than ergosterol, as for instance 24-Methylcholesterol and other cholesterol derivatives (Fontaine et al., 2001; Sancholle et al., 2001). In order to test the possible implication of natural occurring sterols in the splicing reaction, total lipids and sterols from spores and hyphae of *G. intraradices*, mycorrhizal and non-mycorrhizal carrot roots were extracted (see section 4.9). *G. intraradices* was chosen because of its close phylogenetical proximity to *Glomus mosseae*, the occurrence of a GmGIN1 orthologue in this fungus, and the possibility of obtaining a relatively high amount of fungal material under aseptic conditions. Accordingly, derivatives of cholesterol were found to constitute the majority of sterols found in these samples. Cholesterol itself was detected in a very low amount in mycorrhizal roots (see section 4.6).

Cholesterol and lipid extracts were suspended in water prior to splicing reactions according to previous protocols (Porter et al., 1996a, b). Due to its low solubility in water, cholesterol had to be sonified before and after addition to the reaction mixture. Cholesterol was also dissolved in other organic solvents and tested in the splicing reaction with DmHh-C protein. These reactions were carried out in the presence of 1 mM reducing agent (DTT or TCEP) which was also added to the negative control. Cholesterol in water produced splicing of the protein in an extent sufficient for visualization of the two resultant peptides in Coomassie stained gels. On the other hand, cholesterol dissolved in more apolar solvents, such as methanol, was less efficient in inducing the splicing reaction (Fig. 27). Nevertheless, efficiency of the cholesterol induced reaction was much less than with DTT. The attachment of cholesterol to the N-terminal fragment resulting from splicing causes a faster migration in SDS-PAGE gels of this peptide (Fig. 27).

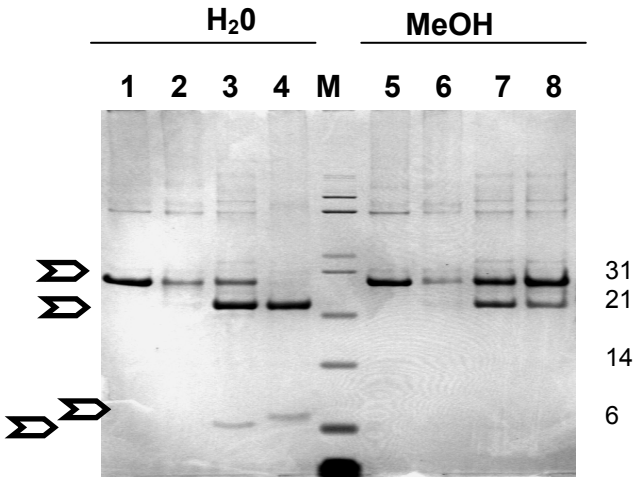

Figure 27. Splicing reaction DmHh-C with cholesterol compared to DTT. 1 and 2-Negative control without (1) and with incubation 17 h at 27°C (2); 3-Splicing with 1mM DTT/cholesterol dissolved in water; 4-100 mM DTT; M-Molecular weight marker; 5 and 6-Negative control (5) and incubated with methanol (6); 7-1mM DTT/cholesterol dissolved in methanol; 8-1mM TCEP/cholesterol dissolved in methanol. Arrows indicate Hh-C precursor and the peptides after splicing positions.

The amount of active protein obtained for GmGIN1-C was not enough to detect splicing with cholesterol or lipid extracts. Splicing reactions with lipid extracts were then performed with the positive control DmHh-C, as it was already described that other sterols could induce splicing of the protein in vitro (Mann and Beachy, 2000). Splicing reaction with lipid extracts were performed in the same conditions, with addition of 1mM TCEP in the splicing reactions. Extracted lipids were resuspended in water with 0.7% TX-100 and sonified. Splicing could be most clearly appreciated in reactions with sterols from mycorrhizal roots (Fig. 28). Accordingly, signals from peptides in the range of 6 kDa corresponding to cholesterol and mycorrhizal roots reactions run faster than the fragment resulting in the reaction corresponding to DTT. These results indicate that a sterol present in mycorrhizal roots is able to provoke splicing in the DmHh-C protein, which supports the hypothesis that GmGIN1 can undergo the same splicing processing as Hedgehog proteins.

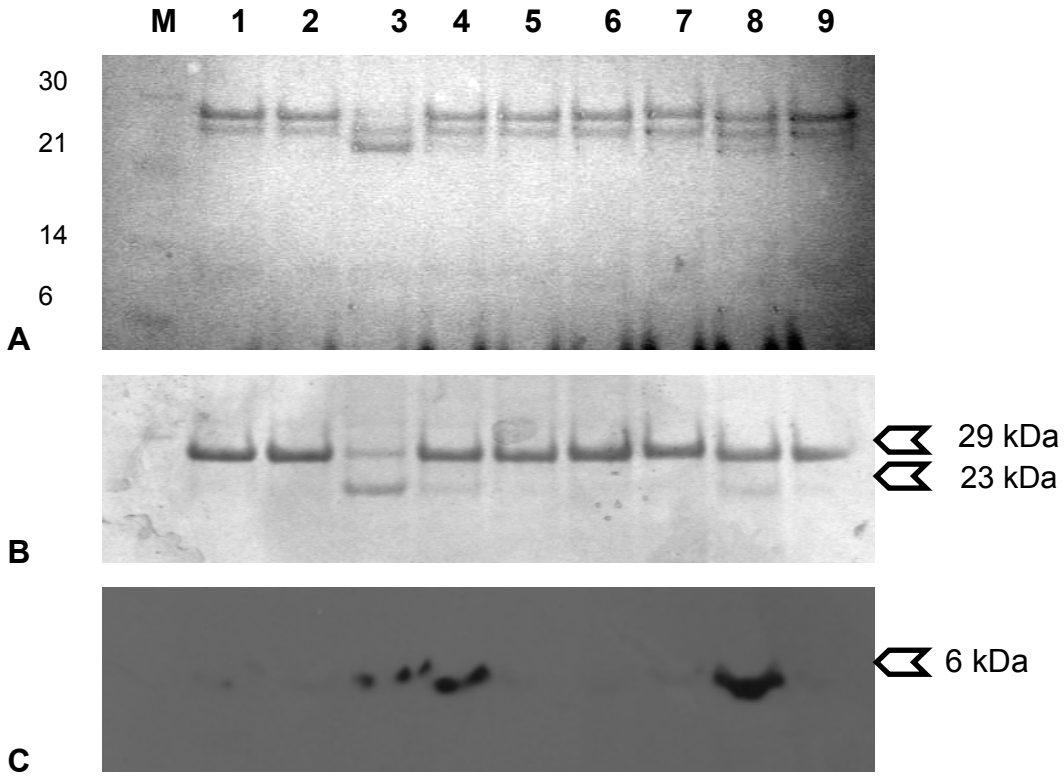

Figure 28. Splicing reaction of DmHh-C with lipid extracts from *G. intraradices* spores, hyphae and mycorrhizal roots. A. Nitrocellulose membrane stained with PonceauS; **B.** Transferred Coomassie stained 12% bis-tris gel; **C-** Immunodetection with AntiXpress antibody. M-Molecular weight marker; 1 and 2-Control without (1) and with incubation (2); 3-100 mM DTT treatment; 4-1 mM TCEP/cholesterol; 5-Spores sterols; 6-Hyphae sterols; 7 to 9-Sample treated with mycorrhizal roots sterols corresponding to different lipid extracts. Arrows indicate Hh-C precursor and the peptides after splicing positions.

4.3 Recombinant expression in *E. coli* of the GiGIN-1 C terminus

4.3.1 Expression using the pTrcHis vector

An orthologue from *GmGIN1* was isolated from *G. intraradices* (Krebs and Requena, unpublished results). In order to study the splicing activity of GiGIN1 its C-terminus was recombinantly expressed in *E. coli* using the same system as for GmGIN1-C. *GiGIN-C* terminus was PCR amplified with the primers GiGINExF1 and GiGINExR1 as described in material and methods. The fragment of 793 bp was ligated into the expression vector pTrcHisTOPO and transformed in chemically competent XL1-Blue *E. coli* cells. Resulting clones were analyzed by plasmid DNA extraction and restriction analysis. Positive clones were checked for the proper orientation of the insert by PCR using the primers pTrcHis Forward and GiGINExR1. Two of the three clones with the

insert in forward orientation were sequenced to make sure they were not containing any sequence mistake. Three different clones were tested for protein expression (Fig. 29). Clone 4, which showed no protein expression, was shown to contain a mistake leading to a stop codon.

First expression studies were preformed with XL1-Blue cells, using empty cells as negative control. Expression was performed at 37°C by induction with 1 mM IPTG at an OD_{600} of 0.6 during 5 hours. Clones 10 and 11 expressed a protein of 33.5 KDa, corresponding to the C-terminus of the GiGIN1 protein, as confirmed by immunodetection (Fig. 29).

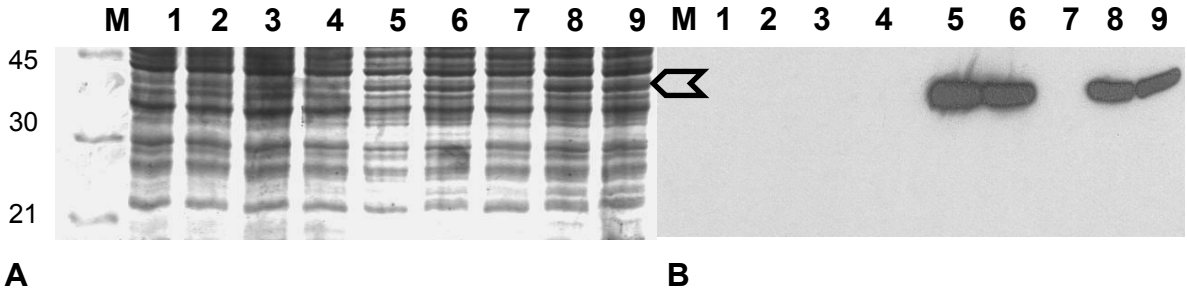

Figure 29. Expression of GiGIN1-C using the pTrcHis vector in *E. coli* XL1-Blue cells. A. Coomassie stained gel, **B.** Immunodetection with AntiXpress antibody.1, 4 and 7-Empty XL1-Blue cells lysates; 2 and 3-Lysates of cells clone 4; 5 and 6-Lysates of cells clone 10; 8 and 9-Lysates of cells clone 11. Arrows indicate GiGIN1-C position.

GiGIN1-C expressed in the pTrcHis vector was also introduced into TOP-10 and M-15[pREP4] *E. coli* cells. The same conditions for induction in XL1-Blue cells were used with these strains. Surprisingly, almost no expression could be detected in TOP-10 cells containing the plasmid expressing GiGIN1-C, although cells seemed to grow normally after induction of production of the protein according to the final OD_{600} (2.1-2.5). On the other hand, M15[pREP4] cells expressing GiGIN1-C in the pTrcHis vector grew to an OD_{600} much lower than other strains after expression of the protein (0.8-1.1), but expressed levels of protein were comparable to these obtained in XL1-Blue cells (Fig. 30).

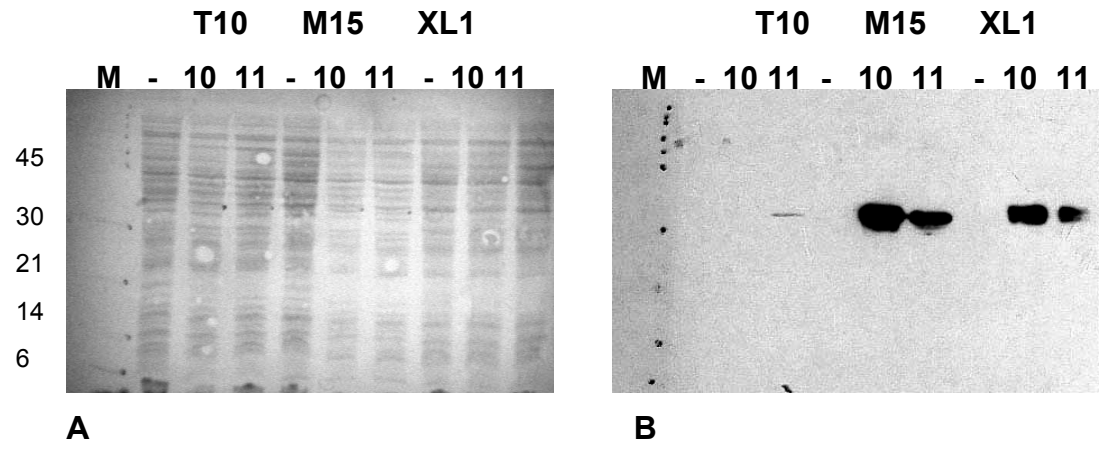

Figure 30. Comparison of expression of GiGIN1-C in pTrcHis vector in different *E.coli* strains, as T10, M15[pREP4] and XL1-Blue. A. PonceauS stained membrane. **B.** Immunodetection with AntiXpress antibody. Clones 10 an 11 were compared to empty cells (-).

4.3.1 Purification of GiGIN1-C expressed in pTrcHis vector

A solubility test was first performed for GiGIN1-C expressed in pTrcHis and XL1-Blue cells, in which lysis was performed under native conditions and the resulting protein amount in the pellet and supernatant were compared. Clones 10 and 11 were tested after inducing expression of GiGIN1-C in two independent cultures. Although most of GiGIN1-C protein is kept in the insoluble fraction, protein was also detected in the supernatant, which enables its purification under native conditions (Fig. 25). Both clones express similar levels of soluble GiGIN1-C. Nevertheless, yields of native purified protein are expected to be rather low.

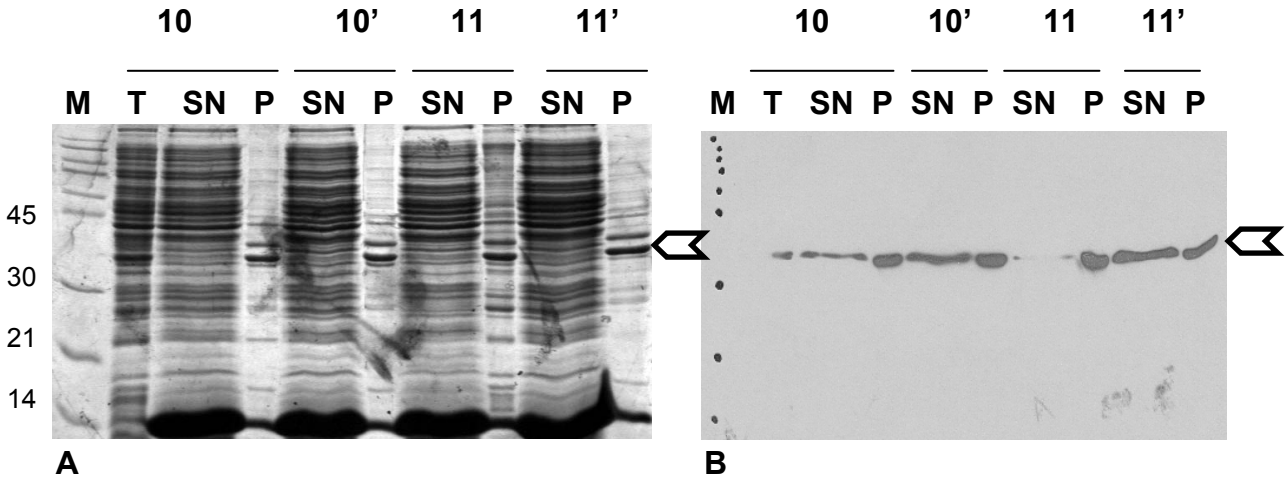

Figure 31. GiGIN1-C solubility expressed in pTrcHis vector in XL1-Blue cells. A. Coomassie stained gel, **B.** Immunodetection with AntiXpress antibody. T- total lysate; SN-supernatant; P-corresponding pellet. Lysis was performed in the two different clones (10 and 11) in cells from two independent cultures. Arrows indicate GiGIN1-C position.

Solubility of GiGIN1-C expressed in M15[pREP4] and TOP10 cells was also tested for both clones and compared to the yields obtained in XL1-Blue (Fig. 32). M15[pREP4] and XL1-Blue cells expressed similar amounts of soluble GiGIN1-C. According to previous results, TOP10 expressed very little protein.

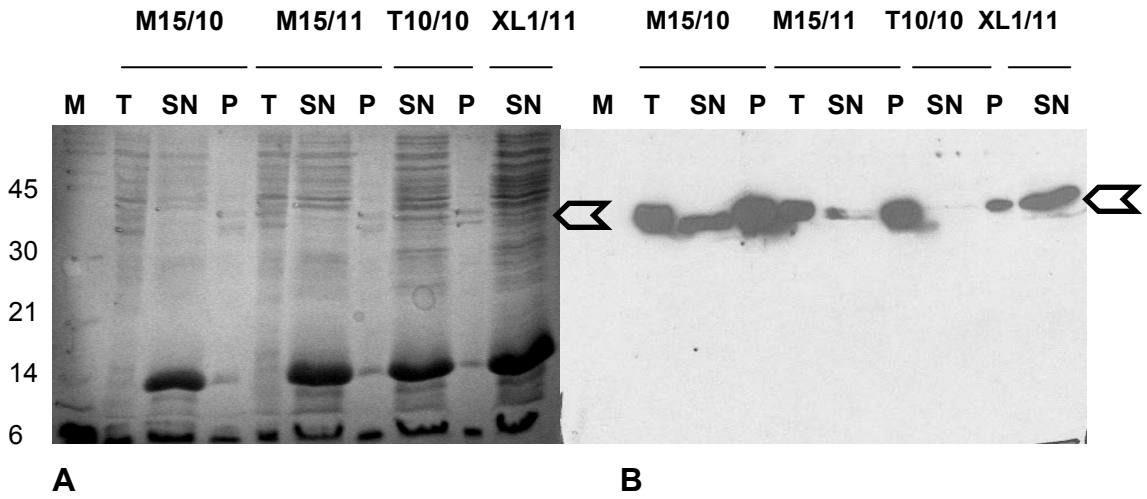

Figure 32. GiGIN1-C solubility expressed in pTrcHis vector in M15, T10 and XL1-Blue cells. A. PonceauS stained membrane., **B.** Immunodetection with AntiXpress antibody. T- total lysate; SN-Supernatant; P-Corresponding pellet. Lysis was performed in the two different clones (10 and 11) expressed in the different *E.coli* strains. Arrows indicate GiGIN1-C position.

In order to know how much protein was expressed, purification of the protein under denaturing conditions by Ni-affinity chromatography was performed in a small scale approach (2 mL culture). A single band corresponding to GiGIN1-C could be observed in Coomassie stained SDS gels (Fig. 33). Purification was carried out from XL1-Blue cells expressing clones 10 and 11, from two independent cultures for each clone.

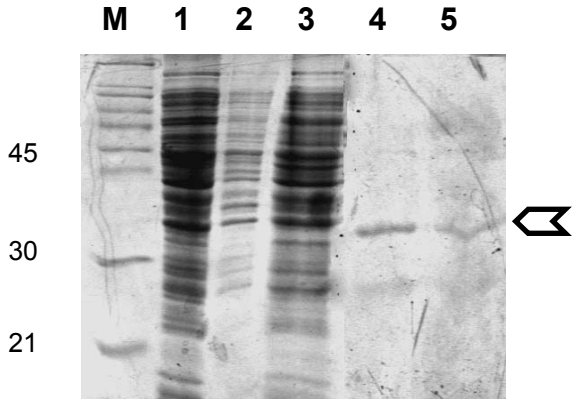

Figure 33. Ni-NTA denaturing purification of GiGIN1-C expressed in pTrcHis and XL1-Blue cells. 1- total lysate, 2-pellet after lysis, 3- Supernatant after incubation with Ni-NTA agarose, 4- Elution 1, 5- Elution 2. Arrows indicate GiGIN1-C position.

4.4 Recombinant expression in *E. coli* of the full length protein GmGIN1

4.4.1 Expression using the pTrcHis-TOPO vector

GmGIN1 protein was expressed heterologously in *E.coli* in order to study the splicing activity of the full length protein and the possible enzymatic activity of the N-terminus of the processed protein. The larger size of the spliced GmGIN1-N terminus was expected to be more easily detectable than the small fragment obtained after splicing of GmGIN1-C. Cloning of the *GmGIN1* full length gene was achieved after PCR amplification with the primers GmGINExF3 and GmGINExR1 as described in material and methods. The fragment of 1298 bp (Fig. 34-A) was ligated into the pTrcHisTOPO expression vector and the resulting reaction was transformed in chemically competent XL1-Blue *E. coli* cells. Resulting clones were analyzed by plasmid DNA extraction and restriction analysis. One of the clones containing the insert in forward orientation was sequenced in order to assure the absence of mistakes. This clone was used for further protein expression studies.

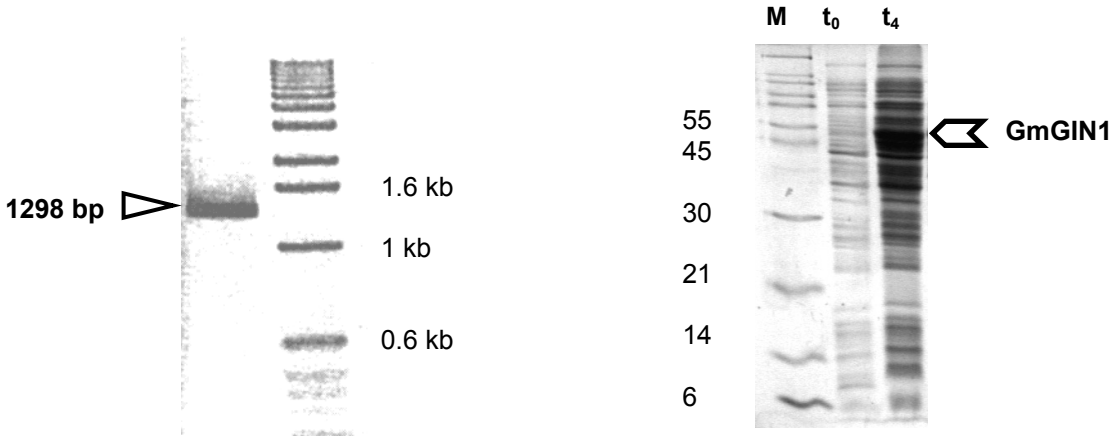

Figure 34. A. PCR product for GinExF3/R1. B. pTrcHisGmGIN1 expression in XL1 Blue cells. Cells expressing GmGIN1 (GIN1) before induction (t_0) and after 4 hours of induction (t_4).

First expression studies were preformed with XL-1 Blue cells, using empty cells as negative control. Standard expression conditions were induction during 4 hours with 0.8 mM IPTG at 37°C once the cells had reached an OD_{600} higher than 0.6 (Fig. 34-B). Protein expression was confirmed by SDS PAGE electrophoresis. A band corresponding to the molecular weight of GmGIN1

expressed in the pTrcHis vector (52 kDa) could be observed in Coomassie stained SDS-gels (Fig. 35-A).

GmGIN1 in pTrcHis vector was also cloned into TOP-10, M-15[pREP4] and BL21 *E. coli* cells. Expression levels of GmGIN1 were compared with empty cells (negative control) and the expression of LacZ protein (positive control) (Fig. 35). The amount of protein expressed in the different strains was quite similar.

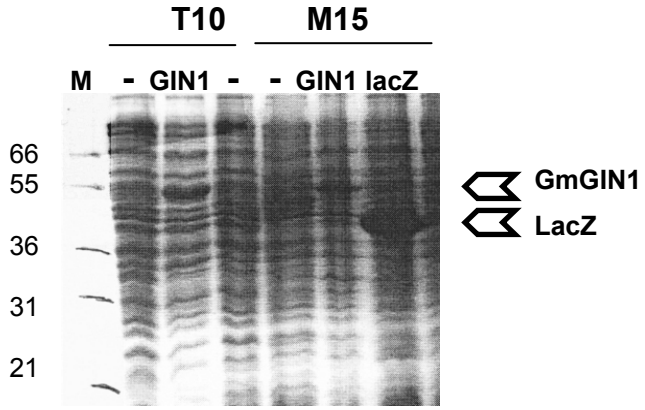

Figure 35. GmGIN1 in pTrcHis expression. T10 and M15 *E. coli* empty cells (-), compared to cells expressing GmGIN1 (GIN1) in TOP10 and M15 cells and M15 cells expressing LacZ protein in the pTrcHis vector.

4.4.2 Expression in pRSETb vector

In order to test whether higher yields of protein could be obtained the *GmGIN1* gene was transferred to the pRSETb vector. The insert in pTrcHis was digested with HindIII and BamHI, and ligated in the linearized pRSETb vector (Fig. 36). Clones were analyzed by plasmid DNA extraction and enzyme restriction analysis.

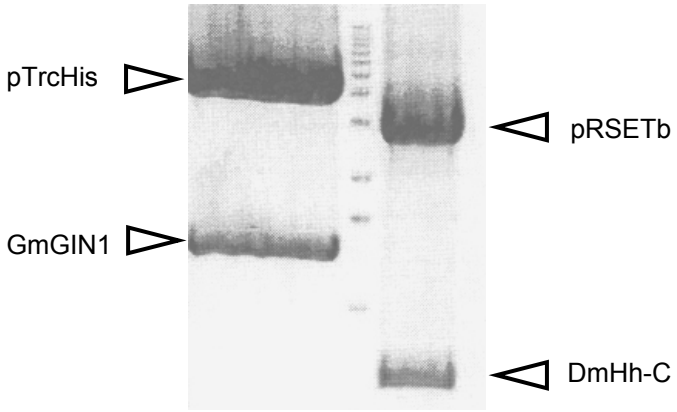

Figure 36. Transfer of the *GmGIN1* gene from pTrcHis to pRSETb vector. Double digestion with HindIII and BamHI of pTrcHis (4.39 Kb) containing *GmGIN1* insert and pRSETb (2.9 Kb) containing *DmHh-C* gene.

GmGIN1 in pRSETb vector was cloned in BL21(DE3) *E. coli* cells for protein expression. Standard expression conditions were induction during 4 hours with 0.8 mM IPTG at 37°C once the cells had reached an OD_{600} over 0.6. Expression of GmGIN1 could be observed even before addition of inducer (IPTG) (t_0 Fig. 37). As observed before for GmGIN1-C and DmHh-C, expression with pRSETb is not controlled, as it should be the case in this vector. A very high amount of total protein was obtained, although very little of this was kept in the soluble fraction after native lysis (Fig. 37 and Fig. 38).

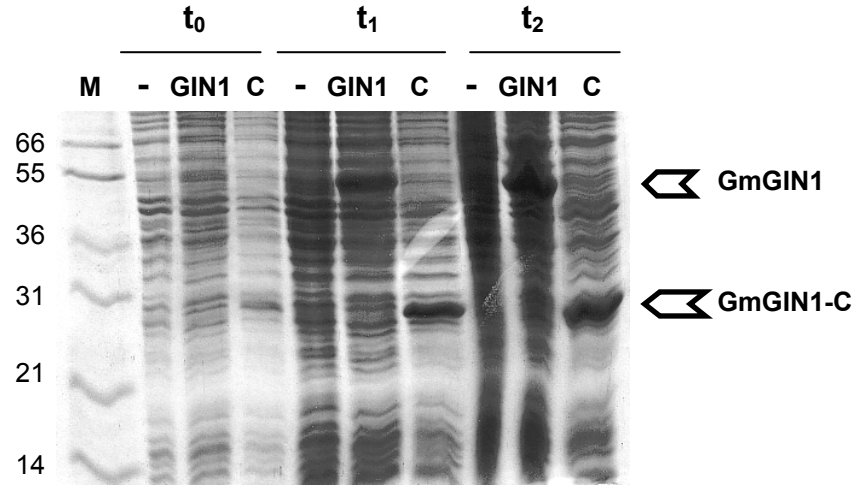

Figure 37. **Expression of GmGIN1 and GmGIN1-C in pRSETb vector.** Comparison between empty BL21(DE3) cells (-) and BL21(DE3) expressing GmGIN1 (GIN1) and GmGIN1-C (C) before induction (t_0), after 1 h (t_1) and 2 h (t_2) of induction with IPTG.

4.4.3 Purification of GmGIN1 by Ni-NTA affinity chromatography

4.4.3.1 Purification under native conditions

The GmGIN1 protein seems to be very insoluble when performing expression from both pTrcHis and pRSETb vectors, as could be assessed by immunodetection of the soluble and insoluble fractions obtained after lysis under native conditions (Fig. 38). The lysate was centrifuged at 10000 rpm for 20 minutes at 4°C, and the supernatant was centrifuged a second time at 35000 rpm for 45 minutes at 4°C. Samples corresponding to the total lysate before (t_0) and after 4 h induction (t_4), supernatant and pellet of the first and second centrifugation were analyzed by SDS-gels, western blot and immunodetection with the AntiXpress antibody. No protein could be detected in any of the two supernatants. GmGIN1 seems to be completely retained in the insoluble fraction. Therefore, no purified protein could be obtained by direct native purification in Ni-NTA resin. Many signals were detected when immunodetection was performed with lysates of cells expressing GmGIN1, possibly showing protein degradation.

4.4.3.2 Purification under denaturing conditions

A first attempt of purification under denaturing conditions was made with a culture of the pTrcHisGmGIN1 construct in XL1 Blue cells (100 ml) which had been induced under standard conditions in LB amp medium. A band (or group of bands) corresponding to the expected 52 kDa molecular weight of GmGIN1 could be observed in Coomassie stained SDS-gels, as well as another band below of 31 kDa (Fig. 39). In case of undergoing self-splicing, GmGIN1 protein would give rise to two peptides of 31 (N-terminus) and 21 (C-terminus) kDa. The His-tag and the Xpress epitope would remain in the GmGIN1-N spliced fragment, and would be recognized by the AntiXpress antibody together with the GmGIN1 precursor. The other half of the protein, GmGIN1-C, would loose the His-tag as a result of the splicing and would not be retained in the resin. Nevertheless, the band around 31 kDa did not give a clear signal when immunodetection with AntiXpress antibody was performed (data not shown).

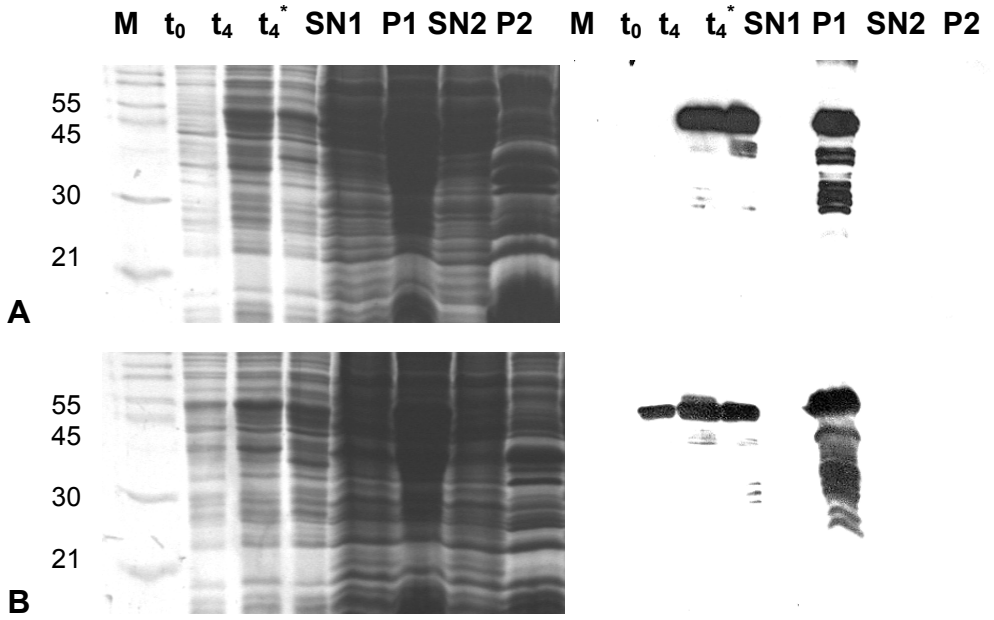

Figure 38. Lysis under native conditions of GmGIN1 expressed in pTrcHis (A) and pRSETb (B) vectors. Left Coomassie stained gels and right immunodetection with AntiXpress antibody. **A.** total lysate in XL1-Blue cells before induction (t_0), after 4 h induction (t_4); total lysate GmGIN1 in pRSETb in BL21(DE3) cells after 4 h induction (t4*); supernatant (SN1) and pellet (P1) 1st centrifugation; supernatant (SN2) and pellet (P2) 2nd centrifugation. **B.** Total lysate in BL21(DE3) cells before induction (t_0) and after 4 h induction (t_4); total lysate GmGIN1 in pTrcHis after 4 h induction (t_{4*}); supernatant (SN1) and pellet (P1) 1st centrifugation; supernatant (SN2) and pellet (P2) 2nd centrifugation.

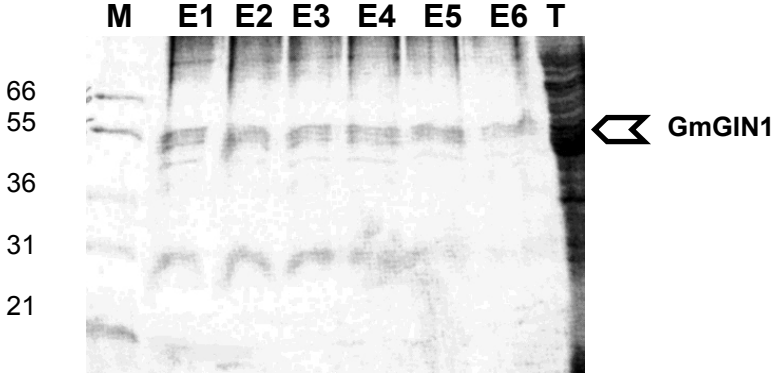

Figure 39. Denaturing purification of HisGmGIN1 expressed in pTrcHis in XL1-Blue cells. E1 to E6 subsequent elutions, T- total lysate XL1-Blue cells expressing GmGIN1 in pTrcHis.

4.4.3.3 Purification under denaturing conditions and refolding

In order to obtain active GmGIN1 protein to perform the splicing assay, denaturing purification of protein expressed in pRSETb/BL21(DE3) cells and

subsequent refolding was carried out. Lysis and purification under denaturing conditions, using 8 M urea as denaturant agent, was performed with buffers containing 50 mM Tris and 300 mM NaCl in lysis buffer and a higher concentration of NaCl of 1 M in the washing buffer, being the rest of the components as described in material and methods. 1L culture BL21(DE3) cells containing the GmGIN1 in pRSETb were resuspended in 25 ml of denaturing lysis buffer. The supernatant was loaded on 1.5 ml Ni-NTA superflow resin (Qiagen) by means of a peristaltic pump with a 0.3 ml/min flow at 4°C. Due to cristalization of the urea the flow was stopped and the washings had to be made at room temperature, at a 0.5 ml to 1 ml/min flow with 20 ml buffer. Refolding was performed at 4°C, with a mixer in which a gradient of decreasing urea was achieved by mixing the refolding buffers A and B. Due to the very slow flow this process lasted 24 h. Elution was performed with 4.5 ml of elution buffer without TX100 and glycerol and was concentrated in one Vivaspin-Hydrosart 10000 kDa MWC device at 3000 rpm 4°C to a final volume of 0.5 ml. All fractions were analyzed by SDS PAGE and by immunodetection with AntiXpress antibody (Fig. 40). Under these conditions a band below 30 kDa appeared. A band corresponding to GmGIN1 could be identified both in Coomassie stained SDS-gels and immunodetection, but elutions carried many contaminant proteins including a main band lower than 30 kDa. This band failed to give a signal when immunodetection with the AntiXpress antibody was performed (Fig. 40-B).

Splicing reactions with this fraction were performed with 18 µl of protein solution and TCEP, cholesterol and DTT were used as nucleophilic agents (Fig. 41). Incubated samples gave many signals, without appearance of a main band. Nevertheless, the amount of loaded sample in the control without incubation seems to be lower, therefore no clear comparison can be established.

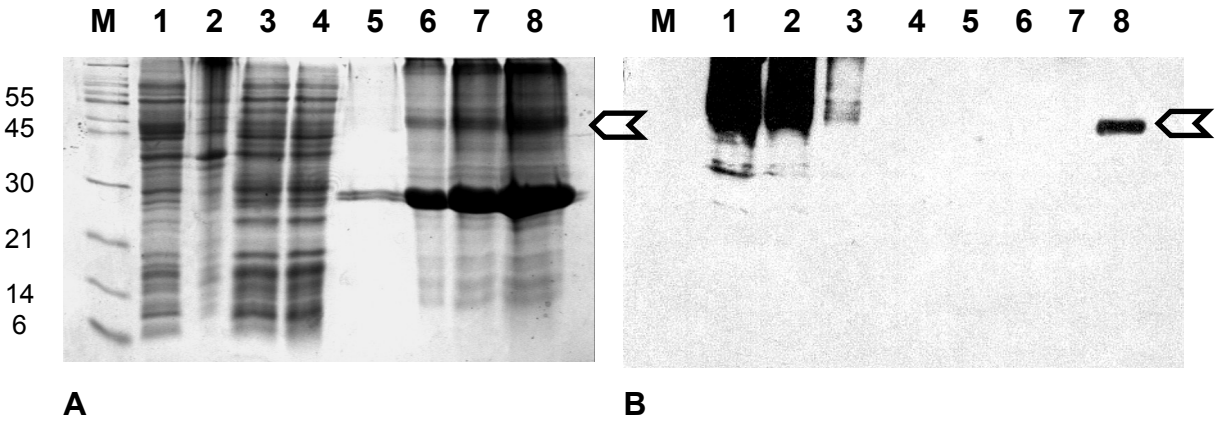

Figure 40. Purification under denaturing conditions and refolding of GmGIN1 expressed in pRSETb vector. M-Molecular weight marker; 1-Total lysate; 2-Pellet after lysis; 3-Supernatant after lysis; 4-Lysate after incubation with Ni-NTA resin; 5-Non concentrated elution; 6-5 μl concentrated eluate; 7-10 μl concentrated eluate; 8-18 μl concentrated eluate. Arrows indicate the position of GmGIN1. Arrows indicate GmGIN1 position.

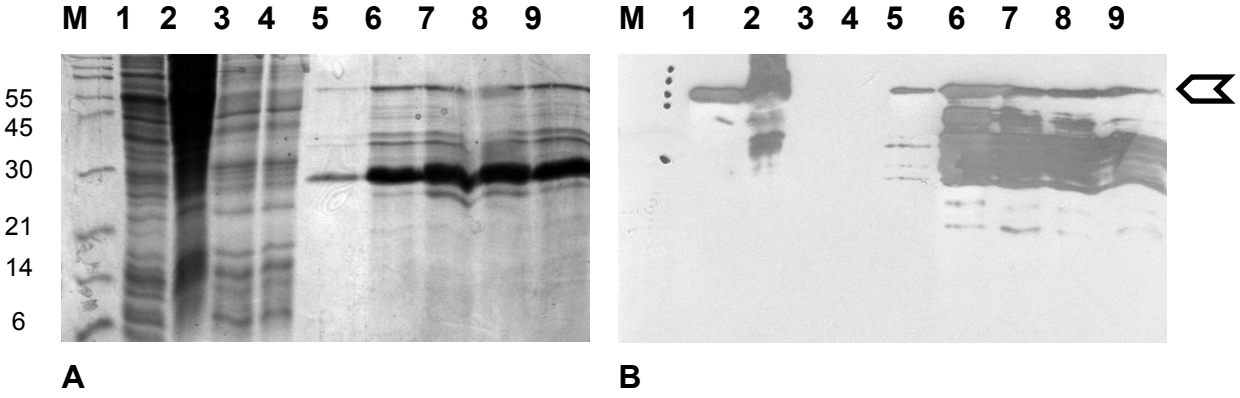

Figure 41. Splicing reaction with GmGIN1 in pRSETb. A. Coomasie stained gel. B. Immunodetection with AntiXpress antibody. 1-Total lysate of BL21(DE3) cells expressing GmGIN1 in pRSETb; 2-Pellet after lysis; 3-Supernatant after incubation with the resin; 4-Flow through the resin; 5 and 6-GmGIN1 without (5) and with (6) incubation for 20h at 27°C without splicing agent; 7 to 9-Splicing reactions with TCEP (7), Cholesterol/1 mM TCEP (8) and DTT (9). Arrows indicate GmGIN1 position.

4.5 Design of specific antibodies versus the N-terminus and C-terminus of GmGIN1

In order to discriminate between amino- and carboxy-terminus of GmGIN1, short peptides of these two regions were selected for production of specific antibodies. One peptide was designed for the GmGIN1-N terminus, the *CREN* peptide with the sequence CRENEYKRKRVNAGLKG (from amino acid 206 to 221 in GmGIN1). Two different antisera, called 461 and 476 *antiCREN*, were produced by SEQLAB. For the GmGIN1-C terminus two different peptides

(*CKQD* and *CRVT*) localized proximal to its carboxy end were designed. *CKQD* corresponds to the peptide CKQDGSQGNLHITPKHH, from amino acids 299 to 314 and *CRVT* corresponds to CRVTKERRKGYYSPLTRSG, from 349 to 366 in GmGIN1. This would allow recognition of the full length protein and exact location of the carboxy terminus after protein splicing. These two peptides were injected together for immunization. Two different antisera, called 474 and 475 *antiCKQD*/*CRVT*, were obtained from SEQLAB. Total lysates from empty *E. coli* and from cells expressing either the GmGIN1-N or the C-terminus cells were tested for specific binding. Thus, preimmune sera and antibodies were used at 1:5,000 and 1:10,000 dilutions. Both sera 461, against the N-terminus, and 474, against C-terminus, gave a more specific signal.

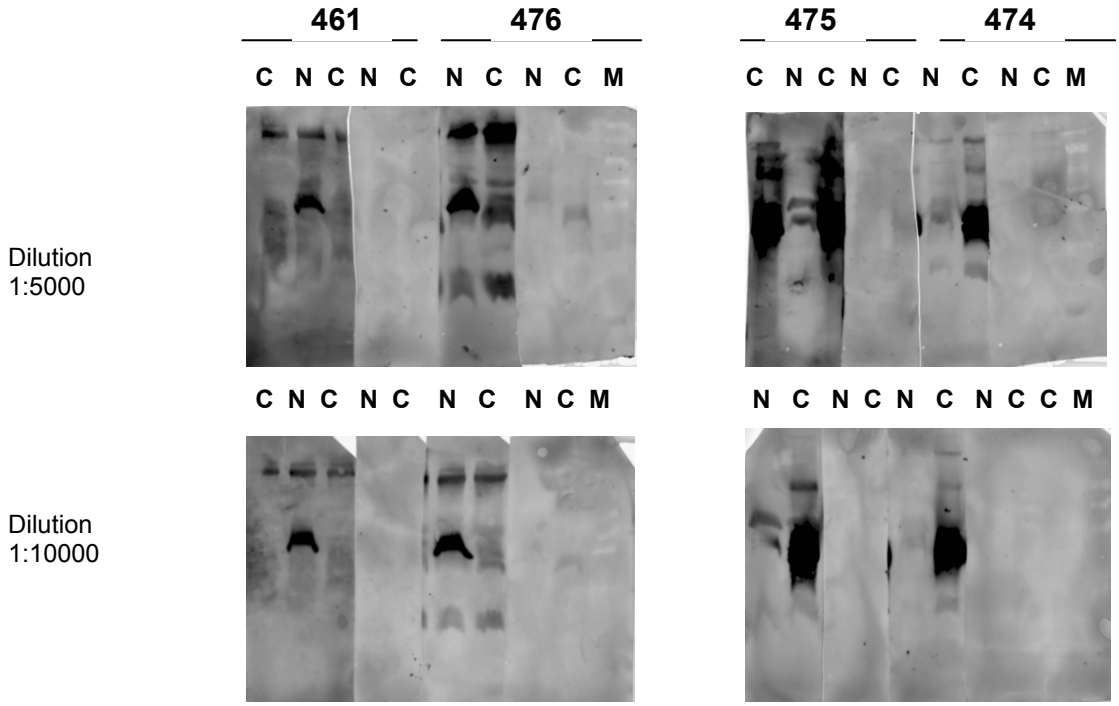

Figure 42. Comparison between preimmune sera and first bleeding for 474 and 475 antiCKQD and CRVT, recognizing GmGIN-C terminus, and 461 and 476 antiCREN sera, recognizing GmGIN-N terminus. N and C correspond to *E. coli* cells expressing GmGIN-N and GmGIN-C lysates respectively; M-Molecular weight marker.

474 *antiCKQD*/*CRVT* antiserum was used for detection of autosplicing of pRSETGmGIN1-C protein. Native lysates (supernatant/soluble fraction) from cells expressing the construct were compared to empty cell lysates. In contrast to detection where the Anti-His antibody was used, signals from two bands in the range from 29 kDa and 25 kDa were observed (Fig. 43).

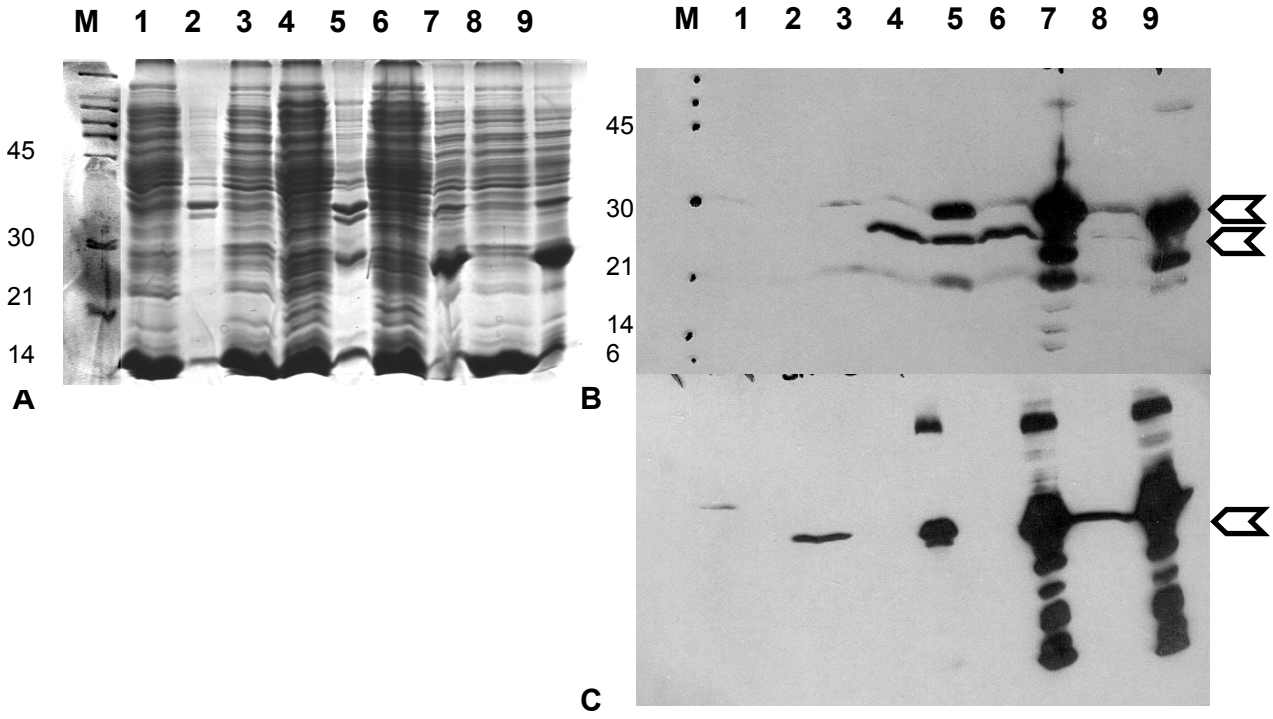

Figure 43. Detection of GmGIN1-C and C-terminal autosplicing fragment with 474 *antiCKQD*/*CRVT* antiserum. A. Coomassie stained gel. **B.** Immunodetection with 474 *antiCKQD*/*CRVT* antiserum. **C-** Immunodetection with Anti-His antibody. 1 and 2- supernatant (SN) and pellet empty BL21(DE3) cells, 3- SN incubation ON/37°C without IPTG induction, 4 and 5- SN and pellet induction IPTG/6 h/37°C, 6-SN induction ON/20°C, 7, 8 and 9- total lysate, SN and pellet incubation ON/37°C without IPTG induction. Arrows indicate GmGIN1-C and the larger of the spliced fragments positions.

antiCREN and *antiCKQD*/*CRVT* antisera were tested for their cross-reactivity with the homolog protein GiGIN1 from *Glomus intraradices*. The full-length GiGIN1 protein has a molecular weight of 54 kDa, and its putative splicing products would have 31.5 (N-terminus) and 22.5 kDa (C-terminus). Total protein extracts were obtained from *G. intraradices* spores and mycorrhizal carrot roots colonized by *G. intraradices*. An *A. muscaria* total protein extract was used as negative control. The *antiCREN* did not recognize any protein from the total protein extracts, while it recognized the positive controls GmGIN1-N and GmGIN1 expressed in *E. coli* (Fig. 44-B).

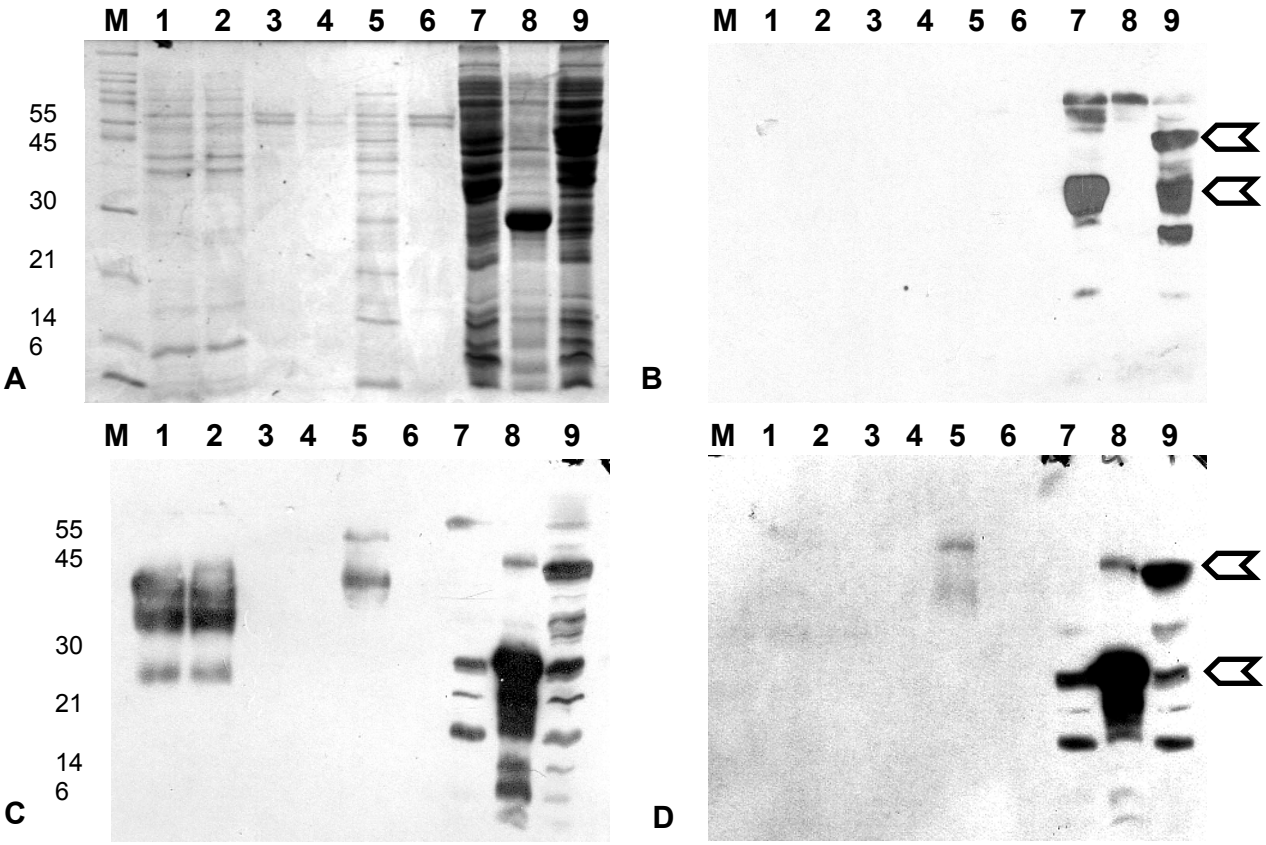

Figure 44. GiGIN1 detection in total protein extracts. A. Coomassie stained gel, **B.** immunodetection with *antiCREN* antiserum (N-terminus), **C and D.** Immunodetection with *antiCKQD*/*CRVT* antiserum (C-terminus). 1-2-*G. intraradices* spores, 3, 4-6 mycorrhizal carrot roots, 5- *A. muscaria*, 7, 8 and 9- total lysate *E. coli* expressing GmGIN1-N, GmGIN1-C and GmGIN1 respectively. Arrows indicate GmGIN1, GmGIN1-N and GmGIN1-C positions.

The *antiCKQD*/*CRVT* antiserum recognized three protein bands of an apparent molecular weight of around 44, 33 and 23 kDa in the spore protein extracts, none in the mycorrhizal root extracts and one protein of an apparent molecular weight of 45 kDa in the protein extracts of *A. muscaria* (Fig. 44-C). In all three detections, the antisera were used at a 1:10000 concentration. These signals were strongly attenuated by further dilution of the second anti-rabbit antibody from 1:3,000 to 1:8,000 (Fig. 44-D). The signal of 23 kDa detected in *G. intraradices* spore protein extracts could correspond to the GiGIN1-C spliced protein (Fig. 44-C).

4.6 Lipid extraction and analysis from *G. intraradices* mycorrhizal samples

4.6.1 Total lipid extraction

In order to analyze which could be the molecule that provokes the self-splicing reaction in GmGIN1, lipid extracts from mycorrrizal samples were extracted, analyzed and tested fro their ability to induce self-splicing. Total lipid extraction from *G. intraradices* spores, *G. intraradices* colonized and non-colonized carrot roots and *Amanita muscaria* mycelium was performed following the Bligh and Dyer protocol (Bligh and Dyer, 1959). Starting fresh weight material and total lipid yield are indicated in Table 3. Lipid extraction from fungal material was much more efficient than extraction from carrot roots. After this, column chromatography was performed to separate the extracts into three mayor groups, in order of increasing polarity.

Sample	Fresh weight (g)	Lipid yield (mg)
G. intraradices spores	2.4	43.8
Mycorrhizal carrot roots	8.3	16.5
Carrot roots	4.75	4.4
Amanita muscaria mycelium	3	42.7

Table 3. Scheme of the different samples used for lipid extraction. Samples fresh weight is compared to total lipid yield. Lipid extraction from root samples was less efficient that from fungal material.

Lipid extracts from *G. intraradices* spores, mycorrhizal and non-mycorrhizal roots, and *A. muscaria* mycelium were subjected to fractionation in silica gel columns, separating fractions corresponding to the dichloromethane elution, which contained neutral lipids, i. e. hydrocarbons, carotenoids, pigments, sterols and sterol esters, glycerides, waxes, fatty alcohols and aldehydes, and fatty acids. The acetone eluates correspond, in plants, to mono- and di-galactosyl glycerides, cerebrosides, steryl glycosides, sulpholipids (plus small amounts of cardiolipin and phosphatidic acid) (Kates, 1972). The methanol eluates contain phosphatides, with only traces of glycolipids. These fractions were analyzed by LC silica gel plates as described in material and methods, and different spots

were identified as compared to several standard lipids. The dichloromethane spore fraction had a high content of triacylglycerol, being the main lipid in this fraction (Fig. 45, lane 1). Triacylglycerol could not be identified by this method in other samples. The sterol precursor squalene, together with hydrocarbons, was mainly eluted in the dichloromethane fraction of all samples (Fig. 45, lanes 1 4, 7, 10). Sterols appeared mainly in the dichloromethane and acetone fractions of all samples. Monoacylglycerol, diacylglycerol and fatty acids appeared mainly in the acetone fraction of all samples. In this elution a spot could be observed corresponding to sterol esters in mycorrhizal and non-mycorrhizal roots (Fig. 45, lanes 4, 7). A prominent spot in methanol eluates was observed in all samples, probably corresponding to phosphatides. Lipids in the different fractions were acetylated and further analyzed by GC-MS.

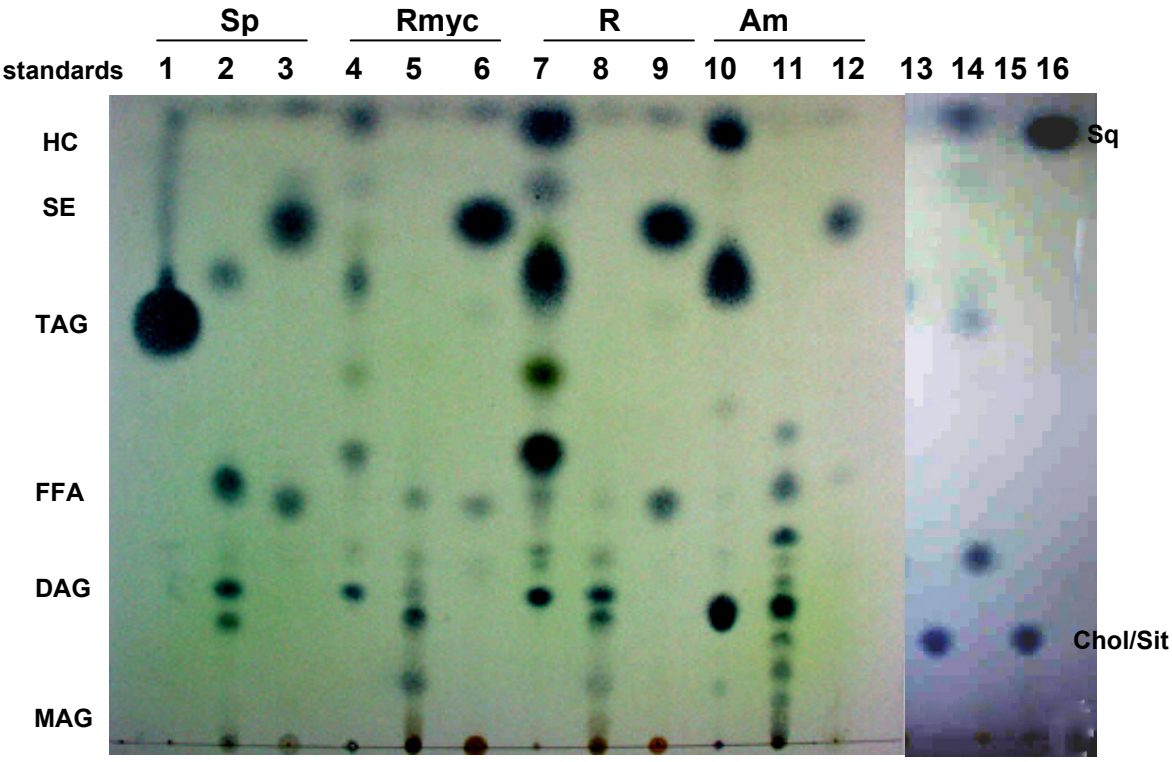

Figure 45. TLC plate silicagel (G60 Merck), washed with Cl_2CH_2/MeOH (1/1, v/v) and developed with hexane/diethyl ether/acetic acid (70/30/1, v/v). **Standards**: Monoacylglycerol (MAG), diacylglycerol (DAG), triacylglycerol (TAG), sterol esters (SE), hydrocarbons (HC). Positions according to www.cyberlipid.org/acylglyt/acyl0003.htm. 1-3 *G. intraradices* spore lipid extract (Sp): 1-Dichloromethane; 2-Acetone and 3-Methanol fraction; 4-6-Mycorrhizal carrot roots lipid extract (Rmyc): 4-Dichloromethane, 5-Acetone and 6-Methanol fraction; 7-9 Non-mycorrhizal carrot roots lipid extract (R): 7-Dichloromethane, 8-Acetone and 9-Methanol fraction; 10-12 *A. muscaria* lipid extract (Am): 10-Dichloromethane, 11-Acetone and 12-Methanol fraction. 13-Free cholesterol (Chol); 14-Mycorrhizal carrot roots acetylated sterols; 15-β-Sitosterol (Sit); 16-Squalene (Sq).

Sterols can be methylated at the carbon 4 (4α-methylsterols), dimethylated (4, 4'-dimethylsterols) or not methylated (4,4-demethylsterols). Ergosterol can be resolved from other 4,4-demethylsterol standards such as cholesterol and sitosterol after acetylation and development with cyclohexane/aceticethylether (9:1, v:v) in silicagel G60 TLC plates (Fig. 46). In the dichloromethane fraction of *A. muscaria* lipid extracts ergosterol was identified, constituting the mayor sterol (Fig. 46, lane 8). Acetylated lanosterol (4, 4'-dimethylsterol) can also be resolved by this method. Results showed that lanosterol is absent as a mayor sterol in all analyzed fractions. In contrast, most of the acetylated sterols seemed to be 4,4-demethylsterols, as later confirmed by GC-MS analysis (Fig. 46, lanes 1 to 6). Squalene was identified in all dichloromethane fractions.

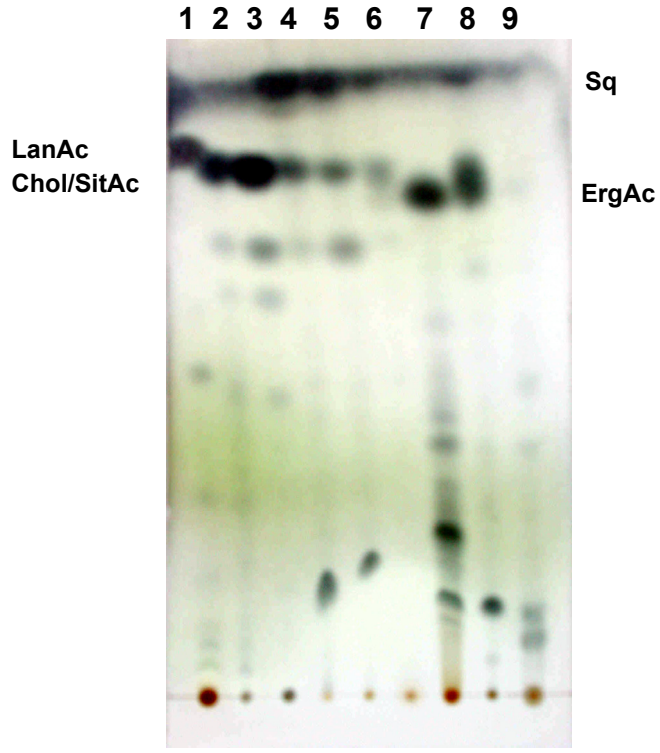

Figure 46. Differentiation between different acetyl-sterols. TLC plate silicagel (G60 Merck), developed with cyclohexane/aceticethylether (9:1, v:v). 1, 2, 3, 7-Acetylated standards: Acetyllanosterol (LanAc), acetylsitosterol (SitAc), acetylcholesterol (CholAc), acetylergosterol (ErgAc), respectively;4 and 5-Acetylated sterols from mycorrhizal (4) and non-mycorrhizal roots (5); 6-Acetyl-Cl_2CH_2 fraction mycorrhizal roots; 8 and 9-Acetylated Cl_2CH_2 (8) and acetone (9) fractions *A. muscaria* .

Further separation of the different sterol acetates was attempted using analytical TLC on 10% $AgNO_3$-silica gel plates. In these plates sterols differing in the degree of unsaturation and position of double bonds, either in the ring

system or in the side chain, can be resolved. Migration was performed as described in material and methods. However, no further distinction between 4,4-dimethyl steryl acetates (i.e. lanosterol), 4-demethyl steryl acetates (i.e. cholesterol, sitosterol and ergosterol) and 4α-methyl steryl acetates could be obtained (data not shown).

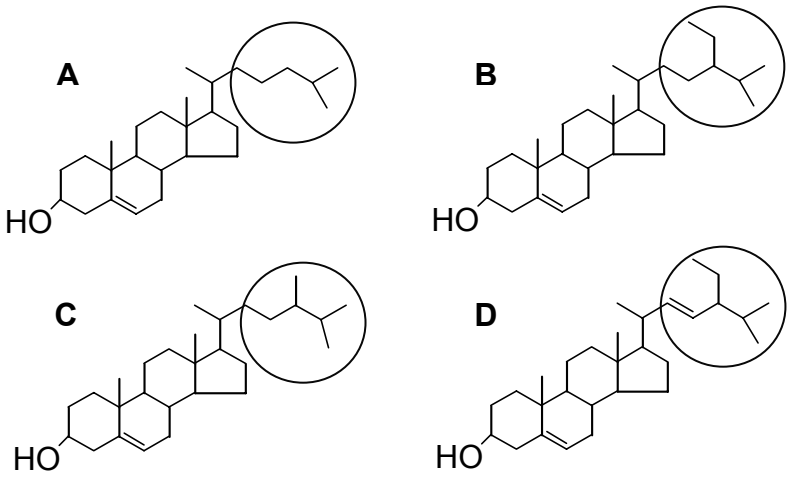

Figure 47. Cholesterol and 24-acyl derivatives. A. Cholesterol. **B.** β-Sitosterol (24-Ethylcholesterol). **C.** Campesterol (24-Methylcholesterol). **D.** Stigmasterol (24-ethylcholesta-5,22-dienol).

4.6.2 Insaponificable lipid fraction extraction

Lipid saponification was performed as described in material and methods with samples of *G. intraradices* spores (3 g), *G. intraradices* extraradical mycelium (3 g), carrot roots colonized by *G. intraradices* (5.56 g) and non-colonized carrot roots (6.47 g). Sample sterols and standards such as cholesterol, sitosterol and squalene, were applied as spots to HPTLC- Alufolien plates (Merck, Silica gel 60 F254). These were developed in a dichloromethane/methanol/water (85/15/0.5) solvent mixture, sprayed with a 0.1% berberin-HCl ethanol solution and made visible under UV-light. Free sterols run with a Rf of 0.78, while hydrocarbons and squalene run with a Rf of 0.92 (Fig. 48, lanes 1 and 2). Free sterols were acetylated overnight and analyzed by GC-MS.

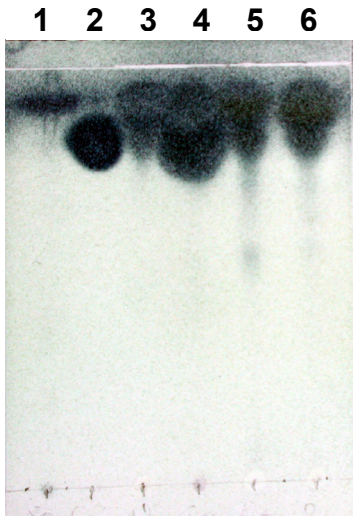

Figure 48. Non-saponifiable extraction fractions.
1-Squalene ; 2-Cholesterol ; 3-Spores *G. intraradices* ; 4-External mycelium G. intraradices ; 5-Carrot roots mycorrhizal with *G. intraradices* ; 6-Non-mycorrhizal carrot roots. Lipids were separated in HPTLC-Alufolien plates (Merck, Silica gel 60 F254), which were developed in a dichloromethane/methanol/water (85/15/0.5) solvent mixture.

4.6.3 Lipid analysis using GC-MS

Analyses by GC-MS showed that campesterol (24-methylcholesterol), stigmasterol (24-ethylcholesta-5,22-dienol) and β-sitosterol (24-ethylcholesterol) were the main sterols found in all samples (Fig. 47). However, the relative levels varied between *G. intraradices* spores and external mycelium (hyphae) and *D. carota* mycorrhizal and non-mycorrhizal roots.

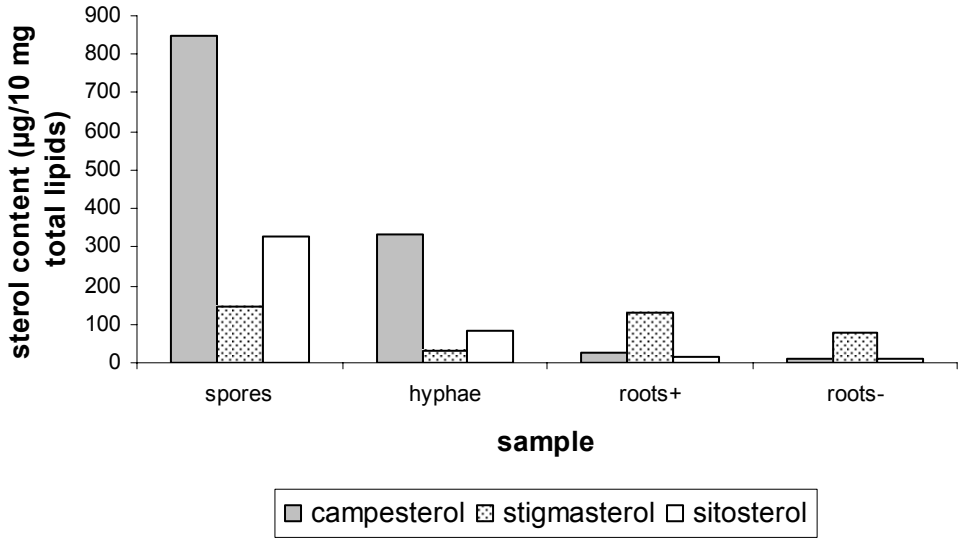

Figure 49. Quantification of main sterols in *G. intraradices* spores and external mycelium (hyphae), and in *D. carota* mycorrhizal (roots+) and non-mycorrhizal (roots-) roots.

Quantification of these sterols was achieved by comparison to the total lipid weight in the sample with cholesterol as internal standard. Thus, it could be shown that spores and hyphae contained high levels of campesterol, while this sterol was not so abundant in mycorrhizal and non-mycorrhizal roots. Thus, the main sterol in these samples was stigmasterol (Fig. 49).

Total lipid fractions and main sterols were analyzed by GC-MS in GC-17A (Shimadzu), coupled to QS-5000 MS (Shimadzu). Main peaks were analyzed according to their mass spectrum, compared to acetylated standard values and patterns (Fig. 50). Other sterols like isofucosterol, lanosterol, and sterol precursors such as cycloartenol were found in spores. Likewise, the external mycelium of *G. intraradices* basically contained the same sterols as the spores. Mycorrhizal carrot roots contained 24-epiclerosterol, isofucosterol, cholesterol and sterol precursors as cycloartenol, obtusifoliol and cycloeucalenol could also be detected. Interestingly, in non-mycorrhizal roots, cholesterol could not be detected. Ergosterol, a typical fungal sterol, could not be detected in any of the samples. However, it could be identified in *A. muscaria* total lipid extracts, in the dichloromethane fraction. Mycorrhizal roots showed a higher content of sterols when compared to non-mycorrhizal roots. The relative amount of 24-methylcholesterol was also increased in mycorrhizal roots (Fig. 50 and Table 5).

Sterol (Acetates)	**Mass spectrum (m/z relative intensity to base peak)**	**Retention time (min)**
24-Methylcholesterol (campesterol) (1)	382(100), 367(14), 274(15), 261(12), 255(17), 213(16), 147863), 81(60)	12.190
24-ethylcholesta-5,22-dienol (stigmasterol) (2)	394(92), 379(3), 351(6), 313(2), 182(6), 255(35), 228(4), 213(6), 81(87), 55(100)	12.620
24-Ethylcholesterol (β-sitosterol) (3)	396(100), 381(14), 288(13), 275(13), 255(19), 213(17), 147(52), 81(56)	13.280
Cholesterol	368(100), 353(14), 260(15), 255(13), 247(18), 213(14), 147(48), 145(37), 81(74), 55(71)	10.790
Isofucosterol	394(12), 379(1), 296(100), 281(19), 253(8), 228(7), 213(11), 55(87)	13.490
24-epiclerosterol	394(100), 379(22), 352(3), 310(7), 296(19), 281(25), 255(14), 253(33), 228(13), 213(20), 211(14)	13.110

Table 4. Sterol acetates with their mass spectrum and the relative intensity of the peak compared to the maximum peak in the spectrum and retention time.

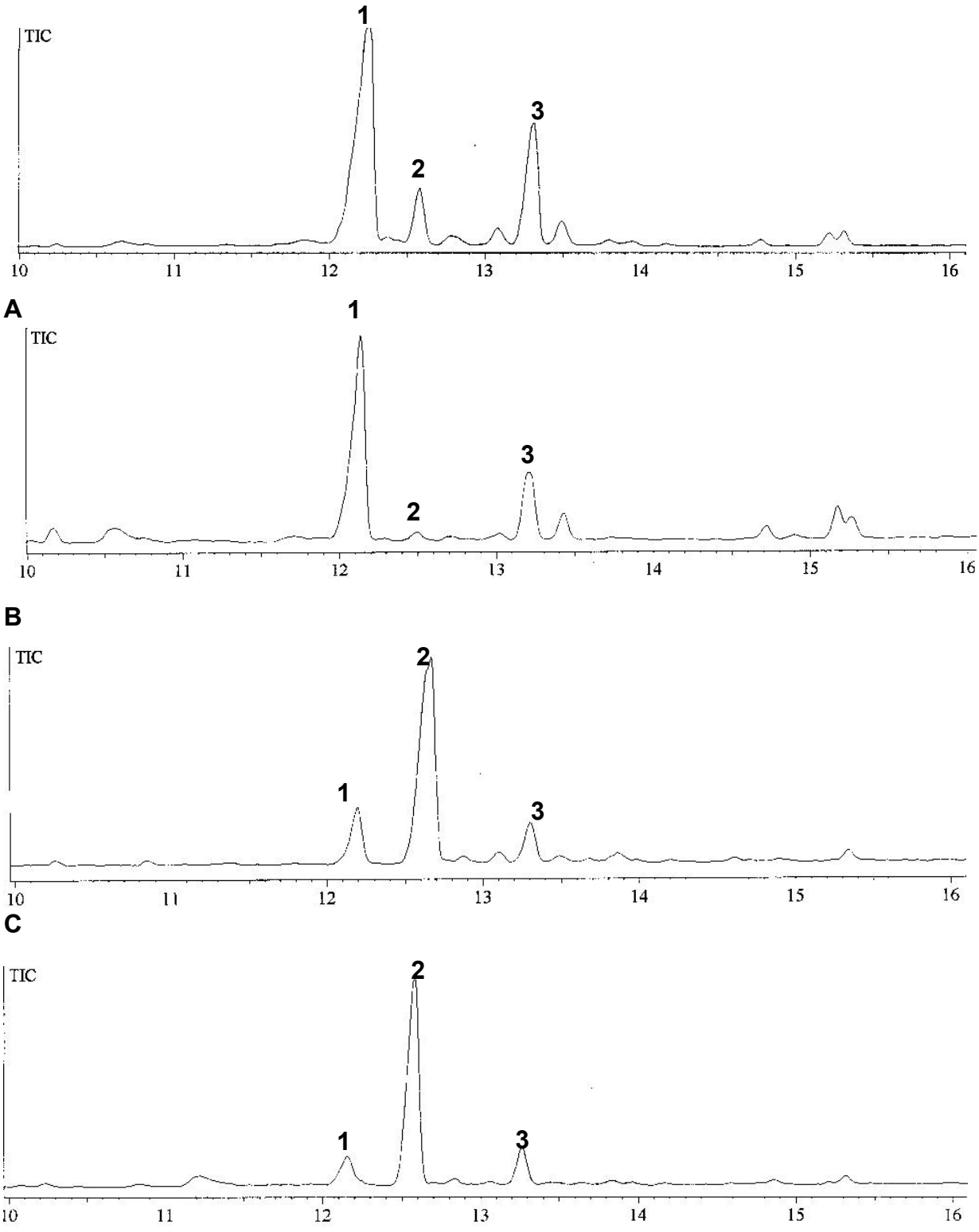

Figure 50. GC-MS chromatrogram from acetylated non-saponificable fractions. A. Spores from *G. intraradices.* **B.** External mycelium from *G. intraradices.* **C.** Carrot roots mycorrhizal with *G. intraradices*, **D.** Non-mycorrhizal carrot roots. 1-Campesterol (24-methylcholesterol); 2-Stigmasterol (24-ethylcholesta-5,22-dienol); 3-β-sitosterol (24-ethylcholesterol).

sterol / sample	Campesterol (1)	Stigmasterol (2)	βSitosterol (3)	Cholesterol	Lanosterol	Isofucosterol
Spores	++++	++	+++	-	*	+
Hyphae	+++	+	++	-	-	+
Mycorrhizal roots	++	++++	+	*	-	+
Non-mycorrhizal roots	+	++++	+	-	-	+

Table 5. Main sterols detected in spores and external mycelium (hyphae) from *G. intraradices*, mycorrhizal and non-mycorrhizal carrot roots. Relative amounts (+, ++, +++, ++++) are indicated when quantification was possible. (*) means the sterol was detected by GC-MS but the amount was too low for quantification. (-) non-detected.

4.7 Recombinant expression and purification of GmGIN1-N terminus

The N-terminus of GmGIN1 (GmGIN1-N) shares similarity with the new family of GTPases called AIG/IAN/GIMAP family (Krücken et al., 2004) (Fig. 52). Accordingly, GmGIN1-N contains a nucleotide binding domain near its amino terminus, as other three conserved cassettes for GTP binding (Fig. 52). Two of them are shared between ATPases and GTPases (Traut, 1994). In order to study the nucleotide affinity of GmGIN1-N as its possible enzymatic activity, GmGIN1-N was expressed heterologously in *E. coli* using the pTrcHis expression vector. The corresponding *GmGIN1-N* gene fragment was PCR amplified with the primers GmGINExF3 and GmGINExR2 as described in material and methods. The fragment of 833 bp (Fig. 51-A) was ligated into the expression vector pTrcHisTOPO and transformed in XL1-Blue *E. coli* cells. Clones were analyzed by plasmid DNA extraction and restriction analysis with EcoRI and BamHI/HindIII. First expression studies were preformed in XL-1 Blue cells, inducing expression of the protein during 4 hours with 0.8 mM IPTG at 37°C, once the cells had reached an OD_{600} over 0.6.

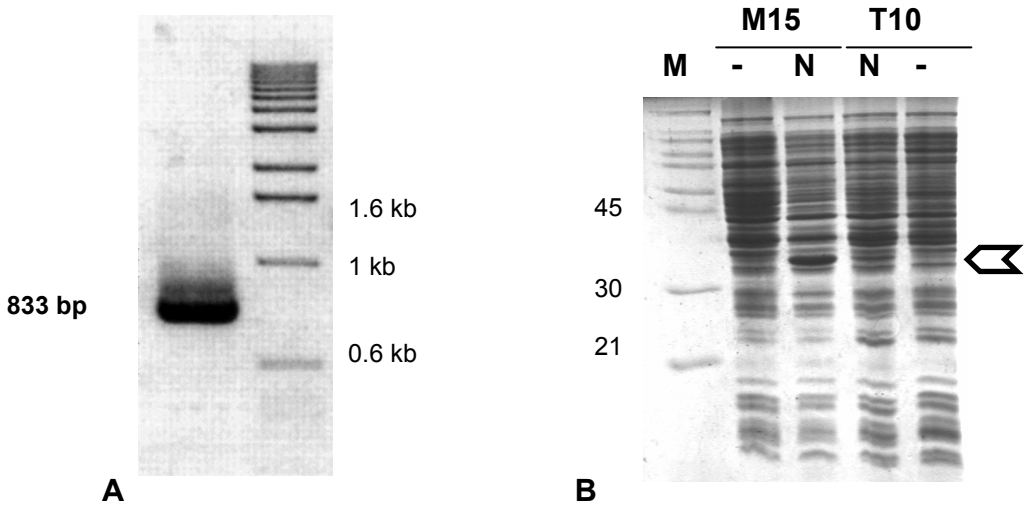

Figure 51. A. PCR product using GinExF3 and GinExR2. B. GmGIN1-N expression using the pTrcHis expression vector. Comparison between M15 *E. coli* empty cells (-), M15 cells expressing GmGIN1-N in pTrcHis (N), T10 cells expressing GmGIN1-N in pTrcHis (N) and T10 *E. coli* empty cells (-). Arrows indicate GmGIN1-N position.

cleavage site	Resulting peptide sequence	Peptide length [aa]	Peptide mass [Da]	$[M+H]^+$	$[M+2H]^{2+}$	Sample1 Detected mass	Sample2 Detected mass
23	23	2465,0	MGGSHHHHHHGMASMTGGQQMGR	2466,0	1234,0	n.d.	n.d.
47	24	2680,2	DLYDDDDKDPTLMSNCPSILLIGK	2681,2	1341,6	n.d.	n.d.
52	5	460,3	TGVGK	461,3	231,6	√	√
62	10	1042,6	STLGNLLLGR	1043,6	522,8	√	√
88	26	2797,3	DVFDVSDSAASLTQGYQTAPIEINEK	2798,3	1400,2	√	√
103	15	1768,8	TFNVVDTHGFFDTNR	1769,8	885,9	√	√
110	7	844,5	TNQEILK	845,5	423,7	√	√
134	24	2736,4	EVTQEILQCENGIQAFVFVIEATR	2737,4	1369,7	n.d.	n.d.
137	3	394,2	FTK	395,2	198,6	√	√
140	3	431,2	EQR	432,2	217,1	√	√
165	25	2695,3	DTINQIINFLGEDSLNNMIAVFSK	2696,3	1349,2	√	√
168	3	405,2	CRK	406,2	204,1	n.d.	n.d.
176	8	882,4	APTINPDR	883,4	442,7	n.d.	n.d.
186	10	1227,6	LFNSFSQEEK	1228,6	615,3	n.d.	n.d.
191	5	663,3	DFLNR	664,3	333,2	√	√
195	4	458,2	IGNR	459,2	230,6	√	√
215	20	2314,1	FTISPNLEIFDEPNDPIVVR	2315,1	1158,6	√	√
219	4	515,3	HMTK	516,3	259,1	√	√
221	2	259,2	LK	260,2	131,1	n.d.	n.d.
238	17	2048,0	EYIVNFPDLYTTAVFEK	2049,0	1025,5	√	√
243	5	588,3	VLMAR	589,3	295,7	√	√
248	5	681,3	ENEYK	682,3	342,1	√	√
249	1	174,1	R	175,1	88,6	n.d.	n.d.
250	1	146,1	K	147,1	74,6	n.d.	n.d.
251	1	174,1	R	175,1	88,6	n.d.	n.d.
257	6	600,4	VNAGLK	601,4	301,7	√	n.d.
262	5	592,3	GFLTR	593,3	297,7	√	n.d.
273	11	1259,6	KPVELINDFEG	1260,6	631,3	√	n.d.

Table 6. Resulting peptides after trypsin digestion of pTrcHisGmGIN1-N and detection of the different peptides by mass spectrometry. Detected (√) and non detected (n. d.) peptides. sample 1 corresponds to the upper band running in SDS-PAGE gels, corresponding to GmGIN1-N; sample 2 corresponds to the lower running band, in which at least the final 22 amino acids could not be detected.

Cells containing GmGIN1-N in pTrcHis expressed a protein of 31 KDa, corresponding to the N-terminus of the GmGIN1 protein fused to the His-tag, as confirmed by immunodetection using the AntiXpress antibody (Fig. 51) and mass spectrometry (table 6). GmGIN1-N in pTrcHis vector was also cloned into TOP-10, M-15[pREP4] and BL21 *E. coli* cells. M15 cells yielded higher amounts of protein, and could be differentiated in Coomassie stained gels in comparison with empty cells (Fig. 51-B).

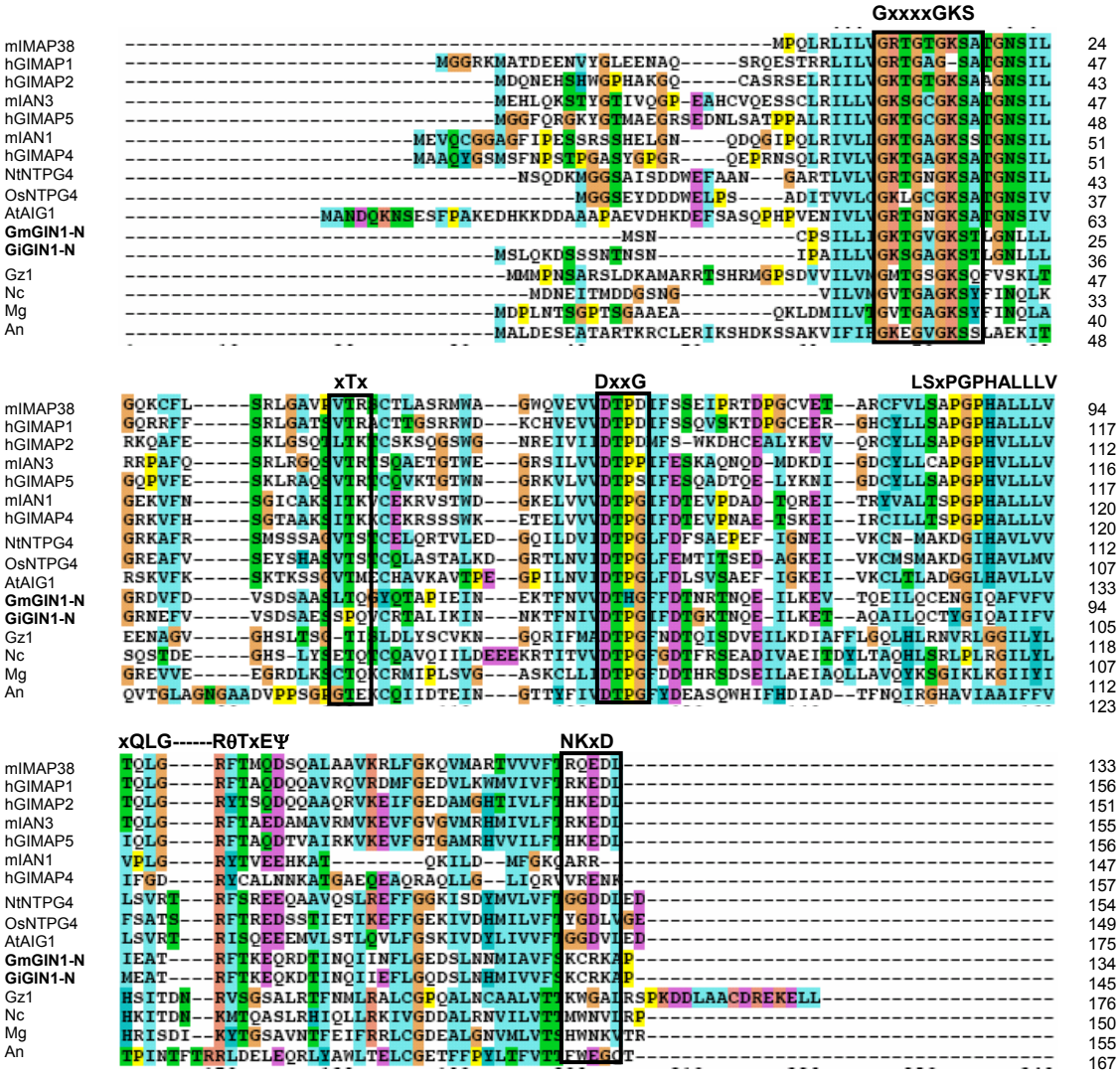

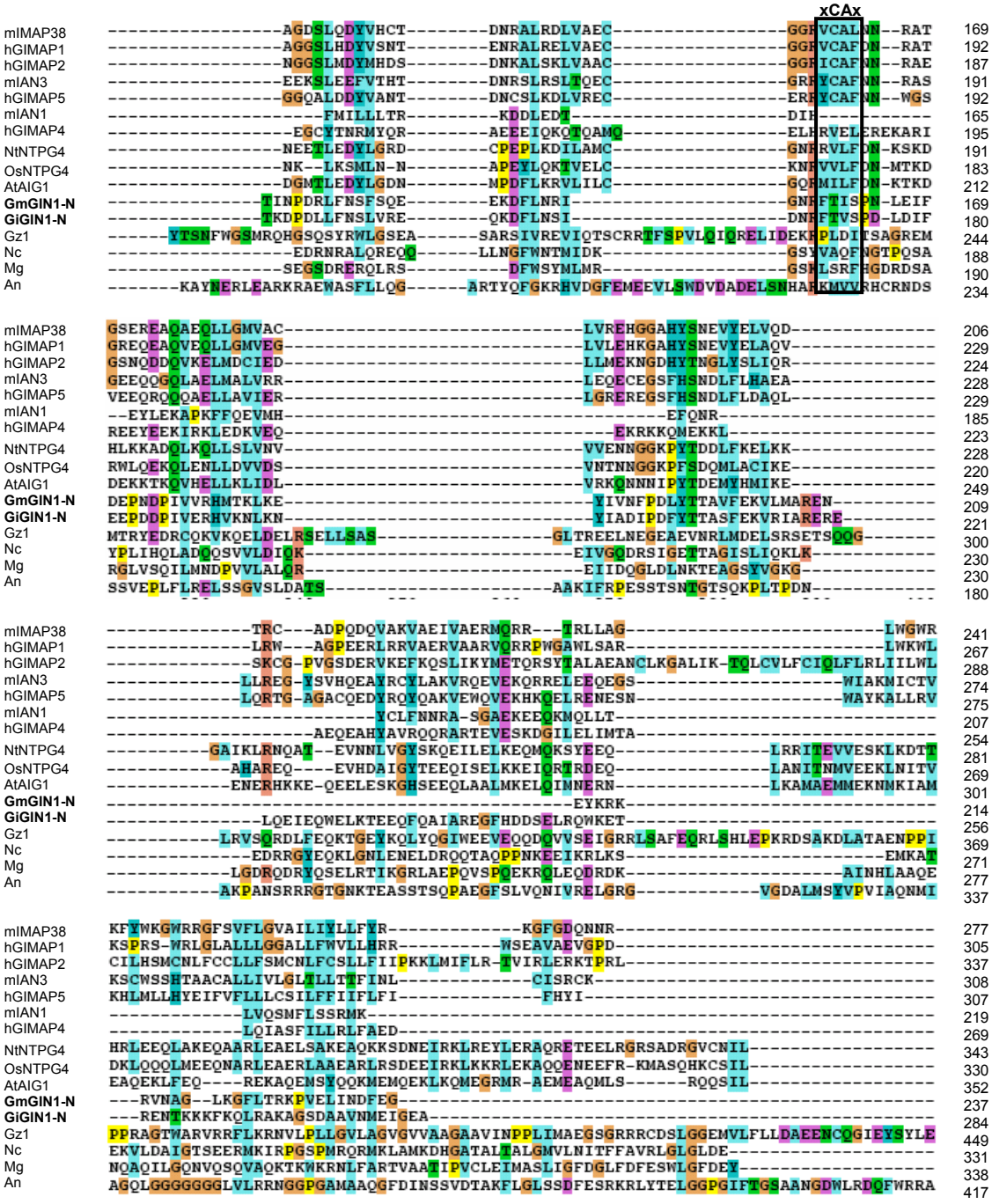

Figure 52. Multiple sequence alignment of animal, plant and fungal members of the AIG/IAN/GIMAP family of proteins with GmGIN1-N and GiGIN1-N h, human; m, mouse; mIMAP38 (NM008376), hGIMAP1 (AJ306287), hGIMAP2 (AL110151), mIAN3 (NM146167), hGIMAP5 (AK002158), mIAN1 (NM174990), hGIMAP4 (AK001972), At, *A. thaliana* AIG (NP174657); Nt, *Nicotiana tabacum* NTPG4 (AAD09518); Os, *Oriza sativa* NTGP4 (XP_466219); Gz, *Gibberella zeae* (1, accession number EAA74755); Nc, *Neurospora crassa* (EAA28888); Mg, *Magnaporthe grisea* (EAA47306); An, *Aspergillus nidulans* (XP_407465). GTP-binding motifs (G1 to G5) are boxed and conserved amino acids are stated. The conserved hydrophobic region between G3 and G4 is also remarked.

GmGIN1-N expressed in pTrcHis vector was more soluble than GmGIN1 full length and GmGIN1-C. Therefore, much of the protein was detected in the supernatant after native lysis. Expression and purification of GmGIN1-N in pTrcHis was compared using three different *E. coli* strains: XL-1 Blue (data not shown), M15 [pREP4] and TOP-10. Best results were obtained performing minipurifications from 2 mL cultures, with addition of 10 mM β-mercaptoethanol and 5 mM $MgCl_2$ in the lysis and washing buffers (Fig. 53). Surprisingly, after scale up of the culture and purification, purified GmGIN1-N gave two different signals after immunodetection with antiXpress antibody (Fig. 54-B). Both bands were recognized by specific antibodies versus the N-terminus (data not shown). Mass spectrometry analyses after trypsin digest also indicate that both bands correspond to the same protein, although a peptide corresponding to the last C-terminal amino acids could not be detected in the lower molecule weight band (table 6).

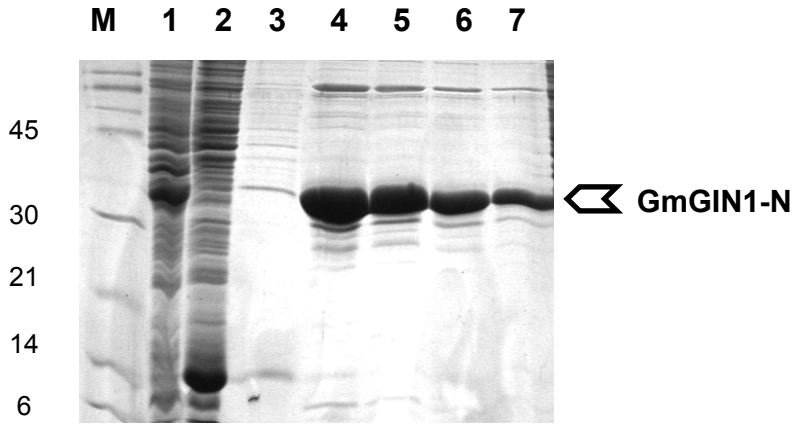

Figure 53. Minipurification of GmGIN1-N expressed in pTrcHis in M15[pREP4] *E. coli* cells. Coomassie stained SDS-PAGE gel. 1-Total cell lysate after induction; 2-SN after Ni-NTA resin incubation; 3-Last wash; 4-7-Subsequent eluted fractions.

Purification of GmGIN1-N under denaturing conditions realized using M15 [pREP4] and TOP-10 *E. coli* strains. These results were compared to the corresponding purifications under native conditions. Under denaturing conditions the lower molecular weight band appears in a much lower relative amount, if at all, and only in the elutions (Fig. 55). These results indicate that GmGIN1-N is susceptible to proteolytic degradation despite PMSF addition

during purification, which is avoided by addition of denaturants and a faster minipurification.

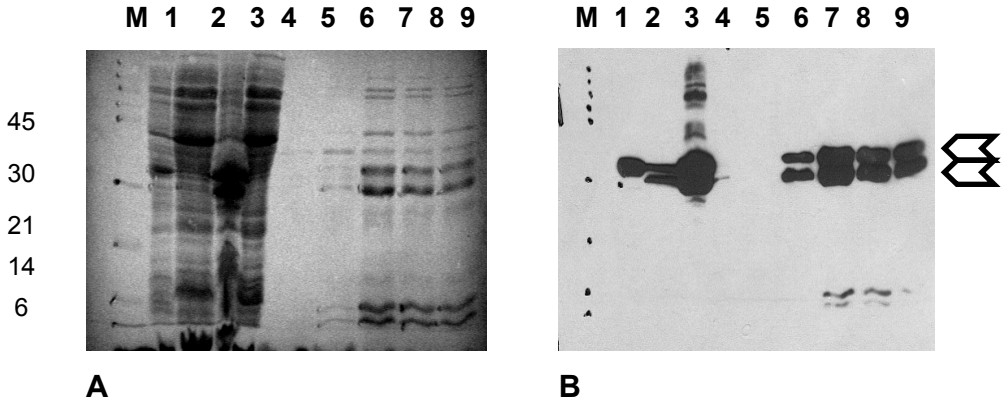

Figure 54. Scale up native purification GmGIN1-N in pTrcHis using M15[pREP4] cells. **A. PonceauS stained nitrocellulose membrane. B. Immunodetection with AntiXpress antibody.**, 1-Total cell lysate after induction; 2-SN after lysis; 3-Pellet after lysis; 4-SN after Ni-NTA resin incubation; 5-Last wash; 6-Wash with 50 mM ImH; 7-9-Eluted fractions. Arrows indicate GmGIN1-N and the degraded product position.

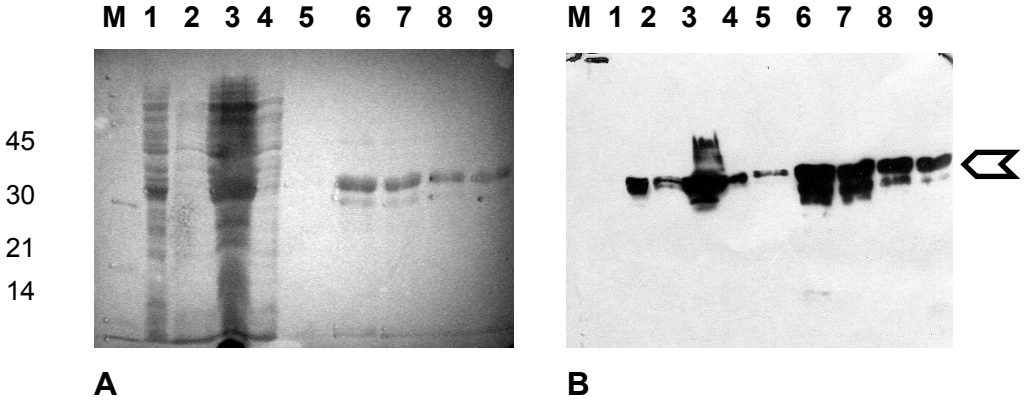

Figure 55. Denaturing purification GmGIN1-N in pTrcHis using M15[pREP4] cells. A. PonceauS stained nitrocellulose membrane. B. Immunodetection with AntiXpress antibody. 1-total cell lysate after induction, 2-SN after lysis, 3-pellet after lysis, 4-SN after Ni-NTA resin incubation, 5-last wash Ni-NTA resin, 6-9-eluted fractions from Ni-NTA resin. Arrows indicate GmGIN1-N position.

4.8 Expression and purification of *cdc42* of *Ustilago maydis*

As positive control for the GTP binding assays and GTPase activity, the small Rho GTPase cdc42 from *U. maydis* was used (Bölker et al., 2002). Wild type Umcdc42 and a derivative mutant, which has glutamine 61 (Q) mutated to leucine (L), were heterologously expressed in *E. coli.* Q61L mutation prevents GTP hydrolysis and makes the protein constitutively active (Ziman et al 1991). The proteins carry also a cysteine to serine mutation in order to avoid

posttranscriptional lipid modification (isoprenylation) at its carboxy terminus (Aspenström and Olson 1995). Nevertheless, this kind of modification would not occur in the *E.coli* expression system. The constructs were expressed in the pET15b vector (Novagen), which incorporates an N-terminal six histidine tag. Expression was induced in BL21(DE3) cells by addition of 0.5 mM IPTG once the cells had reached the exponential growth fase. Protein was purificated by Ni-NTA affinity chromatography under native conditions. Plenty of native protein could be obtained (Fig. 56).

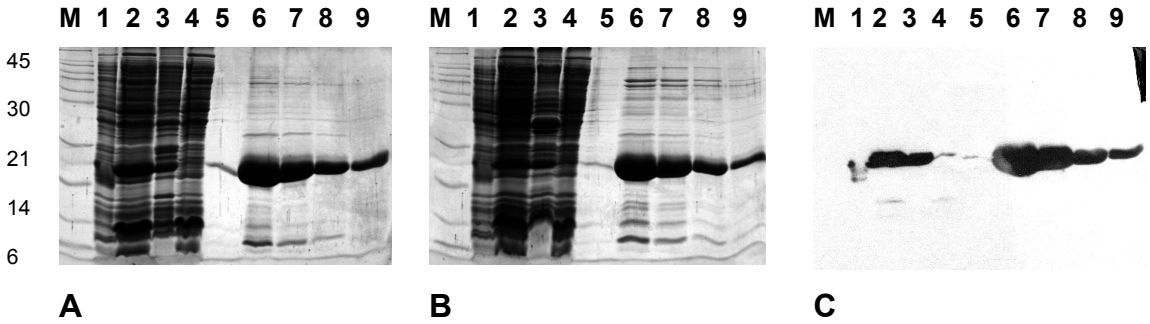

Figure 56. *U. maydis* cdc42 and cdc42(Q-L) proteins expressed in pET15b vector and BL21(DE3) cells and purified under native conditions in Ni-NTA resin. A. Umcdc42(Q-L) mutant. **B.** Umcdc42 Wild type. 1-Total cell lysate after protein induction; 2-Supernatant after lysis; 3-Pellet after lysis; 4-Supernatant after Ni-NTA resin incubation; 5-Last wash Ni-NTA resin; 6 to 9-Eluted fractions from Ni-NTA resin. **C.** Immunodetection with AntiHis Novagen of Umcdc42(Q-L) mutant.

4.9 GTP binding activity

4.9.1 GTP overlay assays

GTP binding assays were performed using radiolabelled α-^{32}P-GTP (Amersham). Total lysates of *E.coli* expressing Umcdc42, Umcdc42(Q-L) or GmGIN1-N and purified proteins were run in SDS-PAGE gels and transferred onto nitrocellulose membranes as described in material and methods. The assay was performed using two different binding buffers (see materials and methods). Empty *E. coli* extracts were used as negative control. As controls were also used total protein extracts from *A. muscaria* mycelium, *G. intraradices* spores and mycorrhizal carrot roots. Several protein bands were linked to the labelled GTP (Fig. 57-A), but none of these signals proved to be specific for neither of the tested GTP binding proteins. No differences were observed between binding of negative control, empty *E.coli* cells, and cells expressing

either of the proteins (Fig. 57 B and C, for Coomassie stained gels). Significant reduction of the signal was observed when 30 μM ATP was added in the binding buffer before incubation with the radioactive α-^{32}P-GTP (comparison between D and E in Fig. 57). Signals were also attenuated by increasing the amount of Tween-20 to 0.2%. Both reagents added together lead to the disappearance of any signal.

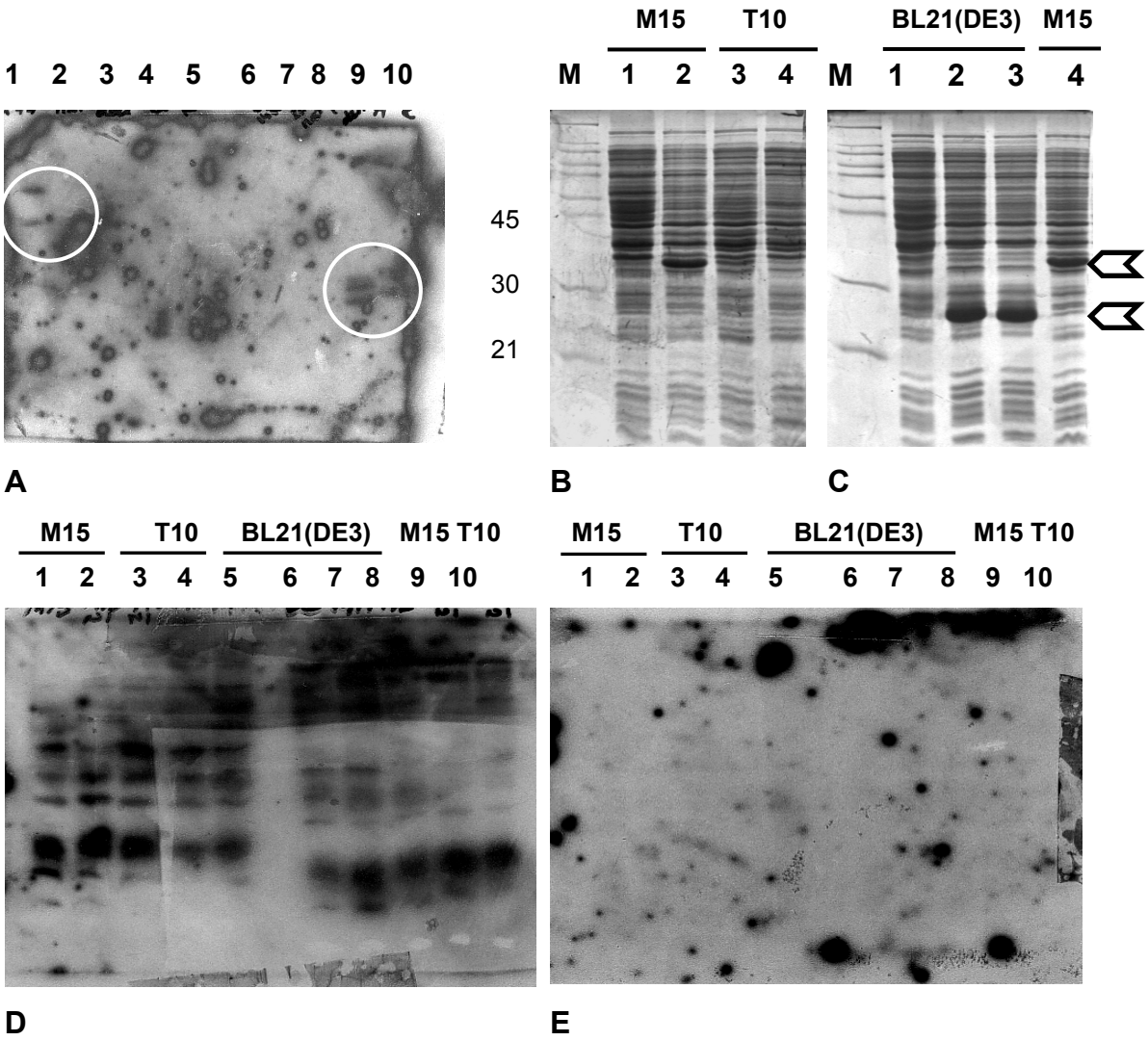

Figure 57. GTP overlays. A. GTP binding assay without ATP. 1-Native purified Umcdc42 WT; 2-Native purified GmGIN1-N (T10); 3-Denatured purified GmGIN1-N (M15); 4-M15 expressing GmGIN1-N; 5-Protein extract from mycorrhizal carrot roots; 6-Native purified Umcdc42(Q-L) mutant; 7-Native purified GmGIN1-N (XL1); 8-Denatured purified GmGIN1-N (T10); 9-Protein extract from *A. muscaria* mycelium; 10-Protein extract from *G. intraradices* spores. **B.** GmGIN1-N expressed in M15 and TOP10 cells (2 and 3), compared to the empty cell lysates (1 and 4). **C.** Umcdc42 and Umcdc42(Q-L) mutant expressed in BL21(DE3) cells (2 and 3) compared to empty cells (1 and 4). Arrows indicate GmGIN1-N and Umcdc42 and Umcdc42(Q-L) positions.
D. GTP binding assay without ATP. E. GTP binding assay with ATP. Negative controls *E. coli* M15 (1), TOP10 (4) and BL21(DE3) (6) cells; GmGIN1-N (N) expressed in M15 (2 and 9) and T10 cells (3 and 10); Umcdc42 WT (5 and 7) and Umcdc42(Q-L) mutant (8) expressed in BL21(DE3) cells.

4.9.2 GTP binding filtration assays

The ability of GmGIN1-N, Umcdc42 and Umcdc42(Q-L) to bind GTP was tested using the so-called GTP binding filtration assay. For that the three proteins purified under native conditions were incubated with the non-hydrolyzable radioactive analogue ^{35}S-γ-GTP. After incubation and subsequent filtration the remaining radioactivity bound to the proteins was measured.

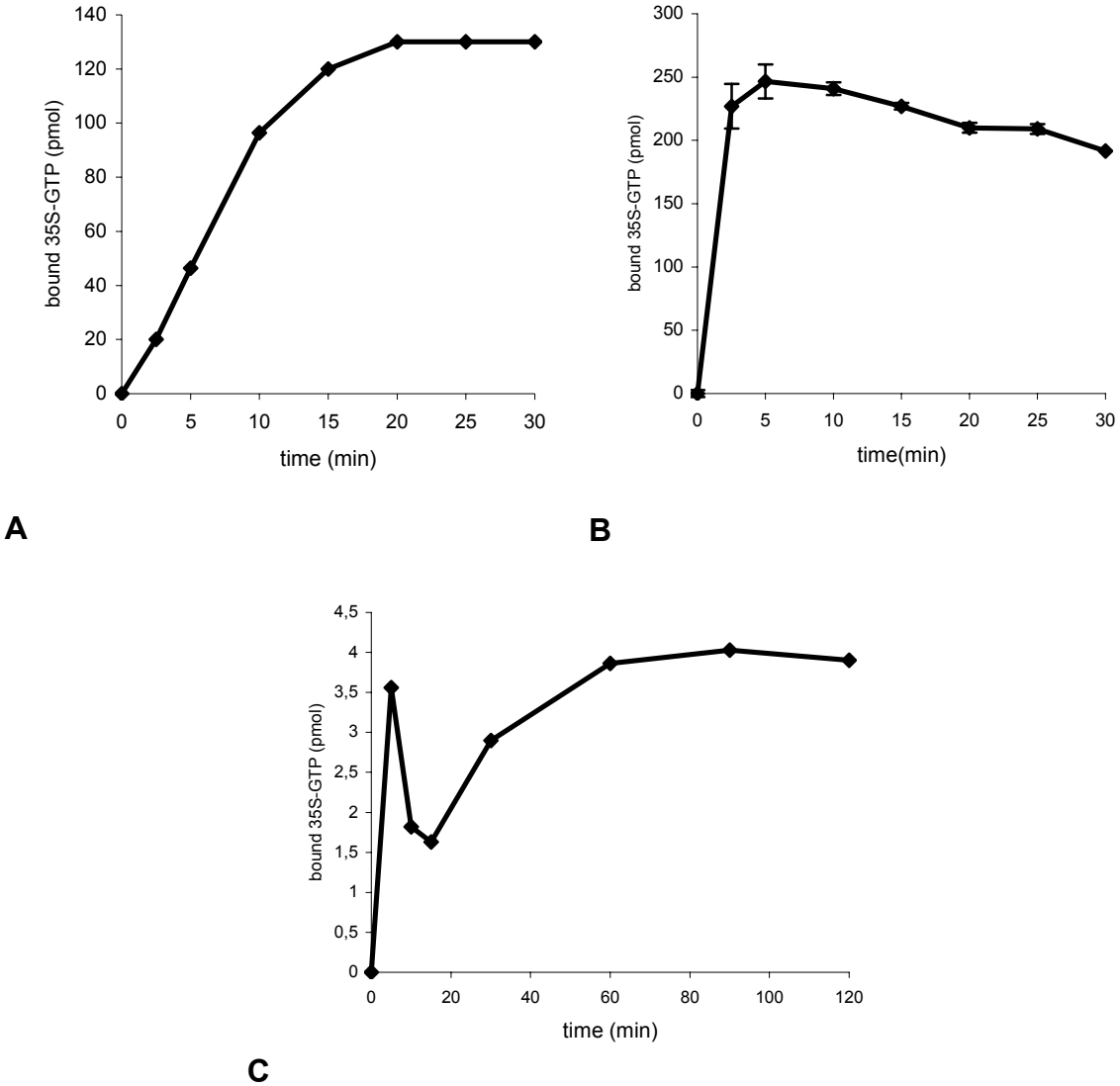

Figure 58. 35S-γ-GTP binding in solution. Binding assays were performed with 10 µM ^{35}S-γ-GTP**. A.** Incubation with 4 µM positive control Umcdc42(Q-L) mutant. **B.** Incubation with 4 µM positive control UmCdc42; **C.** Incubation with 6 µM GmGIN1-N.

A time-course experiment with different incubation times showed that Umcdc42(Q-L) was able to bind ^{35}S-γ-GTP within minutes at a low concentration of free magnesium (1 µM), in an exponential manner with a

saturation kinetics after 20 minutes (Fig. 58-A). In contrast, the wild type form of Umcdc42 bound very rapidly to ^{35}S-γ-GTP using a comparable amount of protein (4 µM) in the binding assay (Fig. 58-B). A difference in the affinity for ^{35}S-γ-GTP would explain the different curves obtained when Umcdc42 (Q-L) mutant was compared to wild type Umcdc42. Levels of ^{35}S-γ-GTP bound by both proteins are very high (15.9 pmoles/µg Umcdc42(Q-L), but even higher for wild type Umcdc42 (24.5 pmoles/µg protein). When the amount of protein in the binding assay was reduced to 0,8 µM Umcdc42, the amount of bound ^{35}S-γ-GTP was reduced to an average of 60 pmoles, but the amount of nucleotide per µg of protein (38.6 pmol/µg protein) was increased. This result is in accordance with the reduction of protein concentration in the assay, although binding seems to be more efficient when the protein is more diluted. The same effect was observed for Umcdc(Q-L) mutant and GmGIN1-N. Nevertheless, no exponential curve was observed with Umcdc42 despite using less protein in the assay.

Very low unspecific binding (0.07 pmoles/µg protein) was detected when DmHhD-C protein was used in the incubation as a negative control, corresponding to less of 1% of the radioactivity in the reaction mixture. Binding of GmGIN1-N, although higher than the negative control (DmHhD-C), was much lower than the values obtained with the positive controls, with a maximum ranging from 0.7 to 8 pmol of ^{35}S-γ-GTP/ µg protein (Fig. 58-C). Protein concentration of GmGIN1-N ranged from 0,5 to 1 µM per assay. An increase of 10 times the protein concentration in the assay did not lead to an increase in the binding to ^{35}S-γ-GTP. Even more, a better binding was observed when using a lower protein concentration. GmGIN1-N purified in the absence or presence of a low amount of GDP showed similar binding capacity at 1 µM free Mg^{+2}. However, a high variability was obtained in both cases. Two other concentrations of $MgCl_2$ were tested, 1 mM and 10 mM. At 1 mM $MgCl_2$ almost no binding could be detected (0.83 pmol ^{35}S-γ-GTP/ µg protein) for GmGIN1-N purified in the absence of GDP. In contrast, protein purified in the presence of GDP showed a relative constant binding capacity of 4 pmol ^{35}S-γ-GTP/ µg protein. At 10 mM concentration of $MgCl_2$ no binding could be detected in any case.

4.9.3 Dissociation assay using competing nucleotides

UmCdc42 and GmGIN1-N were tested for their ability to discriminate between different substrates. Once the proteins were loaded with ^{35}S-γ-GTP, an unlabeled competitor nucleotide in a much higher concentration was added as described in material and methods. Under these conditions UmCdc42 was able to dissociate ^{35}S-γ-GTP and exchange it for GDP when used as a competitor nucleotide as expected (Fig. 59). The same experiment was performed with GmGIN1-N with positive results. ATP and ADP were also used as competitors with this protein. Surprisingly, ATP was the most efficient nucleotide in replacing ^{35}S-γ-GTP, while ADP dissociates ^{35}S-γ-GTP more slowly than the other nucleotides tested (Fig. 60). When GTP was used as a competing nucleotide a quite strange result was obtained. A very fast dissociation within the first 2.5 minutes was followed by a very high binding to ^{35}S-γ-GTP at 7.5 minutes (10 pmoles/µg protein), compared to the initial value of bound ^{35}S-γ-GTP before adding the cold GTP (3.5 pmoles/µg protein). After this increase, binding to ^{35}S-γ-GTP seems to decay again (Fig. 60).

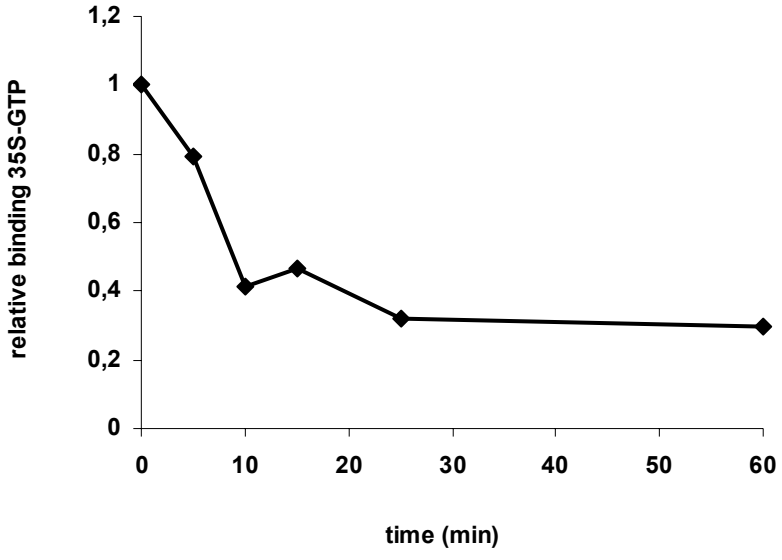

Figure 59. Dissociation assay with UmCdc42 wild type protein using GDP as competing nucleotide. 0.8 µM protein was incubated for 10 minutes with 10 µM ^{35}S-γ-GTP as described in material and methods and 1 mM GDP was added as competitor nucleotide. Aliquots were taken at the indicated time points and ^{35}S-γ-GTP bound to the protein was measured after filtration. Binding before addition of competitor was taken as 100% value.

These experiments were performed with two different batches of purified GmGIN1-N protein, with and without addition of GDP during purification, in triplicate for each time point with similar results. The results indicate that GmGIN1-N has a higher affinity for ATP than for GTP.

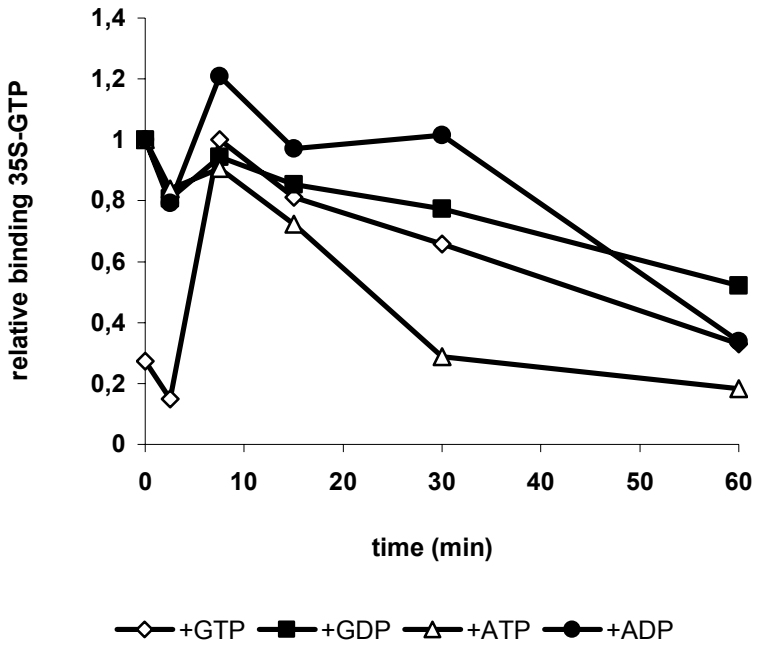

Figure 60. Dissociation assay of GmGIN1-N with competing nucleotides (GTP, GDP, ATP and ADP). 1 µM protein was incubated for 45 minutes with 10 µM ^{35}S-γ-GTP. Values of binding to ^{35}S-γ-GTP before addition of the competing nucleotide were assumed as one unit of binding, excepting for GTP dissociation assay, in which the maximal value of binding (at 7.5 minutes) was considered as the reference unit. Values represent the average from triplicate samples.

4.10 Enzymatic activity of GmGIN1-N

Because of the unexpected results obtained for the competition assays with GmGIN1-N, showing the higher affinity of the protein for ATP, both GTP and ATP hydrolysis experiments were carried out. Twenty pmoles of protein purified in presence of GDP were incubated with 1 µl radiolabelled α^{32}P-ATP or α^{32}P-GTP (10 mCi/ml) (Amersham) in 10 µl hydrolysis buffer at 30°C. Two µl aliquots from the reaction mixture were removed at different time points and frozen to stop the hydrolysis reaction. The same reaction mixture, but lacking the protein, was used as negative control. Aliquots were spotted onto silica gel G60 thin

layer chromatography (TLC) plates and resolved for 12 h with a mixture of isobutyl alcohol:isoamyl alcohol:2-ethoxyethanol:ammonia:water (9:6:18:9:15). Plates were dried and exposed to an X-ray film for 10 h.

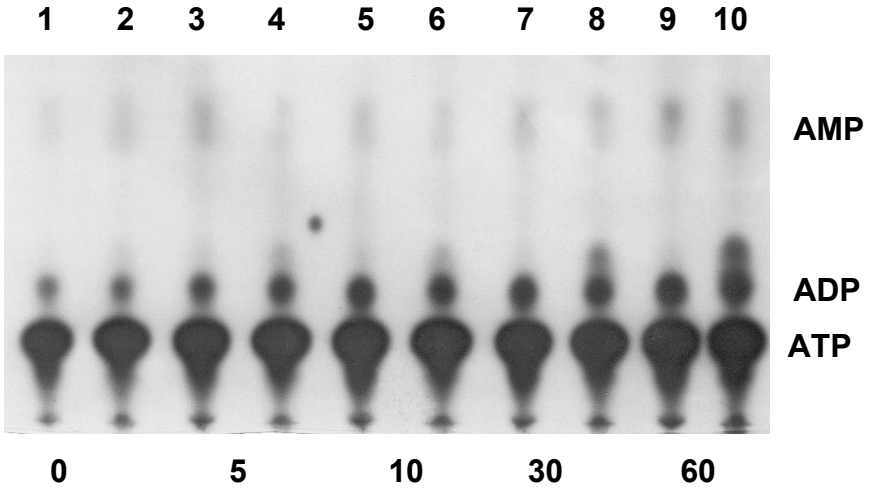

Figure 61. ATPase activity of GmGIN1-N. 20 pmoles (1,6 µM) GmGIN1-N incubated with 1 µl radiolabelled α32P-ATP (10 mCi/ml). Comparison between reaction mixture without protein (1,3,5,7,9) and with GmGIN1-N (2,4,6,8,10) at different time points expressed in minutes.

Appearance of an additional signal in the range of ADP could be observed when α^{32}P-ATP was incubated in the presence of GmGIN1-N (Fig. 61, 63). This indicates that α^{32}P-ATP is being hydrolyzed by the protein. In contrast, when the protein was incubated in the presence of α^{32}P-GTP, no differences could be observed between the negative control and the incubation with GmGIN1-N (Fig. 64). Some background hydrolysis of both nucleotides could be observed. A difference in the running of background α^{32}P-ADP and the specific signal can be observed. This might be due to the binding to the protein. Nevertheless, both signals run in the range described for non-radiolabelled standards (Fig. 63). Incubation of 40 pmoles (3,2 µM) of GmGIN1-N with 0,5 µl radiolabelled α^{32}P-ATP (10 mCi/ml) and 5 µM cold ATP in the same final reaction volume, considerably reduced the background signal of α^{32}P-ADP and increased the intensity of the specific signal (Fig. 62). Moreover, a decrease in the intensity of the signal corresponding to α^{32}P-ATP could be observed in samples incubated with GmGIN1-N.

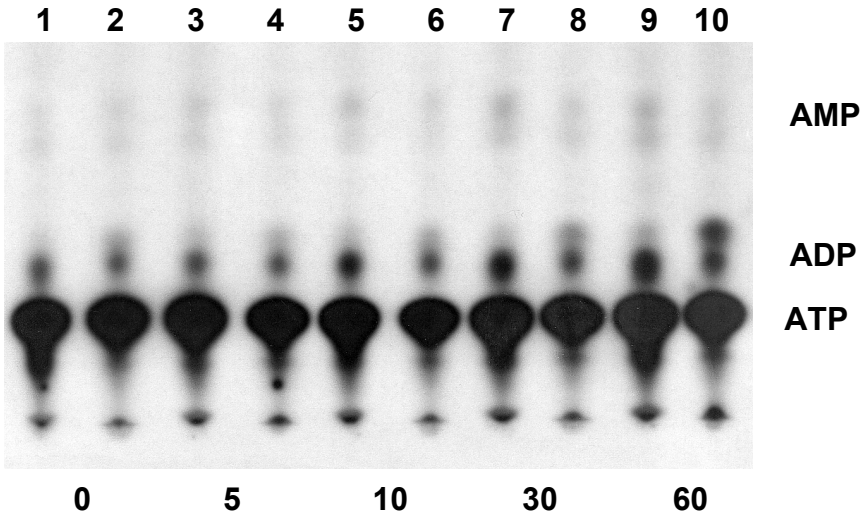

Figure 62. ATPase activity of GmGIN1-N. 40 pmoles (3,2 µM) GmGIN1-N incubated with 0,5 µl radiolabelled α32P-ATP (10 mCi/ml) and 5 µM cold ATP. Comparison between reaction mixture without protein (1,3,5,7,9) and with GmGIN1-N (2,4,6,8,10) at different time points expressed in minutes.

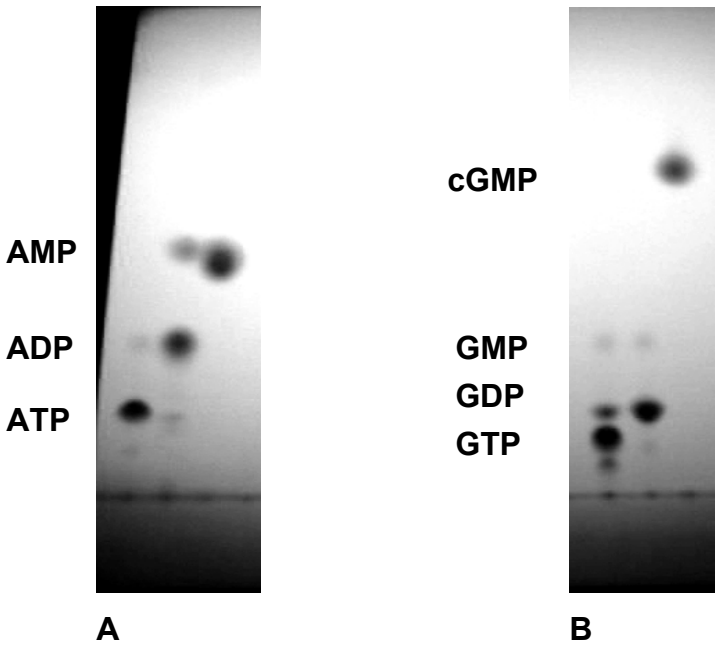

Figure 63. Nucleotide standards. A. Adenosine derivatives. B. Guanosine derivatives. 1 µl of 100 mM stocks from the different nucleotides were spotted onto silicagel G60/F254 TLC plates and resolved for 12 h with a mixture of isobutyl alcohol:isoamyl alcohol:2-ethoxyethanol:ammonia:water (9:6:18:9:15). Spots were visualized by exposure to UV light.

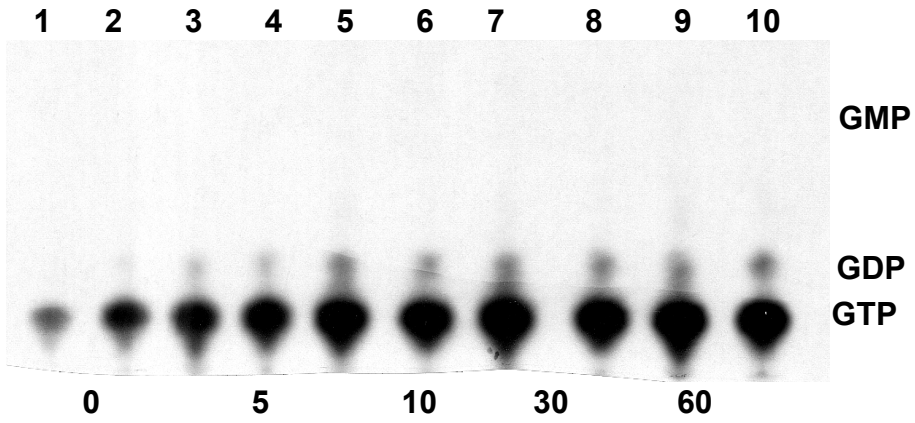

Figure 64. GTPase activity of GmGIN1-N. 20 pmoles (1,6 µM) GmGIN1-N incubated with 1 µl radiolabelled α32P-GTP (10 mCi/ml). Comparison between reaction mixture without protein (1,3,5,7,9) and with GmGIN1-N (2,4,6,8,10) at different time points expressed in minutes.

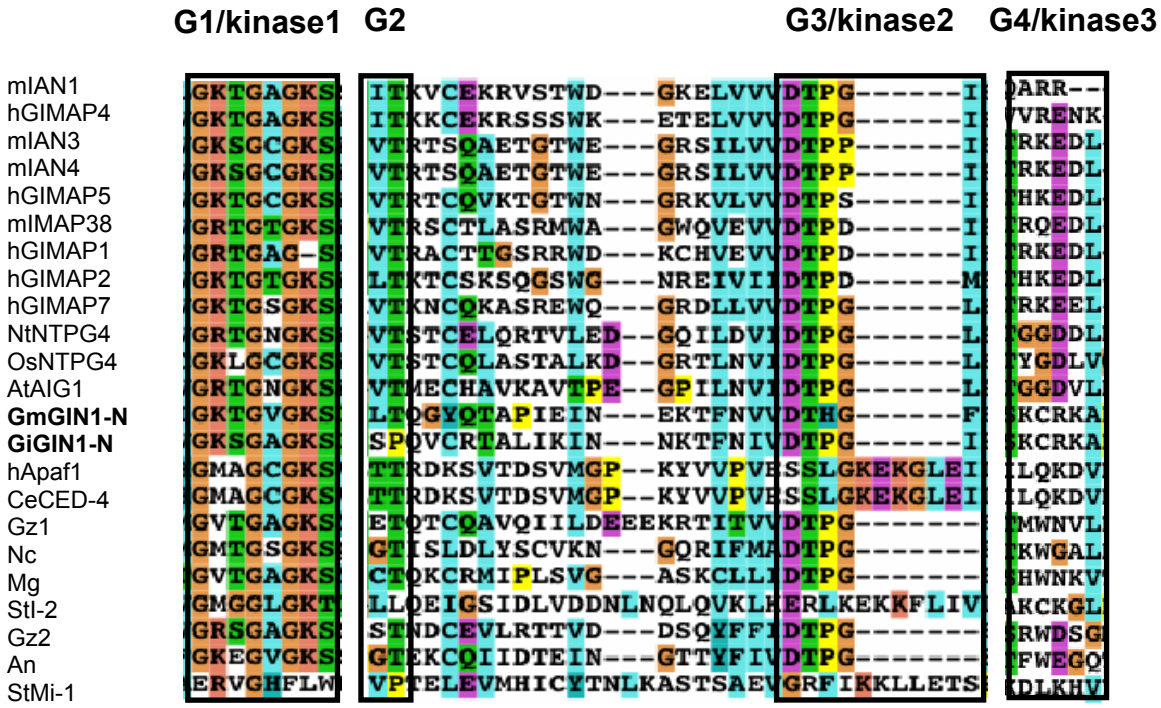

Figure 65. Conserved G1/kinase1, G2, G3/kinase2 and G4/kinase3 motifs in GTP and ATP binding protiens. Comparison of animal, plant and fungal members of the AIG/IAN/GIMAP family of proteins [mIAN1 (NM174990), hGIMAP4 (AK001972), mIAN3 (NM146167), mIAN4 (AF337052), hGIMAP5 (AK002158), mIMAP38 (NM008376), hGIMAP1 (AJ306287), hGIMAP2 (AL110151), hGIMAP7 (NM153236)]with GmGIN1-N and GiGIN1-N and other ATP-binding proteins as human Apaf1 (O14727), *C. elegans* CED-4 (P30429), and *S. tuberosum* I-2 (TO6404) and Mi-1 (AAC97933). h, human; m, mice; At, *A. thaliana* AIG (NP174657); Nt, *Nicotiana tabacum* NTPG4 (AAD09518); Os, *Oriza sativa* NTGP4 (XP_466219); Gz, *Gibberella zeae* (1, accession number EAA74755; 2, EAA74683); Nc, *Neurospora crassa* (EAA28888); Mg, *Magnaporthe grisea* (EAA47306); An, *Aspergillus nidulans* (XP_407465).

5 Discussion

GmGIN1 is mainly expressed at the early developmental stages of the mycorrhizal fungus *Glomus mosseae*, before establishment of the symbiosis with a compatible host plant (Breuninger and Requena, 2004; Requena et al., 2002). GmGIN1 presents a two domain structure. The N-terminal domain shares similarity to a new family of GTP-binding proteins associated with the immune system in animals and with the hypersensitive response against pathogens in plants, the GIMAP/AIG family (Krücken et al., 2004). The C-terminal domain has homology to the C-terminus of Hedgehog proteins, the Hint module (Hall et al., 1997). Because of this similarity, self-splicing of the full length GmGIN1 protein is expected. Consequently, the GmGIN1 amino terminus, with a cholesterol moiety attached, could be localized to raft domains at the cell membrane, similarly to the N-terminus of Hedgehog proteins (Porter et al., 1996a, b). The activated protein could then be implicated in the signaling events leading either to the establishment of the symbiosis with a compatible host or in growth arrest in the absence of a host.

5. 1 Self-splicing of GmGIN1-C

Animal Hedgehog proteins and self-splicing proteins, Inteins, seem to have a common evolutionary origin, as asserts the presence of a domain with a common fold in the crystal structures of the *Drosophila* Hedgehog 151 residue C-terminus (Hh-C_{17}) and the yeast 454 residue intein protein PI-SceI (Hall et al., 1997; Duan et al., 1997). This motif has been called the Hint (Hedgehog Intein) domain (Hall et al., 1997). This evolutionary conservation explains that both types of proteins are processed by partially overlapping mechanisms (Paulus, 2000; Pietrovski, 1994, 1998). In case of Hedgehog proteins, the reaction leads to the incorporation of a cholesterol moiety to the N-terminus after splicing, while in protein splicing the reaction leads to splitting of the intein and peptide linkage of the flanking exteins. The Hint domain is also found in the nematode family of Wart and Ground proteins (Aspöck et al. 1999; Bürgling, 1996). In agreement with the occurrence of this domain, Wrt1 has been shown to undergo auto-splicing when heterologously expressed in *Drosophila* cells

(Porter et al, 1996a). This domain constitutes the fragment of Hh with homology to GmGIN1-C terminus. Moreover, when 3D simulation of GmGIN1-C was realized, the structure resembles the one described for Hh-C_{17}. The Hint domain is able to form the thioester intermediate and undergo self-splicing in the presence of nucleophiles such as DTT, but not sufficient for cholesterol attachment (Hall et al., 1997). Cysteine-258 is indispensable for both steps, the thioester intermediate formation and the cholesterol transfer. This residue corresponds to Cys-238 in GmGIN1-C. This cysteine is localized in the conserved tripeptide Gly-Cys-Phe when compared to Hh proteins, at the splice junction of GmGIN1 (Requena et al., 2002). Polar groups are necessary in the vicinity of this residue to cope with the processing of the protein. In Hh-C Histidine-329, Threonine-326 and Aspartic-303 have been proven to have different functions in the process by mutation of these residues to alanine (Hall et al, 1997; Lee et al., 1994). These amino acids are conserved in GmGIN1-C, corresponding to positions His-310, Thr-313 and Asp-285 (Fig. 1). While the other two amino acids are absolutely conserved among the protein family, Asp-303 can be exchanged for histidine. Cys-258 in Hh constitutes intein Block A (Pietrovski, 1994; Perler, 1997, 2002). His-329 is conserved when compared to inteins, and Thr-326, when not conserved, is replaced by similar amino acids. These two residues relay in inteins Block B (Pietrovski, 1994; Perler, 1997, 2002). No amino acid analog to Asp-303 is present in self-splicing intein proteins. This is in accordance to the fact that Asp-303 has been shown to be indispensable in the cholesterol attachment, but not in the N-S acyl rearrangement leading to the thioester intermediate (Hall et al., 1997). The fact that GmGIN1-C contains an aspartic residue (Asp-285) in an analogous position supports the hypothesis of the attachment of a cholesterol (or sterol) moiety to GmGIN1-N after splicing. In the close homolog GiGIN1 carboxy terminus, glycine is replaced by alanine in the tripeptide GlyCysPhe in the splicing junction, also a non-polar aliphatic amino acid. This change should not affect the ability of this protein to be processed by autocleavage (Perler 2002).

In order to study the ability of GmGIN1 to undergo self-splicing, the C-terminus of GmGIN1 was heterologously expressed in *E. coli*. Expression and purification of GmGIN1-C with a His-tag attached to the N-terminus was performed in the same way as already described for DmHh-C (Lee et al., 1994; Porter et al,

1995, 1996a, b; Hall et al, 1997). DmHh-C was successfully purified and plenty of active protein was obtained after native purification. Under the same conditions, His tagged GmGIN1-C showed splicing activity *in vitro* when DTT was used as nucleophile. As a result, the full GmGIN1-C was processed into two peptides of the expected molecular sizes. In contrast, TCEP seemed not to be as active as nucleophile, neither for the GmGIN1-C nor for the positive control Hh-C. GmGIN1-C was quite insoluble, and therefore kept in inclusion bodies when purified under native conditions. In contrast, denaturing conditions rendered plenty of protein. However, denatured protein did not retain any splicing activity. Renaturation of the protein did not yield a high amount of active protein. Besides the low amount of active native protein obtained in *E. coli*, GmGIN1-C often suffered spontaneous auto-processing during purification. Attempts to avoid this process were not successful. Given the structural similarity of GmGIN1-C to inteins, we tried to inhibit auto-splicing by blocking the reaction by addition of Zn^{+2} ions during purification (Gosh et al., 2001; Mills and Paulus, 2001). This method has been partially useful to avoid splicing of intein proteins, but the yield of purified protein was lower than expected and no progress was observed in this direction (data not shown). Auto-splicing was also observed for the Hh-C protein of *D. melanogaster*, but to a lower extent despite the high amino acid sequence similarity between both proteins (Lee et al., 1992, 1994). *D. melanogaster* Hh-C protein proved to be much more soluble than our protein and thus plenty of functional protein could be recovered. However, when protein concentration was above 1 mg/ml, Hh-C precipitated and lost the autoprocessing activity. This contrasts with the results of Hall et al. (1997), which describe a decreased solubility in the DmHh-C large peptide resulting from the splicing reaction. Therefore, the difference in solubility must depend on the amino acids 83 to 89 from the N-terminus of Hh that are incorporated in the quimeric protein of Hh-C. Accordingly, three of them are polar amino acids (Lee et al., 1992; 1994). After splicing, proteolytic degradation of the Hh-C large fragment results in a 17 kDa peptide, that was much more stable and recovered solubility. This peptide resulted in a loss of the C-terminal hydrophobic tail (Hall et al., 1997). Given the similarity between Hh-C and GmGIN-C in this region, this fact would explain the low solubility of GmGIN1-C. The same reduced solubility was observed for its orthologue GiGIN1-C when

expressed under the same conditions. Strikingly, when the N-terminus of GmGIN1 was expressed and purified under the same conditions the obtained protein was much more soluble.

The amount of GmGIN1-C active protein was not enough to observe a clear effect when commercial lipids like cholesterol or β-sitosterol were tested as splicing agents. In contrast, these lipids provoked the splicing reaction of the positive control Hh-C, in accordance to the results of Mann and Beachy (2000). Similarly, incubation with sterol lipid extracts from mycorrhizal carrot roots was also able to induce Hh-C splicing. The extent of induced splicing was relatively weaker compared with the effect of nucleophiles such as DTT and TCEP. Analysis of total lipid extracts and sterol enriched extracts from spores and external mycelium from *G. intraradices* as well as from mycorrhizal and non-mycorrhizal carrot roots confirmed the presence of cholesterol derivatives in all extracts, as previously described by Fontaine et al. (2001). Cholesterol itself could be detected in mycorrhizal carrot roots, but only as a minor component. Given the high amount of pure cholesterol that had to be added to the incubation with Hh-C to induce splicing, it would not be expected that the low amount in the mycorrhizal roots was responsible for the splicing of Hh-C. Accordingly, splicing of Hh-C has already been described with cholesterol derivatives such as β-sitosterol. So, in principle, any of the cholesterol derivatives would be able to induce the splicing reaction (Mann and Beachy, 2000). As the different tested lipid extracts do not differ in the sterol composition but in their relative amounts, these differences must be responsible to their different capacity of splicing induction. Although the three major sterols in all samples were β-sitosterol (24-ethylcholesterol), stigmasterol (24-ethylcholesta-5, 22-dienol) and campesterol (24-methylcholesterol), their relative amounts differed between them. The main sterol found in spores and hyphae was campesterol (84.7 µg/1 mg lipids), followed by β-sitosterol (32.7 µg/1 mg lipids) and stigmasterol (14.4 µg/1 mg lipids). Strikingly, no splicing induction could be observed in the presence of spore or hyphal sterols, despite their high content of campesterol, which differs from cholesterol only in a methyl group. In both mycorrhizal and non-mycorrhizal roots the most abundant sterol was stigmasterol. Mycorrhizal roots presented higher levels of these lipids than non-

mycorrhizal roots. The order of the relative amount of lipids was altered, as in mycorrhizal roots campesterol was the second most abundant sterol (2.78 versus 0.788 µg/1 mg lipids in non-mycorrhizal roots), while β-sitosterol remained constant. These results are in accordance to the values observed by Fontaine et al. (2001). However, they also report the presence of 24-methylenecholesterol in mycorrhizal roots, which was not detected in non-mycorrhizal roots or germinating spores. We could not differentiate 24-methylenecholesterol from 24-methylcholesterol (campesterol) in any of the samples. It was not possible to determine if 24-methylenecholesterol and 24-methylcholesterol originated from the fungus and therefore appeared respectively as a new component or in a higher amount in mycorrhizal roots compared to non-mycorrhizal roots (Fontaine et al., 2001). Nevertheless, these authors demonstrated that AM fungi are able to synthesize sterols even when they are not in symbiosis, and that synthesis of sterols is more active upon symbiosis establishment. According to these evidences and to our sterol analyses, the increase in the campesterol content in mycorrhizal roots must be either of fungal origin or induced upon mycorrhizal symbiosis. They also showed the presence of lanosterol and 24-methylenelanosterol in mycorrhizal roots, attributed to have a fungal origin, as they were completely absent in non-mycorrhizal roots, and these are usually typical fungal sterols. In this respect, we could also detect lanosterol in spores in a low amount under our experimental conditions. However, it was not detected in any of the other samples, independent whether they were mycorrhizal or not. A higher content of squalene could also be detected in spores as compared to external mycelium (hyphae), suggesting a minor synthesis of sterols at the spore developmental stage. This result is in accordance with Fontaine et al. (2001). It has to be noticed that in our study non-germinated spores of *G. intraradices* were used.

Some part of the 63 carboxy-terminal residues of Hh-C missing in the crystal structure of Hh-C_{17} is required for the second step of the cholesterol transfer (Hall et al., 1997). This region has been called Sterol Recognition Region (SRR). Alignment of several members of the Hedgehog family, and the nematode Warthog and Groundhog sequences reveals a significant degree of similarity in this carboxy terminal region, particularly in the spacing of hydrophobic clusters (Mann and Beachy 2000). This region in the nematode

proteins has been designated as Adduct Recognition Region (ARR). GmGIN1-C also shares similarity in this region with its closest homolog, *Xenopus leavis* Dessert Hedgehog (Xl DHH2) as described in Requena et al. (2002). In Figure 9 can be observed that there is similarity in a conserved hydrophobic domain among the carboxy terminus of the Hedgehog, Groundhog, Wharthog and GIN1 proteins. In accordance, when a hydrophobicity plot was performed with GmGIN1 by the Kyte and Doolittle method (Kyte and Doolittle, 1982), the carboxy tail of GmGIN1-C terminus exhibits a hydrophobic domain. No transmembrane regions were predicted in GmGIN1. GiGIN1 had a very similar distribution of hydrophobic domains compared to GmGIN1. These evidences taken together raise the possibility that molecules other than cholesterol may participate in the processing reaction and constitute novel protein-modifying adducts. Although the function of Hedgehog proteins might differ from that of GmGIN1, given the divergence at their active N-terminus domains, the common feature of posttranslational splicing and cholesterol attachment could be a hint for a similar subcellular localization. Cholesterol modification of proteins has been shown to extend beyond the Hh family. Thus, [H^3] cholesterol has been shown to be incorporated to several other proteins in labeling experiments using COS-7 cells (Porter et al, 1996b).

Cholesterol modified forms of Hedgehog have been found to be predominantly membrane-associated and those lacking this moiety are freely secreted (Burke et al., 1999; Lee et al., 1994; Porter et al., 1995, 1996b). Processed *Drosophila* was shown to be membrane associated (Porter et al., 1996a), most likely into lipid rafts (Rieteveld et al., 1999). Rafts are membrane microdomains that function as platforms for intracellular sorting and signal transduction (Brown and London, 1998). Studies in progress in our group have shown that GiGIN1 seems to be specifically targeted to cell membranes (Ocón, Serrano and Requena, unpublished results).

The lipid modifications of Hh proteins may play a role in targeting them to rafts. Accordingly, overexpressed Sonic hedgehog Shh-N terminus is not localized to rafts because of the lack of the cholesterol moiety. Full length Shh produces the cholesterol and palmitoyl modified Shh-N^{chol}, which is localized to rafts. A mutation in the palmitoylation residue (Shh^{C25S}) does not affect raft localization of Shh-N^{chol} (Chen et al., 2004). Cholesterol was originally

suggested to function as a lipid anchor that restricts the spatial mobility of Hh-N. Thus, in a study using synthetic cholesterol modified peptides it could be demonstrated that this modification targets peptides to membranes almost irreversibly (Peters et al., 2004). But Hh is a secreted signal that diffuses beyond the cell in which it is produced and provokes a signal cascade in cells distant over many diameters (Johnson and Tabin, 1995; Hammerschmidt et al., 1997; Ingham 1998; Lewis et al., 2001). Therefore, a permanent membrane association would not allow Hh-N to act as a morphogen. Nevertheless, this long range signaling pathway is also affected by the cholesterol moiety, as Hh-N lacking this modification is not internalized by the receiving cells in *Drosophila*, an effect mediated by the Hedgehog receptor Patched (Ptc) (Incardona et al., 2000; Johnson et al, 2000). Ptc belongs to a growing family of integral-membrane proteins that posses a Sterol Sensing Domain (SSD), which has been shown to be involved in vesicle trafficking and are involved in cholesterol homeostasis (Carstea et al, 1997). This domain was proposed to interact with Hh-N via its lipid modifications, promoting sequestration of the protein, but mutation in this domain does not compromise binding to Hh or internalization of the complex (Martin et al., 2001; Strutt et al., 2001). Moreover, neither cholesterol nor palmitoyl modification increases the affinity of Hh for Ptc, although the intrinsic activity of the protein is increased (Pepinski et al., 1998). Strikingly, although no proper Hedgehog protein is found in *C. elegans*, two homologs of *Ptc* and numerous *Ptc-related* (*ptc-r*) genes are found (Kuwabara et al., 2000). An explanation of the role of cholesterol modification of Hh-N came with the discovery of the Dispatched (Disp) protein. Dispatched (Disp) also contains an SSD, and has homology to Ptc receptor proteins. It has been shown that this protein is required for the controlled release of the lipid-modified Hh-N (Burke et al., 1999; Gallet et al., 2003; Kawakami et al., 2002; Ma et al., 2002). A member of the Disp family of proteins as well as a homolog of Ptc (Ptc1) have also been found in the *C. elegans* genome (Burke et al., 1999; Kuwara et al., 2000). This is remarkable because no hedgehog proteins are found in this organism. Given that Groundhog and Warthog proteins are likely undergoing self-splicing similar to Hh proteins, it would be interesting to see whether they also interact with Ptc or Disp (Aspöck et al., 1999; Bürgling, 1996; Porter et al, 1996a). Supporting this hypothesis is the fact that *C. elegans*

mutants in *Wrt-6* have a phenotype similar to mutants in *che-14*, a gene related to the Hh receptor Disp (Aspöck, 2000). We performed searches for proteins related to Ptc in the NCBI Blast database, and found several proteins of unknown function in fungi, as *M. grisea* (XP_362552, XP_368425), *U. maydis* (XP_400191), *S. pombe* (NP_596673), *A. nidulans* (XP_406256) and *C. glabra* (XP_449268) among others. Very interestingly, in AM fungi a homologue of NPC1, a protein significantly similar to the Patched receptor, has been identified (Kuhn, Requena and Franken, unpublished results).

Sonic Hedgehog (Shh) proteins are also modified by palmitoylation at the amino terminus of the protein on the α-amino group of Cysteine-24 (Pepinski et al., 1998). This residue is the first N-terminal amino acid of the mature protein, after cleavage of the signaling peptide at its N-terminus (Lee et al, 1992, 1994, 2001). These two processes seem to be conserved among the Hedgehog family of proteins, and although no natural Shh occurring protein has been isolated containing the palmitoyl residue it has been isolated for overexpressed Drosophila Hh, mice and rat Shh in culture cells as well as in different tissues and developmental stages (Chamoun et al., 2001; Chen et al., 2004; Lee et al 2001; Pepinski et al., 1998). Palmitoyltransferases are able to modify secreted proteins, but also intracellular proteins (Linder and Deschenes, 2004). For example, yeast Ras homologs (Ras1p and Ras2p) are both farnesylated at the C-terminus and palmytoilated at the N-terminus in order to localize the protein at the cell membrane (Deschenes and Broach, 1987; Fujiyama and Tamanoi, 1986). Posttranslational lipid modifications of Ras are necessary for its proper localization and biological activity (Takai et al., 2001). Interestingly, a plant homolog of GmGIN1-N, NTGP4, is isoprenylated (Dahéron et al., 2001). Expression of GmGIN1 in a system that allows posttranscriptional modifications and study of the biochemical properties of the resulting protein, as well as localization and identification of the nature of the possible lipid modifications would be necessary to get a clearer picture of the localization and function of this protein. Comparison with expressed GmGIN1-N would also be indispensable.

Rafts are lipid structures at the cell membranes, first described in mammalian cells, which are enriched in sphingolipids and cholesterol (Simons and Ikonen, 1997). Raft domains seem to be involved in asymmetric distribution

of proteins at the cell membrane during polarization and migration (Brown and London, 1998; Gómez-Moutón et al., 2001). Several signaling proteins such as tyrosine kinases from the Src family, heterotrimeric and small G-proteins are recruited to rafts, and are dependent on this recruitment for their function. Several evidences have shown that lipid rafts are also formed in plants and fungi. Thus, in fungi, lipid rafts have been shown to be implicated in polarizing growing processes as yeast mating (Bagnat and Simons, 2002a-b), mating and fission of *S. pombe* (Wachtler et al., 2003), and hyphal growth in *C. albicans* (Martin and Konopka, 2004). They have also been related to delivery of proteins to the cell surface (Bagnat et al., 2000; Frankhauser et al., 1993; Kubler et al., 1996; Sütterlin et al., 1997; Takeda et al., 2004; Umebayashi and Nakano, 2005). In plants, the identification of plasma membrane microdomains insoluble in Triton X-100 containing the Gβ subunit of heterotrimeric G-proteins in tobacco leaves (Peskan et al., 2000), and the differential lipid composition of *Arabidopsis* plasma membrane leaf (Bérczi and Horvath, 2003) suggests that raft domains are also found in plants. But then, other sterols rather than cholesterol might be implicated in raft formation in these organisms. Accordingly, it was shown that cholesterol is not the only sterol capable of contributing to the formation of these structures. Ergosterol, the main sterol found in most fungi, was demonstrated to be even more efficient in raft domain formation than cholesterol (Xu et al., 2001). Stigmasterol and sitosterol, the two major sterols in plants, were also found able to promote raft formation, although stigmasterol domains seem to be less stable. It appears that a mixture of stigmasterol, sitosterol, campesterol and cholesterol takes part of lipid rafts in tobacco leaves (Mongrand et al., 2004). Our sterol analysis of *G. intraradices* showed that stigmasterol, sitosterol and campesterol are the main sterols in spores and hyphae. Although ergosterol, which is the sterol responsible of raft formation in other fungi (Bagnat et al., 2000), was not found, the presence of other cholesterol derivatives could support the formation of lipid rafts in AM fungi. These domains could allocate by similarity lipid modified proteins such as GmGIN1-N. Further studies to clarify the existence and protein composition of such domains are in progress (Ocón, Serrano and Requena, unpublished data). Interestingly, in some other fungi the presence of raft domains has been related to pathogenicity towards animals or plants. Thus, raft formation and proteins

targeted to them have been shown in *C. albicans* to be pathogenicity factors (Martin and Konopka, 2004). Similarly, penetration of the powdery mildew fungus *Blumeria graminis f. sp. hordei* into plant cells after appressoria formation seems to be dependent on its ability to promote plant cell raft domain formation at the penetration locus. This promotes the location at the entry cells of proteins inhibiting the resistance response (Baht et al., 2005). Conversely, lipid rafts in plants have been related to pathogen defense responses, as they are enriched in NtrbohD and the small G protein Ntrac5, upregulated upon interaction with the fungal elicitor cryptogenin (Mongrand et al., 2004). GmGIN1 is mainly expressed during the pre-symbiotic stage of the fungus (Requena et al, 2002; Breuninger and Requena, 2004). Therefore, it could be that targeting of this protein to raft domains could play a role in the establishment of the symbiosis, either by promoting hyphal growth or appressoria formation.

5. 2 Enzymatic activity of GmGIN1-N

Heterologous expression of GmGIN1-N terminus in *E. coli* was performed in order to isolate the protein and analyze its nucleotide binding properties and enzymatic activity. *Ustilago maydis* cdc42 wild type protein and the cdc42(Q-L) mutant were used as positive controls, and purified under the same conditions. The Q-L mutation of cdc42 results in loss of the intrinsic GTPase activity, reducing conversion from bound GTP to GDP and thereby locking the mutant proteins in an activated GTP-bound state (Weinzierl et al., 2002; Ziman et al., 1991). This glutamine residue is part of the conserved G-3 box, implicated in binding of the γ-phosphate of GTP and Mg^{+2}. GTP binding of GmGIN1-N and the cdc42 proteins was first assessed in a membrane assay after transferring of the proteins from SDS gels to nylon membranes. In this denatured stage, incubations of the proteins with α^{32}P-GTP did not show any sign of GTP binding. Several native protein extracts of *G. intraradices* spores and *A. muscaria* mycelium, used as controls, gave positive signals, indicating possible GTP-binding proteins in the extracts. Many signals were obtained when addition of ATP to the binding buffer as competitor was avoided. Nevertheless, none of these signals was different or predominant in cell lysates expressing any of the expressed proteins when compared to empty cell lysates.

Although quite disappointing, this result is not very surprising, as small changes in the binding conditions have been shown to lead to very different results (Bhullar and Haslam, 1987; Vater et al., 1992), reason for which we tried two different buffers in the membrane binding protocol.

A different GTP binding assay, based on GTP binding in solution and further detection after filtration was performed to overcome these difficulties. GmGIN1-N and the positive control proteins purified under native conditions were used in these experiments. Under these conditions UmCdc42 wild type and Q-L mutant strongly bound to the non-hydrolyzable analog of GTP, γ-^{35}S-GTP. This compound has been proven to constitute a good analog for GTP, as diastereomers, isomers with more that one chiral center, are not introduced by the replacement of oxygen by sulfur (Tucker et al., 1986). However, it is important to notice that several GTPases, such as $p21_C$ (Tucker et al., 1986) and EF-Tu (Wittinghofer et al, 1982 and Leupold et al., 1983), have been shown to have a different affinity for γ-^{35}S-GTP than for GTP.

At a low concentration of free Mg^{+2}, which favours the nucleotide exchange, the loading of protein with γ-^{35}S-GTP was very fast. UmCdc42(Q-L) reached a saturation plateau within 20 minutes, in a protein concentration-dependent manner. Wild type UmCdc42 was much faster, with saturation after 2.5 minutes. Indeed, no exponential binding could be observed, even reducing the protein concentration five times compared to the amount used in the binding assay with UmCdc42(Q-L). This could be due to the fact that no nucleotide, usually used GDP, was added during the purification. As a consequence, the protein is empty, and it will have an increased affinity for γ-^{35}S-GTP. Nevertheless, this fact does not explain the differences observed between both proteins, as both were purified under the same conditions. In theory, only the hydrolysis activity of UmCdc42 should be affected by the mutation in the glutamine 61, but the rate of nucleotide exchange also seems to be affected.

Binding of GmGIN1-N to γ-^{35}S-GTP could be also detected, but to a much lower extent. Binding up to 0.7 pmoles γ-^{35}S-GTP/μg protein could be detected, in contrast to the 38.6 pmoles/μg wild type UmCdc42 or 15.93 pmoles/μg UmCdc42(Q-L). The efficiency of the binding was much better when the protein concentration per assay was kept in a range of 0.5-1 μg, in

accordance to Zhang et al. (2003). When the protein concentration of the positive controls was increased, an increase in the molecules of bound GTP could be observed, but the relative binding per μg of protein was reduced. Binding activity of GmGIN1-N protein was very much affected by the concentration of free Mg^{+2} in the binding buffer. This is in accordance to published literature on the subject and it is indicative for the specificity of the binding. At low Mg^{+2} concentrations the nucleotide is not so tightly kept in the coordination site in the protein, which favours the nucleotide exchange. At a higher concentration of Mg^{+2} the nucleotide is stabilized in the binding site, and exchange is inhibited (Franco et al., 1993, 1994, 1996; Perioche et al., 1996; Steinmann et al., 1999). This is the reason why in the washing buffer the concentration of $MgCl_2$ was increased to 10mM. Three different concentrations of Mg^{+2} were tested. Optimal binding results were obtained in an assumed concentration of 1 μM free Mg^{+2} (1 mM $MgCl_2$ and 2 mM EDTA), similar to the results from Franco et al. (1993; 1994). When $MgCl_2$ was raised to 1mM no binding was observed using empty protein purified without GDP. When the protein was purified including a low amount of GDP, the maximum binding to γ-^{35}S-GTP was increased. However, as it happened with the wild type Umcdc42, the protein was not progressively loaded with radiolabelled γ-^{35}S-GTP but it was immediately saturated. The fact that there was more γ-^{35}S-GTP loading when the protein was purified with GDP could be related to the active state of the protein. It has been shown that binding to cofactors or ligands such as GDP or magnesium during purification of GTPases is critical to obtain an active protein (Wagner et. al., 1987). In absence of these cofactors the protein tends to denaturate and precipitate, resulting in lack of activity in the final assay. Binding of γ-^{35}S-GTP for GDP-purified GmGIN1-N and wild type UmCdc42, seems to occur very rapidly, reaching a plateau that can be confused with no binding. In case of UmCdc42 the high binding activity leaves no doubt for the specificity of the interaction, but in case of our protein the binding activity is so low that is difficult to detect. UmCdc42 was proven to dissociate γ-^{35}S-GTP when an excess of a competing nucleotide, GDP, was added to the reaction mixture. GmGIN1-N also dissociated from the radiolabelled γ-^{35}S-GTP under the same conditions. Moreover, when GmGIN1-N was preincubated with an excess of

GDP, no labeling with γ-^{35}S-GTP could be detected. Protein purified in the presence of a low amount of GDP was more efficient in the nucleotide exchange assay, which might be due to the preservation of the protein in a native state due to the addition of the ligand. Surprisingly, when the exchange assay was performed with 1 mM ATP, this nucleotide was also able to displace the bound γ-^{35}S-GTP more efficiently than GDP, or even GTP. When the same assay was performed with 1 mM GTP GmGIN1-N seems to dissociate very quickly from γ-^{35}S-GTP (within 2,5 minutes) and then it binds γ-^{35}S-GTP to a much higher extent (five times more) compared to time point zero (before addition of the competitor). After this, γ-^{35}S-GTP binding decreases again during incubation. Nevertheless, ATP-induced dissociation of γ-^{35}S-GTP was faster and stronger. This indicates that GmGIN1-N has a higher affinity for ATP than for GDP or GTP. Under the same conditions, ADP was also able to compete for the binding to the protein, but to a lower extent, and differences were only evident after 60 minutes of incubation with the competing nucleotide.

It is important not to forget that each GTPase has an intrinsic GTP-binding activity, which differs a lot among the superfamily members and is dependent on many factors like lipid modification, interactions with other proteins, such as GAPs and GEFs, which might be missing in the in vitro assay. The conditions of the interaction or requirements for the binding of GTP and GTPase activity reside in the amino acid sequence of the G1, G3 and G4 boxes. Indeed, GTP binding and GTPase activity was determined for several proteins of the AIG/IAN/IMAP family, homologs to GmGIN1-N, with quite different results (Cambot et al., 2002; Daheron et al., 2001; Stamm et al., 2002). Thus, GST-hIAN1 has an optimal GTP binding and GTPase activity in an *in vitro* assay (Cambot et al., 2002). This assay was performed under similar conditions to the one described in this work, with the exception of a lowered assay temperature (25°C instead of 37°C). The temperature seems to be important for the activation of GmGIN1-N, as the same assay at room temperature led to no binding of γ-^{35}S-GTP.

It is interesting to compare the amino acid sequence at the G3 box (OJOO**D**XA**G**JX) among hIAN1 and Ras (homolog to Cdc42) and GmGIN1-N, where O are hydrophobic and J hydrophilic residues (Bourne et al., 1991). In

the position where mutants for Ras and Cdc42 are described to be affected in GTP-binding and hydrolysis (J) (Weinzierl et al., 2002; Ziman et al., 1991), glutamine-61 from Ras and Cdc42 is replaced for an isoleucine in hIAN1 and for phenylalanine in GmGIN1-N. However, other amino acids in the cassette that are indispensable for the binding are conserved (**D** and **G**) (Fig. 52 and 65). These differences could explain the different affinity of these proteins for GTP. In a review article, Bourne et al. (1991) summarize the mutants existing for this position, pointing towards an important role for this residue (J) in GTP hydrolysis. In the elongation factor Ef-Tu, a histidine residue at this position seems to be completely functional, but replacement by glycine results in a 10-fold reduction of GTPase activity. Nonetheless, other GTPases such as Era in *E. coli* and RSR1 in *S. cerevisiae* contain leucine (Ahnn et al., 1986) and isoleucine (Bender et al., 1989) respectively at this position. However, it is difficult to imagine the uncharged side chains of these residues performing a similar role to the one proposed for glutamine-61. In addition, phenylalanine in GmGIN1-N at this position incorporates an aromatic group, creating a high steric interference as compared with leucine and isoleucine at this position. Dahéron et al. (2001), also studied the GTP binding of mIAN4, which also has an isoleucine at this position, but other amino acids from the cassette are also changed, like glycine (**G**) which is substituted by proline. In that article the authors perform the filtration assay, with enrichment in the protein by immunoprecipitation and compared empty cells to cells expressing the HA-fusion version of the protein. The parameters used do not allow a clear comparison to our data. Although significant differences in binding to GTP are shown by comparison to non-expressing mIAN4 cells, the high standard error of the graphs reflects the high variability of the measurements. This was a constant problem in our experiments with GmGIN1-N, which can be explained by its low binding capacity. The high binding obtained with Umcdc42 and Umcdc42(Q-L) proteins minimized the standard variations observed between triplicate measurements. Glycine (**G**) from the G3 box was changed for aspartic (D) in mIMAP1 and mIMAP38-2, as well as glutamine-61 from Ras and Cdc42 (J) was substituted by isoleucine (Fig. 65). Accordingly, very weak binding of GST-IMAP1 and none for GST-IMAP38-2 was detected in GTP-overlays using α^{32}P-GTP or in binding experiments in solution (Stamm et al., 2002).

The low similarity of the G4 box compared to other AIG/IAN/GIMAP proteins should be taken into consideration when analyzing the GTP binding capacity of GmGIN1-N (Fig. 65). G4 determines the specificity of the binding to the nucleotide base. The G4 box corresponds to the kinase3 motif according to Traut et al. (1994). The kinase3 motif in ATP binding proteins is very variable (Traut et al., 1994). Nevertheless, it can be clearly differentiated from the same motif in GTP-binding proteins. Alignment of GmGIN1-N and GiGIN1-N with AIG/IAN/GIMAP proteins and ATP binding proteins as Apaf1 and CED-4 (Jiang and Wang, 2000; Seiffert et al., 2002) and the plant resistance proteins I-2 and Mi-1 (Tameling et al.,2002) showed that most animal GIMAP proteins have a conserved cassette corresponding to G4, while GmGIN1-N and GiGIN1-N have different motifs (Fig. 65). Accordingly, this motif is also different in the plant and other fungal members of the AIG/IAN/GIMAP family of proteins, as in the ATP binding proteins. Moreover, although a G5 box is described for IAN proteins (Stamm et al., 2002) no clear domain could be found either in GmGIN1-N or in the *A. thaliana* orthologue AtAIG. Strikingly, no G2 motif is found in GiGIN1 amino terminus (Fig. 52). Alignment of all family members also indicates that GmGIN1-N is more closely related to AtAIG and other plant homologs from *Nicotiana tabacum* (NtNPG4) or from *Oriza sativa* (OsNPG4) than to the animal members of this family. Nevertheless, all these proteins contain a conserved hydrophobic motif located between G3 and G4, which has been shown to maintain a certain conformation of the protein in other GTPases (Garnier et al., 1996; Krengel et al., 1990; Krücken et al., 2004). Once again, this motif seems to be more conserved among the animal members of the GIMAP protein family than among plant and fungal members.

All these divergences become more important in the light of our enzyme assay results. The fact of obtaining a very low binding of γ-^{35}S-GTP to GmGIN1-N and its dissociation after addition of ATP prompted us to consider the possibility that GmGIN1-N could have ATPase activity rather than GTPase. Therefore, both ATP and GTP hydrolysis assays using α-^{32}P derivatives were performed. Surprisingly, positive results were obtained when incubation was performed in the presence of α-^{32}P-ATP. Appearance of a spot migrating in the range of α-^{32}P-ADP, compared to unlabeled standards, could be detected with

higher intensity in the reaction mixture in which GmGIN1-N was incorporated. Conversely, no differences were observed when the same reaction was performed in the presence of α-^{32}P-GTP. This difficulty in assigning whether a protein is a GTPase or an ATPase can be explained by the fact that the G1 box or P-loop binding the phosphate of the nucleotide is much conserved among proteins binding GTP and ATP (Saraste et al., 1990; Traut, 1994). A similar situation was described for a group of R (resistant) proteins from plants, the NBS-LRR (Nucleotide Binding Site-Leucine Reach Repeat), which were originally considered to be GTP binding proteins, and only recently have been shown to bind and hydrolyze ATP instead of GTP (Tameling et al., 2002).

Another point to consider is the fact that protein interactions with their natural partners *in vivo* are also missing when expressed *in vitro*. As already commented, GmGIN1-N is supposed to be localized to membranes by means of a cholesterol modification at the C-terminus of this domain, similar to Hh-N proteins (Porter et al., 1996). The cholesterol moiety is not introduced in the *in vitro* system. We tried to express the full length protein GmGIN1 and to perform the splicing *in vitro* with cholesterol, in order to obtain GmGIN1-N bound to cholesterol and test changes in its GTP binding activity. Unfortunately, the full length protein was a completely insoluble protein, which could only be extracted under denaturing conditions in an inactive form. Renaturation of this protein failed to give an active protein.

Other factors, like posttranscriptional modifications, have to be taken into account when considering the activity of the putative GTP or ATPase. As we have already introduced, most of GTPases suffer a lipid modification which is actually critical for their function. Thus, Ras proteins, like Cdc42 from *S. cerevisiae* mutated in the isoprenylation box “CAAX” (C stands for cysteine, A for aliphatic and X for any amino acid), by replacement of the cysteine for serine does not exhibit the same properties like the wild type protein, and proper membrane localization is dependent on its isoprenyl anchor (Ziman et al., 1991). Recombinant protein expression in *E. coli* does not introduce these typical eukaryotic modifications into proteins. Therefore, the subsequent protein activation dependent on these modifications is missing. Hedgehog proteins are also modified in their N-terminus by an acyltransferase (Pepinski et. al., 1998) which enhances the signaling activity of the protein by palmytoylation (Taylor et.

al., 2001). GmGIN1 protein was analyzed using the ScanProsite database and four N-myristoylation sites and two ASN N-glycosylation sites were found. The first myristoylation site forms part of the G1 box or P-loop for ATP/GTP binding proteins, in the Glycine 14. This lipid modification is typical for Arf small proteins and some Gα subunits (Casey, 1995). Myristoylation itself is not enough to recruit Arfs into the cell membranes, as they need a second lipidic modification (Milligan et al., 1995; Wedegaertner et al., 1995) or some lipophilic amino acid residues (Beraud-Dufour et al., 1999). Membrane association is stabilized in the GTP-bound state by a conformational change of the amino-terminal helix that exposes several hydrophobic residues, including Leu-8 and Phe-9, and allows their insertion in the membrane (Antonny et al., 1997; Beraud-Dufour et al., 1999). When myristate is removed, interaction with the lipid bilayer is impeded. (Franco et al., 1995). Myristoylation is normally performed at a N-terminal glycine. This implies that cleavage at the N-teminus should be necessary to get the glycine exposed to this modification. Although a signal peptide was detected at the N-terminus of GmGIN1 and GiGIN1 in the InterProScan database, the presence of this domain was not confirmed when using the SignalP3.0 Server and the NetNGlyc1.0 Server. Two potential N-glycosylation sites, at positions 67 and 327, were confirmed by the NetNGlyc1.0 Server, but in the absence of a signal peptide it is unlikely that these sites are exposed to modification. A similar modification is occurring in Hh-C (Hammerschmidt et al, 1997). Strikingly, GiGIN1 gave the same patterns of posttranslational modifications as GmGIN1 in the predictions of the different programs. Nevertheless, when location prediction was performed using the Predotarv.1.03 service, although no organelle prediction was found for GmGIN1, GiGIN1 was predicted to be localized to endoplasmatic reticulum with a 0.27 probability. Values over 0.2 can be considered reliable. This might be of relevance since cholesterol modification of proteins is usually occurring in this organelle. No GPI site was predicted for any of the two GIN1 proteins by big-OI Predictor.

Recently, a comparative analysis of the IAN family of GTPases, to which GmGIN1-N belongs, has been published (Krücken et al., 2004). The authors have renamed this family of proteins as GTPases from the Immune Associated Protein family (GIMAP). Very interesting is the study over the localization signaling motifs for these proteins. They predicted that hGIMAP4 (or

hIAN1/mIAN1) has both a large coiled-coil and a type II transmembrane domain in its C-terminal region, behind the AIG1 domain. This could imply membrane localization of the protein and the coiled-coil motif could be responsible for protein-protein interactions. hGIMAP2 presents two putative transmembrane domains at the carboxy-terminus, while hGIMAP1 (himap1 or hIAN2 and analogous to mouse imap38) and hGIMAP5 (hIAN5/Irod) contain a putative transmembrane domain also in this region. Several of these proteins, such as hGIMAP1 hGIMAP2, hGIMAP6 and hGIMAP7, contain one or two basic amino acids at the amino- or carboxy-terminus with weak similarity to ER-localization signals of transmembrane proteins. However, the results for localization assays are quite contradictory, as hGIMAP7 (with ER localization signal) and hGIMAP4 (without such a signal) were both located at the ER and Golgi of CHO-K1 cells. A frameshift mutation in *Ian4l1* (rat GIMAP5) results in a truncated protein containing the GTP-binding region but without the transmembrane and the coiled-coil regions (Andersen et al., 2004; Hornum et al., 2002; MacMurray et al., 2002). This results in disruption of mitochondrial localization of the protein (Dahéron et al., 2001), necessary for the antiapoptotic function of this protein (Sandal et al., 2003). Localization studies with GmGIN1 protein, and moreover, with antibodies directed against the N-terminus and C-terminus separately are in progress to verify the processing of the protein *in vivo*, the subcellular localization of the two different domains and their putative interaction partners.

As an attempt to get a hint of which could be the localization of the GiGIN1 protein domains, total protein extracts from spores of *Glomus intraradices* were subjected to immunodetection using antisera raised against the two domains of GmGIN1. The N-terminus antisera recognized no protein in the extracts. This is not surprising as the N-termini of GiGIN1 and GmGIN1 are quite divergent in the region against which the antiserum is directed. When detection of the C-terminus was performed three bands in the spore extracts could be detected, with apparent molecular weights of about 43, 31 and 23 kDa. Full length GiGIN1 has a molecular weight of 54 kDa, while the splicing products would have 31.5 (N-terminus) and 22.5 kDa (C-terminus). The signal of 23 kDa could correspond to the GiGIN1-C spliced protein. Although no signal was detected in the mycorrhizal roots extracts, a band of about 45 kDa was also detected in a protein extract of *A. muscaria*. Nevertheless, the same extract of

A. muscaria did not give any signal when detection versus the N-terminus was performed. Interestingly, immunodetection of spore microsomes directed against the C-terminus revealed that the full length GiGIN1 could be localized to these domains (Ocón, Serrano and Requena, unpublished results). Specific antibodies directed against the N- and C-terminus of GiGIN1 will bring light into this subject, as localization of the N-terminus of the protein, which constitutes the active catalytic domain, is essential to speculate about the role in the life cycle of the fungus or in the establishment of the symbiosis.

First evidence about the function of the different members on the GIMAP family of proteins indicated that in animals these proteins were predominantly expressed in cells and organs of the immune system (Krücken et al., 1997; Poirier et al., 1999; Dahéron et al., 2001; MacMurray et al., 2002). However, recent studies indicate that the expression of these proteins in animals is not restricted to the immune system, but to most cell types (Krücken et al., 2004). This fact points towards a more general role, although these proteins are particularly active in immune related responses and processes. The low expression level, if at all, of these genes in diverse cancer tissues and cell lines is a general feature. This could be interpreted as a role in tumor suppression (Krücken et al., 2004). Lack of *Ian4l1* (human Irod/IAN5) has been demonstrated by RNA interference analysis to lead to apoptosis (Pandarpurkar et al., 2003). This confirms the antiapoptotic effect observed by Sandal et al. (2003). In plants, the first member belonging to this kingdom was induced in the signaling cascade leading to hypersensitive response in *Arabidopsis* in response to the pathogen *P. syringae* (Reuber and Ausubel, 1996). The picture that emerges is that these proteins are involved in signaling pathways which either promote or inhibit cell proliferation, survival, and/or apoptosis respectively. The question is, where in the mycorrhizal symbiosis such an enzyme would play a role? *GmGIN*1 was found to be differentially expressed during development of *Glomus mosseae* mainly in the out-planta phase of the fungus (Requena et al., 2002). GmGIN1 could be involved in the signaling events deciding at this time point the further development towards the establishment of the symbiosis with a compatible partner, or alternatively induce growth arrest and further programmed cell death in the absence of a signal from such a host plant. Thus, it might promote fungal growth. A hint in support of this

hypothesis is the fact that most of the GmGIN1-N domain matches with the GTP CDC cell division motif (pfam 00735.11), which is present in proteins related to control of cell cycle in fungi (Barral et al., 2000; Martin and Konopka, 2004; Roh et al., 2002). Moreover, other heterotrimeric G proteins and small GTPases, as RhoI and cdc42, are implicated in cytokinesis, mating and control of cell growth and development in fungi (Bölker, 1998; Cabib et al., 1998; Cerione, 2004; Dohlman and Thorner, 2001; Drees et al., 2005; Gorfer et al., 2001; Higgs and Pollard, 2001; Posada et al., 1995; Weinzierl et al., 2002; Ziman et al., 1991). The fact that GmGIN1-N is an ATPase, rather than a GTPase, opens new perspectives of which could be the role of this protein in the interaction between the two partners of the mycorrhizal symbiosis. As mentioned before it was recently shown that nucleotide binding proteins involved in plant resistance against pathogens (NBS-LRR) are also ATPases instead of GTPases (Tameling et al., 2002). This family of proteins is related to apoptotic events leading to hypersensitive response (Aravind et al., 1999; Meyers et al., 1999; Pan et al., 2000; Zou et al., 1997). It has been proposed that activation of these proteins by binding and hydrolysis of ATP would lead to the formation of a signalsome protein complex, in analogy to the apoptosome produced by the homolog ATP binding protein Apaf1 (Meyers et al., 1999; Tameling et al., 2002; Zou et al., 1997). The future questions to solve are which could be the molecules or interaction partners that trigger the sequence of events leading to symbiosis formation? If we center our hypothesis in this gene, and given the regulator mechanism of activation and localization of the hedgehog domain, it is tempting to speculate that a sterol molecule provided by a compatible host could set off the signaling cascade of events leading to recognition of the symbiotic partners.

6 Conclusions

The ability of GmGIN1-C to undergo self-splicing was confirmed. Protein, heterologously expressed, could be purified under native conditions and splicing was induced in an analogous manner as proved with Hh-C. This means that GmGIN1 could be processed *in vivo* with a similar mechanism as Hh proteins. In Hh, cholesterol is the molecule that provokes splicing *in vivo*. By means of the cholesterol moiety, the modified N-terminus of Hh proteins is targeted to raft domains at the cell membrane. But cholesterol is not a major sterol in the mycorrhizal symbiosis. So other candidates rather than cholesterol have to be searched. Mycorrhizal lipid extracts were tested for their ability to induce self-splicing in Hh-C. Strikingly, splicing could be detected after incubation with mycorrhizal roots sterols. Given the similarity to the cholesterol molecule of the three main sterols found in all lipid extracts and the even lower yield of lipid extraction in root samples, our results point towards selectivity for a component in mycorrhizal root extracts. Relative amounts of the sterols have to play an important role in this selectivity. The fact that Hh-C is able to undergo self-splicing by sterols other than cholesterol means that other sterols can be responsible for targeting proteins to cellular compartments. Similarly to Hh-N, GmGIN1-N could be targeted to raft domains by a sterol present in the mycorrhizal symbiosis. If this sterol is coming from the host plant, GmGIN1 could be involved in the signaling events that trigger symbiosis establishment.

According to the Hh processing model, by this lipid modification GmGIN1-N would be activated and localized at its site of action. GmGIN1-N was shown to be able to bind to ATP with higher affinity than to GTP, despite its homology to the AIG/GIMAP family of GTPases. Accordingly, it was shown to hydrolyze ATP and not GTP. This fact implies that GmGIN1-N could use the energy released from ATP hydrolysis in triggering itself a sequence of events or promoting interactions with other proteins with this purpose, in analogy to the role purposed for NBS-LRR plant pathogen resistance proteins.

7 Literature

Adjei, A.A. 2001. Blocking oncogenic Ras signaling for cancer therapy. J. Nat.l Cancer Institute 93(14):1062-1073.

Ahnn, J., March, P.E., Takiff, H.E., Inouye M. 1986. A GTP-binding protein of Escherichia coli has homology to yeast RAS proteins. Proc. Natl. Acad. Sci. USA 83(23):8849-53.

Akiyama, K., Matsuoka, H., Hayashi, H. 2002. Isolation and identification of a phosphate deficiency-induced *C*-glycosylflavonoid that stimulates Arbuscular mycorrhiza formation in melon roots. Mol. Plant-Microbe Interact. 15:334-340.

Albrecht, C., Geurts, R., Lapeyrie, F., Bisseling, T. 1998. Endomycorrhizae and rhizobial Nod factors both require SYM8 to induce the expression of the early nodulin genes PSENODS and PsENOD12A. Plant J. 15:605-614.

Alcedo, I., Ayzenzon, M., Vonohlen, T., Noll, M., and Hooper, I. 1996. The *Drosophila* smoothened gene encodes a 7-pass membrane-protein, a putative receptor for the hedgehog signal. *Cell* 86: 221-232.

Alexander, T., Meier, R., Toth, R., Weber, H.C. 1989. Dynamics of arbuscule development and degeneration in onion, bean and tomato with reference to vesicular-arbuscular mycorrhizas with grasses. Can. J. Bot. 67:2505-2513.

Alexandrov, K., Horiuchi, H., Steele-Mortimer, O., Seabra, M. C., Zerial, M. 1994. Rab escort protein-1 is a multifunctional protein that accompanies newly prenylated rab proteins to their target membranes. EMBO J. 13:5262-5273.

Alexandrov, K., Simon, I., Yurchenko, V., Iakovenko, A., Rosttkova, E., Scheidig, A. J., Goody, R. S. 1999. Characterization of the ternary complex between Rab7, REP-1 and Rab geranylgeranyltransferase. Eur. J. Biochem. 265:160-170.

Allen, M.F., Allen, E.B., Friese, C.F. 1989. Responses of the non-mycotrophic plant *Salsola kali* to invasion by vesicular-arbuscular mycorrhizal fungi. New Phytol. 11(1):45-49.

Amitai, C., Belenkiy, O. Dassa B. Shainska, A., Pietrokovski, S. 2003. Distribution and function of new bacterial intein-like rotein domains. Mol. Microbiol. 47(1):61-73

Amor, J.C., Harrison, D.H., Kahn, R.A., Ringe, D. 1994. Structure of the human ADP-ribosylation factor 1 complexed with GDP. Nature 372:704-708.

Andersen, U.N., Markholst, H., Hornum, L. 2004. the antiapoptotic gene Ian4*l* in the rat: genomic organization and promoter characterization. Gene 341:141-148.

Anderson, R. G. W. 1998. The caveolae membrane system. Annu. Rev. Biochem. 67:199-225.

Ane J. M., Kiss G. B., Riely B. K., Penmetsa R. V., Oldroyd G. E., Ayax C., Levy J., Debelle F., Baek J.M., Kalo P., 2004. *Mendicago truncatula DMI1* required for bacterial and fungal symbioses in legumes. Science 303:1364-1367.

Antonny, B., Beraud-Dufour, S., Chardin, P., Chabre M. 1997. N-Terminal Hydrophobic residues of the G-protein ADP-Ribosylation Factor-1 insert into membrane phospholipids upon GDP to GTP exchange. Biochemistry 36:4675-4684.

Aspock, G., Cassata, G., Dozier, C., Kagoshima, G., Niklaus, G., Pretot, R., 2000. The role of the homeobox and Hedgehog-related genes during development of *Caenorhabditis elegans.* In www.biozentrum.unibas.ch/report9899/buerglin.html.

Aspöck, G., Kagoshima, H., Niklaus, G., Bürglin, T.R. 1999. *Caenorhabditis elegans* has scores of hedgehog related genes: Sequence and expression analysis. Genome Res. 9:909-923.

Bagnat, M. and Simons, K. 2002a. Cell surface polarization during yeast mating. PNAS 29:14183-14188.

Bagnat, M. and Simons, K. 2002b. Lipid Rafts in protein sorting and cell polartiy in budding yeast *Saccharomyces cerevisiae*. Biol. Chem. 383:1475-1480.

Bagnat, M., Keränen, S., Shevchenko, A., Shevchenko, A., Simons, K. 2000. Lipid rafts function in biosyhthetic delivery of proteins to the cell surface in yeast. PNAS 97(7):3254-3259.

Bago, B., Pfeffer, P.E., Shachar-Hill, Y. 2000. Carbon metabolism and transport in Arbuscular mycorrhizas. Plant Physiol. 124:949-957.

Barea, I.M., and Jeffries, P.J. 1995. Arbuscular mycorrhizas in sustainable soil-plant systems. In: Varma A, Hock B (eds) Mycorrhiza. Springer, Berlin Heidelberg New York, pp, 521-560

Barker, S.J., Tagu, D., Delp, G. 1998. Regulation of root and fungal morphogenesis in mycorrhizal symbiosis. Plant Physiol. 116:1201-1207.

Barral Y., Meermall V., Mooseker M. S., Snyder M. 2000. Compartmentalization of the cell cortex by septins in required for maintenance of cell polarity in yeast. Mol. Cell 5:841-851.

Baumann, N. A. and Menon, A. K. 2002. D.E. Vance and J. E. Vance (Eds.). *In* Biochemistry of lipids, lipoproteins and membranes (4^{th} edn.). Lipid modifications of proteins, pp, 37-54.

Beachy, P.A., Cooper, M. K., Young, K., E., von Kessler, D. P., Park, W. J., Hall, T. M., Leahy, D. J., Porter, J. A. 1997. Multiple roles of cholesterol in hedgehog biogenesis and signaling. Cold Spring Harb. Symp. Quant. Biol. 62:191-204.

Bécard, G. and Piché, Y. 1989. Fungal growth stimulation by CO_2 and root exudates in vesicular-arbuscular mycorrhizal fungus, *Gigaspora margarita*. New Phytol. 112:77-83.

Bécard, G., Douds, D.D. Pfeffer, P.E. 1992. Extensive hyphal groth of vesicular-arbuscular mycorrhizal fungi in the presence of CO_2 and flavonols. Appl. Enviorn. Microbiol. 58:821-825.

Bécard, G., Kosuta, S., Tamasioukht, M., Séjalon-Delmas, N., Roux, C. 2004. Partner communication in the arbuscular mycorrhizal interaction. Can. J. Bot. 82:1186-1197.

Bécard, G., Piché, Y. 1989a. New aspects on the acquisition of biotrophic status by a vesicular-arbuscular mycorrhizal fungus, *Gígaspora margarita.* New Phytol. 112:77-83.

Bécard, G., Piché, Y. 1989b. Fungal growth stimulation by $C0_2$ and root exudates in vesicular-arbuscular mycorrhizal symbiosis. Appl. Environ. Microb. 55:2320-2325.

Bécard, G., Taylor, L.P., Douds, D.D., Pfeffer, P.E., Doner, L.W. 1995. Flavonoids are not necessary plant signal compounds in arbuscular mycorrhizal symbioses. Mol. Plant Microbe Interact 8:252-258.

Beilby, J.P. And Kidby, D.K. 1980. Biochemistry of ungerminated and Germinated Spores of the Vesicular-arbuscular mycorrhizal fungus, *Glomus caledonius*: Changes in Neutral and Polar Lipids. J. Lipid Research 21:739-750.

Bender, A., and Pringle, J.R. 1989. Multicopy Suppression of the cdc24 Budding Defect in Yeast by CDC42 and Three Newly Identified Genes Including the ras-Related Gene RSR1 Proc. Natl. Acad. Sci. USA 86:9976-9980.

Benito-Moreno, R. M. , Miaczynska, M., Bauer, B. E., Schweyen, R. J., Ragnini, A. 1994. Mrs6p, the yeast homologue of the mammalian choroideraemia protein: immunological evidence for its function as the Ypt1p Rab escort protein. Curr. Genet. 27:23-25.

Bent, A.F., Kunkei, B.N., Dahlbeck, D., Brown, K.L., Schrnidt, R. Giraudat, J., Leung, J., and Staskawicz, B.J. 1994. *RPS2 of Arabidopsis thaliana:* A leucine-rich repeat class of plant disease resistance genes. Science 265:1856-1860.

Beraud-Dufour, S., Paris, S., Chabre, M., Antonny, B. 1999. Dual interaction of ADP ribosylation factor 1 with Sec7 domain and with lipid membranes during catalysis of guanine nucleotide exchange. J. Biol. Chem. 274:37629-37636.

Bérczi, A. and Horvath, G. 2003. Lipid rafts in the plant plasma membrane? Acta Biol. Szegediensis 47(1-4):7-10.

Bethlenfalvay, G.J., Cantrell, I.C., Mihara, K.L., Schreiner, R.P. 1998. Relationships between soil aggregation and mycorrhizae as influenced by soil biota and nitrogen nutrition. Biol. Fertil Soils 28:356-363.

Bhat, R.A., Miklis, M., Schmelzer, E., Schulze-Lefert, P., Panstruga, R. 2004. recruitment and interaction dynamics of plant penetration resitance components in a plasma membrane microdomain. PNAS 102(8):3135-3140.

Bhullar R.P. and Haslam R.J. 1987. Detection of 23-27 kDa GTP-binding proteins in platelets and other cells. Biochem. J. 245:617-620.

Bligh, E.G., Dyer, W.J. 1959. A rapid method of total lipid extraction and purification. Can. J. Biochem. Physiol. 37(8):911-7.

Bölker, M. 1998. Sex and crime: Heterotrimeric G protein in fungal mating and pathogenesis. Fungal Gen. Biol. 25:143-156.

Bonfante-Fasolo P, S Scannerini. 1992. The cellular basis of plant-fungus interchanges in mycorrhizal associations. In: *Mycorrhizal functioning: An integrative plant-fungal process.* Allen MF (ed). pp 65-101, Chapman and Hall, New York.

Bonfante, P., Bianciotto, V. 1995. Presymbiontic versus symbiontic phase in arbuscular endomycorrhizal fungi: morphology and cytology. *In*: Varma, A., Hock, B. (eds). Mycorrhiza. Springer, Berlin Heidelberg New York, pp. 229-247.

Bonfante, P., Genre, A., Faccio, A., Martinin, I., Schauser, L., Stougaard, J., Webb, J., Parniske, M. 2000. The *Lotusjaponicus LjSym4* gene is required for the successful symbiotic infection of root epidermal cells. Mol. Plant Microbe Interact. 13:1109-1120.

Bonfante, P., Perotto, S. 1995. Strategies of arbuscular mycorrhizal fungi when infecting host plants. New Phytol. 130:3-21.

Borkovich, K.A. 1996. Signal transduction pathways and heterotrimeric G proteins. In Brambl, R. and Marzluf, G. A. (eds), The Mycota III. Springer-Verlag, Berlin, pp. 211-228.

Bourne, H.R., Sanders, D.A., McCormick, F. 1990. The GTPase superfamily: a conserved switch for diverse cell functions. Nature 348:125-132.

Bourne, H.R., Sanders, D.A., McCormick, F. 1991. The GTPase superfamily: conserved structure and molecular mechanism. Nature 349:117-127.

Breuninger, M. and Requena, N. 2004. Recognition events in AM symbiosis: analysis of fungal gene expression at the early appressorium stage. Fungal Gen. Biol. 41:794-804.

Brown, D. and Rose, J.K. 1992. Sorting of GPI-anchored proteins to glycolipid-enriched membrane subdomains during transport to the apical cell surface. Cell 68:533-544.

Brown, D.A. and London, E. 1998. Functions of lipid rafts in biological membranes. Annu. Rev. Cell. Dev. Biol. 14:111-136.

Bruns, R. R., an G. E. Palade. 1968. Studies on blood capillaries I. General organization of blood capillaries in muscle. J. Cell Biol. 37:244-249.

Buee, M., Rossignol, M., Jauneau, A., Ranjeva, R., Becard, G. 2000. The pre-symbiotic growth of arbuscular mycorrhizal fungi is induced by a branching factor partially purified from plant root exudates. Mol. Plant. Microbe. Interact. 13:693-698.

Bürglin, T. R. 1996. Warthog and Groundhog, novel families related to Hedgehog. Current Biology 6(9):1047-1050.

Burke, R., Nellen, D., Bellotto, M., Hafen, E., Senti, K.A., Dickson, B.J., Basler, K. 1999. Dispatched, a novel sterol-sensing domain protein dedicated to the release of cholesterol-modified hedgehog from signaling cells. Cell 99:803-815.

Cabib, E., Drgnova, J., Drgon, T. 1998. Role of small G protiens in yeast cells polarization and wall biosynthesis. Ann. Rev. Biochem. 67:307-333.

Cambot, M., Aresta, S., Kahn-Perlès, B., de Gunzburg, J., Romeo, P.H. 2002. Human immtinc associated nucleotide 1: a member of a new guanosine triphosphatase family expressed in resting T and B cells. Blood 99, 3293-3301.

Carstea, E.D., Morris, J.A., Coleman K.G., Loftus, S.K., Zhang, D., Cummings, C., Gu, J., Rosenfeld, M.A., Pavan, W.J., Krizman D.B. 1997. Niemann-Pick C1 disease gene: homology to mediators of cholesterol homeostasis. Science 277:228-231.

Casey, P. J. 1995. Protein lipidation in signal transduction. Science 268:221-225.

Catford, J.G., Staehelin, C., Lerat, S., Piché, Y., Vierheilig, H. 2003. Suppression of Arbuscular mycorrhizal colonization and nodulation in split-root systems of alfalfa after pre-inoculation and treatment with Nod factors. J. Exp. Bot. 54:1481-1487.

Cerione, R.A. 2004. Cdc42:new roads to travel. Trends in Cell Biology 14(3):127-132.

Chabaud, M., Venard, C., Defaux-Petras, A., Bécard, G., Barker, D.G. 2002. Targeted inoculation *of Medicago truncatula* in vitro root cultures reveals *MtENOD1* 1 expression during early stages of infection by arbuscular mycorrhizal fungi. New Phytol. 156:265-273.

Chamoun, Z., Mann, R.K., Nellen, D., von Kessler, D.P., Bellotto, M., Beachy, P.A., Basler, K. 2001. Skinny hedgehog, an acyltransferase required for palmitoylation and activity of the hedgehog signal. Science 293:2080-2084.

Chardin, P., Paris, S., Antonny, B., Robineau, S., Béraud-Bufour, S., Jackson, C.L., Chabre, M. 1996. A human exchange factor for ARF contains Sec7- and pleckstrin-homology domains. Nature 384:481-485.

Chen, J.K., Taipale, J., Cooper, M.K., Beachy, P.A. 2002. Inhibition of Hedgehog signaling by direct binding of cyclopamine to Smoothened. Genes Dev. 16:2743-2748.

Chen, M.-H., Li, Y.-J., Kawakami, T., Xu, S.-M, Chuang, P.-T. 2004. Palmitoylation is required for the production of a soluble multimeric hedgehog protein complex and long-range signaling in vertebrates. Genes and Development 18:641-659.

Chen, Y. and Struhl, G. 1996. Dual roles for patched in sequestering and transducing Hedgehog. Cell 87: 553-563.

Christie, W.W. 1982. *In* Lipid Analysis, 2nd edition. The Isolation of lipids from tissues (Pergamonn Press). pp. 17-23.

Chuang, P.T., McMahon, A.P. 1999. Vertebrate Hedgehog signallinig modulated by induction of a Hedgehog-binding protein. Nature 397:617-621.

Clarke, P. R., Zhang, C. 2001. Ran GTPase: a master regulator of nuclear structure and function during the eukaryotic cell division cycle? Trends Cell Biol. 11(9):366-71.

Cooper, M.K., Porter, J.A., Young, K.E., Beachy, P.A. 1998. Teratogen mediated inhibition of target tissue response to Shh signaling. Science 280:1603-1607.

Cooper, M.K., Wassif, C.A., Krakowiak, P.A., Taipale, J., Gong, R., Kelley, R.I., Porter, F.D., Beachy, P.A. 2003. A defective response to Hedgehog signaling in disorders of cholesterol biosythesis. Nature Genetics 33:508-513.

Dahéron, L., Zenz, T., Siracusa, L.D., Brenner, C., Calabretta, B. 2001. Molecular cloning of lan4: a BCR/ABL-induced gene that encodes an outer-membrane mitochondrial protein with GTP-binding activity. Nucleic Acids Res. 29:1308 1316.

Dangl, J.L., and Jones, J.D.G. 2001. Plant pathogens and integrated defence responses to infection. Nature 411, 826-833.

David-Schwartz, R., Badani, H., Smadar, W., Levy, A.A., Galili, G., Kapulnik, Y. 2001. Identification of a novel genetically controlled step in mycorrhizal colonization: plant resistance to infection by fungal spores but not extra-radical hyphae. Plant J. 27:561-569.

de Vos, A. M., Tong, L., Milburn, M. V., Matias, P. M., Jancarik, J., Noguchi, S., Nishimura, S., Miura, K., Ohtsuka, E., Kim, S. H. 1988. Three-dimensional structure of an oncogene protein: catalytic domain of human c-H-ras p21. Science. 239(4842):888-93.

Debener, T., Lehnackers, H., Arnold, M., and Dangl, J.L. 1991. Identification and molecular mapping of a single *Arabidopsis thallana* locus determining resistance to a phytopathogenic *Pseudomonas syringae* isolate. Plant J. 1:289-302.

Demchenko K., Winzer T., Stougaard J., Parniske M., Pawlowski, K. 2004. Distinct roles of *Lotus japonicus SYMRK* and *SYM15* in root colonization and arbuscle formation. New Phytol. 163:381–392.

Derbyshire, V. and Belfort, M. 1998. Lightning strikes twice: Intron-intein coincidence. Proc. Natl. Acad. Sci. USA 95:1356-1357.

Dohlman, H.G. and Thorner, J.W. 2001. Regulation of G protein-initiated signal transduction in yeast: paradigms and principles. Ann. Rev. Biochem. 70:703-754.

Douds, D.D., Pfeffer, P.E., Shachar-Hill, Y. 2000. Carbon partitioning, cost and metabolism of Arbuscular mycorrhizas. *In* Arbuscular mycorrhizas: physiology and function. Eds. Y. Kapulnik and D.D. Douds. Kluwer Academic Pulishers, Dordrecht, Netherlands. pp. 107-129.

Douds, D.D., Nagahashi, G., Abney, G.D. 1996. The differential effects of cell wall-associated phenolics, cell walls, and cytosolic phenolics of host and non-host roots on the growth of two species of AM fungi. New Phytol. 133:289-294.

Drees, B.L., Sundin, B., Brazeau, E., Caviston, J.P. Chen, G.-C., Guo, W., Kozminski, K.G., Lau, M.W., Moskow, J.J., Tong, A., Schenkman, L.R., McKenzie III, A., Brennwald, P., Longtine, M., Bi, E., Chan, C., Novick, P., Boone, C., Pringle, J.R., Davis, T.N, Fields, S., Drubin, D.G. 2005. A protein interaction map for cell polarity development. J. Cell Biol. 154:549-571.

Duan X., Gimble F. S., Quiocho F. A. 1997. Crystal structure of PI-SceI, a homing endonuclease with protein splicing activity. Cell 89:555-564.

Duc, G., Trouvelot, A., Gianinazzi-Pearson, V., Gianinazzi, S. 1989. First report of non-mycorrhizal plant mutants (Myc-) obtained in pea *(Pisum sativum* L.) and fababean *(Viciafaba* L.). Plant Sci. 60:215-222.

Duncan, J. A. and Gilman, A. G. 1998. A cytoplasmic acyl-protein thioesterase that removes palmitate from G protein alpha subunits and p21(RAS). J. Biol. Chem. 273:15830-15837.

Dunphy, J. T. and Linder, M. E. 1998. Signalling functions of protein palmitoylation. Biochem. Biophys. Acta 1436:245-261.

Echelard, Y., Epstein, D.J., St-Jacques, B., Shnen, L., Mohler, J., McMahon, L.A., McMahon, A.P. 1993. Sonic hedgehog, a member of a family of putative signaling molecules, is implicated in the regulation of CNS polarity. Cell 75:1417-1430

Eisenhaber B., Bork P., Eisenhaber F. 1999. Prediction of potential GPI-modification sites in proprotein sequences. J. Molec. Biol. 292 (3), 741-758.

Endre, G., Kereszt, A, Kevei, Z., Mihacea, S., Kalo, P., Kiss, G.B. 2002. A receptor kinase gene regulating symbiotic nodule development. Nature 417:962-966.

Entenmann, C. 1957. General procedures for separating lipid components of tissue. Methods Enzymol. 3:299-317.

Fang, E.G. and Dean, R. 2000. Site-directed mutagenesis of the magB gene affects growth and development in *Magnaporte grisea.* Mol. Plant Microbe Interact. 13:1214-1227.

Fankhauser, C., Homans, S.W., Thomas-Oates, J.E., McConville, M.J., Desponds, C., Conzelmann, A., Ferguson, M.A.J. 1993. Structures of glycosylphosphatidylinositol membrane anchors from *Saccharomyces cerevisiae*. J. Biol. Chem. 268(35):26365-26374.

Folch, J., Lees, M. Stanley, G.H.S. 1957. A simple method for the isolation and purification of total lipids from animal tissues. J. Biol. Chem. 226:497-509.

Fontaine J., Grandmougin-Ferjani A., Hartmann M.-A., Sancholle, M. 2001. Sterol biosynthesis by the arbuscular mycorrhizal fungus *Glomus intraradices*. Lipids 36(12):1357-63.

Franco, M., Chardin, P., Chabre, M., Paris, S. 1993. Myristoylation is not required for GTP-dependent binding of ADP-ribosylation factor ARF1 to phospholipids. J. Biol. Chem. 268(33):24531-24534.

Franco, M., Chardin, P., Chabre, M., Paris, S. 1995. Myristoylation of ADP-ribosylation factor 1 facilitates nucleotide exchange at physiological Mg^{2+} levels. 1994. J. Biol. Chem. 270(3):1337-1341.

Franco, M., Chardin, P., Chabre, M., Paris, S. 1996. Myristoylation-facilitated Binding of the G Protein ARF1GDP to Membrane Phospholipids is required for its activation by a soluble nucleotide exchange factor. J. Biol. Chem. 271(3):1573-1578.

Franken, P. and Requena, N. 2001a. Molecular analyisis of arbuscular mycorrhiza. *In*: Hock, B. (ed.) The mycota, vol IX. Springer, Berlin Heidelberg New York, pp. 19-28.

Franken, P. and Requena, N. 2001b. Analysis of gene expression in arbuscular mycorrhizas: new approaches and challenges. New Phytol. 150:517-523.

Franken, P., and Gnädinger, F. 1994. Analysis of parsley Arbuscular endomycorrhiza: infection development and mRNA levels of defense-related genes. Mol. Plant-Microbe Interact. 7:612-620.

Franson, A., Ruusala, A., Aspenstrom, P. 2003. Atypical Rho GTPases have roles in mitochondrial homeostasis and apoptosis. J. Biol. Chem. 278:6495-6502.

Friedrichson, T. and Kurzchalia, T. V. 1998. Microdomains of GPI-anchored proteins in living cells revealed by crosslinking. Nature 394:802-805.

Fry, S.C., Smith, R.C., Renwick, K.F., Martin, D.J., Hodge, S.K., Matthews, K.J. 1992. Xyloglucan endotransglycosylase, a new wall-loosening enzyme activity from plants. Biochem. J. 282:821-828.

Fujiyama, A. and Tamanoi, F. 1986. Processing and fatty acid acylation of RAS1 and RAS2 proteins in *Saccharomyces cerevisiae*. Proc. Natl. Acad. Sci. USA 83:1266-1270.

Fuse, N., Maiti, T., Wang, B., Porter, J., Hall, T., Leahy, D., and Beachy, P. 1999. Sonic hedgehog protein signals not as a hydrolytic enzyme but as an apparent ligand for patched. Proc. Natl. Acad. Sci. 96:10992-10999.

Fuse, N., Maiti, T., Wang, B., Porter, J.A., Hall, T.M.T., Leahy, D.J., Beachy, P.A. 1999. Sonic hedgehog protein signals not as a hydrolytic enzyme but as an apparent ligand for Patched. Proc. Natl. Acad. Sci. USA 96:10992-10999.

Gadkar, V., David-Schwartz, R., Kunik, T., Kapulnik, Y. 2001. Arbuscular mycorrhizal fungal colonization. Factors involved in host recognition. Plant Physiol. 127:1493-1499.

Gadkar, V., David-Schwartz, R., Nagahashi, G., Douds, D.D., Winiger, S., Kapulnik, Y. 2003. Root exudates of pmi tomato mutant M161 reduces AM fungal proliferation in vitro. FEMS Microbiol. Lett. 223:193-198.

Gallet A., Rodriguez, R., Ruel, L., Therond, P.P. 2003. Cholesterol modification of hedgehog is required for trafficking and movement, revealing an asymmetric cellular response to hedgehog. Dev. Cell 4:191-204.

Garcia-Garrido, J.M., Ocampo, J.A. 2002. Regulation of the plant defence response in arbuscular mycorrhizal symbiosis. J. Exp. Bot. 53:1377-1386.

Garnier, J., Gibrat, J.-F., Robson, B., 1996. GOR secondary structure prediction method version IV. *In*: Doolittle, R.F. (Ed.), Methods in Enzymol. 266. Academic Press, lnc., San Diego, pp. 540-553.

Genre, A. and Bonfante, P. 2002. Epidermal cells of a symbiosis-defective mutant of *Lotus japonicus* show altered cytoskeleton organisation in the presence of a mycorrhizal fungus. Protoplasma 219:43-50.

Genre, A. and Bonfante, P. 1997. A mycorrhizal fungus changes microtubule orientation in tobacco root cells. Protoplasma 199:30-38.

George E, Marschner H, Jakobsen I, 1995: Role of arbuscular mycorrhizal fungi in uptake of phosphorus and nitrogen from soil. Critical Reviews in Biotechnology 15: 257-270.

Gianinazzi-Pearson V., Dumas-Gaudot, E., Gollote, A., Tahiri-Alaoui, A., Gianinazzi, S. 1996. Cellular and molecular defense-related root responses to invasion by Arbuscular mycorrhizal fungi. New Phytol. 133:45-57.

Gianinazzi-Pearson, V. 1996. Plant cell responsos to arbuscular mycorrhizal fungi getting to the roots of the symbiosis. Plant Cell 8:1871-1883.

Gianinazzi-Pearson, V., Arnould, C., Oufattole, M., Arango, M., Gianinazzi, S. 2000. Differential activation of H-ATPase genes by an arbuscular mycorrhizal fungus in root cells of transgenic tobacco. Planta 211:609-613.

Gianinazzi-Pearson, V., Branzanti, B., Gianinazzi, S. 1989. In vitro enhancement of spore germination and early hyphal growth of a vesicular-arbuscular mycorrhizal fungus by host root exudares and plant flavonoids. Symbiosis 7:243-255.

Gianinazzi-Pearson, V., Smith, S.E., Gianinazzi, S., Smith, F.A. 1991. Enzymatic studies on the metabolism of vesicular-arbuscular mycorrhizas:

V. H^+-ATPase a component of ATP-hydrolyzing enzyme activities in plant-fungus interfaces? New Phytol. 117:61-74.

Giovanetti, M. and Sbrana, C. 1998. Meeting a non-host: the behaviour of AM fungi. Mycorrhiza 8:123-130.

Giovannetti, M., Avio, L., Sbrana, C. 1993a. Factors affecting appressorium development in the vesicular-arbuscular mycorrhizal fungus *Glomus mosseae* (Nicol.and Gerd.) Gerd. & Trappe. New Phytol. 123:114-122.

Giovannetti, M., Sbrana, C., Avio, L. 1993b. Differential hyphal morphogenesis in arbuscular mycorrhizal fungi during preinfection stage. New Phytol. 125:587-593.

Giovannetti, M., Sbrana, C., Citernesi, A.S., Avio, L. 1996. Analysis of factors involved in fungal recognition responses to host derived signals by arbuscular mycorrhizal fungi. New Phytol. 133:65-71.

Giovannetti, M., Sbrana, C., Citernesi, A.S., Avio, L., Gollote, A., Gianinazzi-Pearson, V., Gianinazzi, S. 1995. Recognition and infection process, basis for host specificity of AMF. *In*: Gianinazzi, S. and Schüepp, H. (Eds). Impact of arbuscular mycorrhizas on sustainable agriculture and natural ecosystems. Birkháuser, Basel, pp. 61-72.

Goldberg, J. 1998. Structural basis for activation of ARF GTPase: mechanisms of guanine nucleotide exchange and GTP-myristoyl switching Cell 95:237-248.

Gollote, A., Gianinazzi-Pearson, V., Giovannetti, M., Sbrana, C., Avio, L., Gianinazzi, S. 1993. Cellular localization and cytochemical probing of resistance reactions to arbuscular mycorrhizal fungi in a "locus a" mutant *Pisum sativum* L. Planta 191:112-122.

Gomez-Moutón, C., Abad, J.L., Mira, E., Lacalle, R.A., Gallardo, E., Jiménez-Baranda, S., Bernad, A., Manes, S., Martínez, A.C. 2001. Segregation of leading-edge and uropod components into specific lipid rafts during T cell polarization. PNAS 98:9642-9647.

Gorfer, M., Tarkka, M.T., Hanif, M., Pardo, A.G., Laitiainen, E., Raudaskoski, M. 2001. Characterization of small GTPases Cdc42 and Rac and the relationship between Cdc42 and Actin cytoskeleton in vegetative and ectomycorrhizal hyphae of *Suillus bovinus*. Am. Phytopathol. Soc. 14(2):135-144.

Gosh, I., Sun, L., Xu, M. 2001. Zinc Inhibition of Protein trans-Splicing and Identification of Regions Essential for Splicing and Association of a Split Intein, Journal of Biol. Chem. 276:24051-24058.

Grant, M.R., Godiard, L., Straube, E., Ashfield, T., Lewald, J., Sattler, A., Innes, R.W., Dangl, J.L. 1995. Structure of the *Arabidopsis RPM1* gene which enables dual-specificity disease resistance. Science 269:843-846.

Guenoune, D., Galili, S., Phillips, D.A., Volpin, H., Chet, I., Okon, Y., Kapulnik, Y. 2001. The defense response elicited by the pathogen *Rhizoctonia solani* is suppressed by colonization of the AM-fungus *Glomus intraradices*. Plant Sci. 160:925-932.

Guttenberger M and Hampp R 1992. Ectomycorrhizins-symbiosis-specific or artifactual polypeptides from ectomycorrhizas? Planta 188:129-136.

Hall, T.M., Porter, J.A., Young, K.E., Koonin, E.V., Beachy, P.A., Leahy, D.J. 1997. Crystal structure of a hedgehog autoprocessing domain: homology between hedgehog and selfs-splicing proteins. Cell 91:85-97.

Harley JL & Smith SE. 1983. Mycorrhizal Symbiosis. Academic Press, London.

Hamm, H. E. and Gilchrist, A. 1996. Heterotrimeric G proteins. Curr. Opin. Cell Biol. 8:189-196.

Hammerschmidt, M., Brook, A., McMahon, A.P. 1997. The world according to hedgehog. Trends Genet. 13(1):14-21.

Hause, B., Maier, W., Miersch, O., Kramell, R., Strack, D. 2002. Induction of jasmonate biosynthesis in arbuscular mycorrhizal barley roots. Plant Physiol. 130:1213-1230.

Higgs, H.N., Pollard, T.D. 2001.Regulation of actin filament network formation through ARP2/3 complex: activation by a diverse array of proteins. Annu. Rev. Biochem. 70:649-76.

Hirata, R., Ohsumk, Y., Nakano, A., Kawasaki, H., Suzuki, K., Anraku, Y. 1990. Molecular structure of a gene, VMA1, encoding the catalytic subunit of H(+)-translocating adenosine triphosphatase from vacuolar membranes of *Saccharomyces cerevisiae*. J. Biol. Chem. 265(12):6726-33.

Hirschman, J. E. and Jennes, D. D. 1999. Dual lipid modification of the yeast Gγ subunit Ste18p determines membrane localization of Gβγ. Mol. and Cellular Biol. 19(11):7705-7711.

Hoffman, G. R., Nassar N., Cerione R. A. 2000. Structure of the Rho family GTP-binding protein cdc42 in complex with the multifunctional regulator RhoGDI. Cell 100:345-356.

Hornum, L., Romer, J., Markholst, H. 2002. The diabetes-prone BB rat carries a frameshift mutation in lan4, a positional candidate of Iddm1, Diabetes 51:1972 1979.

Hooper, L. 1994. Distinct pathways for autocrine and paracrine Wingless signalling in *Drosophila* embryos. Nature 372:461-464.

Incardona, J.P., Lee, J.H., Robertson, C.P., Enga, K., Kapur R.P., Roelink, H. 2000. Receptor-mediated endocytosis of a soluble and membrane-tethered sonic hedgehog by Patched-1. PNAS 97(22):12044-12049.

Incardona, J.P., Gaffield, W., Kapur, R.P., Roelink, H. 1998. The teratogenic Veratrum alkaloid cyclopamine inhibits Sonic hedgehog signal transduction. Development 125:3553-3562.

Ingham, P.W. 2001. Hedgehog signaling: a tale of two lipids. Science 294:1879-1881.

Ingham, P.W. 1998. Transducing Hedgehog: the story so far. EMBO J. 17:3505-3511.

Ingham, P.W. and McMahon, A.P. 2001. Hedgehog signaling in animal development: paradigms and principles. Genes and Development 15:3059-3087.

Ingram, W.J., Wicking, C.A., Grimmond, S.M., Forrest, A.R., Wainwright, B.J. 2002. Novel genes regulated by Sonic Hedgehog in pluripotent mesenchymal cells. Oncogene 21:8196-8205.

Innes, R.W., Bisgrove, S.R., Smith, N.M., Bent, A.F, Staskawicz, B.J., Liu, Y.-C. 1993. Identification of a disease resistance locus in *Arabidopsis* that is functionally homologous to the RPG1 locus of soybean. Plant J. 4:813-820.

Isshiki, T., Mochizuki, N., Maeda, T., Yamamoto, M. 1992. Charachterization of a fision yeast gene, *gpa2* , that encodes a G_{α} subunit involved in the monitoring of nutrition. Genes Dev. 6:2455-2462.

Jaffe, A. B., Hall, A. 2002. Rho GTPases in transformation and metastasis. Adv Cancer Res., 84:57-80.

Jahnen, W. and Hahlbrock, K. 1988. Cellular localization of non-host resistance reaction of parsley (*Petroselinun crispum*) to fungal infection. Planta 173:197-204.

Jeong, J., McMahon, A.P. 2002. Cholesterol modification of Hedgehog family proteins. J. Clin. Invest. 110:591-596.

Jiang, X., & Wang, X. 2000. Cytochrome C promotes caspase-9 activation by inducing nucleotide binding to Apaf-1. J. Biol. Chem. 275:31199-31203.

Johnson, R.L. and Tabin, C. 1995. The long and the short of hedgehog signaling. Cell 81:313-316.

Johnson, R., Milenkovic, L., Scott, M. 2000. In vivo functions of the Patched protein: Requirement of the C terminus for target gene inactivation but not Hedgehog sequestration. Mol. Cell 6:467-478.

Jurnak, F. 1985. Structure of the GDP domain of EF-Tu and location of the amino acids homologous to ras oncogene proteins. Science. 230(4721):32-6.

Kahn, R.A., Yucel, J.K., Malhotra, V. 1993. ARF signaling: a potential role for phospholipase D in membrane traffic. Cell 75(6):1045-8.

Kane, P.M., Yamashiro, C.T., Wolczyk, D.F., Neff, N., Goebl, M., Stevens, T.H. 1990. Protein splicing converts the yeast TFP1 gene product to the 69-kD subunit of the vacuolar H(+)-adenosine triphosphatase. Science 250(4981):651-7.

Karpen, H. E., Bukowski, J.T., Hughes, T., Gratton, J-P., Sessa, W.S., Galiani, M.R., 2001, The Sonic Hedgehog receptor patched associates with caveolin-1 in cholesterol-rich microdomains of the plasma membrane. J. Biol. Chem. 276(22):19503-19511.

Kawakami, T., Kawcak, T., Li, Y.J., Zhang, W., Hu, Y., Chuang, P.T. 2002. Mouse dispatched mutants fail to distribute hedgehog proteins and are defective in hedgehog signaling. Development. 129:5753-5765.

Koonin, E.V. 1995. A protein splice-junction motif in hedgehog family proteins. *Trends Biochem. Sci.* 20:141-142.

Koske, R.E. 1982. Evidence for a volatile attractant from plantroots affecting germ tubes of a VA mycorrhizal fungus. Trans. Br. Mycol. Soc. 79:305–310.

Kosuta, S., Chabaud, M., Lougnon, G., Gough, C., Dénarié, J., Barker, D.G., Bécard, G. 2003. A diffusible factor from Arbuscular mycorrhizal fungi

induces symbiosis-specific MtENOD11 expression in roots of *Medicago truncatula*. Plant Physiol. 131:952-962.

Krengel, U., Schlichting, L., Scherer, A., Schtinlann, R., Frech, M., John, J., Kabsch, W., Pai., E.F., Wittinghofer, A. 1990. Three-dirmensional structures of 11-ras p21 mutants: molecular basis for their inability to switch molecules. Cell 62:539-548.

Krücken, J., Schroetel, R.M.U., Müller, I.U., Saidani, N., Marinovski, P., Benten, W.P.M., Stamm, O., Wunderlich, F. 2004. Comparative analysis of the human *gimap* gene cluster encoding a novel GTPase family. Gene 341:291-304.

Krücken, J., Stamm, O., Schmitt-Wrede. H.-P., Mincheva, A., Lichter, P., Wunderlich, F. 1999. Spleen-specific expression of the malaria-inducible intronless mouse gene *imap38.* J. Biol. Chem. 274:24383-24391.

Krücken, J., Schmitt-Wrede, H.-P., Markmann-Mulisch, U., Wunderlich, F. 1997. Novel gene expressed in spleen cells mediating acquired testosterone-resistant immunity to *Plamodium chabaudi* malaria. Biochem. Biophys. Res. Commun. 230:167-170.

Kruger, M., Mennerich, D., Fees, S., Schafer, R., Mundlos, S., and Braun, T. 2001. Sonic hedgehog is a survival factor for hypaxial rnuscles during mouse developrnent. Development 128:743-752.

Kübler, E., Dohlman, H.G., Lisanti, M.P. 1996. Identification of Triton X-100 insoluble membrane domains in the yeast *Saccharomyces cerevisiae*. J. Biol. Chem. 271(51):32795-32980.

Kunkel, B.N., Bent, A.F., Dahlbeck, O., lnnes, R.W., Staskawicz, B.J. 1993. *RPS2,* an Arabidopsis disease resistance locus specifying recognition of *Pseudomonas syringae* strains expressing the avirulence gene *avrRpt2.* Plant Cell 5:865-875.

Kuwabara, P.E., Lee, M.-H., Schedl, T., Jefferis, S.X.E. 2000. A *C. elegans* patched gene, ptc-1, functions in germ-line cytokinesis. Genes and Development 14:1933-1944.

Kytte, J. and Doolittle, R. F. 1982. A simple method for displaying the hydropathic character of a protein. J. Mol. Biol. 157:105–132.

Lapopin, L., Gianinazzi-Pearson, V., Franken, P. 1999. Comparative differential RNA display analysis of arbuscular mycorrhiza in *Pisum sativum* wild type

and a mutant defective in late stage development. Plant. Mol. Biol. 41:669-677.

Larose, G., Chnevert, R., Moutoglis, P., Gagne, S., Piché, Y., Vierheilig, H. 2002. Flavonoid levels in roots of *Medicago sativa* are modulated by the developmental stage of symbiosis and the root colonizing arbuscular mycorrhizal fungus. J. Plant Physiol. 159:1329-1339.

Lee, J.D., Kraus, P., Gaiano, N., Nery, S., Kohtz, J., Fishell, G., Loomis, C.A., Heisman, J.E. 2001. An acylatable residue of Hedgehog is differentially required in *Drosophila* and mouse limb development. Dev. Biol. 233:122-136.

Lee, J.D., Treisman, J.E. 2001. Sightless has homology to transmembrane acyltransferases and is required to generate active Hedgehog protein. Curr. Biol. 233:1147-1152.

Lee, J.J., Ekker, S.C., Park, W-J., von Kessler, D.P., Porter, J.A., Sun, B.I., Beachy, P.A. 1994. Autoproteolysis in Hedgehog Protein Biogenesis. *Science* 266:1528-1537.

Lee, J.J., von Kessler, D.P., Parks, S. Beachy, P.A. 1992 secretion and localized transcription suggests a role in positional signalling for products of the segmentation gene hedgehog. Cell 70:777-789.

Lehmann, P. 2002. Structure and evolution of plant disease resistence genes. J. Appl. Gen. 43(4):403-414.

Lerat, S., Lapointe, L., Piché, Y., Vierheilig, H. 2003. Variable carbon-sink strength of different *Glomus mosseae* strains colonizing barley roots. Can. J. Bot. 82:886-889.

Leupold, C.M., Goody, R.S., Wittinghofer, A. 1983. Stereochemistry of the elongation factor Tu X GTP complex. Eur. J. Biochem. 135(2):237-41.

Lewis, P.M., Dunn, M.P., McMahon, J.A., Logan, M., Martin, J.F., St-Jacques, B., McMahon, A.P. 2001. Cholesterol modification of Sonic Hedgehog is required for long-range signaling activity and effective modulation of signaling by Ptc1. Cell 105:599-612.

Linder, M.E. and Deschenes, R.J. 2004. Model organisms lead the way to protein palmitoyltransferases. J. Cell Sci. 117:521-526.

Lisanti, M.P., Sargiacomo, M., Scherer, P.E. 1999. Purification of caveolae-derived membrane microdomains containing lipid-anchored signaling

molecules, such as GPI-anchored proteins, H-Ras, Src-farnily tyrosine kinases, eNOS and G-protein alpha-, beta-, and gamma-subunits. Methods Mol. biol. 116:51-60.

Lisanti, M.P., Tang, Z.-T., Scherer, P., Sargiacomo, M. 1995. Caveolae purification and GPI-linked protein sorting in polarized epithelia. Methods Enzymol. 250:655-668.

Liu, S. and Dean, R. 1997. G proteins alpha subunits genes control growth, development and pathogenicity of *Magnaporte grisea.* Mol. Plant Microbe Interact. 10:1075-1086.

Lobo, S., Greentree, W.K., Linder, M.E. Deschenes, R.J. 2002. Identification of a Ras palmitoyltransferase in *Saccharomyces cerevisiae*. J. Biol. Chem. 277:41268-41273.

Logi, C., Sbrana, C., Giovanetti, M. 1998. Cellular events involved in survival of individual arbuscular mycorrhizal symbionts growing in the absence of the host. Appl. Environ. Microbiol. 64:3473-3479.

Lorenz, M.C. and Heitman, J. 1997. Yeast pseudohyphal growth is regulated by GPA2, a G protein homolog. EMBO Journal 16(23):7008-7018.

Ma, Y., Erkner, A., Gong, R., Yao, S., Taipale, J., Basler, K. 2002. Hedgehog-mediated patterning of the mammalian embryo requires transporter-like function of dispatched. Cell 111:63-75.

MacMurray, A.J., Moi alejo, D.H., Kwitek, A.E., Rütledge, H.A., Van Yserloo, B., Gohlke, P., Speros, S.J., Snyder, B., Schaefer, J., Bieg, S., Jiang, J., Ettinger, R.A., Fuller, J., Daniels, T.L., Pettersson, A., Orlebcke, K., Birren, B., Jacob, H.J., Lander, E.S., Lernmark, A. 2002. Lymphopenia in the BB rat model of type 1 diabetes is due to a mutation in a novel immune-associated nucleotide (lan)-related gene. Genome Res. 12:1029-1039.

Magee, A.I., Gutierrez, L., McKay, C.J., Marshall, I.A., Hall, A. 1987. Dynamic fatty acylation of $p21^{N\text{-}ras}$. EMBO J. 6:3353-3357.

Manenti, S., Sorokine, O., Van Dorsselaer, A., Taniguchi, H. 1994. Demyristoylation of the major substrate of protein kinase C (MARCKS) by the cytoplasmic fraction of brain synaptosomes. J Biol Chem. 269(11):8309-13.

Mann, R. K. and Beachy, P. A. 2000. Cholesterol modification of proteins. Biochem. Biophys. Acta 1529:188-202.

Marigo, V., Davey, R., Zuo, Y., Cunningham, I., Tabin, C. 1996a. Biochemical evidence that patched is the hedgehog receptor. Nature 384:176-179.

Martin, S.W. and Konopka, J.B. 2004. Lipid raft polarization contributes to hyphal growth in *Candida albicans*. Eukaryotic Cell 3(3):675-684.

Martin, V., Carrillo, G., Torroja, C., Guerrero, I. 2001. The sterol-sensing domain of Patched protein seems to control Smoothened activity through Patched vesicular trafficking. Current Biol. 11:601-607.

Martin-Laurent, F., van Tuinen, D., Dumas-Gaudot, E., Gianinazzi-Pearson, V., Gianinazzi, S., Franken, P. 1997. Differential display analysis of RNA accumulation in arbuscular mycorrhiza of pea and isolation of a novel symbiosis-regulated plant gene. Mol. Gen. Genet. 256:37-44.

Maurer-Stroh, S., Washielt, S., Eisenhaber, F. 2003. Protein prenyltransferases. Genome Biol. 2:212-218.

McArthur, D.A.J., and Knowles, N.R. 1992. Resistance responses of potato to vesicular-arbuscular mycorrhizal fungi under varying abiotic phosphorus levels. Plant Physiol. 100:341-351.

McLaughlin, S. and Aderem, A. 1995. The myristoyl-electrostatic switch: a modulator of reversible protein-membrane interactions. Trends Biochem. Sci. 20:272-275.

Meyers, B.C., Dickerman, A.W., Michelniore, R.W., Sivararnakrishnan, S., Sobral, B.W., and Young, N.D. 1999. Plant disease resistance genes encode members of an old and diverse protein family within the nucleotide-binding superfamily. Plant J. 20:317-332.

Micchelli, C.A., The, I., Selva, E., Mogila, V., Perrimon, N. 2002. rasp, a putative transmembrane acyltransferase, is required for hedgehog signaling. Development 129:843-851.

Milburn, M.V., Tong, L., deVos, A.M., Brunger, A., Yamaizumi, Z., Nishimura, S., Kim, S.H. 1990. Molecular switch for signal transduction: structural differences between active and inactive forms of protooncogenic ras proteins. Science. 247(4945):939-45.

Milligan, G., Grassie, M.A., Wise, A., MacEwan, D.J., Magee, A.I., Parenti, M. 1995. G-protein palmitoylation: regulation and functional significance. Biochem. Soc. Trans. 23:583-587.

Mills, K.V. and Paulus, H. 2001. Reversible Inhibition of Protein Splicing By Zinc Ion, Journal of Biol. Chem. 276:10832-10838.

Mindrinos, M., Katagiri, F., Yu, G.-L., Ausubel, F.M. 1994. The *A. thaliana* disease resistance gene RPS2 encodes a protein containing a nucleotide-binding site and leucine-rich repeats. Cell 78:1856-1860.

Mitra R. M., Gleason C.A., Edwards A., Hadfield J., Downie J.A., Oldroyd G.E., Long S.R. 2004. A Ca^{+2}/calmodulin-dependent protein kinase required for symbiotic nodule development: gene identification by transcript-base cloning. PNAS 101:4701-4705.

Moffett, S., Brown, D.A., Linder, M.E. 2000. Lipid-dependent targeting of G proteins into rafts. Am. Soc. Biochem. Mol. Biol. 275(3):2191-2198.

Mongrand, S., Morel, J., Laroche, J., Claverol, S., Carde, J-P., Hartmann, M-A., Bonneu, M., Simon-Plast, F., Lessire, R., Bessoule, J-J. 2004. Lipid rafts in Higher Plant Cells: Purification and characterization of Triton X-100-Insoluble microdomains from Tobacco plasma membrane. J. Biol. Chem. 279(35):36277-36286.

Morandi, D., Bailey, J.A, Gianinazzi-Pearson, V. 1984. Isoflavonoid accumalation in soybean roots infected with vesicular-arbuscular mycorrhizal fungi. Physiol. Plant Pathol. 24:357-364.

Morandi, D., Sagan, M., Prado-Vant, E., Duc, G. 2000. Influence of genes determinine supernodulation on root colonization by the mycorrhizal fungus *Glomus mosseae* in *Pisum sativum* and *Medicago truncatula* mutants. Mycorrhiza 10:37-42.

Mosse, B. 1959. The regular germination of resting spores and some observations in the growth requirements of *anendogone* sp. causing vesicular-arbuscular mycorrhiza. Trans. Br. Mycol. Soc. 42:273-286.

Mosse, B. 1988. Some studies relating to "independent" growth of vesicular-arbuscular endophytes. Can. J. Bot. 66:2533-2540.

Mukherjee, S. and Maxfield, F. R. 2004. Membrane Domains. Annu. Rev. Cell Biol. 20:839-866.

Murone, M., Rosenthal, A., de Sauvage, F.J. 1999. Sonic hedgehog signaling by the patched-smoothened receptor complex. Curr. Biol. 9:76-84.

Murphy, P.J., Langridge, P., Smith, S.E. 1997. Cloning plant genes differentially expressed during colonization of roots of *Hordeum vulgare* by the vesicular-

arbuscular mycorrhizal fungus *Glomus intraradices.* New Phytol. 135:291-301.

Nagahashi, G. and Douds, D.D. 2000. Partial separation of root exudates components and their effects upon the growth of germinated spores of AM fungi. Funct. Ecol. 104:1453-1464.

Nagahashi, G., and Douds, D.D. 1997. Appressorium formation by AM fungi on isolated cell walls of carrot roots. New Phytol. 136:299-304.

Nair, M.G., Safir, G.R., Siqueira, J.O. 1991. Isolation and identification of vesicular-arbuscular mycorrhiza stimulatory compounds from clover *(Trifolium repens)* root. Appl. Environ. Microbiol. 57:434-439.

Neer, E.J. 1995. Heterotrimeric G proteins: Organizers of membrane signals. Cell 80:249-257.

Nichols, B., Harris, R., James, A., 1965. Biochem. Biophys. Res. Commun. 20:256.

Nimchuk, Z., Eulgem, T., Hollt III, B.F., Dang, J.L. 2003. Recognition and response in the plant immune system. Annu. Rev. Genet. 37:579-609.

Novero, M., Faccio, A., Genre, A., Stougaard, J., Webb, K.J., Mulder, L., Parniske, M., Bonfante, P. 2002. Dual requirement of the *LjSym4* gene for mycorrhizal development in epidermal and cortical cells of *Lotus japonicus* roots. New Phytol. 154:741-749.

Ocón Garrido, A. 2004. Characterization of the role of trehalose in arbuscular mycorrhizal fungi. Doctoral thesis.

Okamoto,T., Schlegel, A., Scherer, P.E., Lisanti, M.P. 1998. Caveolins, a family of scaffolding proteins for organizing “preassembled signaling complexes“ at the plasma membrane. J. Biol. Chem. 273:5419-5422.

Pai, E. F., Kabsch, W., Krengel, U., Holmes, K. C., John, J., Wittinghofer A. 1989. Structure of the guanine-nucleotide-binding domain of the Ha-ras oncogene product p21 in the triphosphate conformation.Nature. 341(6239):209-14.

Pai, E.F., Krengel, U., Petsko, G.A., Goody, R.S., Kabsch, W., Wittinghofer, A. 1990. Refined crystal structure of the triphosphate conformation of H-ras p21 at 1.35 A resolution: implications for the mechanism of GTP hydrolysis. EMBO J. 9(8):2351-9.

Pan, Q., Wandel, J., and Fluhr, R. 2000. Divergent evolution plant NBS-LRR resistance gene homologues in dicot and cer genomes. J. Mol. Evol. 50, 203-213.

Pandarpurkar, M., Wilson-Fritch, L., Corvera, S., Markholst, H., Hornum, L., Greiner, D.L., Mordes, J.P., Rossini, A.A., Bortell, R., 2003. Ian4 is required for mitochondrial integrity and T cell survival. Proc. Nat. Acad. Sci. USA. 100:10382-10387.

Parton, R.G. and Hancock, J.F. 2004. Lipid rafts and plasma membrane microorganization; insights from Ras. Trends in Cell Biol. 14:141-147.

Pasqualato, S., Renault, L. & Cherfils, J. 2002. Arf, Arl, Arp and Sar protein: a family of GTP-binding proteins with a structural device for “front-back” communication. EMBO Reports 3(11):1035-1041.

Paszkowski, U., Shi, L., Bi-Yu, L., Xun, W., Briggs, S., Boller, T. 2001. A single gene mutation in the maize nope1 mutant abolishes the recognition of arbuscular mycorrhizal fungi. *In*: 10th International Congress, Molecular Plant-Microbe Interactions, Madison, WI, July10-14, Poster abstract n° 686.

Paulus, H. 2000. Protein splicing and related forms of protein autoprocessing. *Annu Rev Biochem* 69:447-496.

Pei, J. and Grishin, N.V. 2001. The CaaX prenyl endopeptidases belong to a novel superfamily of putative membrane-bound metalloproteases. Trends Biochem. Sci. 26:275-277.

Peitzsch, R.M., McLaughlin, S. 1993. Binding of acylated peptides and fatty acids to phospholipid vesicles: pertinence to myristoylated proteins. Biochemistry. 32(39):10436-43.

Pepinsky, R.B., Zeng, C., Wen, D., Rayhorn, P., Baker, D.P., Williams, K.P. 1998. Identification of a palmitic acid-modified form of human Sonic hedgehog. J. Biol. Chem. 273:14037-14045.

Pereira-Leal, J.B., Hume, A.N., Seabra, M.C. 2001. Prenylation of Rab GTPases: molecular mechanisms and involvement in genetic disease. FEBS Lett. 498:197-200.

Perler, F.B. 2002. Inbase, the new England biolabs intein database protein splicing mechanism and intein structure. Nucleic Acids Res. 30:383-384.

Peskan, T., Westermann, M.G., Oelmäller, R. 2000. Identification of low-density Triton X-100-insoluble plasma membrane microdomains in higher plants. Eur. J. biochem. 267:6989-6995.

Peters, C., Wolf, A., Wagner, M., Kuhlmann, J., Waldmann, H. 2004. The cholesterol membrane anchor of the hedgehog protein confers stable membrane association to lipid-modified proteins. PNAS 101(23):8531-8536.

Pietrokovski, s. 1994. conserved sequence features of inteins (protein introns) and their use in identifying new inteins and related proteins. Protein Sci. 3:2340-2350.

Pirozynski, K.A., Malloch, D.W. 1975. The origin of land plants a matter of mycotrophism. Biosystems 6:153-164.

Poirier, G.M., Anderson, G., Huvar, A., Wagaman, P.C., Shuttleworth, J., Jenkinson, E., Jackson, M.R., Peterson, P.A., Erlander, M.G., 1999. Immune-associated nucleotide-1 (IAN-1) is a thymic selection marker and defines a novel gene family conserved in plants. J. Immunol. 163:4960-4969.

Porter, J.A., Ekker, S.C., Park, W-J., von Kessler, D.P., Young, K.E., Chen, C-H., Ma, Y., Woods, A.S., Cotter, R.J. Koonin, E.V., Beachy, P.A. 1996a. Hedgehog patterning activity: Role of a Lipophilic Modification Mediated by the Carboxy-terminal Autoprocessing Domain. Cell 86:21-34.

Porter, J.A., von Kessler, D.P., Ekker, S.C., Young, K.E., Lee, J.J., Moses, K., Beachy, P.A. 1995. The product of hedgehog autoproteolytic cleavage active in local and long-range signalling. Nature 374:363-366.

Porter, J.A., Young, K.E, Beachy, P.A. 1996b. Cholesterol Modification of Hedgehog Signalling Proteins in Animal Development. Science, 274: 255-259.

Posada, J., Miller, P.J., McCullough, J., Ziman, M., Johnson, D.I. 1995. Genetic and biochemical analysis of Cdc42p function in *Saccharomyces cerevisiae* and *Schizosaccharomyces pombe.* Methods Enzymol. 256:281-290.

Poulin, M.J., Simard, J., Catford, J.-G., Labrie, F., Piché, Y. 1997. Response of symbiotic endomycorrhizal fungi to estrogen and antiestrogens. Mol. Plant Microbe Interact. 10:481-487.

Redecker, D., Kodner, R., Graham, L.E. 2000b. Glomalean fungi from the Ordovician. Science 289:1920-1921.

Redecker, D., Morton, J.B., Bruns, T.D. 2000a. Ancestral lineages of arbuscular mycorrhizal fungi (Giomales). Mol. Phylog. Evol. 14:276-284.

Regenfelder, E., Spellig, T., Hartmann, A., Lauenstein, S., Bölker, M., Kahmann, R. 1997. G proteins in *Ustilago maydis*: transmission of multiple signals? EMBO Journal 16(8):1934-1942.

Remy, W., Taylor, T.N., Hass, H., Kerp, H. 1994. Four hundred-million-year-old mycorrhizal vesicular arbuscular mycorrhizae. Proc. Nat. Acad. Sci. USA 91:11841-11843.

Requena, N. 1998. Mycorrhizal interactions in the rhizosphere. *In:* Varma A (ed) Microbes: for health, wealth and sustainable environment. MPH New Delhi, India. pp. 726-735.

Requena, N., Breuninger, M., Franken, P., Ocón, A. 2003. Symbiotic status, phosphate and sucrose regulate the expression of two plasma membrane H^+-ATPase genes from the arbuscular mycorrhizal fungus *Glomus mosseae.* Plant Physiol. 132(3):1540-1549.

Requena, N., Jeffries, P., Barea, J.M. 1996. Assessment of natural mycorrhizal potential in a desertified semiarid ecosystem. Appl. Environ. Microbiol. 62:842-847.

Requena, N., Mann, P., Hampp, R., Franken, P. 2002. Early developmentally regulated genes in the arbuscular mycorrhizal fungus *Glomus mosseae:* identification of GmGIN1*,* a novel gene with homology to the C-terminus of metazoan hedgehog proteins. Plant Soil 244:129-139.

Requena, N., Pérez-Solis, E., Azcón-Aguilar, C., Jefries, P., Barea, M. 2001. Increased establishment of mycorrhizal plants inoculated with native endophyles in semi-arid degraded mediterranean ecosystems. Appl. Environ. Microbiol. 67:495-498.

Resh, M. D. 1999. Fatty acylation of proteins: new insights into membrane targeting of myristoylated and palmitoylated proteins. Biochim. Biophys. Acta 1451:1-16.

Reuber, T.L. and Ausubel, F.M. 1996. Isolation of Arabidopsis Genes that differentiate between resistance responses mediated by the *RPS2 and RPM1* disease resistance genes. Plant Cell 8:241-249.

Rietveld, A., Neutz, S., Simons, K., and Eaton, S. 1999. Association of sterol- and glycosylphosphatidylinositol-linked proteins with *Drosophila* raft lipid microdomains. J. Biol. Chem. 274:12049-12054.

Roh, D.H., Bowers, B., Schmidt, M., Cabib, E. 2002. The septation apparatus, an autonomous system in budding yeast. Mol. Biol. Cell. 13(8):2747-59.

Rothberg, K.G., Heuser, J.E., Donzell, W.C., Ying, Y., Glenney, J.R., Anderson, R.G.W. 1992. Caveolin, a protein component of caveolae membrane coats. Cell 68:673-682.

Roussel, H., van Tuinen, D., Franken, P., Gianinazzi, S., Gianinazzi-Pearson, V. 2001. Signalling between arbuscular mycorrhizal fungi and plants: identification of a gene expressed during early interactions by differential RNA display analysis. Plant Soil 232:13-19.

Ruiz-Lozano, J.M., Roussel, H., Gianinazzi, S., Gianinazzi-Pearson, V. 1999. Defense genes are differentially induced by a mycorrhizal fungus and *Rhizobium* sp. in wild-type and symbiosis-defective pea genotypes. Mol. Plant Microbe Interact. 12:976-984.

Salzer, P., Bonamoni, A., Beyer, K., Vógeli-Lange, R., Aeschbacher, R.A., Lang, J., Wiemken, A., Kim, D., Cook, D.R., Boller, T. 2000. Differential expression of eight chitinase genes in *Medicago truncatula* roots during mycorrhiza formation, nodulation and pathogen infection. Mol. Plant Microbe Interact. 13:763-777.

Salzer, P., Corbière, H. Boller, T. 1999. Hydrogen peroxide accumulation in *Medicago truncatula* roots colonized by the arbuscular mycorrhiza-forming fungus *Glomus intradices*. Planta 208:319-325.

Sancholle M., Dalpe Y., Grandmougin-Ferjani A., 2001. *In*: The Mycota IX (Springer-Verlag eds). Lipids of Mycorrhizae. pp. 63-93.

Sandal, T., Aumo. L., Hedin, L., Gjertsen, B.T., Doskeland, S.A., 2003. Irod/lan5: an inhibitor of γ-radiation and okadaic acid induced apoptosis. Mol. Biol. Cell 14:3292-3304.

Saraste, M., Sibbald, P.R., Witinghofer, A. 1990. The P-loop: A common motif in ATP- and GTP-binding proteins. Trends Biochem. Sci. 15:430-434.

Sargiacomo, M., Sudol, M., Tang, M., Lisanti, M.P. 1993. Signal trasducing molecules and glycosyl-phosphatidylinositol-linked proteins form a caveolin-rich insoluble complex in MDCK cells. J. Cell Biol. 122:789-807.

Schauser L., Roussis A., Stiller J., Stougaard J. 1999. A plant regulator controlling development of symbiotic nodules. Nature 402:191-195.

Scherer, P.E., Okamoto, T., Chun, M., Nishimoto, L., Lodish, H.F., Lisanti. M.P. 1996. Identification, sequence, and expression of caveolin-2 defines a caveolin gene family. Proc. Nat. Acad. Sci. USA 93:131-135.

Scherer, P.E., Lewis, F.-Y., Volonte, D.J., Engelman, A., Galbiati, F., Couet, J., Kohtz, D.S., van Donselaar, E., Peters, P., Lisanti, M.P. 1997. Cell-type and tissue-specific expression of caveolin-2. Caveolins 1 and 2 co-localize and form a stable hetero-oligomeric complex in vivo. J. Biol. Chem. 272:29337-29346.

Scheres, B., van Dewiel, C., Zalensky, A., Horvath, B., Spaink, H., van Eck, .H, Zwartkruis, F., Wolters, A.M., Gloudemans, T., van Kammen, A. 1990. The ENOD12 gene product is involved in the infection process during the *pea-Rhizobium* interaction. Cell 60:281-294.

Schroeder R., London E., Brown D. 1994. Interactions between saturated acyl chains confer detergent resistance to lipids and glycosylphosphatidylinositol (GPI)-anchored proteins: GPI-anchored proteins in liposomes and cells show the same behavior. 91:12130-12134.

Schüßler, A., Gehrig, H., Schwarzott, D., Walker, C. 2001a. Analysis of partial Glomales SSU RRNA gene sequences: implications for primer design and phylogeny. Mycol. Res. 105:5-15.

Schüßler, A., Schwarzott, D., Walker, C. 2001b. A new fungal phylum, the Glomeromycota: phylogeny and evolution. Mycol. Res. 105:1413-1421.

Seabra, M.C., Goldstein, J.L., Sudhof, T.C., Brown, M.S. 1992. Rab geranylgeranyl transferase. A multisubunit enzyme that prenylates GTP-binding proteins terminating in Cys-X-Cys or Cys-Cys. J. Biol. Chem. 267(20):14497-503.

Seabra, M.C., Brown, M.S., Slaughter, C.A., Sudhof, T.C., Goldstein J.L. 1992. Cell 70:1049-1067.

Seiffert, B.M., Vier, J., Hacker, G. 2002. Subcellular localization, oligomerization, and ATP-binding of *Caenorhabditis eiegans* CED-4. Biochem. Biophys. Res. Commun. 290:359-365.

Simon, L., Bousquet, J., Levesque, R.C., Lalonde, M. 1993b. Origin and diversification of endomycorrhizal fungi and coincidence with vascular plants. Nature 363:67-69.

Simon, L., Levesque, R.C., Lalonde, M. 1993a. Identification of endomycorrhizal fungi colonizing roots by fluorescent single-strand conformation polymorphism-polymerase chain reaction. Appl. Environ. Microbiol. 59:4211-4215.

Simoneau, P., Lousy-Louis, N., Plenchette, C. Strullu, D.G. 1994. Accumulation of new polypetides in Ri-T-DNA-transformed roots of tomato (*Lycopersion esculentum*) during the development of vesicular-arbuscular mycorrhizae. Appl. Environ. Microbiol. 60:1810-1813.

Simons, K. and Ikonen, E. 1997. Functional rafts in cell membranes. Nature 387:569-572.

Sinensky, M. 2000. Recent advances in the study of prenylated proteins. Biochem. Biophys. Acta 1484:93-106.

Siqueira, J.O., Safir, G.R., Nair, M.G. 1991. Stimulation of vesicular-arbuscular mycorrhiza formation and growth of white clover by flavonoid compounds. New Phytol. 118:87-93.

Smart, E.J., Graf, G.A., McNiven, M.A., Sessa, W.C., Engelman, J.A., Scheref, P.E., Okamoto, T., Lisanti, M.P. 1999. Caveolins, liquid-ordered domains, and signal transduction. Mol. Cell. Biol. 19(11):7289-1304.

Smith, F.A. and Smith, S.E. 1997. Structural diversity in vesicular-arbuscular mycorrizal symbiosis. New Phytol. 137:373-388.

Smith, S.E. and Smith, F.A. 1996. Membranes in Mycorrhizal Interfaces: Specialised functions or not? In: Membranes, Specialised Functions in Plant Cells. Ed. Smallwood, M. Knox, J. and Bowles, D. Bios, Oxford pp 525-542.

Smith, S.E. and Smith, F.A. 1990. Structure and function of the interfaces in biotrophic symbiosis as they relate to nutrient transporte. New Phytol. 114:1-38.

Smith, S.E., Read, D.J. 1997. Mycorrhizal symbiosis, 2nd edn. Academic Press, London Smith S.E. and Smith F.A. 1990. Structure and function of the interfaces in biotrophic symbiosis as they relate to nutrient transporte New Phytol. 114:1-38.

Solaiman, M.Z., Senoo, K., Kawaguchi, M., Imaizumi-Anraku, H., Akao, S., Tanaka, A., Obata, H. 2000. Characterization of mycorrhizas formed by *Glomus sp*. on roots of hypernodulating mutants of *Lotus japonicus*. J. Plant Res. 113:443-448.

Sorokina, E.M., Chernoff, J. 2005. Rho-GTPases: new members, new pathways. J. Cell. Biochem. 94:225-231.

Sprang, S. R. 1997. G proteins mechanism: Insights from structural analysis. Annu. Rev. Biochem. 66:639-678.

Stamm, O., Krücken, J., Schinitt-Wrede, H.-P., Benten, W.P.M., Wunderlich, F. 2002. Human ortholog to mouse gene *imiap38* encoding an ERlocalizable G-protein belongs to a gene family clustered on chromossome 7q32--36. Gne 282:159-167.

Steinmann, T., Geldner, N., Grebe, M., Mangold, S., Jackson, C.L., Paris, S., Gälweiler, L., Palme, K., Jürgens, G. 1999. Coordinated polar localization of auxin efflux carrier PIN1 by GNOM ARF GEF. Science 286:316-318.

Stenmark, H. and Olkkonen, V. M. 2001. The Rab GTPase family. Genome Biol. 2(5):1-7.

Stone, D., Hynes, M., Armanini, M., Swanson, T., Gu, Q., Johnson, R., Scott, M., Pennica, D., Goddard, A., Phillips, H. 1996. The tumor-suppressor gene patched encodes a candidate receptor for Sonic hedgehog. *Nature* 384: 129-134.

Stracke, S., Kistner, C., Yoshida, S., Mulder, L., Sato, S., Kaneko, T., Tabata, S., Sandal, N., Stougaard, J., Szczyglowski, K., Parniske, M. 2002. A plant receptor-like kinase required for both bacteria¡ and fungal syrnbiosis. Nature 417:959-962.

Sütterlin, C., Doering, T.L., Schimmöller, F., Schröder, S., Riezman, H. 1997. Specific requirements for the ER to Golgi transport of GPI-anchored proteins in yeast. J. Cell Science. 110:2703-2714.

Taipale, J., Chen, L., Cooper, M., Wang, B., Mann, R., Milovic, L., Scott, M., and Beachy, P. 2000. Effects of oncogenic mutations in Smoothened and patched can be reversed by cyclopamine. *Nature* 406:1005-1009.

Taipale, J., Cooper, M.K., Maiti, T., Beachy, P.A. 2002. Patched acts catalytically to suppress the activity of Smoothened. Nature 418: 892-896.

Takai, Y., Sasaki, T., Matozaki, T. 2001. Small GTP-Binding protiens. Phys. Reviews 81:153-194.

Takeda, T., Kawate, T., Chang, F. 2004. Organization of a sterol-rich membrane domain by cdc15p during cytokinesis in fission yeast. Nature Cell Biol. 6(11):1142-1144.

Tamasloukht, B., Séjalon-Delmas, N., Kluver, A., Roux, C., Bécard, G., Franken, P. 2003. Root factor induce mitochondrial-related-gene expression and fungal respiration during the developmental switch from asymbiosis to presymbiosis in the Arbuscular mycorrhizal fungus *Gigaspora rosea*. Plant Physiol. 131:1468-1478.

Tameling, W.I.L., Elzinga, S.D.J., Darin, P.S., Vossen, J.H., Takken, F.L.W., Haring, M.A., Cornelissen, B.J.C. 2002. The tomato R gene products I-2 and Mi-1 are functional ATP binding proteins with ATPase activity. The Plant Cell 14:2929-2939.

Taussig, R., Iniguez-Lluhi, J.A., Gilman, A.G. 1993. Inhibition of adenylyl cyclase by Gi alpha. Science 261(5118):218-21.

Taylor, F.R., Wen, D., Garber, E.A., Carmillo, A.N., Baker, D.P., Arduini, R.M. 2001. Enhanced potency of human Sonic hedgehog by hydrophobic modification. Biochem. 40:4359-4371.

Taylor, T.N., Remy, W., Hass, H., Kerb, H. 1995. Fossil arbuscular mycorrhizae from the early Devonian. Mycologia 87:560-573.

The, I., Bellaiche, Y., Perrimon, N. 1999. Hedgehog movement is regulated through tout velu-dependent synthesis of a heparan sulfate proteoglycan. Mol. Cell 4:633-639.

Tommerup, I.C. 1984. Persistence of infectivity by germinated spores of vesicular-arbuscular mycorrhizal fungi in soil. Trans. Br. Mycol. Soc. 82:275-282.

Traut, T.W. 1994. The functions and consensus motifs of nine types of peptide segments that form different types of nucleotide binding sites. Eur. J. Biochem. 222:9-19.

Trueblood, C.E., Boyartchuk, V.L., Picologlou, E.A., Rozema, D., Poulter, C.D., Rine, J. 2000. The CaaX proteases, Afc1p and Rce1p, have overlapping but distinct substrate specificities. Mol. Cell Biol. 20:4381-4392.

Tsai, S.M. and Philips, D.A. 1991. Flavonoids released naturally from alfalfa promote development of symbiotic *Glomus* spores *in vitro*. Appl. Environ. Microbiol. 57:1485-1488.

Tucker, J., Sezzakiel, G., Feuerstein, J., John, J., Goody, R.S., Wittinghofer, A. 1986. Expression of p21 proteins in *Escherichia coli* and sterochemistry of the nucleotide-binding site. EMBO J. 5(6):1351-1358.

Umebayashi, K & Nakano, A. 2005. Ergosterol is required for targeting of tryptophan permease to the yeast plasma membrane. J. Cell Biol. 161(6):1117-1131.

Valzer, P. and Boller, T. 2000. Elicitor-induced reactions in mycorrhizae and their suppression. *In*: Current advances in mycorrhizae research. *Eds.*G.K. Podila and D.D. Douds. APS Press, St. Paul, Minn. pp. 1-10.

Van Brussel, A.A.N. , Bakhuizen, R. , Van Spronsen, P.C. , Spaink, H.P. , Tak, T. , Lugtenberg, B.J.J. and Kijne, J.W. (1992) Induction of pre-infection thread structures in the leguminous host plant by mitogenic lipo-oligosaccharides of *Rhizobium. Science*, 257, 70-71.

van den Heuvel, M. and Ingham, P.W. 1996. Smoothened encodes a serpentine protein required for hedgehog signaling. *Nature* 382:547-551.

van der Heijden, M.G.A., Klironomos, J.N., Ursic, M., Moutoglis, P., Streitwolf-Engel, R., Boller, T., Wiemken, A., Sanders, I.R. 1998. Mycorrhizal fungal diversity determines plant biodiversity, ecosystem variability and productivity. Nature 396:69-72.

van Rhijn, P., Fang, Y., Galili, S., Shaul, O., Atzmon, N., Wininger, S., Eshed, Y., Lum, M., LiY, T.O.V., Fujishige, N., Kapulnik, Y., Hirsch, A.M. 1997. Expression of early nodulin genes in alfalfa mycorrhizae indicates that signal transduction pathways used in forming arbuscular mycorrhizae and rhizobium-inducednodules maybe conserved. Proc. Natl. Acad. Sci. USA 94:5467-5472.

Varma, R. and Mayor, S. 1998. GPI-anchored proteins are organized in submicron domains at the cell surface. Nature 394:798-801.

Vater C. A., Raymond C. K., Ekena K., Howaald-Stevenson I., Stevens T. H. 1992. The VSP1 protein, homolog of dynamin required for vacuolar protein sorting in *Saccharomyces serevisiae*, is a GTPase with two functionally separable domains. J. Cell Biol. 119:773-786.

Vernoud, V., Horton, A. C., Yang, Z., Nielsen, E. 2003. Analysis of the small GTPase gene superfamily of Arabidopsis. Plant Physiol. 131(3):1191-208.

Vierheilig, H. 2004. Regulatory mechanisms during the plant-arbuscular mycorrhizal fungus interaction. Can. J. Bot. 82:1166-1176.

Vierheilig, H., Alt, M., Mohr, U., Boller, T., Wiemken, A. 1994. Ethylene biosyhtesis and activities of chitinase and ß-1,3-glucanase in the roots of host and non-host plants of vesicular-arbuscular mycorrhizal fungi after inoculartion with *Glomus mosseae*. J. Plant. Physiol. 143:337-343.

Volpin, H., Elkind, Y., Okon, Y., Kapulnik, Y.A. 1994. A vesicular-arbuscular mycorrhizal fungus (*Glomus intraradix*) induces a defese response in alfalfa roots. Plant. Phsiol. 104:683-689.

von Heijne, G. 1986. A new method for predicting signa1 sequence cleavage sites. Nucleic Acids Res. 14:4683-4690.

Wachtler, V., Rajagopalan, S., Balasubramanian, M.K. 2002. Sterol-rich plasma membrane domains in the fission yeast *Schizosaccharomyces pombe*. J. Cell. Sci. 116(5):867-874.

Wagner P., Molenaar C. M. T., Rauh A. J. G., Brokel R., Schmitt H. D., Gallwitz, 1987. Biochemical properties of the ras-related YPT protein in yeast: a mutational analysis. EMBO J., 6(8):2373-2379.

Wallace, C.J. 1993. The curious case of protein splicing: mechanistic insights suggested by protein semisynthesis. Protein Sci. 2(5):697-705.

Wedegaertner, P.B., Wilson, P.T., Bourne, H.R. 1995. Lipid modifications of trimeric G proteins. J. Biol. Chem. 270(2):503-506.

Wegel, E., Schauser, L., Sandal, N., Stougaard, J., Parniske, M. 1998. Mycorrhiza mutants of *Lotus japonicus* define genetically independent steps during symbiotic infection. Mol. Plant Microbe Interact. 11:933-936.

Weinzierl, G., Leveleki, L., Hassel, A., Kost, G., Wanner, G., Bölker, M. 2002. Regulation of cell separation in the dimorphic fungus *Ustilago maydis*. Mol. Microbiol. 45(1):219-231.

Wittinghofer, A., Goody, R.S., Roesch. P., Kalbitzer, H.R. 1982. Eur. J. Biochem. 124:109-115.

Wyss, P.T., Boller, T. Wiemken, A. 1991. Phytoalexin in response is elicited by a pathogen (*Rhizoctonia solani*) but not by a mycorrhizal fungus (*Glomus mosseae*) in bean roots. Experientia 47:395-399.

Xu, X., Bittman, R., Duportail, G., Heissler, D., Vilchezes, C., London, E. 2001. Effect of the structure of natural sterols and sphingolipids on thhe formation of ordered sphingolipid/sterol domains (Rafts). J. Biol. Chem. 276(36):33540-33546.

Yu, G.-L., Katagiri, F., and Ausubei, F.M. 1993. *Arabidopsis muta*tions at the *RPS2* locus result in loss of resistance to *Pseudomonas syringae* strains expressing the avirulence gene *avrRpt2.* Mol. Plant Microbe Interact. 6:434-443.

Zhang, F. L. and Casey, P. J. 1996. Protein prenylation: molecular mechanisms and functional consequences. Annu. Rev. Biochem. 65:241-169.

Zhang, J., Zhang, Y., Inouye, M. 2003. Thermotoga maritima MazG protein has both nucleoside triphosphate Pyrophosphohydrolase and Pyrophosphatase activities. J. Biol. Chem. 278(24):21408-21414.

Zeng, X., Goetz, J.A., Suber, L.M., Scott, W.J. Jr., Schreiner, C.M., Robbins, D.J. 2001. A freely diffusible form of Sonic hedgehog mediates long-range signalling. Nature 411:716-720.

Ziman, M., Obrien, J. M., Oulette, L. A., Church, W. R., Johnson, D. I. 1991. Mutational analysis of *cdc42Sc*, a *Saccharomyces cerevisiae* gene that encodes a putative GTP-binding protein involved in the control of cell polarity. Mol. Cell. Biol. 11:3537-3544.

Zou, H., Henzel, W.J., Liu, X., Lutschg, A., and Wang, Y. 1999. Apaf-1, a human protein Homologous to C. *elegans* CED-4, participates in cytochrome c-dependent activation of caspase-3. Cell 90:405-413.

Zuber, S., Hynes, M.J. & Andrianopoulos, A. 2002. G-Protein signaling mediates asexual development at 25°C but has no effect on Yeast-like growth at 37°C in the dimorphic Fungus *Penicillium marneffei. Eukaryotic* Cell 1(3):440-447.

Curriculum vitae

First name	Esther
Family name	Serrano Padial
Date of Birth	May 12, 1977
Place of Birth	Elda, Alicante (Spain)

Education

1983-1991	Primary school at “Colegio Padre Manjón” in Elda, Alicante (Spain)
1991-1995	Secondary school at “Colegio Sagrada Familia” in Elda, Alicante (Spain)
1995-2000	Studies of Pharmacy in the University of Granada (Spain)
December 2001	Master thesis “*Un quelato de Cobre (II) conteniendo formas protonadas de eilendiaminotetraacetato y adenina: síntesis, estructura cristalina y propiedades.”* at the Inorganic Chemistry Department, University of Granada, Spain.
June 2005	Doctoral thesis at the Department of Physiological Ecology of Plants, Faculty of Biology, University of Tübingen.